Ministère de l'Enseignement Supérieur et de la Recherche Scientifique
Université Hassiba Benbouali de Chlef
Faculté de Technologie
Département de Mécanique

THÈSE

Présentée en vue de l'obtention du diplôme de

DOCTORAT EN SCIENCES

Spécialité : Génie mécanique

Par

Ali TETBIRT

Thème :

TRANSFERTS CONVECTIFS MAGNETOHYDRODYNAMIQUES DES FLUIDES MICROPOLAIRES ET VISQUEUX DANS UN CANAL VERTICAL

Soutenance le 04/07/2017 devant le jury composé de :

Hamou ZAHLOUL	Professeur	UHB Chlef	Président
Abdelkader YOUCEFI	Professeur	UST Oran	Rapporteur
Ridha MAZOUZI	MCA	UDB El-Khemis	Rapporteur
Abdallah BENAROUS	MCA	UHB Chlef	Rapporteur
Miloud TAHAR ABBES	Professeur	UHB Chlef	Directeur de Thèse
Mohamed Nadjib BOUAZIZ	Professeur	UYF Médéa	Co-directeur de Thèse

Ministry for Higher Education and Scientific Research
University Hassiba Benbouali of Chlef
Faculty of Technology
Department of Mechanical Engineering

THESIS

OF DOCTORATE IN SCIENCES

Mechanical Engineering

Presented by

Ali TETBIRT

Theme:

MAGNETOHYDRODYNAMIC CONVECTIVE TRANSFERS OF MICROPOLAR AND VISCOUS FLUIDS IN A VERTICAL CHANNEL

In 04 / 07 / 2017, in front of jury members:

Hamou ZAHLOUL	Professor	UHB Chlef	President
Abdelkader YOUCEFI	Professor	UST Oran	Examinator
Ridha MAZOUZI	MCA	UDB Khemis Miliana	Examinator
Abdallah BENAROUS	MCA	UHB Chlef	Examinator
Miloud TAHAR ABBES	Professor	UHB Chlef	Supervisor
Mohamed Nadjib BOUAZIZ	Professor	UYF Médéa	Co-Supervisor

بسم الله الرحمن الرحيم

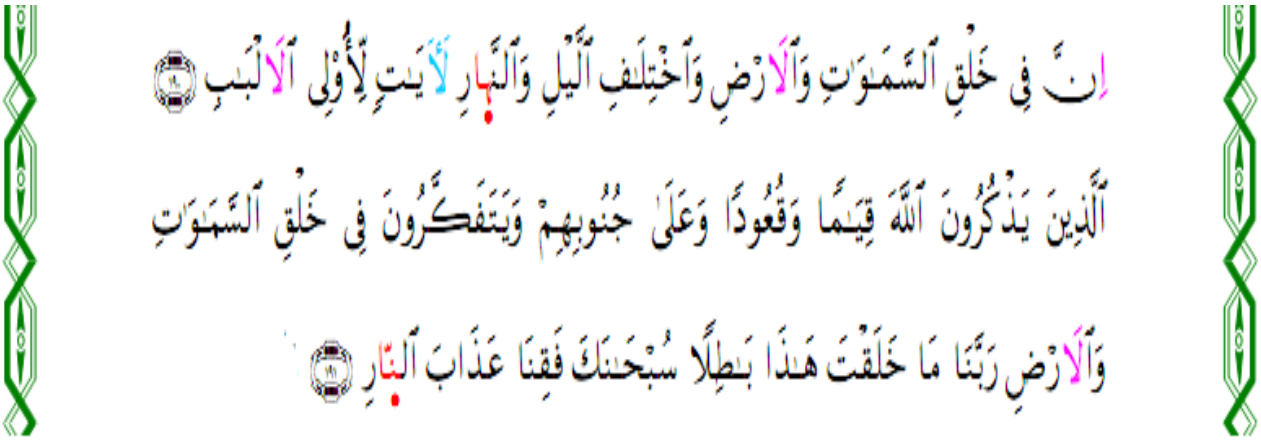

سورة آل عـمران، ألآية 190

Dedications

With all my heart, as a sign of honor, respect and recognition, as a result this dissertation is dedicated to the memory of my father, my grandmother and my brothers, Mohamed, Benyucef, and Djamel. I wish from Allah to give clemency and forgiveness for them.

I would like to dedicate this modest work to my dear mother for her supplication to Allah for helping me to success in my work.

This dissertation is dedicated to my wife for her patience during the time required to its completion. This dissertation is dedicated to my brothers, my sisters, and all members of my large family.

In the end, I would like to dedicate this work to all my colleagues and friends who know me and love the best things happening to me.

Ali TETBIRT

About the Author

Full Name: **Ali TETBIRT**
Permanent researcher at UDES/CDER, Developing Unit of Solar Equipments Developing Center of Renewable Energy.

Mob: (+213) 06 67 88 01 69/05 40 03 21 04

e-mail: tetbirtali@yahoo.fr

Presenter's Name. Ali TETBIRT. In 1989, I received the Bachelor's degree in mathematical from Hamza Ben-Abdelmotalib's college, Khemis Miliana, Ain Defla. Then, in 2008, I finished engineer's degree, in climatic engineering from the Faculty of Sciences and Technology, University Djilali Bou-Naama of Khemis Miliana (UDBKM), Ain Defla, Algeria. After that, in 2011, I received the Magister degree in energy and transfer from Department of Mechanic, Faculty of Sciences and Technology, University Yahia Fares of Médéa (UYFM), Algeria. Finally, in May 12, 2013, I started working as a researcher in Developing Unit of Solar Equipments (UDES/CDER), Bou-Ismail, Tipaza, Algeria.

Acknowledgements

About this degree, there have been many people who have assisted, encouraged and supported me in my doctorate. In particular, I wish to thank my supervisor, Pr. Miloud TAHAR ABBES and Pr. Mohamed Nadjib BOUAZIZ, for their guidance, advice, comments and support throughout this research work were fundamental for its development in all this investigate.

I would also like to thank Dr. Benyucef KHELIDJ, because He was the first who gave me advices to continue in the same Magister degree project. He had also given me the possibility to work in this topic with Pr. M. N. BOUAZIZ. I would like to express my great respect to my lab-mates Djelloul BELKACEMI and Fateh BOUZEFFOUR, all of the administrative staff, and members of the Mechanical and Energy Laboratory of UHB Chlef.

Then I should not forget to acknowledge all my colleagues in FTEER-teams at Developing Unit of Solar Equipments (UDES), Bou-Ismail, Tipaza.

I would like also to thank my Mother and wife for their patience, Brother, Sisters for their encouragement, and other friends, particularly Mahdi Morane, Mohamed Azizou, Ridha Allich, Mahmoud Kadhi Mohamed Ali Djebiret, Mamer Ouali, Mohand Berdja, Ferhat Yahi for their patience, good humor, unfailing Interest in my work, indeed who made all together our workspace enjoyable.

Finally, I'll never forget that I had my doctorate degree in July 4th, 2017, when I was very happy of that event. That is how I'd like to thank a lot Pr. Hamou ZAHLOUL, Dr. Ridha MAZOUZI, Dr. Abdallah BENAROUS, and Pr. Abdelkader YOUCEFI for the valuable scientific criticism, good cooperation, and their patience.

Ali Tetbirt

In July 4th, 2017

ملخص

هذا العمل يمثل دراسة نظرية ورقمية لظاهرة انتقال الحرارة بواسطة الحمل من نوعين مختلفين من سوائل غير قابلة للامتزاج في قناة عمودية مع وجود تأثير لمجال مغناطيسي خارجي على القناة، وتشمل الدراسة عدة تطبيقات في منظومة السوائل الميكانيكية و الطاقة في المجالين: الصناعي و البيولوجي، مثل تدفق الدم داخل جسم الإنسان وحركة السائل الزليلي في المفاصل.

إن الموائع و السوائل الميكروقطبية هي سوائل تحتوي على جسيمات دقيقة عالقة ذات حركة دورا نية مجهريه معقدة تحت تأثير عدة خصائص الفيزيائية و كهروطيسية .... لأجل التوصل إلى فهم صحيح للخصائص الفيزيائية و الميكانيكية المجهرية لحركة الموائع الميكروقطبية، عملنا على صياغة نموذج رياضي يأخذ في الحسبان انتشار المجال المغناطيسي و أثره على إنتشار الطاقة أو إحتباسها في الموائع و كذالك أثره على حركة الجزيئات الدقيقة داخل القناة. النموذج المقترح للحل و الدراسة هو مجموعة من المعادلات تصف حفظ المادة، حفظ الحركة و حفظ الطاقة. الحل المقدم سمح بظهور بعض المعاملات بدون وحدات (متر، الثانية، الحريرة، الخ...)، نذكر على سبيل المثال لا الحصر: معامل المادة (K)، معامل برونت (Pr)، معامل الحمل المختلط (GR)، معامل المغنطة (Ha)، معامل إيكرت (Ec).

وعليه فإن النتائج التحليلية و الرقمية التي تم الحصول عليها من نموذج الرياضي المبرمج آليا (برنامج Matlab) تم استثمارها و استخدامها و التعليق عليها، ولقد بدا جليا و واضحا تأثير الحقل المغناطيسي على السرعة الخطية وسرعة دوران الجزيئات حول نفسها داخل الموائع الميكروقطبية و اللزجة. ومن ثم فإن هذه النتائج قد خضعت لمناقشة و دراسة مقارنة بين النموذج الحالي و دراسات سابقة منشورة في مقالات علمية.

كلمات المفاتيح: مائع مبكروقطبي، تأثير الهيدروديناميك الممغنطة، تدفق الحمل الحراري، الميكروقطبية، الميكرودوراني.

Abstract

This work is devoted to the theoretical, analytical, and numerical study of a free-convective flow in a vertical channel, it's consisting of two immiscible fluid regions, the first region is filled of a non-Newtonian fluid of micropolar type, and the second region is filled with Newtonian-viscous fluid. Both fluids are under effects of the temperature gradient and magnetic field.

In a microscopic scale, non-Newtonian micropolar fluids contain suspended fine particles in complex rotating motion, complex microstructure under the influence of several physicochemical characteristics….. The behavior of micropolar fluid flow is influenced by its microstructure characteristics which these have an effect on the distribution of velocities field. (ie linear or axial and microrotation velocities).

To achieve a good understanding about the complexity of this type of flow, a mathematical model was developed in considering the term of magnetic diffusivity and the term of thermal diffusivity in the energy balance equation. This allows the appearance of some dimensionless parameters such as the material parameter (K), the Prandtl number (Pr), the mixed convection parameter (GR), the magnetic parameter (Ha) and the Eckert number (Ec).

Therefore, the numerical results obtained from the model were used to assume an apparent effect of the magnetic field on linear and spin velocities within micropolar and viscous fluids. Hence, those results obtained from the mathematical model are used in a comparative study between the current studied model in considering terms of the magnetic diffusivity and thermal diffusivity, and others works which didn't consider those terms.

Key words: Micropolar Fluid; Magnetohydrodynamic effect; Convective flow; Micropolarity; Microrotation.

Résumé

Ce travail est consacré à l'étude théorique, analytique et numérique d'un écoulement convectif, mixte et magnétohydrodynamic dans un canal vertical composé de deux régions de fluides immiscibles, la première région est remplie d'un fluide non-Newtonien de type micropolaire et la seconde région du canal est remplie d'un fluide Newtonien visqueux. Le modèle physique à étudier – canal et les deux fluides – sont sous l'influence d'un gradient de température et d'un champ magnétique.

À l'échelle microscopique, les fluides non-Newtoniens de type micropolaire contiennent des particules fines en suspension et en mouvement rotatif et avec microstructure complexe sous l'influence de plusieurs caractéristiques physico-chimiques…Le comportement de fluide micropolaire en écoulement convectif est influencé par ses caractéristiques de la microstructure qui ont un effet sur le champ de distribution des vitesses. (C.-à-d. vitesses linéaires ou axiales et la microrotation). L'écoulement naturel a lieu dans le canal vertical comme dans le cas de l'industrie mécanique, tels que : les colloïdes, fluides contenant des particules fines en suspension, cristaux liquides, fluides polymères à longue chaîne et fluides pétillants (brillant, coloré, etc.).

Aussi, l'objectif de cette étude est d'examiner le comportement des fluides micropolaires vis-à-vis au comportement des fluides Newtoniens en analysant les profils de la vitesse linéaire et la vitesse de microrotation ainsi que l'effet de taux de frottements aux parois du canal en fonction de certains paramètres appropriés résultant de la formulations mathématiques et cela dans les deux cas : sans ou avec champ magnétique.

Afin d'atteindre ces objectifs cités ultérieurement et aussi prédire le comportement de ce type d'écoulement complexe, un modèle mathématique a été développé qui prend en considération le terme de la diffusivité magnétique et le terme de diffusivité thermique de l'équation de bilan énergétique, cela a permis l'apparition de certains paramètres et nombres adimensionnels tels que le paramètre matériel (K), le nombre de Prandtl (Pr), le paramètre de convection mixte (GR : définit par le rapport du nombre de Grashof sur le nombre de Reynolds), le nombre de Hartmann (Ha) qui caractérise le flux linéaire, surfacique et/ou volumique du champ magnétique et le nombre d'Eckert (Ec).

Les résultats obtenus à partir du modèle mathématique final, ont permis d'une part d'analyser l'effet du champ magnétique sur la distribution du champ des vitesses linéaires et de la microrotation (spin) aux seins des fluides micropolaires et visqueux, d'autre part, ces résultats sont utilisés dans l'étude comparative entre des travaux déjà faites qui négligent les termes de la diffusivité thermique et la diffusivité magnétique dans l'équation de bilan énergétique et le modèle en cours qui prend en considération ces termes.

Mots clés : Fluide Micropolaire, Effet magnétohydrodynamique, Ecoulement Convectif, Micropolarité, Microrotation.

Communications

1) Ali TETBIRT, Benyucef KHELIDJ, Miloud TAHAR ABBES, Ahmed KELLACI, Ridha MAZOUZI, Ecoulement convectif magnétohydrodynamique des fluides immiscibles : micropolaire et visqueux dans un canal vertical, 2ème Conférence Internationale sur les Energies, Matériaux et Environnement, le 2 et 3 Décembre 2012, Université Djilali Bounaama de Khemis Miliana.

2) Ali TETBIRT, Benyucef KHELIDJ, Miloud TAHAR ABBES, Etude numérique de la variation des vitesses d'un écoulement convectif libre sous l'influence d'un champ magnétique des fluides micropolaire et visqueux dans un canal vertical**,** Journées d'Etudes des Doctorants **(**JED'1), le 18 et 19 juin 2013, Université Hassiba Benbouali de Chlef.

3) Ali TETBIRT, Benyucef KHELIDJ, Miloud TAHAR ABBES, Influence du champ magnétique sur le transfert de chaleur de l'écoulement convectif naturel des fluides micropolaires et visqueux dans un canal vertical, Journées d'Etudes des Doctorants **(**JED'2), le 25 et 26 juin 2014, Université Hassiba Benbouali de Chlef.

4) Ali TETBIRT, Benyucef KHELIDJ, Miloud TAHAR ABBES, Transferts convectifs MHD de fluides non-Newtonien micropolaire et fluide Newtonien visqueux dans un canal vertical, Journées d'Etudes des Doctorants **(**JED'3), le 07 et 08 Octobre 2015, Université Hassiba Benbouali de Chlef

Publication

1) Ali Tetbirt, Mohamed Nadjib Bouaziz, Miloud Tahar Abbes, Numerical study of magnetic effect on the velocity distribution field in a macro/micro-scale of a micropolar and viscous fluid in vertical channel, Journal of Molecular Liquids , Vol. 216, (2016), page 103–110.

Nomenclature

Latin alphabet

Symbol	Designation	Unit
A	Surface	m^2
C_h	Constant of Hamaker	---
B_0	Magnetic field coefficient	---
C_p	Specific heat at constant pressure	kj/kg.K
d_p	Diameter of particle	meter(m)
F	Force	$m.kg.s^{-2}$ (N)
F_B	Brownian force	$m.kg.s^{-2}$
F_{gr}	Gravitational force	$m.kg.s^{-2}$
F_{in}	Force of inertia	$m.kg.s^{-2}$
F_{vd}	Van-Der Waals force	$m.kg.s^{-2}$
F_{vs}	Viscous force	$m.kg.s^{-2}$
h^*	Width ratio	----
J	Elastic complication	$m / kg\ s^2$ ou 1/Pa
j	Micro-inertia density	---
k	Boltzmann constant	---
k	Structural index	---
k	Thermal conductivity	W/m.K
k_i	Thermal conductivities of both fluids	W/m.K
k^*	Thermal conductivities ratio	---
K	Material parameter	---
k_C	Critical fluid consistency	---
m	Microscopic structure parameter	---
n	Parameter characterizing the type of fluid	---
P	Pressure	$kg.m^{-1}.s^{-2}$ (Pa)
T	Temperature	Kelvin(K)
t_1	Characteristic time	Second (s)
t_m	Characteristic period	s
S	Coefficient which characterizes the degree of particle-particle	---

	interaction	
U_i	Linear velocities of both fluids	m/s
y	Dimensionless variable	---

Greek alphabet

β	Coefficient of thermal dilation at constant pressure	---
η	Particle Viscosity	$kg.m^{-1}.s^{-1}$
η	Similarity variable	---
ρ	Density	Kg/m^3
ρ^*	Densities ratio	---
λ	Thermal conductivity	W/m.K
γ	Deformation	---
μ_0	Initial viscosity	
μ_m	Average viscosity	
μ^*	Viscosities ratio	---
Φ_m	Maximum packing fraction	---
τ	Tangential shear stress	$kg.m^{-1}.s^{-2}$
σ_0	Modulus of elasticity	
σ	Swirling viscosity	---
σ^*	Electrical conductivity of fluid	---
θ	Dimensionless variable that characterizes the temperature	---
χ	Constant linked μ_∞ and the shear rate of viscosity at very low value	---

Dimensionless numbers

Ec	Eckert number	----
Gr	Grashof number	----
Ha	Hartmann number	----
Nu	Nusselt number	----
Pr	Prandtl number	----
Re	Reynolds number	----

List of Acronyms and Abbreviation

BEM	Boundary Element Method
CSCM	Cubic Spline Collocation Method
KBM	Keller Box Method
LGAM	Lie Group Analysis Method
MHD	MagnetoHydroDynamic
MF	Micropolar Fluid
MV	Microrotation Velocity
NSM	Network Simulation Methodology
LV	Linear Velocity
UHF	Uniform Heat Flow
UWT	Uniform wall Temperature
VF	Viscous Fluid

Table of contents

Chapter 3: Mixed Convection and MHD effect on Newtonian and non-Newtonian-micropolar fluid flows

Part III

Chapter 4: Modeling and solving the immiscible non-Newtonian-micropolar and Newtonian-viscous fluids flow in vertical channel

List of figures

List of Tables

Background Introduction

The research works on immiscible flows of micropolar non-Newtonian fluids and Newtonian viscous fluids under the effect of magnetic field and temperature gradient are based on the theories of micro-continuum carried out by the physicist **A. Cemal Eringen** [1-6]. Consequently, several axes of theoretical and experimental research have been created to explain certain thermomechanical phenomena in microscopic scale, for example**: A. Ishak & all** [7] have studied a uniform mixed convective flow and magnetohydrodynamic through a stopping point (stagnation point) on a vertical surface immersed in an incompressible micropolar fluid. This study shows us the existence of a reversed flow region (the velocity of flow changes direction). They also found that the studies of the convective flow of viscous and micropolar fluids without a magnetic field influence have failed to prove the existence of a transitional flow regime. Another types of research are carried out on free convective flows in the absence of the magnetic field such as the study by **Z. Chahoui & all** [8], examining the effects of microstructure and microrotation on the devices Of lubrication in the boundary layer, the effect of particle size (the particle size relative to the thickness of the lubricant film) and the shear torque have apparent effects on flow perturbation and Equivalent viscosity of the micropolar fluid.

According to **J. P. Kumar & all** [9], the free convective flow under the established regime of the micropolar and viscous fluids in a vertical channel is studied, they observed that the parameter of mixed convection favors the linear velocity which is the cause Of an increase in the buoyancy force which represents an advantage for the lubrication systems, whereas the material parameter does not favor the linear speed, which is a disadvantage for the lubrication systems, they have also observed that the parameter of The mixed convection and the material parameter favor the speed of the microrotation. **Youn J. Kim** [10], have studied the instability of the convective flow of micropolar fluids through a vertical, porous and movable plate in a porous medium, he found that the suction speed of the micropolar fluid through the porous media decreases when the parameter Magnetic field (Ha) increases, while the latter increases as the number of Grashof increases**. K. L. Hsiao** [11-15]**,** has studied the mixed flows and heat and mass transfer of viscoelastic fluids and nanofluids under the effect of the magnetic field, he found that the increase of the magnetic parameter decreases the rate of heat transfer and the profile of the Speed, while increasing number of Prandtl and Grashof number improves energy efficiency (heat transfer), he also observed that the increase in buoyancy force, also improves the heat transfer in the presence Of a

porous material from the flow of mixed convection of viscoelastic fluids. For nanofluids, the variation of the magnetic parameter decreases, on the one hand, the rate of increase of the flow velocity of the nanofluid in the boundary layer, on the other hand it causes the increase of heat transfer and this Is also noted for the Prandtl number while the upward variation of the Eckert number causes the heat transfer decrease**. A. K. Piętal [16],** has studied the possibility of applying the theory of micropolar fluids on flow models in microchannels and the calculation as a function of the geometric dimension of the flow field, he showed that for linear dimension of flow sufficiently The equations of the flow of the micropolar fluid take the form of the Navier-Stokes equations, and then the POISEUILLE flows in a microchannel are studied as a function of the diameter of the maximum section of the channel. He confirmed that the micropolar model is applicable for a small geometric dimension characteristic of the flow. The results indicate that this "limiting dimension" depends on the rheological properties of the fluid which can be expressed through dimensionless microstructure parameters defined herein. For the larger microchannels, the flow is silent, well described by the classical fluid model, and it pays to perform the calculations on the basis of classical dynamics, the Navier-Stokes equations, which are simpler than those of Dynamic equations fluids micropolar. The results obtained correspond to some experimental estimates obtained earlier. The lower limit of applicability of the theory of micropolar fluids to the modeling of microflows as mentioned above results from fundamental questions on how the small dimensions of the flow field the micropolar fluid model can be treated as A continuous environment. This problem has been studied in other articles in detail. On the basis of the results, we can conclude that the micropolar theory is applicable to the modeling of fluid flows in channels of width not less than 10 diameters of the fluid molecule**.** Using the method of Nachtsheim Swigert, **Md. Z. Haque et al [17],** have studied numerically the behavior of micropolar fluids in free convective flow MHD, with heat and mass transfer through a porous medium whose heat and mass flux Are constant. The main results obtained from this study are: the velocity of micropolar fluid flow and the local friction coefficient vary in proportion to the density of the light particles and the air. While microrotation varies proportionally with the high density of heavy particles and water (inversely proportional with micropolar fluids and air density of light particles). They also observed that the temperature of the micropolar fluid is higher for air than water. It is hoped that scientific investment is useful for plasma as well as in electrical engineering, extractions of geothermal energy, generators and control of parameters in the boundary layer in the field of aerodynamics**.** In 2013, **B. Madhusudhana et al [18]**, have studied the free convective transfer of heat and mass MHD from the flow over a semi-infinite vertical plate,

mobile and permeable under the effect of heat absorption, Radiation, chemical reaction and sore. By the analytical solution of the governing differential equations of the flow, they noted that as the number of thermal Grashof increases, the velocity of fluid flow increases, so increasing the heat source and radiation Decrease in the temperature of the fluid and the speed of flow of the fluid. In addition, the local friction coefficient is increased due to the increase of the sore parameter. Similarly, the local friction coefficient and the Nusselt number are decreased due to the increase in radiation and heat source parameters. In 2008, **Jian-Jun Shu et al** [19], proposed a new fundamental solution for micropolar fluids, they wrote the Navier-Stokes and Oseen differential equations of the uniform flow in explicit form and unbounded two- Point two-dimensional micropolar, Stokes two-dimensional and three-dimensional micropolarities, the three-dimensional Oseenlet micropole, and the three-dimensional Oseen micropolar pair, hence these fundamental solutions are not defined for the flows of Newtonian fluids due to the lack of microrotaction velocity field. As an application, the drag coefficients of a solid sphere or a circular cylinder are determined which results in a micropolar flow of low Reynolds number and are compared with those corresponding to the Newtonian flow. The drag coefficient in the micropolar fluid is greater than that of a Newtonian fluid. **A. A. Siddiqui** [20], has formulated the non-uniform flow due to a uniformly accelerated circular cylinder and rotates in a stationary, viscous, incompressible and micropolar fluid. This flow problem is examined numerically by adopting a special scheme including the Adams-Bashforth temporal Fourier series method and the Runge-Kutta finite special finite difference method. He observed in this experimental study that if the effects of micropolarity are intensified, the lift increases and the drag force is reduced. The same thing happens if the rotation of the cylinder increases. In addition, rotation not only dampens vortices and unfavorable pressure adjacent the cylinder region, but also dissolves the boundary layer separation. In addition, rotation reduces the micropolar spin boundary layer as well. **M. Ashraf and A. R. Wehgal** [21], have studied MHD flow and heat transfer of micropolar fluid over a deceived disk. Research suggests that the heat transfer rate at the disc surface increases with increasing values Of micropolar parameter. Also the magnetic field improves the shear stresses and the torque. The shear stress factor is lower for micropolar fluids than for Newtonian fluids, which can be beneficial in controlling the flow and heat of the polymer treatment. **M. Zadravec et al.** [22], have contributed in numerical simulation of the flow of micropolar fluid in a channel, describing the flow of rigid particles in suspension, undeformable and in its own rotation. By applying the Boundary Element Method (BEM) method, the results show that the ratio between the viscosity coefficient of turbulence and the coefficient of a viscosity of the spin gradient

control the microrotation in the microchannel. **D. Gupta [23],** have worked in the aim to obtain a mathematical model for various nonlinear flow problems of micropolar fluids and determining the numerical solution of these problems. He studied the effect of various parameters on the flow rate and the heat transfer characteristics of the micropolar fluid. Also, he had worked to find the parameters responsible for the reduction of friction, and studied the parameters which increase the rate of Transfer of heat. **Xinhui Si et al. [24],** Have studied the influence of viscous dissipation in the energy equation of the flow and heat transfer of incompressible micropolar fluid in a channel, which walls are expanding or contracting. They have focused on the influence of certain physical parameter values on velocity, microrotation, and heat transfer. They concluded that the value of the microrotation close to the suction wall is a decreasing function and the temperature is an increasing function. Due to the existence of injection on the walls, the profile of the microrrotation is antisymmetric and the minimum value of the temperature decreases. The maximum value of the flow velocity is an increasing function. The value of the microrotation and the temperature at the wall, both are decreasing functions. The value of microrotation at the wall is an increasing function. The speed of the microrotation is zero in the center of the channel because the directions of the speed of the microrotation are opposite**. P. Muthu et al. [25]**, have studied the oscillatory flow of micropolar fluid in an annular region with constriction, provided by the variation of the radius of the outer tube, is studied. The nonlinear governing equations of the flux are solved using the perturbation method to determine the flow characteristics. The main contribution of this article is to see the micropolar nature of blood flow in a catheterized artery. They found that a mean zero flow, continuous flow analysis predicted a non-zero mean pressure drop. The variation in the size of the catheter has an effect on the shear of the wall. **G. M. Abdel-Rahman [26],** has studied the effect of magnetohydrodynamics on thin layers of unstable micropolar liquid through a porous medium. These thin films are considered for three different geometries. The governing differential equations are solved numerically using the Shooting Method. From the present study, Abdel-Rahman found that the rotation of the microparticles at the limit increases the speed with respect to the case where there is no rotation at the limit.

Thesis contribution and outlines

Consequently, we will limit our discussion on the transport phenomena (thermomechanics) involved in this type of flow as a function of the variation of certain physical parameters; our doctoral thesis has been divided into two parts.

First, we started with part one, which is presented by chapter one. This chapter represents a literature synthesis of current studies done on flows Newtonian fluids and non-Newtonian-micropolar in presence or in absence of magnetic field effect, This study provides a rich area of scientific of physical, energetic researchers and companies, whether in nature flows (ex. blood, sediment transport...) or industrial processes (stirring and mixing suspension, liquid-liquid extraction, solid-liquid separation, fermentation, fluidization, etc. ...) these are complex environments which are developing thermo-physical phenomena and interaction between a various suspended particles at micro/nano-scales. In order to have an approach between the various collected works and our study; we will analyze the work of researchers available in this area by giving some tables summarizing these studies.

The second part consists of three chapters devoted to the theoretical study of non-Newtonian micropolar fluids, their rheological behavior, and the laws and equations that govern the kinematics and dynamics of fluids of this type. The details in this part are as follows:

- In chapter two, we are focused on the definition of micropolar fluids by giving examples of this type of non-Newtonian fluids, in the other hand present rheological behavior of micropolar fluids. **Eringen [5]**, has formulated the micro-continuum micropolar theory, which has been used by many authors in a variety of physical conditions, **M. M. Rahman [27].** Micropolar fluids are non-Newtonian fluids with the internal structures in which the coupling between the rotational speed of each particle and the macroscopic velocity field is considered. Examples: The flows colloids and suspension of fine particles. The long chain polymer liquid crystals, blood, sparkling fluids (bright, colorful, etc.), **Y. A. Buyevich, [28]**. The microfleece theory is adopted to examine the effects of microstructure and microrotation on lubrication devices in the thin layer of lubricant. The micropolarity will result in an increase of the equivalent viscosity which later leads to improved lubrication, **Z. Chaohui, et al, [8].**
- After, in chapter three, we have presented a case of convective heat transfer phenomenon which was at one time a type of theoretically negligible flow but actually its impact on the boundary layer is experimental proved. This thermal phenomenon is called combined free and forced convection, In the treatment of forced convection, generally the effects of free convection are ignored, this was a hypothesis and this is evident when there is an unstable temperature gradient and the flow is convective free, presumably, by hypothesis, forced convection is supposed

negligible. It is time to note that, this situations will be different when the effects of forced and free convection are comparable, in which case it is inappropriate to neglect both processes. It has indicated that free convection is negligible if (Gr_L/Re_{2L}) and that forced convection is negligible if (Gr/Re^2) << 1. Hence the mixed convection regime is generally one for which (Gr/Re^2) ≈1. The effect of buoyancy on heat transfer in a forced flow is strongly influenced by the direction of the buoyancy force relative to that of the flow, **Theodore L. Bergman, et al, [29]**. So the effect of buoyancy is to alter the velocity and temperature fields in the forced convection flow, and this in turn alters the Nusselt number and friction coefficient. Consider the case of upward forced convection over a vertical surface, thus in vertical tube in both cases, external and internal flow. If the temperature wall is up then the fluid temperature (T_w>T), the resulting buoyancy force support the convection flow, especially in close to wall-region, **W. M. Kays, et al, [30]**. The free convection may be significant, however, when low-velocity fluids flow over heated (or cooled) surfaces. A measure of the influence of free convection is provided by the ratio, **D. R. Pitts, [31]**.

- Then, in chapter four, we have presented in firsthand, the basic formulation of viscous fluid equations of mechanics, as well as the equations of the continuity, the continuum, and the energy. Moreover, we have added another type of equations which describe a micro-continuum and magnetic field effects. In result, we will find together that the classical form of Navier-Stokes equations cannot describe certain types of flows, such as micropolar fluid motions, **Eringen, [3-4], Buyevich, [28]**. This is applied in many fields, especially in engineering, which are clearly indicates the far-reaching applications of polar fluid-mechanics knowledge and their importance in various fields of engineering, whereas, it necessary to carry out a special fluid mechanics considerations for each of the areas listed below. The objective of the derivations in this section is to formulate the conservation laws for mass, momentum, energy, in such a way that they can be applied to all these cases of flow problems.

Finally, the third part, consist of two chapters involved the physical model to be studied, the mathematical formulation and the analytical and numerical solutions of this model. These both chapters are as follow.

- In chapter five, we have presented an analytical and numerical study of a convective flow model of MHD micropolar and viscous fluids in a vertical

channel, in this work we have considered two incompressible and immiscible fluids in different regions, first region is occupied by non-Newtonian micropolar fluid and the second region is occupied by Newtonian-viscous fluid. The channel is subjected to the influence of a transverse magnetic field and temperature gradient. To provide an understanding of the complexity of this type of flow, a mathematical model is considered take into account the magnetic diffusivity term in equation of the energy balance, the model is investigated and allows appearance to certain dimensionless parameters such as a material parameter (K), Prandtl number (Pr), a mixed convection parameter defined by the Grashof number and Reynolds number (GR) ratio, a magnetic parameter called a Hartmann number (Ha) and Eckert number (Ec), as well as dimensionless ratios such us the widths ratio of fluids (H); the thermal conductivity ratio (k*); the thermal expansion coefficients ratio (β*); the viscosities ratio (μ*) and the ratio of the densities (ρ*). The final results of the mathematical model are used to deduce the effect of the magnetic field on the variation of the linear velocities (axial), the microrotation velocity field and temperatures field -transfer heat - so these results are subject to a comparative discussion in the conclusion between our numerical model study taking into account the term of the magnetic diffusivity with another models studied analytically with or without magnetic effect.

- In chapter six, we found two means of figures, curves obtained from analytical solution using Microsoft Excel for the model without magnetic field effect. Thus a numerical solution is done for the model with a magnetic field effect by computing "Matlab". The obtained figures show us dimensionless linear velocities and dimensionless microrotation velocity into both regions of a channel. So the structure of the flow is represented by dimensionless velocities $u_1, u_2\ et\ N$.

Part I

Chapter 1

Literature review

1.1. Introduction

This chapter represents a literature synthesis of current studies done on flows Newtonian fluids and non-Newtonian-micropolar in presence or in absence of magnetic field effect, This study provides a rich area of scientific of physical, energetic researchers and companies, whether in nature flows (ex. blood, sediment transport...) or industrial processes (stirring and mixing suspension, liquid-liquid extraction, solid-liquid separation, fermentation, fluidization, etc. ...) these are complex environments which are developing thermo-physical phenomena and interaction between a various suspended particles at micro/nano-scales. In order to have an approach between the various collected works and our study, we will analyze the work of researchers available in this area by giving some tables summarizing these studies.

1.2. Convective flows without magnetic field effect

1.2.1. With porous medium

In 2004, the researcher's team: **Zhang Chaohui and all**, have studied the effects of microstructure and micro-rotation lubrication devices in the boundary layer lubrication. They analyzed the lubricating properties where the film thickness approaches to nano scale, to design reliable lubrication systems. They noted that the movement is affected by the viscous share, the effect of shear couples and direct connection to the microstructure velocity field. As result the micro-polarity increase in equivalent viscosity which later leads to better lubrication. They have concluded that the theory of micro-polarity is used to investigate execution of lubrication fluids in thin layers (boundary layer). The effects of microstructure and micro-rotation are combined into the viscosity modification of the formula (the formula Hamrock and Dowson), the main property distinguished of lubrication with micropolar fluids is the effect of particle size (the dimensions of the particle with respect to the thickness of the lubricant thin layer), they said that the thinner fluid film is the more anomaly to the lubrication phenomenon (non-polar case) **[8]**.

In 2005, **Chun-I Chen** have studied a linear and non-linear stability analysis for characterization of micropolar film flowing down the inner surface of a rotating infinite vertical cylinder is given. A generalized non-linear kinematic model is derived to represent the physical system and is solved by the long wave perturbation method in the following

procedure. First, the normal mode method is used to characterize the linear behaviors. Then, an elaborated non-linear film flow model is solved by using the method of multiple scales to characterize flow behaviors at various states of sub-critical stability, sub-critical instability, supercritical stability, and supercritical explosion. The modeling results indicate that by increasing the rotation speed, X, and the radius of cylinder, R, the film flow will generally stabilize the flow system **[32].**

In 2009, **M. M. Rahman**, have studied a free-forced convective laminar in two-dimensional flow and heat transfer of micropolar fluids past a vertical radiate isothermal permeable surface with viscous dissipation and Joule heating is investigated numerically. The local similarity solutions for the flow, microrotation (angular velocity) and heat transfer characteristics are illustrated graphically for various material parameters. The effects of the pertinent parameters on the local skin friction coefficient, plate couple stress and the rate of heat transfer are also calculated. It was shown that micropolar fluids presented lower viscous drag and heat transfer values than those of the Newtonian fluids. The effect of radiation on the rate of heat transfer in a weakly concentrated micropolar fluid is higher than a strongly concentrated micropolar fluid. Results also show that full radiation has significant effect on the rate of heat transfer compared to the linear radiation **[27].**

1.2.2. Without porous medium

In 1998, **M. A. Hossain, and M. K. Chowdhury** have studied a steady two-dimensional mixed convection flow of viscous incompressible micropolar fluid past an isothermal horizontal heated plate with uniform free stream and variable spin-gradient viscosity is considered. With appropriate transformations the boundary layer equations are transformed into non-similar equations appropriate for three distinct regimes, namely, the forced convection regime, the free convection regime and the mixed convection regime. Solutions of the governing equations for these regimes are obtained by an implicit finite difference scheme developed for the present problem. Results are obtained for the pertinent parameters, such as the buoyancy parameter, ~ in the range of 0 to 10 and the vortex viscosity parameters, A = 0.0, 1.0, 3.0, 5.0 and 10.0 for fluid with Prandtl number Pr - 0.7 and are presented in terms of local shear-stress and the local rate of heat transfer. Effects of these parameters are also shown graphically on the velocity, temperature and the couple stress distributions. From the present analysis, it is observed that both the momentum boundary layer and the thermal boundary layer increase due to an increase in the vortex viscosity of the fluid **[33]**.

In 1988, **S. P. Singh, et al**, are studied numerically a physical model similar as the human joints. They introduced a continuously varying porosity mode for lower plate instead of usual uniform mono or multi-layered models, taking within a micropolar fluid film is taken as a lubricant, by suitable choice of non-dimensional porosity variation parameter, they analyzed the variation of pressure and load capacity with reference. As result as, trends of variations are fairly in agreement with those recorded in earlier investigations. They conclude that the decrease in $L=\beta_0/l$ (the initial film thickness of fluid/the width of cartilage), provoke an increase of the effective viscosity, but the axial pressure decrease, in the other hand, when the porosity in the interface, cartilage-fluid, increases the pressure decreases, which causes the increase in velocity in the porous media, while in the case of non-porous cartilage pressure is maximum **[34].**

In 2006, **Y. Y. Lok , et al**, are studies the unsteady mixed convection boundary-layer flow of a micropolar fluid near the region of the stagnation point on a double infinite vertical flat plate is studied. It is assumed that the unsteadiness is caused by the impulsive motion of the free stream velocity and by sudden increase or sudden decrease in the surface temperature from the uniform ambient temperature. The problem is reduced to a system of non-dimensional partial differential equations, which is solved numerically using the Keller-Box Method (KBM). This method may present well-behaved solutions for the transient (small time) solution and those of the steady-state flow (large time) solution. It was found that there is a smooth transition from the small-time solution (initial unsteady-state flow) to the large-time solution (final steady-state flow). Furthermore, it is shown that for both, assisting and opposing cases, and fixed value of the Prandtl number, the reduced steady-state skin friction and the steady-state heat transfer from the wall (or Nusselt number) decrease with the increase of the material parameter. On the other hand, it is shown that with the increase of the Prandtl number and a fixed value of the material parameter, the reduced steady-state skin friction decreases when the flow is assisting and it increases when the flow is opposing **[35].**

In the work done in 2008, **C. Y. Cheng**, has analyzed the boundary-layer of natural convection heat transfer near a vertical truncated cone with power-law variation in surface temperature in a micropolar fluid. In this, a transformed boundary layer governing equations are solved by the Cubic Spline Collocation Method (CSCM). Results for local

Nusselt numbers are presented as functions of vortex viscosity parameter, the surface temperature exponent, and the Prandtl number. The heat transfer rates of the truncated cones with higher surface temperature exponents are higher than those with lower surface temperature exponents. Moreover, the heat transfer rate from a vertical truncated cone in Newtonian fluids is higher than that in micropolar fluids. Cheng has concluded that the Increase in the parameter of the swirling viscosity micropolar fluid has a tendency to retard the flow and reduces the heat transfer rate. Moreover, the temperature increase of lateral surface of the cone promotes the increase of the buoyant force and thus leads to increase the heat transfer rate, **[36].**

In 2009, **J. P. Kumar, et al**, have studied fully-developed laminar free-convection flow in a vertical channel, and the analytical solution is given, the channel consist of two immiscible fluid regions, one region is filled with micropolar fluid and the other region is filled with viscous fluid. Using the boundary and interface conditions proposed by previous investigators, analytical expressions for linear velocity, micro-rotation velocity and temperature have been obtained. Numerical results are presented graphically for the distribution of velocity, micro-rotation velocity and temperature fields for varying physical parameters such as the ratio of Grashof number to Reynolds number, viscosity ratio, width ratio, conductivity ratio and micropolar fluid material parameter. It is found that the effect of the micropolar fluid material parameter suppress the velocity whereas it enhances the micro-rotation velocity. The effect of the ratio of Grashof number to Reynolds number is found to enhance both thelinear velocity and the micro-rotation velocity. The effects of the width ratio and the conductivity ratio are found to enhance the temperature distribution. **[9]**.

In 2016, **J. Raza, et al**, have studied numerically in order to investigate a multiple solutions of micropolar fluid in a channel with changing walls. Mathematical modeling of laws of conservation of mass, momentum, angular momentum and energy is performed and governing partial differential equations are converted into self-similar ordinary differential equations by applying suitable similarity transformation and then solved numerically by *shooting method.* A new branch of solutions is found and presented in graphically and numerically for the various values of parameters, which this method has never been reported, **[37]**.

In 2009, **Md. A. Ikbal, et al**, have did a theoretical investigation of atherosclerotic arteries deals with mathematical models that represent non-Newtonian flow of blood

through a stenosed artery in the presence of a transverse magnetic field. They conclude that the magnetic field causes substantial reduction of the flow rate. The form of magnetic field gradient plays an important role and substantially determines the flow field, [38].

In 2009, **V. P. Srivastava et al**, have studied a problem of blood flow in a narrow catheterized artery, using two-phase macroscopic model of blood (i.e., red cells suspended in plasma). It is found that the effective viscosity and the frictional resistance increase with hematocrit. Flow characteristics assume lower magnitudes in catheterized artery as compared to uncatheterized artery for any given set of parameters. Numerical results reveal that the effective viscosity and the increased frictional resistance assume their minimal magnitude and consequently the volumetric flow rate assumes its maximal magnitude during the artery catheterization at the catheter size approximately fifty percent of the artery size **[39].**

In 2007, **F. Shahzad, et al**, have studied the time-independent equations for the two dimensional incompressible micropolar fluid. They have used the Lie Group Analysis Method (LGAM) to reduce the governing complex differential equations of a micropolar fluid flow to ordinary differential equations which have solved analytically. Finally the boundary value problem has been discussed, and the graphical results are in good agreement with the numerical solution. The group of researchers has concluded that the magnetic parameter holds the angular velocity. But the velocity components decrease in reference of magnetic parameter. They also conclude that the behavior of magnetic parameter is opposite on the angular velocity than on linear velocities **[40]**.

1.3. Convective flows with magnetic field effect

1.3.1. With porous medium

In 2001, **Y. J. Kim** has studied two-dimensional laminar flow of a viscous incompressible electrically conducting fluid in the vicinity of a semi-infinite vertical porous moving plate in the presence of a transverse magnetic field, the plate moves with constant velocity in same direction with fluid flow, and the free stream velocity follows the exponentially increasing small perturbation law. A uniform magnetic field acts perpendicular to the porous surface which absorbs the fluid with a suction velocity varying with time. The effects of material parameters on the velocity and temperature fields across the boundary layer are investigated. Numerical results show that for a constant plate moving velocity with a given magnetic and permeability parameters, and

Prandtl and Grashof numbers, the effect of increasing values of suction velocity parameter results in a slight increasing surface skin friction for lower values of plate moving velocity. It is also observed that for several values of Prandtl number, the surface heat transfer decreases by increasing the magnitude of suction velocity **[10].**

In 2010, a paper entitled fully developed electrically conducting micropolar fluid flow and heat transfer along a semi-infinite vertical porous moving plate is studied by **R. Sharma et al**, including the effect of viscous heating and in the presence of a transverse magnetic field in the flow direction. They have conclude that the velocity increases with the increase of plate velocity or Darcy number but it decreases as each of magnetic parameter value, Forchhimer number and the micropolar parameter increases. The temperature decrease as heat absorption coefficient increases, but it increases as each of plate velocity, Forchhimer number and the micropolar parameter increases. The skin friction coefficient decreases as exponential index n* increases, while it increases with the increase of the magnetic parameter. The Nusselt number is increased due to the magnetic parameter and exponential index n*. The magnetic field can be used effectively for controlling the rate of heat transfer as required in MHD applications like MHD generators, nuclear reactor, where it is required to control the enormous temperature **[41].**

In 2013, a problem under title, A magnetohydrodynamic (MHD) flow of a viscous fluid on a nonlinear porous shrinking sheet is studied by **F. Md Ali et al**. They have used the Shooting Method (SM), this method is used to solve numerically the boundary layer partial differential equations. They are found that dual solutions only exist for positive values of the controlling parameter, it can conclude that the controlling parameter accelerated the boundary layer separation; however, the magnetic parameter delayed the boundary layer separation **[42]**.

In 2015, **Z. Abbas, et al**, have studied the analysis of a second-grade fluid in a semi-porous channel in the presence of a chemical reaction is carried out to study the effects of mass transfer and magnetohydrodynamics. The upper wall of the channel is porous, while the lower wall is impermeable. The basic governing flow equations are transformed into a set of nonlinear ordinary differential equations by means of a similarity transformation. An approximate analytical solution of nonlinear differential equations is constructed by using the homotopy analysis method. The features of the flow and concentration fields are analyzed for various problem parameters. Numerical values of the skin friction coefficient and the rate of mass transfer at the wall are found. In this study, they have concluded that

the mass transfer analysis on the laminar flow of an MHD second-grade fluid in the presence of a chemical reaction is discussed. A set of nonlinear ordinary differential equations is solved by the homotopy analysis method to obtain an approximate analytical solution. The physical effects of various involved parameters on the flow and concentration fields are analyzed. The following observations are made in this study: with an increase in the Reynolds number Re, the shear stress increases; the fluid velocity at the center of the channel decreases with an increase in M; the concentration increases with increasing K and decreases with increasing Re; finally, the rate of mass transfer at the wall decreases as the values of Sc and γincrease **[43].**

In 2008, the application of Lie group analysis method is investigated by **S. M. M. EL-Kabeir et al**, for solving the problem of heat transfer in an unsteady, three-dimensional, laminar, boundary layer flow of a viscous, incompressible and electrically conducting fluid over inclined permeable surface embedded in porous medium in the presence of a uniform magnetic field and heat generation/absorption effects. They have concluded that the unsteady three-dimensional laminar boundary-layer flow of a viscous, incompressible and electrically conducting fluid over an inclined permeable surface embedded in porous medium in the presence of a uniform magnetic field and heat generation/absorption effects are treated. Using Lie group method, we have presented the transformation groups for the problem, apart from the scaling group; the system admits a group of translations, as well, concerning thegroup of scaling and the associated self-similar solutions. Moreover, due to the generality of our procedure and the lackof unnecessary assumptions, we have obtained the general form of the functions involved in the boundary conditions. Finally, the application of three-independent-variable partial differential equations transformed to two-independent variable system by using one subgroup of the general group. The resulting system of governing equations is solved numerically using perturbation technique for various values of physical parameters **[44]**.

In 2012, **N. T. M. Eldabe, et al**, have studied the problem of free convection heat with mass transfer for MHD non-Newtonian Eyring–Powell flow through a porous medium, over an infinite vertical plate is studied taking into account the effects of both viscous dissipation and heat source. They have concluded that as the non-Newtonian and magnetic parameters increase, the value of the velocity decreases. This conclusion meets the logic of the magnetic field exerting a retarding force on the free convection flow **[45]**.

A problem of a theoretical study of unsteady magnetohydrodynamic viscous Hartmann–Couette laminar flow and heat transfer in a Darcian porous medium intercalated between parallel plates, under a constant pressure gradient is presented. Viscous dissipation, Joule heating, Hall current and ionslip current effects are included as is lateral mass flux at both plates is investigated by **O. A. Bèg et al**. (2009). They have used a computational technique known as Network Simulation Methodology (NSM) to examine graphically the velocity distributions (u*,w*) and temperature distribution (T*) at the channel centre (y* = 0) over time (t*) for the effects of multiple dimensionless numbers as Darcy (Da), Hartmann (Ha), etc…, with Prandtl number prescribed at 7.0 (electrically conducting water), Eckert number held constant at 0.25 (heat convection from the plates to the fluid) and Reynolds number (Re) fixed at 5.0 (for Re < 10, Darcian model is generally valid). They observed that increasing Darcy number causes an increase in temperature, T*; values are however significantly reduced for the higher Hartmann number case (Ha = 10). For the case of low transpiration (it corresponds to weak suction at the upper plate and weak injection at the lower plate), both primary velocity (u*) and secondary velocity (w*) are increased with a rise in Darcy number (owing to a simultaneous decrease in Darcian porous drag); temperature T* is also increased considerably with increasing Da. However, temperature, T* is strongly increased with a rise in pressure gradient parameter, dP*/dx*, as is primary velocity (u*); however, secondary velocity (w*) is reduced **[46]**.

A problem of two dimensional unsteady laminar boundary-layer flow of a viscous, incompressible, electrically conducting and heat-absorbing fluid along a semi-infinite vertical permeable moving plate with a uniform transverse magnetic field in presence of radiation, chemical reaction, soret effect and thermal diffusion effects, is investigated by **B. Madhusudhana Rao et al**. they have observed that when the Thermal Grashof number and Mass Grashof number increased, the fluid velocity increased. The presence of heat source effects and radiation effects caused the reductions in the fluid temperature which resulted in decreasing in the fluid velocity. Also, when Schmidt number was increased, the concentration was decreased, this resulted in decreasing in the fluid velocity **[47]**.

A numerical study is carried out for the axisymmetric steady laminar incompressible flow of an electrically conducting micropolar fluid between two infinite parallel porous disks with the constant uniform injection through the surface of the disks. This problem was treated by **ASHRAF and WEHGAL**. They observed that the heat transfer rate at the surfaces of the disks increases with the increases in the Reynolds number, the magnetic parameter,

and the Prandtl number. The shear stresses decrease with the increase in the injection while increase with the increase in the applied magnetic field. The shear stress factor is lower for micropolar fluids than for Newtonian fluids, which may be beneficial in the flow and thermal control in the polymeric processing [48].

1.3.2. Without porous medium

In 2008, **A. Ishak, et al**, had studied a steady MHD mixed convection stagnation point flow towards a vertical surface Immersed in a incompressible micropolar fluid. The external velocity impinge normal to the wall and the wall temperature is assumed to vary linearly with the distance from the stagnation point. The governing partial differential equations are transformed into a system of ordinary differential equations, which is then solved numerically by a finite-difference method. The features of the flow and heat transfer characteristics for different values of the governing parameters are analyzed and discussed. Both assisting and opposing flows are considered. It is found that dual solutions exist for the assisting flow, be sides that usually reported in the literature for the opposing flow [7].

In 2015, **Y. Liu et al**, have studied an alternating current (AC) Magnetohydrodynamic (MHD) electro-osmotic flow of incompressible Maxwell fluids between micro-parallel plates. They are investigated by using the separation variables method. Fluids were driven under the Lorentz force produced by the interaction of a vertical magnetic field and two horizontal electrical fields. The solution involves analytically solving the linearized Poisson–Boltzmann equation, the Navies–Stokes equation and the constitutive equation of Maxwell fluids. They are conclude that at low values of Hartmann number (Ha) the magnitude of velocity decreases with Ha when the transverse electric field disappeared (S=0) due to the opposing magnetic force. However, the magnitude velocity increases with Ha when the transverse electric field appears (S = 10) and the aiding magnetic force exceeds the opposing magnetic force. At high values of Hartmann number Ha, the magnitude of steady velocity decreases with Ha because Ha beyond a critical value, the retarding force is dominant over the driving force [49].

In 2015, a problem of magnetohydrodynamic flow of Jeffrey fluid through a circular micro-channel is treated by **Chonghua et al,** they have used the variable separation method, the analytical solutions to both DC-operated MHD and AC-operated MHD micro-pumps are found. The flow is assumed to be laminar, unidirectional, one dimensional and driven by the Lorentz force. The Lorentz force can be taken as hydrostatic pressure gradient in the

momentum equation of the MHD micro-channel flow model. The effects of Hartmann number Ha, dimensionless relaxation time λ_1 and retardation time λ_2 on the velocity and volumetric flow rate are investigated. The velocity and volumetric flow rate grow and then reduce with Hartmann number Ha. There is a critical value of the Ha for MHD velocity and an optimum Ha for maximum volumetric flow rate. In addition, a comparison with previous works is also provided to confirm the validity of the present results **[50]**.

In 1996, **A. A. Mohammadein et al**, have studied the effects of magnetic field with vectored surface mass transfer and induced buoyancy stream-wise pressure gradients on heat transfer to a horizontal plate placed in a micropolar fluid, they have used boundary layer equations for the mixed convection flow over a semi-infinite horizontal plate with vectored mass transfer in a transverse magnetic field. The mathematical model obtained is solved numerically in aim to obtain the mass transfer, the buoyancy, and material parameters for different values of the magnetic parameter. A discussion is provided for the effects of the transverse magnetic field on micropolar fluid behavior. The results indicate that micropolar fluids display a reduction in drag as well as heat transfer rate when compared with the Newtonian fluids. The transverse magnetic field is observed to reduce the overall heat transfer to the surface **[51]**.

In 2016, **Z. Y. Huang, et al,** have studied numerically the characteristics of laminar MHD fluid hammer. A non-dimensional fluid hammer model, based on Navier–Stocks equations, coupling with Lorentz force is numerically solved in a reservoir–pipe–valve system with uniform external magnetic field. The MHD effect is represented by the interaction number which associates with the conductivity of the MHD fluid as well as the external magnetic field and can be interpreted as the ratio of Lorentz force to Joukowsky force. The transient numerical results of pressure head, average velocity, wall shear stress, velocity profiles, and shear stress profiles are provided. The additional MHD effect hinders fluid motion, weakens wave front and homogenizes velocity profiles, contributing to obvious attenuation of oscillation, strengthened line packing and weakened Richardson annular effect. Studying the characteristics of MHD laminar fluid hammer theoretically supplements the gap of knowledge of rapid-transient MHD flow and technically provides beneficial information for MHD pipeline system designers to better devise MHD systems. As a result phenomena made by MHD effects, a high initial pressure gradient is required to drive the MHD fluid in order to achieve a specific Reynolds number. Another conclusion is that a homogeneous initial velocity profile of Newtonian fluid, which can be induced by magnetic

field, tends to induce large line packing because it has better ability to resist velocity reversal near the pipe wall. Some extreme cases where very large strength of external magnetic field or conductivity of MHD fluid is required are also studied. Line packing keeps intensifying and finally takes the place of wave oscillation while Richardson annular effect gets weak and finally is thoroughly eliminated. The MHD effects to homogenize velocity profile and to attenuate the wave front are increasingly intensive when the interaction number is larger so that the velocity profiles can stay uniformity as far as possible during transient process. So in an extreme case of laminar MHD fluid hammer, no wave oscillation or Richardson annular effect but line packing and relatively homogenous velocity profile exist **[52].**

In 2016, **Ruchika Dhanai, et al**, have studied a various applications of nanofluids, by the numerical investigation of multiple solutions in MHD boundary layer flow and heat transfer of power-law nanofluid past a permeable nonlinear shrinking sheet with heat source/sink. They concluded that the rate of heat transfer at the surface decreases for increasing value of Eckert number but heat transfer rate increases with increasing of Prandtl number **[53]**.

In 2012, **M. Turkyilmazoglu**, has investigated the problem of magnetohydrodynamic slip flow of an electrically conducting, non-Newtonian fluid past a shrinking sheet is of concern of the present paper. The physical pure exponential type solutions are targeted to investigate whether they are unique or multiple under the influence of slip flow conditions. He has observe that the physical parameters as magnetic parameter, has an effect as well as unique or multiple slip flow solutions. In the presence of a magnetic field has also substantial effects on velocity and temperature fields, **[54]**.

In 2015, **Hari R. Kataria et al**, have studied theoretically the boundary layer flow of an incompressible micropolar fluid under uniform magnetic field and motion takes place due to the buoyancy force between vertical walls. They concluded that the velocity of the fluid decreases with increasing Prandtl number. The velocity amplitude as well as the boundary layer thickness decreases when magnetic parameter increased. Magnitude of the micro-rotation has an increasing tendency with the material parameter and vortex viscosity decreases with increase in Prandtl number. The steady state time of fluid velocity as well as microrotation is more for symmetric cases compared to asymmetric cases. The velocity and micro-rotation fluid profiles decrease at any point of fluid regime with magnetic parameter. The velocity decreases and micro rotation profile of fluid increases at any point of fluid

regime with vortex viscosity parameter. The steady state time of velocity profile and micro-rotation have a decreasing tendency with material parameter [55].

In 2015, **M. M. Rashidi, et al**, have studied and analyzed the convective flow of a third grade non-Newtonian fluid due to a linearly stretching sheet subject to a magnetic field, they have also studied in detail the entropy generation. They have used, in solving the governing equations analytically by means, the Optimal Homotopy Analysis Method (OHAM), they have concluded that the effect of various parameters on the velocity and temperature, such as the magnetic parameter and Prandtl number are investigated. In addition, the dependence of the entropy generation number on the magnetic parameter, Prandtl, Reynolds, Hartmann numbers and the dimensionless temperature difference is investigated. From the obtained results it can note the following: Brownian motion plays an important role to improve thermal conductivity of the fluid. The thermal boundary-layer thickness gets decreased with increasing magnitude of the Prandtl number. Effect of the magnetic field on the fluid flow and temperature distribution is important. By increasing the magnitude of the magnetic parameter, the entropy generation function increases [56].

In 2015, **Neela Rani, et al**, have studied the onset of instability in a layer of dielectric micropolar fluid under the simultaneous action of – an AC – electric field and temperature gradient has been investigated. In summary, they concluded that the role of electric field is to destabilize the convection in the fluid layer in the case of stability motions only for negative values of electric Rayleigh number. They have also noted that the role of micropolarity is to stabilize the convection in fluid layer in stability as well as in over-stability motions. As well as the role of Prandtl number is again to stabilize the fluid layer in the case of over-stability only. In case of stability, in end they observed that the expression of thermal Rayleigh number is independent of Prandtl number and hence Prandtl number has no role to play [57].

In 2016, **Madhu, and Kishan** have studied numerically the Magnetohydrodynamic mixed convection boundary layer flow of heat and mass transfer stagnation-point flow of a non-Newtonian power-law nanofluid towards a stretching surface in the presence of thermal radiation. They have concluded that the effect of magnetic field parameter reduces the velocity profiles, but the presence of the thermophoresis parameter increase the velocity, temperature and concentration profiles for both newtonian and non-Newtonian fluids. The Brownian motion number increases the temperature profiles and decreases the concentration profiles. The velocity and concentration profiles are increases with the

increase of radiation parameter for both Newtonian and non-Newtonian fluids. They have observed that the mixed convection parameter and velocity ratio parameter are to increase the velocity profiles and reduces the temperature and concentration profiles. Also, the skin friction co-efficient f(0) increases with the increase of thermophoresis parameter and it decreases with the increase of Brownian motion parameter and the power law index **[58]**.

In 2011, **B. S. Babu, et al**, have proposed a physical model to study. The model is as flows, a vertical channel divided into two regions one region is filled with Micropolar fluid and the other region is filled with viscous fluid. The channel is subjected to the transverse magnetic field. The coupled governing equations are solved numerically by using the regular Galerkin Finite Element Methode (GFEM). The results are compared with those computed by **Kumar et al**. It is found that the increase in the magnetic field reduces the micro-rotation (N) and velocity. Then, the increase in Eckert number provokes a decrease in the linear, and microrotation velocities **[59]**.

In 2015, **Cha'o-Kuang Chen, et al**, have studied numerically the heat transfer performance and entropy generation characteristics of a mixed convection magnetohydrodynamic flow of Al_2O_3–water nanofluid in a vertical asymmetrically-heated parallel-plate channel subject to viscous dissipation effects. In performing the analysis, the effects of the Lorentz force and Joule heating are modeled using the transverse momentum balance equation and energy balance equation, respectively. Moreover, the Hartmann number is assigned a value of Hm = 0 (no magnetic field) or Hm = 2 (weak magnetic field). The results show tha the presence of the magnetic field increases the local Nusselt number at the hot wall. Moreover, the enhancement in the heat transfer performance increases with an increasing nanoparticle concentration. Also, the local Nusselt number at the cold wall also increases with an increasing nanoparticle concentration. However, for a constant particle concentration, the Nusselt number reduces given the application of a magnetic field. Finally, the average entropy generation number also reduces when a magnetic field is applied **[60].**

In both investigated problems, first study is on two dimensional stagnation point flow of an electrically conducting micropolar fluid impinging normally on a heated surface in the presence of a uniform transverse magnetic field. The second one is on magnetohydrodynamics (MHD) flow and heat transfer characteristics of a viscous incompressible electrically conducting micropolar fluid in a channel with stretching walls. **M. ASHRAF, M. M. ASHRAF, N. JAMEEL, and K. ALI [61-62]**, had observed, in the first, that the study shows that the velocity and thermal boundary layers become thinner as the

magnetic parameter is increased. The micropolar fluids display more reduction in shear stress as well as heat transfer rate than that exhibited by Newtonian fluids, which is beneficial in the flow and thermal control of polymeric processing. Moreover, the second study may be involved beneficially in the flow and thermal control of polymeric processing.

In 2010, **M. Kumari, et al**, have studied the transient boundary layer flow and heat transfer of a viscous incompressible electrically conducting non-Newtonian power-law fluid in a stagnation region of a two-dimensional body in the presence of an applied magnetic field have been studied when the motion is induced impulsively from rest. The nonlinear partial differential equations governing the flow and heat transfer have been solved by the Homotopy Analysis Method (HAM), and by an implicit finite-difference scheme. For some cases, analytical or approximate solutions have also been obtained. The special interest is the effects of the power-law index, magnetic parameter and the generalized Prandtl number on the surface shear stress and heat transfer rate. In all cases, there is a smooth transition from the transient state to steady state. The shear stress and heat transfer rate at the surface are found to be significantly influenced by the power-law index N except for large time and they show opposite behavior for steady and unsteady flows. The magnetic field has strongly shear stress effect on the surface, but the heat transfer rate effect on the surface is comparatively weak except for a large time. On the other hand, the generalized Prandtl number exerts a strong influence on the surface heat transfer. Therefore, the skin friction coefficient decreases rapidly in a small interval from 0.0 – 0.1, **[63]**.

In 2013, **R. Ellahi**, in his paper, has examined the magnetohydrodynamic (MHD) flow of non-Newtonian nanofluid in a pipe in using analytical solution. The temperature of the pipe is assumed to be higher than the temperature of the fluid. In particular two temperature dependent viscosity models have been considered. It is observed that the MHD parameter decreases the fluid motion and the velocity profile is larger than that of temperature profile even in the presence of variable viscosities. They observed a strong dependence of the velocity and temperature on viscosity indexes **[64]**.

In 2016, **K. Tzirakis et al**, have steadied the problem of blood flow dynamics which have an integral role in the formation and evolution of cardiovascular diseases. Simulation of blood flow has been widely used in recent decades for better understanding the symptomatic spectrum of various diseases, in order to improve already existing or develop new therapeutic techniques. The mathematical model describing blood Rheology is an important component of computational hemodynamics. Blood as a multiphase system can

yield significant non-Newtonian effects thus the Newtonian assumption, usually adopted in the literature, is not always valid. To this end, they have conclude that the convergence rate, however, of the Newtoniteration was not significantly affected preserving the computational efficiency of the method. The ability of the method to accurately resolve 2D and 3D benchmark problems was demonstrated. The method is subsequently utilized to assess the effects of magnetic fields on biomagnetic fluid flow. To this end, the magnetization force generated by an externally applied magnetic field is added in the RHS of the momentum equations, resulting in considerable flow deviation, even for moderate field intensity. Magneto-viscous effects are also taken into account through the generated additive viscosity of the fluid and were found to be important. Applications of interest can be foreseen by exploiting magnetic fields for blood flow control, such as reduction of blood loss during surgery and targeted drug delivery **[65]**.

A problem of free convection MHD flow of micropolar and viscous fluids in a vertical channel with dissipative effects was investigated by **B. S. Babu et al.** to solve the governing differential equations, they had used the Finite Element Method (FEM), the obtained results were compared with those given by **J. P. Kumar and N. Kumar [9],[21]. Babu et al.** conclude that the increase in the magnetic field reduces the micro rotation (N) and velocity and enhances the temperature. Increase in the Eckert number (Ec), decreases the velocity, temperature and micro rotation. The Nusselt number and shear stress values are also analyzed **[66]**.

1.4. Problematic

The approach of many study papers presented by many researcher teams in different ways of scientific research areas of fluid flows such as, biological or industrial flows, in porous or without porous media and in absence or in presence of magnetic field, **J. P. Kumar et al, C. Y. Cheng, J. Raza et al, [9,36,37],** and many others researchers are worked on some different models in many ways, analytically and numerically, in aim to understand the behavior of non-Newtonian micropolar fluids flow in micro-scale, furthermore, to detect which dimensionless parameter, number or coefficients have a positive or a negative effect on microstructure, microinertia, and material parameter,…..etc, at each point into a fluid. In literature, I was involved by some studies which are focused on the research area of non-Newtonian micropolar fluids as well as it has been of great interest because the Navier–Stokes equations for Newtonian fluids cannot successfully describe the characteristics of fluid with suspended particles. There exist more than a few approaches to study the mechanics of fluids with a substructure. Some of these studies are paying attention on free convective flows of immiscible micropolar fluids in channel, for example, in 2009, **J. P. Kumar et al. [9]**, have proposed a model of free-convective flow in vertical channel, the flow is considered fully-developed, the channel was divided into two immiscible regions, one of them is filled with Micropolar fluid and the other is filled with viscous fluid, in first way, the coupled governing equations were solved analytically using the boundary and interface conditions proposed by previous investigators. In second way, in 2011, **B. S. Babu et al**, **[66],** have used the same physical model with the same boundary conditions, moreover, the channel was subjected to transverse magnetic field with dissipative effects, and the coupled governing equations are solved numerically by using a regular Galerkin Finite Element Method (GFEM). In 2012, **N. Kumar et al**. **[21]**, have used the same model as the researcher team refer in **[66]**, involve more change into channel, as well as, a porous medium was immerged in immiscible fluids. So, **J. P. Kumar and D. Gupta** had solved analytically the coupled governing equations. In observing studies referenced in **[9] & [21]**, we think that both ways of solutions are simplified terms of the thermal diffusivity and magnetic diffusivity in the energy conservation equation. We think that coupled Navier-Stokes equations had missed energy in both analytical solution. Also, in viewing the GFEM method used to find the solution of differential equations of fluid flow, We observed that our mathematical model can be studied numerically using the similarity method**.**

Part II

Chapter 2

Non-Newtonian micropolar fluids and Rheology

2.1. Introduction

In this chapter we presented in first hand definition of micropolar fluids by giving examples of this type of non-Newtonian fluids, in the other hand present rheological behavior of M.F. Eringen formulated the micro-continuum theory micropolar, which has been used by many authors in a variety of physical conditions, . Micropolar fluids are non-Newtonian fluids with the internal structures in which the coupling between the rotational speed of each particle and the macroscopic velocity field is considered, **M. M. Rahman** [27]. Examples: The flows colloids and suspension of fine particles. The long chain polymer, crystal liquids, blood, and sparkling fluids (bright, colorful, etc…) **Y. A. Buyevich** [28]. The micropolar fluids theory is adopted to examine the effects of microstructure and microrotation on lubrication devices in the thin layer of lubricant. The micropolarity will result in an increase of the equivalent viscosity which later leads to improved lubrication, **Z. Chaohui, et al,** [8].

2.2. Micropolar fluids

2.2.1. A flow of fine suspended particles

One gives some examples of the existence of this type of non-Newtonian fluids.

A. Fluids of suspended polymer particles

These fluids are considered as non-Newtonian solutions of low concentration of polymer, for example, latex particles molecules dissolved in water (Figure 2.7). **Nicodemo et al,** had observed that the addition of latex particles in a fluid sheared simply didn't have influence on the viscosity curve, [28].

B. Colloids

Colloidal fluids are fluids which contain similar fine particles contains glue or gelatin and which does not crystallize, wherein the Brownian forces and particle-particle interactions play an important role [28].

The internal forces can be divided into hydrodynamic forces that are responsible for migration, alignment or orientation of particles in the case of non-spherical particles and collapsed structure when it comes to rainfall and aggregates, these forces result in relative movements of suspended particles, Einstein confirmed were the only forces in the analyzes of the viscosity of a dilute suspension ball in a Newtonian fluid. [28].

Non-hydrodynamic internal forces consist Brownian forces responsible for internal movement and distribution of the particles they have the strength of physical and chemical

interactions that can affect the internal structure of colloidal particles in suspension. Brownian motion allows for low-range attractive forces to promote the flocculation of construction and training of low gel network. Not to say that the external forces such as due to an electric field can drastically modify the rheological properties of suspensions **[28]**. The table.2.1 summarizes the main forces acting the colloidal particles with some basic mathematical formulas to calculate the magnitude:

Table .2.1: The forces focus on colloid suspensions (Adapted by **Russel et al**). **[28]**.

Force	**the magnitude**	**Definition**
Brownian	$F_B = \frac{kT}{d_p}$ (2.1)	k: Boltzmann's constant T: temperature [K] dp: particle diameter
Van Der Waals	$F_{Vd} = \frac{A}{d_p}$ (2.2)	A: constant Hamaker
Viscous	$F_{Vs} = \eta d_p^2 U = \eta d_p \dot{\gamma}$ (2.3)	η: viscosity on particle
Inertia	$F_{In} = d_p^2 \rho_p U^2$ (2.4)	U: relative speed of particle
Gravitational	$F_{gr} = d_p^2 \Delta \rho g$ (2.5)	Δ ρ: difference between fluid density and particle

C. Bloods

The flows of the blood are considered fluids deformable vesicle suspension of non-Newtonian character, its behavior in motion is as a shear thinning fluid and its viscosity decreases when the shear rate (velocity gradient) increases noted in references **[1-6]**, see the example given by **N. Midoux** and **D. Quemada**, **[67-68]**. (figure2.1).

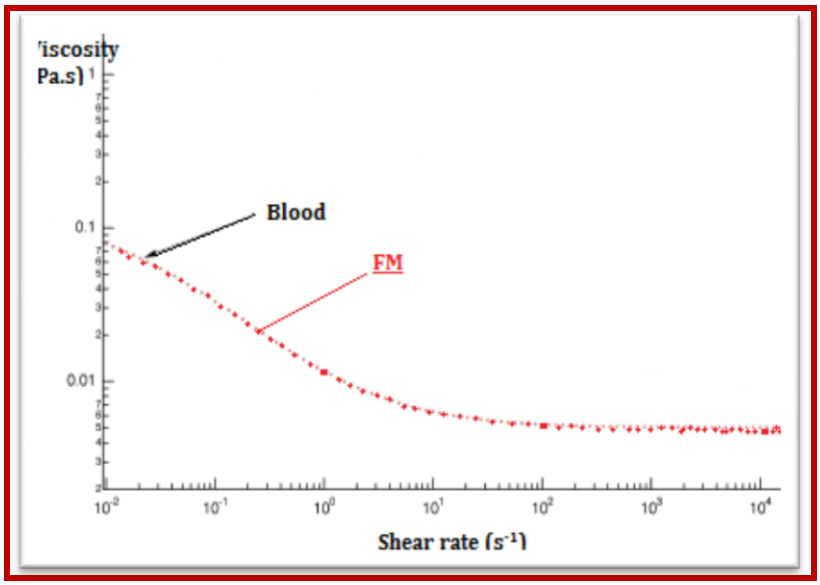

Figure 2.1: Viscosity versus shear rate for the blood, **[38]**.

D. Synovial fluid or human joint liquid

About a rheological behavior studies of synovial fluid, we can sited for examples the study of Ogston and Stanier, they have brought out the visco-elastic character behavior while Dowson and Mow noted that the human joints liquid have the same rheological behavior as a lubricant, Jones agree too, Dintenfass found that synovial fluid is non-Newtonian due to the presence of molecules of byaluronique acid (long chain polymer), and its viscosity decreases with the increase of shear rate, this view was experimentally supported by Bloch and Dintenfass, Maroudas and Dowson. **S. P. Singh, et al**, **[34]**.

E. Liquid Crystals

There exist a large number of organic compounds that exhibit simultaneously solid and liquid behavior, at the same time they flow like fluids. These substances are called liquid crystals. Liquid crystals are constituted of rod-like, disk-like, or arbitrary-shaped molecules in a fluent environment. There are many different types of liquid crystals. Liquid crystals, that possess rod-like molecules, are divided into two classes: nematic and smectic (Figure.2.2) **[1]**.

- In nematic liquid crystals, the mass centers of the molecules are distributed randomly in three dimensions.
- In smectics, they are arranged in equidistant planes.

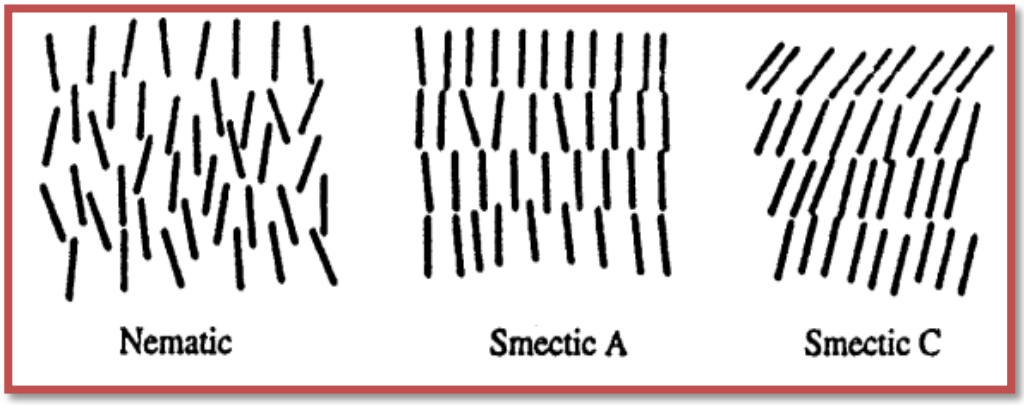

Figure 1.2: Nematic and smectic liquid crystals **[1]**.

When the rod-like elements of nematics are organized into adjacent planes, slightly rotated forming a helical structure is called *cholesteric* or chiralnematic phase (Figure.2.3). Cholesterics exhibit birefringence and optical activity. It can cite an other types of liquid crystals, the polymeric which molecules consist of rigid bars attached to each other by

flexible chains or by a single long flexible fiber with attached bars as side chains (Figure2.4), polymeric liquid crystals can be in nematic, chiralnematic, or smectic orders [1].

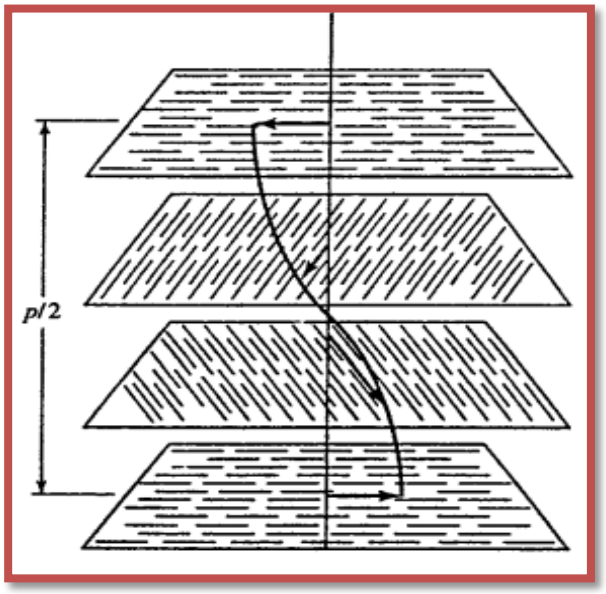

Figure 2.3: Cholesteric phase [1].

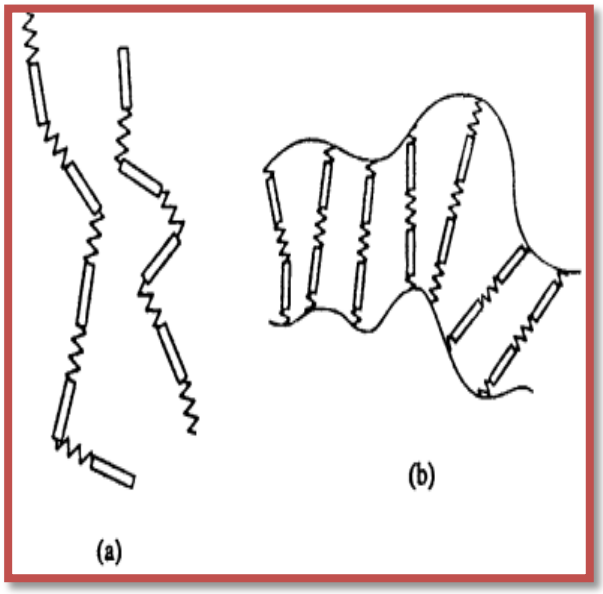

Figure 2.4: Liquid crystalline polymers; (a) main chain, (b) side chain [1].

A different class of liquid crystals has biologically important molecules, such as, phospholipids, called Amphiphilic molecules, which are either water seeking or water repelling (Figure2.5).

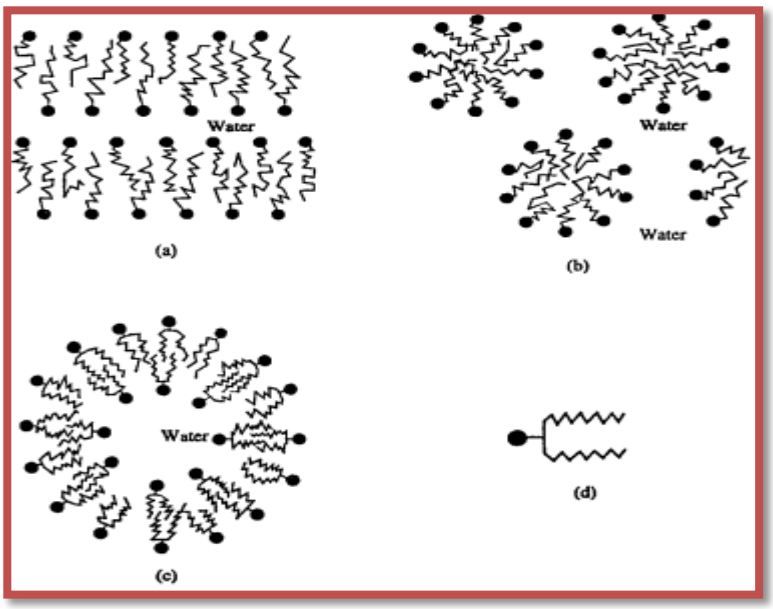

Figure 2.5: Amphiphilic molecules: (a) soap molecules; (b) micelle; (c) vesicle; (d) phospholipid molecule [1].

2.2.2. Some rheological models of micropolar fluids

In the literature, there are several models that explain the rheological behavior of non-Newtonian micropolar fluids because their rheological behavior is independent of time and included in the category of pseudo-plastic (shear thinning) fluids **[28]**.

A. Carreau and modified Carreau models

One can distinguish this type of fluids; low concentration polymer melt model is proposed (Table 2.2), for high concentrations of solids, or low viscosity matrices, interactions particle per particle can become significant, as for polystyrene melts filled with black coal, Titanium dioxide and calcium carbonate. Poslinski and others proposed a Carreau model changed **[28].**

Table 2.2: Rheological laws of micropolar fluid shear-thinning not present a critical stress**. N. Midoux, D. Quemada and H. A. Barnes [67-68] & [74]**.

Model	**Rheological laws**	**Parameters** n < 1
Ostwald De Waele	$\tau = k.\dot{\gamma}^{n}$ (2.6)	n, k: parameter and consistency index, respectively.
Ostwald De Waele	$\mu = m.\dot{\gamma}^{n-1}$ (2.7)	m : is parameter, mischaracterized behavior at low shear rates.
Carreau	$\tau = \left[\mu_{\infty} + (\mu_0 - \mu_{\infty})[1 + (\lambda.\dot{\gamma})^2]^{\frac{n-1}{2}}\right].\dot{\gamma}$ (2.8)	$\mu_0, \mu_{\infty}, \lambda$ n : structure index
Cross	$\tau = \left[\mu_{\infty} + \frac{\mu_0 - \mu_{\infty}}{1+(\dot{\gamma}.t_1)^p}\right].\dot{\gamma}$ (2.9)	μ_{∞} : presents the viscosity at very high shear rate.
Ellis	$\tau = \left[\frac{\mu_0}{1+\left(\frac{\tau}{\tau_{1/2}}\right)^{\alpha-1}}\right].\dot{\gamma}$ (2.10)	$\mu_0, \tau_{1/2}, \alpha$ $\tau_{1/2}$: Presents half of the applied shear stress.

$$\mu = \frac{\sigma_0}{\dot{\gamma}} + \frac{\mu_0}{(1+(t_1\dot{\gamma})^2)^{(1-n)/2}} \quad (2.11)$$

With, $\sigma_0 = G_0 \times \gamma_0$ & G_0 is the modulus of elasticity, with: $\sigma_0 < |\sigma|$ & $\dot{\gamma}_0 \geq |\dot{\gamma}|$, μ_0 zero-viscosity, and the characteristic time (t_1) are described by Maron Pierce, giving the following expressions [28].

$$t_1 = t_{1m} \frac{\mu_0}{\mu_m} \tag{2.12}$$

$$\frac{\mu_0}{\mu_m} = \left(1 - \frac{\phi}{\phi_m}\right)^{-2} \tag{2.13}$$

With: μ_m & t_{1m} are respectively the viscosity and the characteristic period of the polymer matrix, ϕ_m: is the maximum fraction of packaging $= 0.80$; $\frac{\mu_0}{\mu_m} = \frac{2}{5}$.

Poslinski and al, obtained a good agreement between the proposed model and the experimental data, they found that the rheological behavior of the suspended particles is very similar to the behavior of non-saturated polymer particles (low polymer concentration) and suspended spherical particles of Glass. (Figure 2.6) [28].

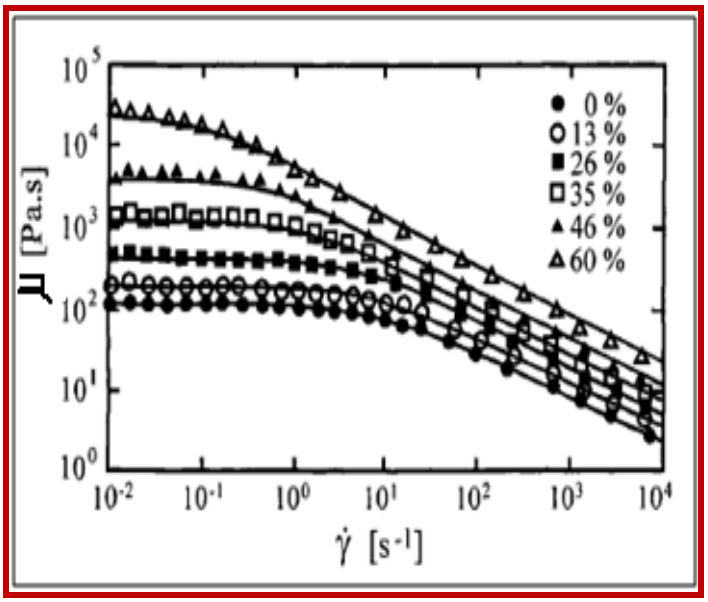

Figure 2.6: the shear viscosity of the spherical particles of suspended glass for different percentages of volume, dispersed in a thermoplastic polymer at 150 ° C, [28].

B. Human blood models

In Pathological narrowing the flow of human blood in the stenosis of a blood vessel or artery is provided under the micropolar fluid model following, **Md. Ikbal** [38].

$$\tau = -m\left\{\left|\sqrt{\frac{1}{2}(\dot{\gamma}:\dot{\gamma})}\right|^{n-1}\right\}\dot{\gamma} \tag{2.14}$$

$$\text{With: } \frac{1}{2}(\dot{\gamma}:\dot{\gamma}) = 2\left\{\left(\frac{\partial v}{\partial r}\right)^2 + \left(\frac{v}{r}\right)^2 + \left(\frac{\partial u}{\partial z}\right)^2\right\} + \left(\frac{\partial u}{\partial r} + \frac{\partial v}{\partial z}\right)^2 \tag{2.15}$$

τ : Shear-stress tensor; $\dot{\gamma}$: Tensor of shear rate;

m & n : are respectively, consistency index and the index parameter of fluid behavior; z and r are the polar coordinates; u and v are respectively the velocity components along the axis (oz) and the pole (r).

There is a particular pattern of blood flow through a catheterization narrow artery; this model is given by the formula of following effective viscosity, **V. P. Srivastava et al, [39]**.

$$\mu_e = \frac{(1-C)\mu_s}{1-\varepsilon^4+\beta(1-\varepsilon^2)+(1-\varepsilon^2)^2/\log\varepsilon} \qquad (2.16)$$

With: μ_s : is an empirical relationship to the viscosity of a suspension; $\varepsilon = \frac{a_1}{a}$, where a; a_1 are the limit values taken by the radius r of a hollow cylinder; $\beta = \frac{8C(1-C)\mu_s}{Sa^2}$; S is the coefficient which characterizes the degree of particle by particle interaction. C: the particle density in the volume fraction of blood.

2.2.3. Shear-thinning or Pseudoplastic fluid

Generally, this type of fluids do not exhibit critical stress of flow or very low critical stress, for exemple: cements, adhesives, fluids containing suspended particles of detergent, and some paints, suspended particles of latex (polymer) in water, aqueous solution of polyacrylamide (figure.2.6 and 2.7). According to the experiments on this type of fluids, the gradient of apparent viscosity decreases while the shear rate increases **[67-69]**.

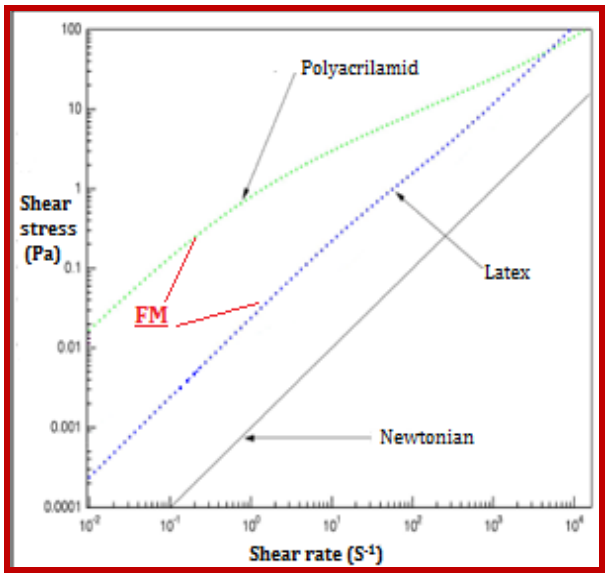

Figure 2.7 : profile of curves obtained from aqueous solution of polyacrylamide and latex (polymer) in water **[38]**.

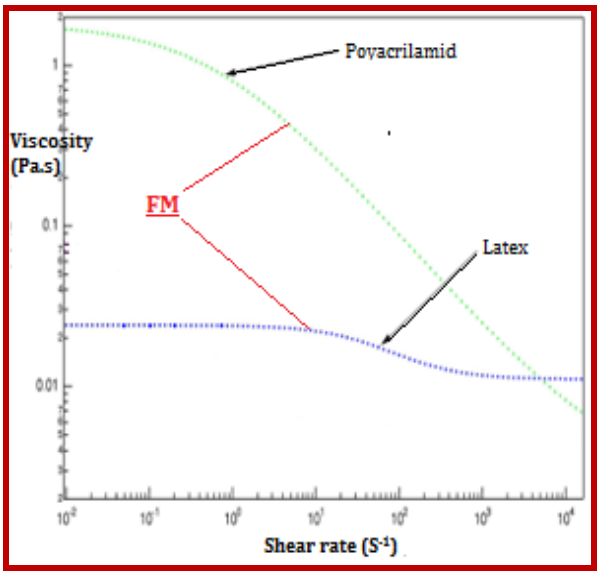

Figure 2.8: the viscosity depending of shear rate of the aqueous solution of polyacrylamide and latex (polymer) in water **[38]**.

2.3. General characteristics of micropolar fluid

The micropolar fluid is characterized by the Brownian movement, the rotary motion (spin), the vortex viscosity, the viscosity of spin gradient, the density of micro-inertia of suspended solid particles, **C. Y. Cheng [36]**.

2.3.1. Micro-rotation (vortex)

The theorem that defined the proper rotation of the particles, denounced that when the fluid particles rotate around their own axis, the fluid flow is called rotational movement, the properties of this type of flow is important and different properties to potential flow (i-rotational). The rotation of a particle is described by its mean angular velocity given by differential called formulas angular variations given by the following formulas, **R. P. Chhabra and E. Krause [69],[84]**.

$$\begin{cases} d\alpha = \frac{\partial v}{\partial x} dt \\ d\beta = \frac{\partial u}{\partial y} dt \end{cases} \tag{2.17}$$

Generalizing the relation (2.17) in other form in three dimensions of the space we obtain the vector of rotation, **[68-69],** or vector swirling is according to:

$$\vec{\omega} = \xi\vec{i} + \eta\vec{j} + N\vec{k} = \frac{1}{2}\left(\vec{\nabla} \times \vec{v}\right) \tag{2.18}$$

With: $\vec{\nabla} = \frac{\partial}{\partial x}\vec{i} + \frac{\partial}{\partial y}\vec{j} + \frac{\partial}{\partial z}\vec{k}$; $\vec{v} = u\vec{i} + v\vec{j} + w\vec{k}$

The component of the angular velocity of moving particle in rotation in different planes: (yoz), (xoz) & (xoy), are ξ, η and N, respectively given by:

$$\xi = \frac{1}{2}\left(\frac{\partial v}{\partial z} + \frac{\partial w}{\partial y}\right) \tag{2.19}$$

$$\eta = \frac{1}{2}\left(\frac{\partial u}{\partial z} + \frac{\partial w}{\partial x}\right) \tag{2.20}$$

$$N = \frac{1}{2}\left(\frac{\partial v}{\partial x} + \frac{\partial u}{\partial y}\right) \tag{2.21}$$

2.3.2. Viscosity of the vortex

It is usually given by a coefficient σ* characterizes the viscosity at the microscale to the border separating the fluid layer and the wall of the fine solid particles in suspension (related to fluid-solid contact area) in σ* balance equations is bound by the dynamic

viscosity μ in the momentum equation, the relationship between σ*, μ, and γ is called the viscosity of spin gradient. It given by the following formula, **[68-69].**

$$\gamma = (\mu + 0{,}5.\sigma^{*})j \qquad (2.22)$$

With: j: the density of micro-inertia.

σ^{*}: Viscosity of the vortex (spin).

2.4. Main parameters affecting the viscosity

The main parameters that have an apparent effect on the viscosity are: The temperature for liquids and semi-solids, expressed by the Arrhenius law; Pressure; The chemical nature of the fluid; The concentration of the solution in case of material; The weather; The shear stress on site both first parameters. **[69]**, we given you in table2.3, some types of viscosities.

A. Temperature and pressure Effects

Practically, the temperature of incompressible fluid rise causes the expansion of volume (increase of intermolecular distances). The same result, when the pressure becomes very high, more than 40 bars, the viscosity (μ) increases, less than 40 bars, the variation of viscosity is neglected, but for incompressible fluids, the threshold pressure is counted in start of 20 bars **[69].**

Table 2.3: Relations of different viscosity coefficients **[69].**

Coefficient	**formula**	**Character**
Dynamic viscosity (absolute) μ	$\mu = \frac{\tau}{D}$ (2.23)	-----
Cinematic Viscosity, ν	$\nu = \frac{\mu}{\rho}$ (2.24)	μ : Dynamic viscosity of the dispersion.
Relative viscosity, μ_r	$\mu_r = \frac{\mu}{\mu_s}$ (2.25)	μ_s : Dynamic viscosity of the solvent.
Specific viscosity, μ_{sp}	$\mu_{sp} = \frac{(\mu - \mu s)}{\mu s}$ (2.26)	-----
intrinsic viscosity, μ_i	$\mu_i = \lim_{\substack{C\to 0 \\ \varepsilon\to 0}} [\frac{\mu_{sp}}{C}]$ (2.27)	C: Presents the concentration of dispersed phase.

2.5. Conclusion

From this theoretical analysis, we can conclude that there is an important link between the microscopic structure and fluid flow behavior. So, it's possible to have certain desired characteristics of a product by manipulating the structure using a range of additives. Vice versa, harnessing rheological measurements to obtain insights at the microstructure scale, on the current basis, it is constructed materials in a convenient form in the industry (for example: personal care drugs, paintings, etc ....).

Chapter 3

Mixed Convective and MHD effect on Newtonian and non-Newtonian-micropolar fluid flows

Chapter 3: Mixed Convective and MHD effect of Newtonian and non-Newtonian micropolar fluid flows

3.1. Introduction

In this chapter, in the first part, we have presented a case of convective heat transfer phenomenon which was at one time a type of theoretically negligible flow but actually its impact on the boundary layer is proved experimentally. This thermal phenomenon is called combined free and forced convection, In the treatment of forced convection, generally the effects of free convection are ignored, this was a hypothesis and this is evident when there is an unstable temperature gradient and the flow is convective free, presumably, by hypothesis, forced convection is supposed negligible. It is time to note that, this situations will be different when the effects of forced and free convection are comparable, in which case it is inappropriate to neglect both processes. It has indicated that free convection is negligible if (Gr_L/Re_{2L}) and that forced convection is negligible if (Gr/Re^2) << 1. Hence the mixed convection regime is generally one for which (Gr/Re^2) ≈1. The effect of buoyancy on heat transfer in a forced flow is strongly influenced by the direction of the buoyancy force relative to that of the flow, **Theodore L. Bergman, et al, [29]**. So the effect of buoyancy is to alter the velocity and temperature fields in the forced convection flow, and this in turn alters the Nusselt number and friction coefficient. Consider the case of upward forced convection over a vertical surface, thus in vertical tube in both cases, external and internal flow. If the temperature wall is up then the fluid temperature (T_w>T), the resulting buoyancy force support the convection flow, especially in close to wall-region, **W. M. Kays, et al, [30]**. The free convection may be significant, however, when low-velocity fluids flow over heated (or cooled) surfaces. A measure of the influence of free convection is provided by the ratio in relation (3.1) gives by **D. R. Pitts, [31]**.

in the second part, we present the writing of basic formulation of mechanical equations of viscous fluids, so, it is easy to formulate the mass conservation, momentum, and energy equations, in second hand we will add another type of equations or terms which describe a micro-continuum and magnetic field effect, we will find together that the classical form of the Navier-Stokes equations does not describe certain types of flows, such as moving micropolar fluids. Fluid mechanics considerations are applied in many fields, especially in engineering. Below a list is provided which clearly indicates the far-reaching applications of fluid-mechanics knowledge and their importance in various fields of engineering, whereas it necessary to carry out special fluid mechanics considerations for each of the areas listed

below. The objective of the derivations in this section is to formulate the conservation laws for mass, momentum, energy, in such a way that they can be applied to all the flow problems. The aim in this step is to derive local formulations of the conservation equations and to introduce field quantities into the mathematical representations of the conservation equations is sought for solutions of fluid flow problems. This requires one to express temporal changes of substantial quantities as temporal changes of field quantities. Also, our discussion will consider some of the simple relations of fluid dynamics and boundary layer analysis that are important for a basic understanding of convection heat transfer.

3.2. Mixed convection regime

$$\frac{\mathrm{Gr}}{\mathrm{Re}^2} = \frac{buoyancy\ \ force}{Inertia\ \ force} \tag{3.1}$$

The regimes of convection are:

Free convection: Gr >> Re^2; Forced convection: Gr << Re^2, and Mixed free and forced convection: Gr ≈ Re^2.

3.3. Free and forced combined convection in tube

A summary of combined free-forced convection effects in tubes has been given by **Metais and Eckert**, as indicated in figure 3.1, which presents regimes for mixed convective flow in vertical tubes. Two different combinations are indicated in figure indicated above.

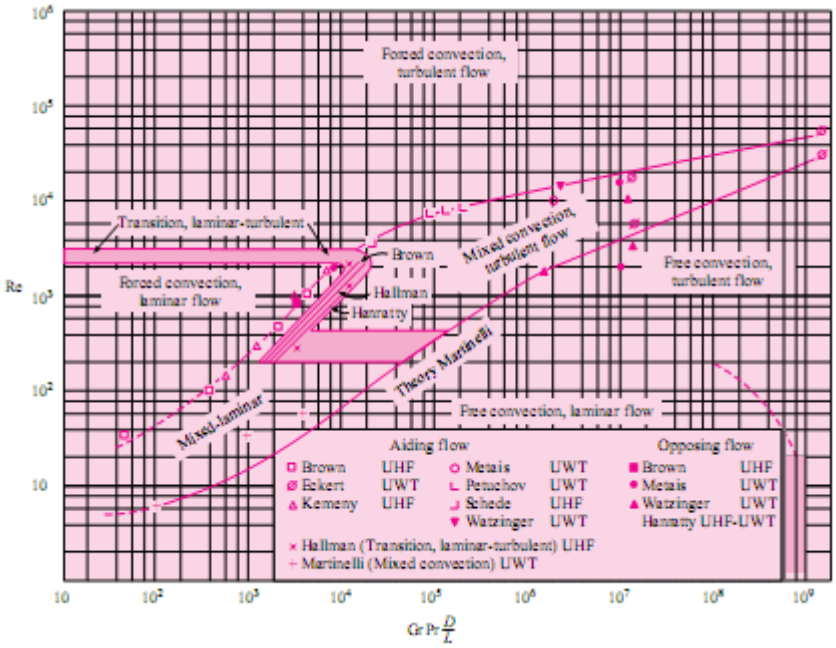

Figure 3.1: Regimes of free, forced, and mixed convection for a flow through vertical tubes [76].

Aiding flow means that the forced-free-convection currents are in the same direction, while the flow is opposing, it means that they are in the opposite direction. The abbreviation UWT means Uniform Wall Temperature, and the abbreviation UHF indicates data for Uniform Heat Flux, **J. P. Holman** & **M. F. Marinet et al**. [76-77]. It is fairly easy to anticipate the qualitative results of the figure 3.1.

A large Reynolds number implies a large forced-flow velocity, and hence less influence of free-convection currents. Large values of Grashof and Prandtl product more mixed convection, this would expect free-convection effects to prevail. The figure 3.2 shows us regimes for combined convection in horizontal tubes. On this figure, **J. P. Holman,** [76], the Graetz number is defined as follows.

$$Gz = Re.Pr\frac{d}{L} \tag{3.2}$$

The correlations on figures 3.1 and 3.2 are applicable for the follow range.

$$10^{-2} < Re.Pr\frac{d}{L} < 1 \tag{3.3}$$

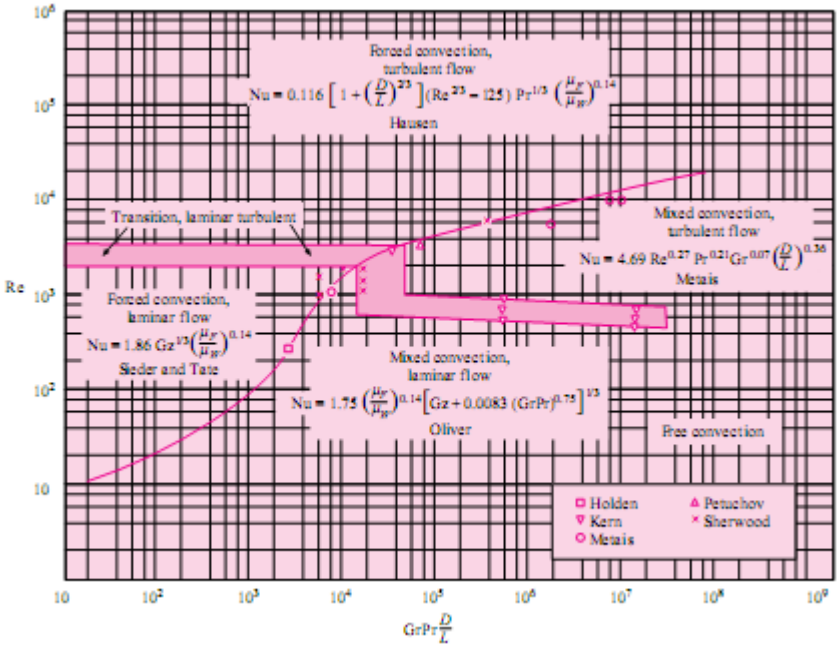

Figure 3. 2: Regimes of free, forced, and mixed convection for flow through horizontal tubes, [76].

The correlations presented in the figures are for constant wall temperature, all properties are evaluated at the film temperature. Involves for the region of laminar flow and mixed convection, Brown and Gauvin (Figure3.2) developed a improved correlation, [76], it's as following.

$$Nu = 1.75\left(\frac{\mu_b}{\mu_w}\right)^{0.14}\left[Gz + 0.012(Gz.Gr^{1/3})^{4/3}\right]^{1/3} \quad (3.4)$$

Than, μ_b is evaluated at the bulk temperature. This relation is preferred over that shown in Fig. 3.2. The problem of combined free and forced convection from horizontal cylinders is treated in detail by Fandand Keswani, **[76].**

3.4. Criteria for the free or forced convection

In general notion, a majority of combined-convection analysis of heat-transfer mode is governed by the fluid velocity, for a forced-convection situation involving a fluid velocity of 30 m/s, for example, probably is to overshadow most free-convection effects encountered in ordinary gravitational fields because the free-convection flow velocities are small comparing with 30 m/s. In another way, a forced flow situation at very low velocities (~0 3 m/s) might be influenced appreciably by flows due by free-convection. An order of magnitude analysis of the free-convection boundary layer equations will indicate a general criterion for determining whether free-convection effects dominate. The criterion is that once, **[76].**

$$Gr/_{Re^2} > 10 \quad (3.5)$$

3.5. External mixed convection

We can distinguish two types of external convective flows, flow over a vertical plate and flow over a horizontal plate. The flow in mixed convection near a vertical plate, results from a combination of natural and forced convection. It considered that the wall is porous and is crossed by a uniform suction velocity flow (v_0: velocity, counted positively for suction). Suction prevents the thermal and velocity boundary layers from growing and, as a consequence, they are spatially uniform. $\frac{d\delta}{dx} = \frac{d\delta_T}{dx} = 0$, **M. F. Marinet, et al, [77].**

Conclude that:

- The temperature and velocity distribution; the friction coefficient. $C_f = \tau_w/\rho v_0^2$. Divide the assistance of natural and forced convection to C_f.

Example of theoretical model of vertical plate heated with constant flux

The two equations above about the isothermal plane wall can be used with high-quality of accuracy of constant heat flux problem provided that $\widehat{Nu}_L$ and Ra, are based on the difference of height midpoint temperature of plate. Therefore, ΔT and properties are based on $\Delta T_{L/2} = T_S\,(L/2) - T_\infty$. Then $\hat{h} = q_S^{"}/\Delta T_{L/2}$, and A solution and error test is required. **[62]**. This problem is solved using Pohlhausen's similarity parameter and steam function in two dimensions (x,y), this is as follows.

$$\eta = \frac{y}{x}\left(\frac{Gr_x}{4}\right)^{\frac{1}{4}} \tag{3.6}$$

$$\psi(x,y) = f(\eta)\left[4v\left(\frac{Gr_x}{4}\right)^{\frac{1}{4}}\right] \tag{3.7}$$

Using: $\frac{\partial\psi}{\partial y} = u$; $\frac{\partial\psi}{\partial x} = -v$; $then$: $\theta = \frac{T-T_\infty}{T_s-T_\infty}$.

Using terms above in continuity and energy equations of Navier-Stokes, we will obtain the following dimensionless mathematical model.

$$f^{'''} + 3ff^{''} - 2(f')^2 + \theta = 0 \tag{3.8}$$

$$\theta^{''} + 3Prf\theta^{'} = 0 \tag{3.9}$$

It is simpler to consider them as simultaneous equations coupled through the function *f*. η: is the variable of similarity. Although, the dimensionless temperature θ, each solution must be for a particular Prandtl number, since *Pr* appears as a parameter. The boundary conditions are:

At $\eta = 0$: $f = 0, f' = 0, \theta = 1$ (3.10)

As $\eta \to \infty$: $f \to 0, \theta \to 0$ (3.11)

The solution of this dimensionless differential equations is given as curves for wide range of Prandtl numbers, see figures 3.3 & 3.4

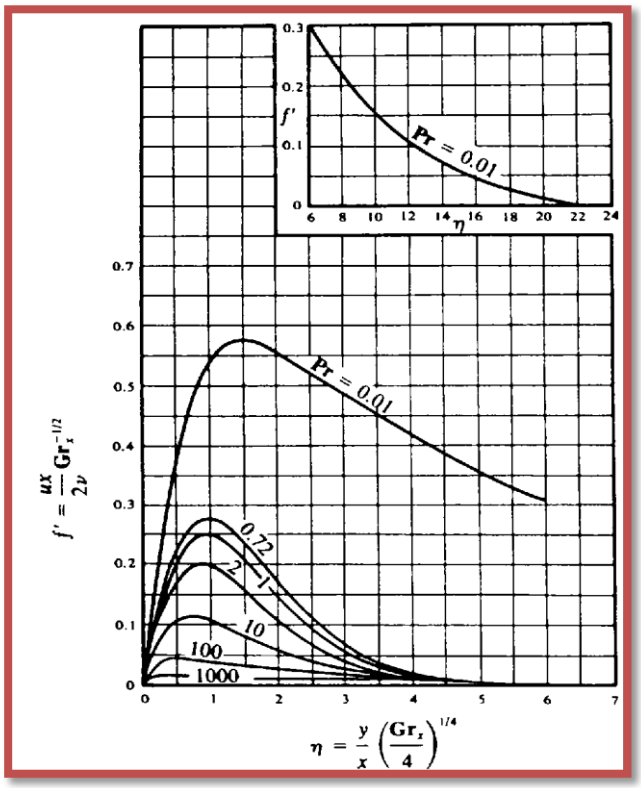

Figure 3. 3: Laminar, free velocity temperature profiles [76].

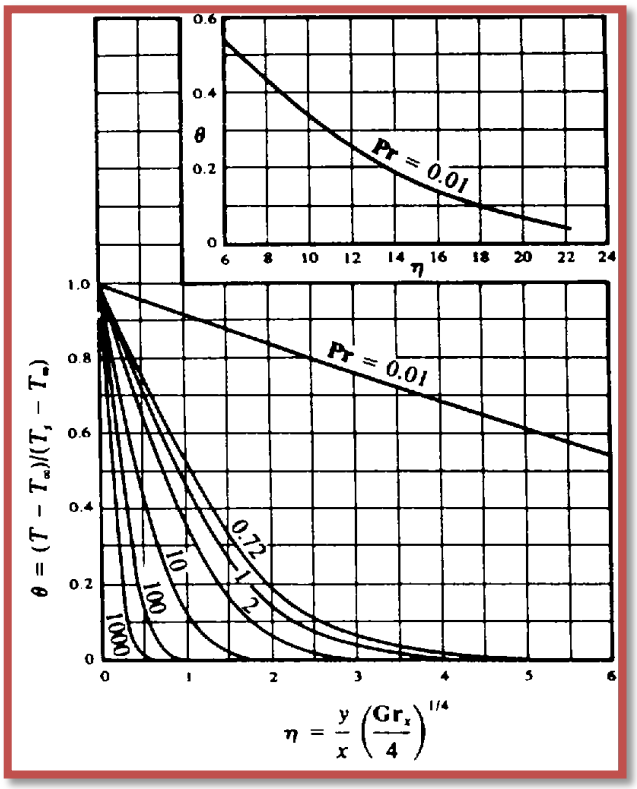

Figure 3. 4: Laminar, free convective temperature profiles [76].

3.6. Internal Natural mixed convection

In free configurations, external natural convection flows developing freely under the influence of the various forces carried hinto play. In many situations, however, confinement effects are present because the space offered to flows and heat transfer has limited dimensions, so that distances between walls are of the order of the length scale of the flow or are even smaller. These confined situations correspond to natural convection in open ducts (chimneys) or in closed cavities. Main applications are in the domain of housing, in particular solar energy, and also in the domain of nuclear safety (in the case of pump failure) or concern the cooling of electrical or electronic components, [77].

3.7. More recent correlations

Newer correlation is carried on to be equations in the area of natural convection. It may be found in more extensive heat transfer texts, only a few of the more frequently encountered geometries/empirical equations are introduced, especially, those for the vertical plane wall and the horizontal cylinder with constant surface temperatures, **Rohsenow and Martynenko** [78-79].

3.7.1. Infinite Horizontal Circular Cylinder with constant temperature Surface

Churchill and Chu are given a correlation that is generally used and covers a wide range of Rayleigh numbers, it's as follows [79].

$$\widehat{Nu_D} = \left\{0.60 + \frac{0.387 Ra_D^{1/6}}{\left[1+(0.559/Pr)^{9/16}\right]^{8/27}}\right\}^2 \quad (3.12)$$

Which is valid for $10^{-5} < Ra_D < 10^{12}$ and properties are estimated at T_f. For gases $\beta = 1/T_f$.

3.7.2. Vertical plate with constant temperature surface

For constant $T_{,}$ Churchill and Chu recommend the following correlation which is valid over the entire range of Ra_L, with properties evaluated at T_f, [79].

$$\widehat{Nu_L} = \left\{0.825 + \frac{0.387 Ra_D^{1/6}}{\left[1+(0.492/Pr)^{9/16}\right]^{8/27}}\right\}^2 \quad (3.13)$$

Precision results are somewhat improved for laminar flow, with T_f, by using

$$\widehat{Nu_L} = 0.825 + \frac{0.670 Ra_D^{1/4}}{\left[1+(0.492/Pr)^{9/16}\right]^{4/9}} \quad (3.14)$$

In which, properties are evaluated at T_f and $R_{aL} \leq 10^9$.

3.8. Governing equations of classical fluid mechanics

Four differential equations of continuity and three equations of momentum, called again, Navier-Stokes equations, contain five remaining unknowns P, ρ, U_j, so that an incomplete system of partial differential equations still exists. With the aid of the thermal energy equation and the thermodynamic state equation, valid for the considered fluid, it is possible to obtain a complete system of partial differential equations that permits general solutions for flow problems, when initial and boundary conditions are present by **Holman**, **Schetz, Kothandaraman & LIENHARD** [76], [80-82].

3.8.1. Newtonian viscous fluid flow

Let us consider that the flow of fluids is Newtonian, where the influence of the viscous forces and the gravitational force has a significant impact. These viscous forces are described in terms of a shear stress (τ) between the fluid layers. Assuming that this constraint is proportional to the normal velocity gradient, [76],[77], [79], [84].

A. The continuity equation

In considerations of fluid mechanics, (closed fluid system) can always be found, i.e. a system whose total mass, $\sum_{i=1-n} m_i = \mathrm{M} = \text{constant}$. This is easily seen for a fluid mass, which is stored in a container. For all other fluid flow considerations, control volumes can always be defined within which the system's total mass can be stated as constant. So, the general vector form of the mass conservation (continuity equation) is as fellows.

$$\frac{DM}{Dt} = \frac{\partial M}{\partial t} + \left(\vec{V}.\overrightarrow{grad}\right)M = 0 \qquad (3.15)$$

With $\vec{V} = x\vec{\imath} + y\vec{\jmath} + z\vec{k}$ and $\overrightarrow{grad} = \frac{\partial}{\partial x}\vec{\imath} + \frac{\partial}{\partial y}\vec{\jmath} + \frac{\partial}{\partial z}\vec{k}$.

The differential form of continuity equation holds for steady or unsteady flow. In Cartesian coordinates, with: V is the volume, ρ is the density of fluid, considered constant, it is reduces and (3.15) take the following form.

$$\vec{\nabla}.\vec{V} = 0 \qquad (3.16)$$

B. Momentum equation

The derivations of the momentum equations of fluid mechanics are usually given for the three coordinate directions *j* = 1, 2, 3. They express Newton's second law and are easiest formulated in their Lagrange forms. For a fluid element, it is stated that the time derivative of the momentum in the *j* direction is equal to the sum of the external forces acting in this direction on the fluid element, plus the molecular-dependent input of momentum per unit time. The forces can be stated as mass forces, caused by gravitation forces and electromagnetic forces, as well as surface forces caused by pressure. Here, fluid elements act like rigid bodies. They do not change their state of motion, i.e. their momentum, if no mass or surfaces forces act on the fluid elements and no molecular-dependent momentum input is present. However, when forces are present, or when molecular momentum input occurs, a considered fluid element changes. Fluids, as they are treated in classical books, i.e. liquids (incompressible fluids), furthermore, For the pressure force, in considering axes for, *j* = 1, 2, 3. We can write:

$$\rho\left(\frac{\partial U_j}{\partial t} + U_i\frac{\partial U_j}{\partial x_i}\right) = -\frac{\partial P}{\partial x_j} - \frac{\partial \tau_{ij}}{\partial x_j} + \rho.g \qquad (3.17)$$

For Newtonian fluids.

$$\tau_{ij} = -\mu\left(\frac{\partial U_j}{\partial x_i} + \frac{\partial U_i}{\partial x_j}\right) + \frac{2}{3}\delta_{ij}\frac{\partial U_k}{\partial x_k} \tag{3.18}$$

$\delta_{ij}\frac{\partial U_k}{\partial x_k}$: present the spatial variation of velocity components. As in this equation the element volume of the fluid, appearing in all terms, was eliminated, the equations of momentum are given by (3.17) per unit volume, the momentum equations in the three coordinate directions (Cartesian coordinates), and result:

$$\rho\left(\frac{\partial U_1}{\partial t} + U_1\frac{\partial U_1}{\partial x_1} + U_2\frac{\partial U_1}{\partial x_2} + U_3\frac{\partial U_1}{\partial x_3}\right) = -\frac{\partial P}{\partial x_1} - \frac{\partial \tau_{11}}{\partial x_1} - \frac{\partial \tau_{21}}{\partial x_2} - \frac{\partial \tau_{31}}{\partial x_3} \tag{3.19}$$

$$\rho\left(\frac{\partial U_2}{\partial t} + U_1\frac{\partial U_2}{\partial x_1} + U_2\frac{\partial U_2}{\partial x_2} + U_3\frac{\partial U_3}{\partial x_3}\right) = -\frac{\partial P}{\partial x_2} - \frac{\partial \tau_{12}}{\partial x_1} - \frac{\partial \tau_{22}}{\partial x_2} - \frac{\partial \tau_{32}}{\partial x_3} \tag{3.20}$$

$$\rho\left(\frac{\partial U_3}{\partial t} + U_1\frac{\partial U_3}{\partial x_1} + U_2\frac{\partial U_3}{\partial x_2} + U_3\frac{\partial U_3}{\partial x_3}\right) = -\frac{\partial P}{\partial x_1} - \frac{\partial \tau_{13}}{\partial x_1} - \frac{\partial \tau_{23}}{\partial x_2} - \frac{\partial \tau_{33}}{\partial x_3} \tag{3.21}$$

So, $\tau_{ij} \neq 0$, for fluids in general but for ideal in terms of fluid mechanics, the molecular momentum transport turns out to be $\tau_{ij} = 0$. Hence the following forms of the momentum equations can be written as follow:

<u>For viscous fluids</u>.

$$\rho\left(\frac{\partial U_j}{\partial t} + U_i\frac{\partial U_j}{\partial x_i}\right) = -\frac{\partial P}{\partial x_j} - \frac{\partial \tau_{ij}}{\partial x_j} + \rho.g \tag{3.22}$$

<u>For ideal fluids</u>**.**

$$\rho\left(\frac{\partial U_j}{\partial t_i} + U_i\frac{\partial U_j}{\partial x_i}\right) = -\frac{\partial P}{\partial x_j} + \rho.g \tag{3.23}$$

This system of equations comprises four equations for the four unknowns P, U_1, U_2, U_3. In principle, it can be solved for all flow problems to be investigated if suitable initial and boundary conditions are given. For thermodynamically ideal liquids, i.e. ρ = constant, a complete system of partial differential equations exists through the continuity equation and the momentum equations, which can be used for solutions of flow problems.

The Navier-Stokes equations of momentum in Cartesian coordinates in taking account that: ρ and μ , are constant, then $\tau_{ij} = -\mu\frac{\partial U_j}{\partial x_i}$.

$$\rho\left(\frac{\partial U_1}{\partial t}+U_1\frac{\partial U_1}{\partial x_1}+U_2\frac{\partial U_1}{\partial x_2}+U_3\frac{\partial U_1}{\partial x_3}\right)=-\frac{\partial P}{\partial x_1}+\mu\left(\frac{\partial^2 U_1}{\partial x_1^2}+\frac{\partial^2 U_1}{\partial x_2^2}+\frac{\partial^2 U_1}{\partial x_3^2}\right) \quad (3.24)$$

$$\rho\left(\frac{\partial U_2}{\partial t}+U_1\frac{\partial U_2}{\partial x_1}+U_2\frac{\partial U_2}{\partial x_2}+U_3\frac{\partial U_3}{\partial x_3}\right)=-\frac{\partial P}{\partial x_2}+\mu\left(\frac{\partial^2 U_2}{\partial x_1^2}+\frac{\partial^2 U_2}{\partial x_2^2}+\frac{\partial^2 U_2}{\partial x_3^2}\right) \quad (3.25)$$

$$\rho\left(\frac{\partial U_3}{\partial t}+U_1\frac{\partial U_3}{\partial x_1}+U_2\frac{\partial U_3}{\partial x_2}+U_3\frac{\partial U_3}{\partial x_3}\right)=-\frac{\partial P}{\partial x_3}+\mu\left(\frac{\partial^2 U_3}{\partial x_1^2}+\frac{\partial^2 U_3}{\partial x_2^2}+\frac{\partial^2 U_3}{\partial x_3^2}\right) \quad (3.26)$$

3.8.2. Thermal Energy Equation

For the temporal change of the total energy of a fluid element, one obtains with $\delta m = \text{constant}$, i.e. $\frac{d(\delta m)}{dt}=0$, see references **[76]**,**[77], [79], [84]**:

$$\frac{d}{dt}\left(\delta m_R\left[\frac{1}{2}U_1^2+e+G\right]\right)=\delta m_R\frac{D}{Dt}\left(\frac{1}{2}U_1^2+e+G\right) \quad (3.27)$$

The equation (3.27) presents the total energy change with time of a fluid element which has to be considered concerning the derivation of the total energy equation. The change in the total energy of the fluid element can emanate from the heat conduction, which yields the following inputs minus the output of heat. There are different forms of the thermal energy equation can be derived from equation (3.27), generally, the thermal energy equation can be written for thermodynamically simple fluids.

$$\rho\frac{De}{Dt}=-\frac{\partial \dot{q}_i}{\partial x_i}-P\frac{\partial U_i}{\partial x_i}-\tau_{ij}\frac{\partial U_j}{\partial x_i} \quad (3.27)$$

For a thermodynamically ideal liquid, with $\frac{\partial Ui}{\partial xi}=0$ and $Cv = Cp$, the equation (3.27), becomes:

$$\rho C_p\frac{DT}{Dt}=\lambda\frac{\partial^2 T}{\partial x_i^2}-\tau_{ij}\frac{\partial U_j}{\partial x_i} \quad (3.28)$$

3.8.3. Heat transfer in fluid flows

The differential equations carried out in (3.19)-(3.21), that should be satisfied in the flow field about body while there is heat transfer between fluid and material body, The Navier-Stokes equations structured by the continuity, momentum and energy equations are developed in laminar boundary layer case of a general viscous fluid in the cartesian coordinate system taking in consideration C_p = C_v, ρ = constant, they could be shown in others forms us equations (3.15), (3.24)-(3.27), as follows, see reference **[84].**

- Mass conservation balance.

$$\frac{\partial u}{\partial x}+\frac{\partial v}{\partial y}+\frac{\partial w}{\partial z}=0 \tag{3.29}$$

- Movement conservation balance.

$$\frac{\partial u}{\partial x}+v\frac{\partial u}{\partial y}+w\frac{\partial u}{\partial z}=-\frac{1}{\rho}\frac{dp}{dx}+\frac{\mu}{\rho}\left(v\frac{\partial^2 u}{\partial y^2}+w\frac{\partial^2 u}{\partial z^2}\right) \tag{3.30}$$

$$u\frac{\partial v}{\partial x}+v\frac{\partial v}{\partial y}+w\frac{\partial v}{\partial z}=-\frac{1}{\rho}\frac{dp}{dy}+\frac{\mu}{\rho}\left(u\frac{\partial^2 v}{\partial x^2}+w\frac{\partial^2 v}{\partial z^2}\right) \tag{3.31}$$

$$u\frac{\partial w}{\partial x}+v\frac{\partial w}{\partial y}+w\frac{\partial w}{\partial z}=-\frac{1}{\rho}\frac{dp}{dz}+\frac{\mu}{\rho}\left(v\frac{\partial^2 w}{\partial x^2}+w\frac{\partial^2 w}{\partial y^2}\right) \tag{3.32}$$

- Equation of thermal energy balance.

$$\rho\left(\frac{\partial e}{\partial t}+U_i\frac{\partial e}{\partial x_i}\right)=-\frac{\partial \dot{q}_i}{\partial x_i}-P\frac{\partial U_i}{\partial x_i}-\tau_{ij}\frac{\partial U_j}{\partial x_i} \tag{3.33}$$

We not that ρ*:* is the density of the fluid, e: its inner energy, t: the time, U_i: the fluid velocity, $\dot{q}_i$ the heat flux, P: the pressure and τ_{ij} : the molecular-dependent momentum transport. This equation can now be employed for a thermodynamically ideal fluid, i.e. for ρ = constant and thus for $\left(\frac{\partial Ui}{\partial xi}\right)=0$, and also for

$$\dot{q}_i=-\lambda\frac{\partial T}{\partial x_i}\text{; and } \tau_{ij}=-\mu\left(\frac{\partial U_j}{\partial x_i}+\frac{\partial U_i}{\partial x_j}\right) \tag{3.34}$$

A heat transfer computations, can be written in another simple form, in taken into consideration that: $c_v=c_p=c$, and ρ = constant:

$$\rho.C\left(\frac{\partial T}{\partial t}+U_i\frac{\partial T}{\partial x_i}\right)=\lambda\frac{\partial^2 T}{\partial x_i}+\mu\left(\frac{\partial U_j}{\partial x_i}\right)^2 \tag{3.35}$$

In the cartesian coordinate system (3.35) will take the following form.

$$\left(\frac{\partial T}{\partial t}+u\frac{\partial T}{\partial x}\right)=\frac{\nu}{P_r}\frac{\partial^2 T}{\partial x}+\eta\left(\frac{\partial u}{\partial x}+\frac{\partial v}{\partial x}+\frac{\partial w}{\partial x}\right)^2 \tag{3.36}$$

$$\left(\frac{\partial T}{\partial t}+v\frac{\partial T}{\partial y}\right)=\frac{\nu}{P_r}\frac{\partial^2 T}{\partial y}+\eta\left(\frac{\partial u}{\partial y}+\frac{\partial v}{\partial y}+\frac{\partial w}{\partial y}\right)^2 \tag{3.37}$$

$$\left(\frac{\partial T}{\partial t}+w\frac{\partial T}{\partial z}\right)=\frac{\nu}{P_r}\frac{\partial^2 T}{\partial z}+\eta\left(\frac{\partial u}{\partial z}+\frac{\partial v}{\partial z}+\frac{\partial w}{\partial z}\right)^2 \tag{3.38}$$

With: $\alpha = \frac{\lambda}{\rho.C}$; $P_r = \frac{\upsilon}{\alpha} \Rightarrow \frac{\lambda}{\rho.C} = \frac{\nu}{P_r}$ and $\eta = \frac{\mu}{\rho.C}$; α: present a thermal diffusion coefficient; η: is the viscous diffusion coefficient, P_r is dimensionless number named Prandtl number.

3.9. Micropolar fluid mechanics

The aim of this part of theoretical study is to present the mechanics of micropolar continua (also known as Cosserat Continua), see reference, **V. A. Eremeyev et all [85]**. In focus of scientists since the end of the nineteenth century. A first review of the theory with independent force and moment (couple) actions was given in 1909 by the Cosserat brothers in their centurial French book "Théorie des corps déformable''. While this moment, it was published in this field tens of books and thousands of articles. Continuum theory is focused on the fact that the continuum translations and rotations can be defined independently.

In other words, force and moment actions in the continuum can be introduced independently as in dynamics of rigid body or structural mechanics. In a micropolar medium, each material particle has six freedom degrees; they are three translational and three rotational freedom degrees. These characteristic features of the Cosserat continuum model give a possibility to describe more complex media, for example, micro-inhomogeneous materials, foams, cellular solids, lattices, masonries, particle assemblies, magnetic rheological fluids, liquid crystals, etc. Starting with the symbol papers by Eringen and others, the micropolar continuum is applied to the model of fluids. This branch of the hydrodynamics is called the micropolar or asymmetric hydrodynamics.

The micropolar hydrodynamics is applied to describe the behavior of magnetic liquids, polymer suspensions, liquid crystals, and other types of fluids with microstructure. Within the Cosserat continuum theory, many problems were successfully solved. They demonstrate qualitative and quantitative difference between the solutions by micropolar and classic elasticity models. One of the principal difficulties of any micropolar theory is to establish its constitutive equations. This question was not discussed in the Cosserats' original monograph, and it was a reason why the ideas of micropolar continuum were not recognized by many researchers.

But even if for a material the constitutional equations are formulated we are faced with a new hard problem: the identification of the material parameters.

3.9.1. Micropolar continuum kinematics

This part presents a summary of general relations of the kinematics of micropolar continuum. The description of a particle motion of a micropolar continuum (medium) is based on the assumption that each particle of the micropolar body has six degrees of freedom; this hypothesis is similar to the description of a rigid body in classical mechanics. Three freedom degrees are translational as in classic elasticity, and three other degrees are rotational.

In the actual configuration **x** at instant t, the position of a particle of micropolar continuum is given by the position vector $\mathbf{V_P}$; $\mathbf{O_{Pj}}$ (j = 1, 2, 3) is an orthogonal Trihedron define a particle orientation (Fig. 3.5), which present vectors called the directors. The two vector field's V_P and O_{Pj} are respectively the particle translational and rotational motions. In the aim to describe the medium relative deformation, we use some fixed position of the body that may be taken at **t = 0** or another fixed instant; we call this position the reference configuration $\mathbf{C_r}$. for this case the state of particle is defined by the position vector **R**, whereas its orientation by directors $\mathbf{D_j}$. we note that as the reference configuration can be chosen not only the real state but also any one. The motion of a micropolar continuum is described by, see **[85]**.

$$V_p = V_p(R,t);\ \mathrm{O_{Pj}} = \mathrm{O_{Pj}}(R,t) \tag{3.39}$$

In the process of deformation the trihedron $\mathrm{O_{Pj}}$ stays orthonormal, $\mathrm{O_{Pj}} \cdot \mathrm{O_m} = \delta_{\mathrm{km}}$. The change of directors is described by an orthogonal tensor is as follows.

$$H = \mathrm{O_{Pj}} \otimes \mathrm{D_j} \tag{3.40}$$

H is the microrotation tensor, and then V_P describes the particle position of the continuum at time t, whereas H defines its orientation. The orientation of D_j and O_{Pj} can be selected the same, so H is proper orthogonal. Hence, the micropolar continuum deformation is described by relations as follows.

$$V_p = V_p(R,t);\ H = H(R,t) \tag{3.41}$$

A linear velocity is given by the following relation.

$$V = \dot{V}_p \tag{3.42}$$

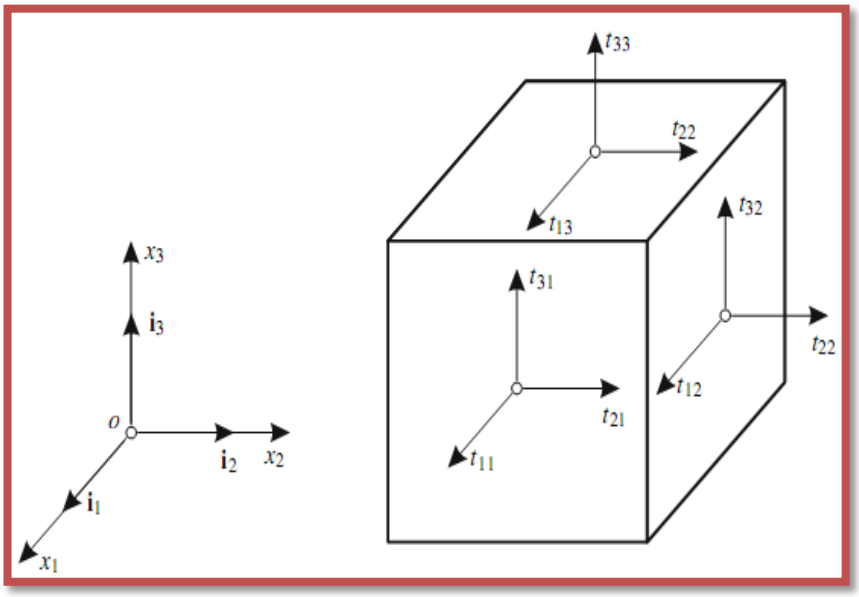

Figure.3.5: Positive stresses of orthogonal Tetrahedron shape **[85].**

The angular velocity vector, called vector of microgyration, is given by the following relation.

$$\omega = -\frac{1}{2}(H^T.\dot{H})_X \tag{3.43}$$

Where the dot (.) denotes the inner product, $(\ldots)^{\mathrm{T}}$ is the transposed form of vector H. The symbol $(\ldots)_\times$ stands for the vector invariant of a second-order tensor. In particular, for a dyad $a \otimes b$, it has $(a \otimes b)_X = a \times b$, where x is the vector (cross) product relation (3.43), means that ω is the axial vector associated with the skew-symmetric tensor $H^T.\dot{H}$.

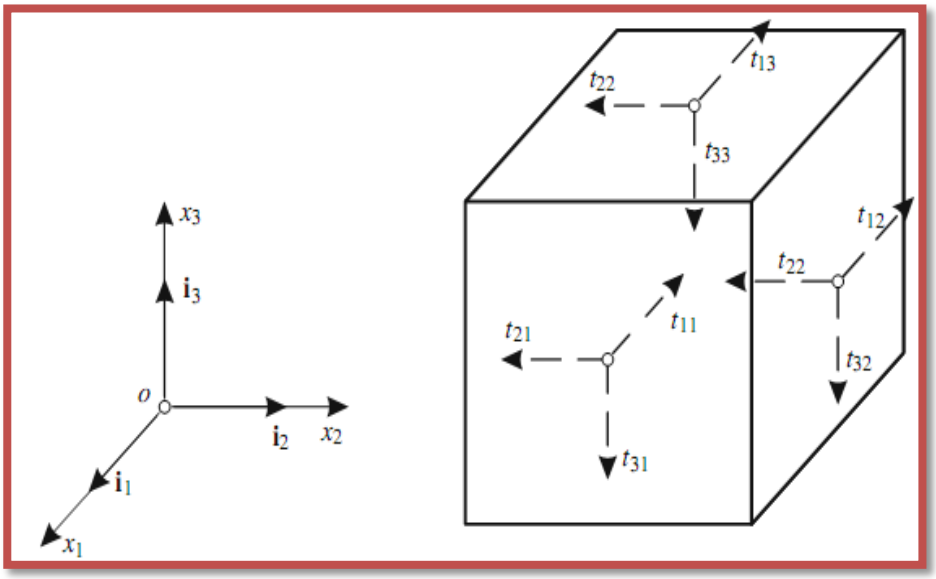

Figure.3.6: Negative stresses, of orthogonal Tetrahedron shape **[85]**.

3.9.2. Equations of the movement

The dynamic equations of micropolar continuum in the local form are done us in transforming Euler's laws of motion as in the proof of Cauchy; see the work given by **Victor A. Eremeyev and all, [85]**. The form of equations are as flows:

$$\rho \frac{d\boldsymbol{V}}{dt} = div\boldsymbol{T} + \rho \boldsymbol{f} \tag{3.44}$$

$$J \frac{d\omega}{dt} = divM - T_x + \rho m \tag{3.45}$$

In cartesian coordinates, equations (3.44) and (3.45) take the following form.

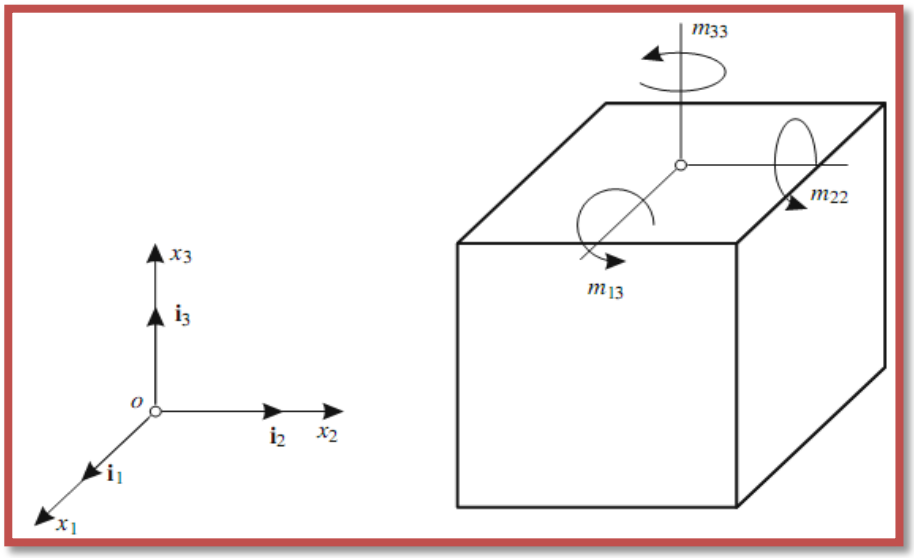

Figure 3.7: Couple stresses of orthogonal tetrahedron shape, **[85]**.

$$\rho \frac{d\mathrm{v_s}}{dt} = \frac{\partial t_{sj}}{\partial x_j} + \rho f_s \tag{3.46}$$

$$J \frac{d\omega_s}{dt} = \frac{\partial m_{sj}}{\partial x_j} + t_{mn}\, \varepsilon_{mns} + \rho m_s \tag{3.47}$$

$$\varepsilon_{mns} = -(i_m \times i_n).\,\mathrm{i_s} \tag{3.48}$$

Where: T is the Cauchy stress tensor, M is the couple stress tensor, m is the volume couples, t_{sj} and m_{sj} are matrices represent the components of the stress tensor and of the couple stress tensor in Cartesian basis i_j . j is the rotation inertia.

When the medium does not possesses couple's properties that are rotation interaction of particles is negligible, we obtain the following equation:

$$T_\times = 0 \tag{3.49}$$

Its solution is the symmetric stress tensor, that is $T = T^T$. therefore when couple stresses and the distributed external couples in the moment balance equation of momentum are absent, It depends on the symmetry of the Cauchy stress tensor which is a property of continuous classical mechanics.

For the classical continuum, that is when couple stresses and the external couples are absent, (3.49) holds automatically as a consequence of the constitutive equations. for this reason, the balance equation of moment of momentum take part in less important role in the Cauchy continuum.

In order to solve the model indicated by equations (3.44) & (3.45), that describes any phenomenon of flow of micropolar fluids must obey to setup a boundary-value problem for a micropolar body, we should supplement the motion equations with boundary and initial conditions, see reference **[85]**, have put in our hands rules for this.

3.10. Electromagnetic, production and effects on materials in flow

In microscopic scale, the presence of electrical and magnetic fields has an effect on the response characteristics of many materials. As well, an electro-Rheology is the name given to the mechanics branch that is concerned with the material flow of that is primarily affected by the electrical field action. Usually, electro-rheological materials are dielectrics or semi-conductors in a non-conducting fluid, though recently Ferroelectrics have also been used. Starting at a microscopic level or within the context of continuum mechanics in a homogenized sense, the electro-rheological fluids are modeled. Thus we should restrict ourselves to continuum models, otherwise, even in the case of continuous-field mechanics (continuum mechanics); there are several methods of modeling electro-rheological fluids, **D. A. Siginer, et al. & H. K. Moffat [75-86]**.

Moreover, we think that not only earth and sun generate and safe a magnetic field, this state normally is accompaniment to any cosmic body that is both – wholly or fluid in part – flows and rotates. So, it appears to be a sort of universal validity about this statement which applies quite irrespective of the length-scales considered. Such us, the planet in macroscopic-scale. For example, Jupiter shares with the Earth the property of strong rotation. Within, they have a fluid interior composed of an alloy of liquid metallic hydrogen and helium. Furthermore, this character happening naturally, occurring-magnetic fields, see reference, **H. K. Moffat, [86]**.

3.10.1. Kinematics and balance laws

In this part it is sufficient to say that by the same analogy as in paragraph 3.8, the writing of general relations of the kinematics of micropolar continuum keep in the same laws. Furthermore, the approach in kinematics are similar in order to lay down the laws governing this type of flows taking into account the generation of the electrically-force and Magnetic field due to the proper electrical conductivity of fluids.

3.10.2. Equations of the movement

The kinematical definitions are keeping our more then, the minimum of the basic equation documentations while ensuring that the treatment be self-contained. A complete and proper frame-work for the reading of electro-rheological fluids would involve the laws of electromagnetism in addition to the usual laws of thermo-mechanics. To express the equations of electro-magnetic, it exists many ways; we shall use the Minkowskian formulation. For any details of discussion of basic laws of field dependant materials within the background of continuum mechanics can be found in reference **[86]**.

- The conservation of mass (continuity equation) is as follows.

$$\frac{\partial \rho}{\partial t} + div(\rho V) = 0 \tag{3.50}$$

- The balance of linear momentum the following form.

$$divT^T + \rho f + f_e = \rho \frac{dV}{dt} \tag{3.51}$$

$f \; and \; f_e$ Are respectively, the external mechanical body and the electromagnetic force density. Where f_e is given by the following formula.

$$f_e = q_e E + \frac{1}{C} J_c \times B + \frac{1}{C} \frac{\partial P}{\partial t} \times B + \frac{1}{C} div[(P \times B) \otimes V] + [gradB]^T M + [gradE]P \tag{3.52}$$

$q_e, E, c, J_c, B \; and \; P$. Are respectively, the electric charge density; the electric field; the capacity of current ;the conduction current; the magnetic flux and the electric polarization. Then M is defined as follows.

$$M = \mathrm{M_p} + \frac{1}{\mathrm{C}} \mathrm{V} \times \mathrm{P} \tag{3.53}$$

M is the magnetic polarization. Thus, the angular momentum balance is given by the following formula.

$$div(x \times T) + x \times \rho f + l_e = x \times \rho \frac{dV}{dt} \quad (3.54)$$

Where: l_e is the electromagnetic angular momentum density given by the following equation.

$$l_e = x \times f_e + P \times \mathcal{F} + M \times B \quad (3.55)$$

Where: $\mathcal{F}$ was the electromotive force intensity given by the following formula.

$$\mathcal{F} = \mathrm{E} + \frac{1}{\mathrm{C}}\mathrm{V} \times \mathrm{M} \quad (3.56)$$

The energy balance equation is given by the following form.

$$\rho \frac{\partial}{\partial t}\left(e + \frac{1}{2}|V|^2\right) + div\ q = div(TV) + \rho f.V + \rho.r + w_e \quad (3.57)$$

Where: $e, q, r\ and\ w_e$. are respectively, the specific internal energy; the heat flux vector; the radiant heating and the energy production density which is given by.

$$w_e = f_e.V + \rho\mathcal{F}.\frac{d}{dt}\left(\frac{P}{\rho}\right) - M.\frac{dB}{dt} + J.\mathcal{F} \quad (3.58)$$

And J: takes the following form expression.

$$J = J_c - q_e V \quad (3.59)$$

3.11. Conclusion

From these theoretical studies, we can conclude that:

- In the first part which consists of the mixed convection due by heat transfer is associated with flows in a wide spectrum various domains of biological or industrial flows. From this theoretical study we understand that this type of flow cooperate with an important part in the energy transfer problems and for environment, so, free-forced convection under external or internal effects as thermal inertia, force due to magnetic field, present a large domain of studies that we should work on.

- from the second part which present a simply theoretical study. We have observed that general laws of continuous media mechanics can be sufficiently used to develop and study general models that can describe the rheological characteristics of electro-conducting fluids and the behavior of certain types of fluids possessing criteria in flow of electrical conductor. Of course, such a model could be further simplified by taking into account initial conditions and boundaries.

Part III

Chapter 4

Modeling and solving the immiscible non-Newtonian-micropolar and Newtonian-viscous fluids flow in vertical channel

Chapter 4: Modeling and solving the immiscible non-Newtonian-micropolar and Newtonian-viscous fluids flow in vertical channel

4.1. Introduction

In this chapter we present an analytical and numerical study of a convective flow model of MHD micropolar and viscous fluids in a vertical channel, in this work we have considered two incompressible and immiscible fluids in different regions, first region is occupied by non-Newtonian micropolar fluid and the second region is occupied by Newtonian-viscous fluid. The channel is subjected to the influence of a transverse magnetic field and temperature gradient. To provide a right understanding of complexity of this type of flow, a mathematical model proposed considering thermal diffusivity and magnetic diffusivity terms in the equation of the energy balance. The model is investigated and allows appearance to certain dimensionless parameters such as a material parameter (K), Prandtl number (Pr), a mixed convection parameter defined by the Grashof number and Reynolds number (GR) ratio, a magnetic parameter called a Hartmann number (Ha) and Eckert number (Ec), as well as dimensionless ratios such us the widths ratio of fluids (H); the thermal conductivity ratio (k*); the thermal expansion coefficients ratio (β*); the viscosities ratio (μ*) and the ratio of the densities (ρ*). The final results of the mathematical model are used to deduce the effect of the magnetic field on the variation of the linear velocities (axial), the microrotation velocity field and temperatures field -transfer heat - so these results are subject to a comparative discussion in the conclusion between our numerical model study taking into account the term of the magnetic diffusivity with another models studied analytically with or without magnetic effect.

4.2. Configuration of the physical model

Because of their high consistencies, non-Newtonian materials are most frequently processed under conditions of laminar flow. Furthermore, shear stresses are generally so high that viscous generation of heat can rarely be neglected, and the distribution of temperature dependence of the rheological properties adds to the complexity of the mass, momentum and energy balance equations. Numerical techniques are often needed to obtain solutions, even for highly idealized conditions of flow. Much of the research activity in this area has related to heat transfer to inelastic non-Newtonian fluids in laminar flow in circular and non-circular ducts, **A. C. Eringen [5-6].** The suggested model theoretically and numerically studied, concerns a vertical channel, figure 1, composed of two infinite isothermal parallel plates, negligible thickness in (OX) axis

direction, limited in (OY) axis direction and maintained at different temperatures T_1 and T_2 where $T_2 > T_1$, under ($B=\sigma^* B_0^2$) a constant magnetic field influence in (OY) axis direction. The channel is composed of two regions filled with an immiscible micropolar and a viscous fluids, the first one is limited by the following condition $-h < y < 0$, with : ρ_1 is a density, μ_1 is a dynamic viscosity, σ is a spinning viscosity, σ^* is a magnetic permeability of fluid, B_0 is a magnetic field coefficient, k_1 is a thermal conductivity, β_1 is a thermal dilation coefficient at a constant pressure and the second region is limited by the following condition $0 < y < h_2$, occupied by a viscous fluid with ρ_2 is a density, μ_2 is a dynamic viscosity, k_2 is a thermal conductivity and β_2 is a thermal dilation coefficient.

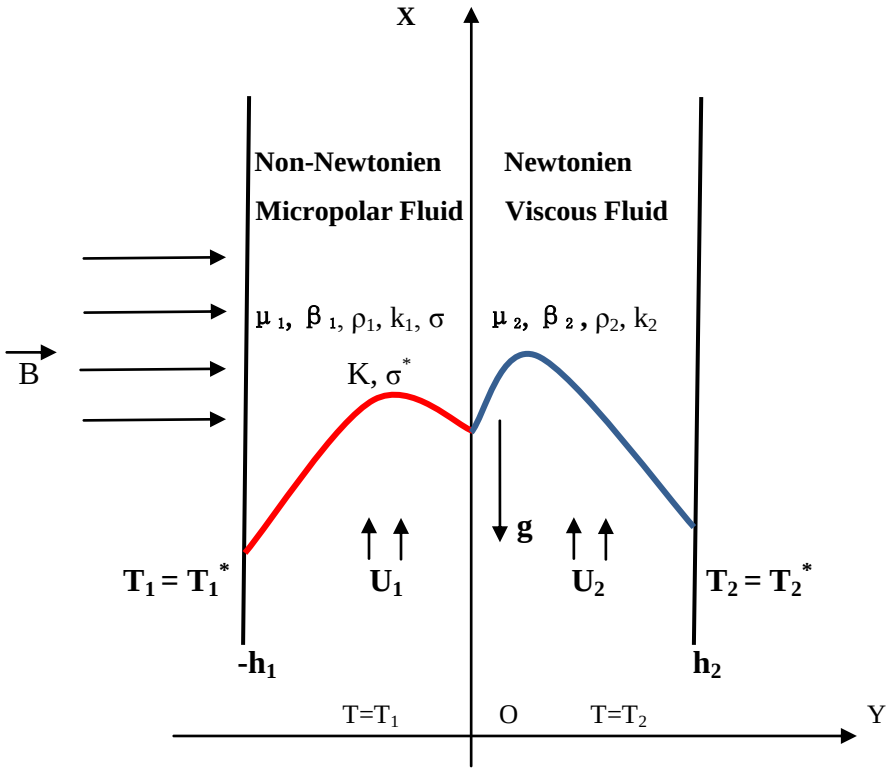

Figure 4.1: suitable diagram of a vertical channel formed of two regions of different type of immiscible fluids, under influence of gravity, magnetic and temperature fields.

4.3. Mathematical formulation

4.3.1. The balances of Continuity, micro/macro Continuum, and energy

In general the two-dimensional Navier-Stocks equations of mass conservation (continuity), macro/micro-continuum and energy equations can be written in forms definite by the physician Eringen for the Non-Newtonian micropolar fluids in the first region.

The two-dimensional continuity equations of both regions.

- First region.

- Continuum balance.

$$\frac{\partial U_1}{\partial X} + \frac{\partial V_1}{\partial Y} = 0 \tag{4.1}$$

- micro/macro momentum.

$$U_1 \frac{\partial U_1}{\partial X} + V_1 \frac{\partial U_1}{\partial Y} = -\frac{1}{\rho_1}\frac{\partial P_1}{\partial X} + \frac{(\mu_1+\sigma)}{\rho_1}\left(\frac{\partial^2 U_1}{\partial X^2} + \frac{\partial^2 U_1}{\partial Y^2}\right) + \frac{\rho_1 g \beta_1 (T_1 - T_1^*)}{\rho_1} + \frac{\sigma}{\rho_1}\frac{\partial n}{\partial Y} - \frac{\sigma^* B_0^2 U_1}{\rho_1} \tag{4.2}$$

$$U_1 \frac{\partial V_1}{\partial X} + V_1 \frac{\partial V_1}{\partial Y} = -\frac{1}{\rho_1}\frac{\partial P_1}{\partial Y} + \frac{(\mu_1+\sigma)}{\rho_1}\left(\frac{\partial^2 V_1}{\partial X^2} + \frac{\partial^2 V_1}{\partial Y^2}\right) - \frac{\sigma}{\rho_1}\frac{\partial n}{\partial X} \tag{4.3}$$

$$j\left(U_1 \frac{\partial n}{\partial X} + V_1 \frac{\partial n}{\partial Y}\right) = -\frac{2\sigma n}{\rho_1} + \frac{\sigma}{\rho_1}\left(\frac{\partial V_1}{\partial X} - \frac{\partial U_1}{\partial Y}\right) + \frac{\gamma}{\rho_1}\left(\frac{\partial^2 n}{\partial X^2} + \frac{\partial^2 n}{\partial Y^2}\right) \tag{4.4}$$

- Energy balance.

$$U_1 \frac{\partial T_1}{\partial X} + V_1 \frac{\partial T_1}{\partial Y} = \frac{k_1}{\rho_1 c_{p1}}\left(\frac{\partial^2 T_1}{\partial X^2} + \frac{\partial^2 T_1}{\partial Y^2}\right) + \frac{\sigma^* B_0^2 U_1^2}{\rho_1 c_{p1}} \tag{4.5}$$

The microrotation viscosity (spin gradient) γ and micro-inertia density j, in the literature, several studies consider the density of the micro-inertia by the following equation:

$$\gamma = \left(\mu_1 + \frac{\sigma}{2}\right) j \tag{4.6}$$

With $j = h_1^2$ the recent model studied, n represents the microrotation velocity designated by the normal vector on the plane (XoY), g represents respectively the gravity acceleration in the first region and the linear or axial velocity in the second region.

- Seconde region

- Continuum balance.

$$\frac{\partial U_2}{\partial X} + \frac{\partial V_2}{\partial Y} = 0 \tag{4.7}$$

- Macroscopic momentum balance

$$U_2\frac{\partial U_2}{\partial X}+V_2\frac{\partial U_2}{\partial Y}=-\frac{1}{\rho_2}\frac{\partial P_2}{\partial X}+\frac{\mu_2}{\rho_2}\left(\frac{\partial^2 U_2}{\partial X^2}+\frac{\partial^2 U_2}{\partial Y^2}\right)+\frac{\rho_2 g\beta_2(T_2-T_2^*)}{\rho_2}-\frac{\sigma^* B_0^2 U_2}{\rho_2} \tag{4.8}$$

$$U_2\frac{\partial V_2}{\partial X}+V_2\frac{\partial V_2}{\partial Y}=-\frac{1}{\rho_2}\frac{\partial P_2}{\partial Y}+\frac{\mu_2}{\rho_2}\left(\frac{\partial^2 V_2}{\partial X^2}+\frac{\partial^2 V_2}{\partial Y^2}\right) \tag{4.9}$$

- Energy balance.

$$U_2\frac{\partial T_2}{\partial X}+V_2\frac{\partial T_2}{\partial Y}=\frac{k_2}{\rho_2 c_p}\left(\frac{\partial^2 T_2}{\partial X^2}+\frac{\partial^2 T_2}{\partial Y^2}\right)+\frac{\sigma^* B_0^2 U_2^2}{\rho_2 c_{p2}} \tag{4.10}$$

4.3.2. Data and hypothesis

We have imagine that each particle of a Non-Newtonian micropolar fluid can translate and independently rotate; this translation is described by the classical motion. Further, we assume that the motion and micromotion are everywhere continuous **[6]**, the fluids were supposed to have constant physical properties except the densities, both fluids are considering incompressible, the flow mode is permanent, regular, laminar and entirely developed, the variation of the densities is considered weak and negligible except in the term gravity force, **J. P. Kumar, N. Kumar, M. Madhu et al, [9],[21],[58]**. It was assumed that the fluid properties, such as the density ρ, the dynamic viscosity μ and the heat conduction λ, are constants. They could therefore be considered as predefined and did not enter into the fluid-mechanical considerations of the quantities of the flow problem as unknowns that were to be computed. Thus the complexity of flow-problem solutions was considerably reduced, as with constant values for ρ, μ and λ the strong coupling between the momentum equations and the energy equation was broken. For the solution of flow problems, it was therefore sufficient to solve the continuity and the momentum equations, i.e. the energy equation had only to be employed when, in addition to the knowledge of the flow field, information on the temperature field of the fluid was needed. In this section, a flow problem will be considered for which it is no longer permissible to neglect the density modifications that occur. Restrictively, it will be assumed, however, that only small density modifications arise, so that the following holds, see **[9],[21],[66],** and **M. A. Hosain et al. & Y. Y. Lok et al, [33],[35]** are given by

$$\rho_1=\rho_0[1-\beta_1(T_1-T_1^*)] \tag{4.11}$$

$$\rho_2=\rho_0[1-\beta_2(T_2-T_2^*)] \tag{4.12}$$

4.4. Physical model without magnetic field effect

In using the hypothesis set out in subsection (4.3 .2) we obtained.

$$V_1 = V_2 = 0 \tag{4.13}$$

$$\frac{dU_1}{dX} = \frac{dU_2}{dX} = 0 \tag{4.14}$$

The motion equations of region 1, will be.

$$\frac{dU_1}{dX} = 0 \tag{4.15}$$

$$(\mu_1 + \sigma)\frac{d^2U_1}{dY^2} + \rho_1 g\beta_1(T_1 - T_1^*) + \sigma\frac{dn}{dY} = 0 \tag{4.16}$$

$$\gamma\frac{d^2n}{dY^2} - \sigma(2n + \frac{dU_1}{dY}) = 0 \tag{4.17}$$

$$\frac{d^2T_1}{dY^2} = 0 \tag{4.18}$$

The motion equations of region 2, will be :

$$\frac{dU_2}{dX} = 0 \tag{4.19}$$

$$\mu_2\frac{d^2U_2}{dY^2} + \rho_2 g\beta_2(T_2 - T_2^*) = 0 \tag{4.20}$$

$$\frac{d^2T_2}{dY^2} = 0 \tag{4.21}$$

4.4.1. Analytical solution

To solve the differential equations (4.15) - (4.21) which represent the free-convective flow in first and second regions, the equations (4.6), (4.11) & (4.12) are used in the absence of magnetic field, six boundary conditions were considered about velocity profiles and four boundary conditions for temperature profiles, in supposing that the flow is null for Y=- h_1 and Y = h_2 (points in front of the both walls); for Y=0 the immiscibility interface separate the fluids it's supposed that the continuity of linear velocity, equality between the shearing forces and the microrotation velocity is constant there, see **A. Ishak et al, [7]**.

A. The boundary and interface conditions

Thus the mathematical relations of the boundary conditions are as follows:

Velocities:

$$Y = -h_1 \Longrightarrow U_1 = 0\ ; Y = h_2 \Longrightarrow U_2 = 0\ ; Y = 0 \Longrightarrow U_1(0) = U_2(0) \tag{4.22}$$

$$\text{et}\ \frac{dn}{dY} = 0\ ; (\mu_1 + \sigma)\frac{dU_1}{dY} + \sigma n = \mu_2 \frac{dU_2}{dY} \tag{4.23}$$

$$Y = -h_1 \Rightarrow n = 0 \tag{4.24}$$

Temperatures:

$$Y = -h_1 \Rightarrow T_1 = T_1^*\ ; Y = h_2 \Rightarrow T_2 = T_2^*;\ Y = 0\ \Longrightarrow T_1(0) = T_2(0)\ \&\ k_1 \frac{dT_1}{dY} = k_2 \frac{dT_2}{dY} \tag{4.25}$$

B. Introduce the dimensionless variables

This step consist to introduce a dimensionless variables, because we're eliminated all dimensions (put, second, Kelvin, ...), h_1, h_2, T_1, T_2, ... and we limit our study to an interval the variable will be dimensionless and ranges over the interval defined and takes the values of [-1,0] ∪ [0.1] respectively for the two regions, the procedures are.

$$u_1 = \frac{U_1}{U_0}; u_2 = \frac{U_2}{U_0}; \theta_1 = \frac{T_1 - T_1^*}{\Delta T}\ ;\ \theta_2 = \frac{\mathbf{T_2 - T_2^*}}{\mathbf{\Delta T}} \text{ with } \Delta T = T_1^* - T_2^*\ \&\ T_1^* > T_2^*$$

$$N = \frac{h_1}{U_0} n; K = \frac{\sigma}{\mu_1}\ ; d\theta_1 = \frac{dT_1}{T_1^* - T_2^*} \Leftrightarrow dT_1 = \Delta T\, d\theta_1\ \&\ dT_2 = \Delta T\, d\theta_2$$

$$y = \frac{Y}{h_i}\ \left(y = \frac{Y}{h_1}, \text{region1};\ y = \frac{Y}{h_2}, \text{region2}\right); \text{Moreover } dY = h_1 dy\ \&\ dY = h_2 dy$$

- First region

Introduce the dimensionless variables - above paragraph (B) - in equations (4.15) - (4.18), we obtain:

Dimensionless motion equations of region1

$$U_0 \frac{du_1}{dx} = 0, U_0 \neq o \Longrightarrow \frac{du_1}{dx} = 0 \tag{4.26}$$

$$\mu_1 \frac{U_0}{h_1^2}(1 + K)\frac{d^2 u_1}{dy^2} + \rho_1 g \beta_1 (T_1 - T_1^*) + \sigma \frac{U_0}{{h_1}^2}\frac{dN}{dy} = 0 \tag{4.27}$$

$$\mu_1 \frac{U_0}{{h_1}^3} h_1^2 \left(1 + \frac{K}{2}\right) \frac{d^2N}{dy^2} - \sigma(2\frac{U_0}{h_1} N + \frac{U_0}{h_1}\frac{du_1}{dy}) = 0 \quad (4.28)$$

$$\Delta T \frac{d^2\theta_1}{dy^2} = 0 \quad (4.29)$$

$$\frac{\mu_1 U_0}{h_1^2}(1+K)\frac{d^2u_1}{dy^2} + \rho_1 g \beta_1 (T_1 - T_1^*) + \sigma \frac{U_0}{{h_1}^2}\frac{dN}{dy} = 0$$

$$\frac{d^2u_1}{dy^2} + \frac{1}{(1+K)}\frac{h_1^2 \rho_1 g \beta_1}{\mu_1 U_0}(T_1 - T_1^*) + \frac{1}{(1+K)}\frac{\sigma}{\mu_1}\frac{dN}{dy} = 0$$

$$\frac{d^2u_1}{dy^2} + \frac{1}{(1+K)}\frac{1}{\left(\frac{U_0 h_1 \rho_1}{\mu_1}\right)}\left(\frac{h_1^3 \rho_1^2 g \beta_1 \Delta T}{\mu_1^2}\right)\theta_1 + \frac{K}{(1+K)}\frac{dN}{dy} = 0$$

$$\frac{d^2u_1}{dy^2} + \frac{1}{(1+K)}\frac{Gr}{Re}\theta_1 + \frac{K}{(1+K)}\frac{dN}{dy} = 0 \quad (4.30)$$

Following the changes of variables specified in paragraph (B), equations (4.28), (4.29) are as follows:

$$\frac{\mu_1 U_0}{h_1}\left(\frac{2+K}{2}\right)\frac{d^2N}{dy^2} - \frac{\sigma U_0}{h_1}(2N + \frac{du_1}{dy}) = 0$$

$$\frac{d^2N}{dy^2} - \frac{2}{(2+K)}\frac{\sigma}{\mu_1}(2N + \frac{du_1}{dY}) = 0$$

$$\frac{d^2N}{dy^2} - \frac{2K}{(2+K)}(2N + \frac{du_1}{dy}) = 0$$

$$\frac{d^2N}{dy^2} - \frac{2K}{(2+K)}\left(2N + \frac{du_1}{dy}\right) = 0 \quad (4.31)$$

$$\frac{d^2\theta_1}{dy^2} = 0 \quad (4.32)$$

With: $GR = \frac{Gr}{Re}$; $Gr = \frac{h_1^3 \rho_1^2 \beta_1 g \Delta T}{\mu_1^2}$ & $Re = \frac{\rho_1 h_1 U_0}{\mu_1}$; $K_1 = \frac{1}{(1+K)}$; $K_2 = \frac{K}{(1+K)}$; $K_3 = \frac{2K}{(2+K)}$;

The final dimensionless differential equations that describe the motion in the first channel region (4.26), (4.30), (4.31), and (4.32) takes the following form.

$$u_1'(x) = 0 \quad (4.33)$$

$$u_1''(y) + K_1 . GR . \theta_1(y) + K_2 . N'(y) = 0 \quad (4.34)$$

$$N''(y) - 2K_3 . N - K_3 . u_1'(y) = 0 \quad (4.35)$$

$$\theta_1'' = 0 \tag{4.36}$$

- Second region

By the same method, one replace the dimensionless variables in equations from (4.19) - (4.21):

$$\frac{du_2}{dx} = 0 \tag{4.37}$$

$$\frac{\mu_2 U_0}{h_2^2}\frac{d^2u_2}{dy^2} + \rho_2 g\beta_2(T_1^* - T_2^*)\theta_2 = 0$$

$$\frac{d^2u_2}{dy^2} + \frac{h_2^2\rho_2 g\beta_2 \Delta T}{\mu_2 U_0}\theta_2 = 0$$

$$\frac{d^2u_2}{dy^2} + \frac{h_2^2\rho_2\mu_1 g\beta_2 h_1^3\rho_1^2\beta_1\Delta T}{\rho_1 h_1^2\mu_2\beta_1\left(\frac{U_0 h_1\rho_1}{\mu_1}\right)\mu_1^2}\theta_2 = 0$$

$$\frac{d^2u_2}{dy^2} + \frac{h_2^2\rho_2\mu_1\beta_2}{h_1^2\rho_1\mu_2\beta_1}\frac{\left(\frac{h_1^3\rho_1^2\beta_1 g\Delta T}{\mu_1^2}\right)}{\left(\frac{U_0 h_1\rho_1}{\mu_1}\right)}\theta_2 = 0$$

$$\frac{d^2u_2}{dy^2} + h^{*2}.\rho^*.\mu^*.\beta^*\frac{Gr}{Re}.\theta_2 = 0 \tag{4.38}$$

$$\frac{(T_1^* - T_2^*)}{h_2^2}\frac{d^2\theta_2}{dy^2} = 0$$

$$\frac{d^2\theta_2}{dy^2} = 0 \tag{4.39}$$

The final dimensionless differential equations that describe the motion in the second region of the channel (4.36) - (4.38) takes the following form.

$$u_2'(x) = 0 \tag{4.40}$$

$$u_2''(y) + h^{*2}.\rho^*.\mu^*.\beta^*.\frac{Gr}{Re}.\theta_2(y) = 0 \tag{4.41}$$

$$\theta_2''(y) = 0 \tag{4.42}$$

C. The interface and boundary conditions

The final dimensionless of interface and boundary conditions are as follows:

- Velocities forms.

$Y = -h_1 \Rightarrow y = -1,\ u_1 = 0$ et $N = 0$

$Y = h_2 \Rightarrow y = 1 \Rightarrow u_2 = 0$

$u_1(0) = u_2(0),\ N'(0) = 0$; $(\mu_1 + \sigma)\frac{U_0}{h_1}\frac{du_1}{dy} + \sigma\frac{U_0}{h_1}N = \mu_2\frac{U_0}{h_2}\frac{du_2}{dy} \Leftrightarrow (\mu_1 + \sigma)\frac{du_1}{dy} + \sigma N =$

$\mu_2\frac{h_1}{h_2}\frac{du_2}{dy}$

$\Leftrightarrow (\mu_1 + \sigma)\frac{du_1}{dy} + \sigma N = \mu_2\frac{h_1}{h_2}\frac{du_2}{dy} \Leftrightarrow (1 + K)\frac{du_1}{dy} + K.N = \frac{\mu_2}{\mu_1}.\frac{h_1}{h_2}.\frac{du_2}{dy}$

$$\frac{du_1}{dy} + \frac{K}{(1+K)}N = \frac{1}{\mu^* h^* (1+K)}\frac{du_2}{dy}$$

$$\Longrightarrow u_1' + K_2.N = \frac{K_1.h^*}{\mu^*}u_2' \qquad (4.43)$$

- Temperature forms.

$\theta_1(-1) = 0$ et $\theta_2(1) = 0$;

Et $Y = 0 \Rightarrow y = 0 \Longrightarrow T_1 = T_2 \Longrightarrow T_1 - T_1^* - T_2^* = T_2 - T_2^* - T_1^* \Rightarrow \frac{T_1 - T_1^*}{\Delta T} - \frac{T_2^*}{\Delta T} = \frac{T_2 - T_2^*}{\Delta T} - \frac{T_1^*}{\Delta T}$

$$\frac{T_1 - T_1^*}{\Delta T} = \frac{T_2 - T_2^*}{\Delta T} - \frac{T_1^*}{\Delta T} + \frac{T_2^*}{\Delta T} \Longrightarrow \theta_1(0) = \theta_2(0) - \frac{(T_1^* - T_2^*)}{\Delta T} \Rightarrow \theta_1(0) = \theta_2(0) - \frac{\Delta T}{\Delta T}$$

$$\Rightarrow \theta_1(0) = \theta_2(0) - 1 \qquad (4.44)$$

et $\frac{k_1}{h_1}\frac{d\theta_1}{dy} = \frac{k_2}{h_2}\frac{d\theta_2}{dy} \Leftrightarrow \frac{k_1}{k_2}\frac{d\theta_1}{dy} = \frac{h_1}{h_2}\frac{d\theta_2}{dy}$

$$\Leftrightarrow \theta_1' = \frac{h}{k^*}\theta_2' \qquad (4.45)$$

With: $\mu^* = \frac{\mu_1}{\mu_2}; h^* = \frac{h_1}{h_2}; k^* = \frac{k_1}{k_2}; \beta^* = \frac{\beta_1}{\beta_2}; \rho^* = \frac{\rho_1}{\rho_2}$

According to the hypothesis specified in paragraph (4.2), equations (4.34) - (4.36) (4.40) - (4.42) can be written as follows:

$$u_1''(y) + K_1.GR.\theta_1(y) + K_2.N'(y) = 0 \qquad (4.46)$$

$$N'' - 4K_3.N - 2K_3.u_1' = 0 \qquad (4.47)$$

$$\theta_1'' = 0 \tag{4.48}$$

$$u_2'' + h^{*2}\rho^*.\mu^*.\beta^*.GR.\theta_2 = 0 \tag{4.49}$$

$$\theta_2'' = 0 \tag{4.50}$$

We integrate the differential equations, (4.48), (4.50) we obtain:

$$\frac{d^2\theta_1}{dy^2} = 0 \Longrightarrow \frac{d\theta_1}{dy} = c_1 \Longrightarrow \int d\theta_1 = c_1 \int dy \Longrightarrow \theta_1 = c_1 y + c_2$$

$$\frac{d^2\theta_2}{dy^2} = 0 \Longrightarrow \frac{d\theta_2}{dy} = c_3 \Longrightarrow \int d\theta_2 = c_3 \int dy \Longrightarrow \theta_2 = c_3 y + c_4$$

So the dimensionless functions of temperatures.

$$\theta_1 = c_1.y + c_2 \tag{4.51}$$

$$\theta_2 = c_3.y + c_4 \tag{4.52}$$

With the following differential equations:

$$u_2'' + h^{*2}.\rho^*.\mu^*.\beta^*.GR.\theta_2 = 0 \Longrightarrow u_2'' + h^{*2}\rho^*.\mu^*.\beta^* GR.(c_3.y + c_4) = 0 \Longrightarrow$$

$$u_2'' = -c_3.h^{*2}.\rho^*.\mu^*.\beta^*.GR.y - h^{*2}.\rho^*.\mu^*.\beta^*.GR.c_4$$

By double integral we obtained:

$$u_2' = -\frac{c_3.h^{*2}.\rho.\mu^*.\beta^*.GR}{2}y^2 - c_4.h^{*2}.\rho.\mu^*.\beta^*.GR.y - c_9$$

$$u_2 = -\frac{h^{*2}.\rho.\mu^*.\beta^*.GR}{6}(c_3y^3 + 3c_4y^2) - c_9y - c_{10} \tag{4.53}$$

To solve the equation (4.47), we are used the method of parameter variations, the form of the equation (4.47) shows that N has a solution of the following form. See **R. Branson,** [87].

$$N = N_h + N_p \tag{4.54}$$

$N_h'' - \frac{4K}{(2+K)}N_h = 0$; The form of this equation is: $f'' + D.f = 0$ it admits a solution under form: $N_h = c_5\,ch(\sqrt{D}.y) + c_6 sh(\sqrt{D}.y)$; et $D = \frac{4K}{(2+K)}$.

So the solution of N is:

$$N = c_5\,\mathrm{ch}\left(\sqrt{D}.y\right) + c_6\,\mathrm{sh}\left(\sqrt{D}.y\right) + N_p \tag{4.55}$$

The particulate solution of N is.

$$N_p = C_1(y)N_1 + C_2(y)N_2 \tag{4.56}$$

$$\text{with : } N_1 = \mathrm{ch}\left(\sqrt{D}.y\right) \text{ et } N_2 = \mathrm{sh}\left(\sqrt{D}.y\right)$$

$C_1(y)$ and $C_2(y)$ are Two functions to determine, that represent a solutions for the system of equations (4.55) &(4.56), written in matrix form to solve:

$$\begin{cases} C_1'N_1 + C_2'N_2 = 0 \\ C_1'N_1' + C_2'N_2' = \frac{2K}{(2+K)}u_1' \end{cases} \tag{4.57}$$

$$\Longrightarrow \begin{pmatrix} N_1 & N_2 \\ N_1' & N_2' \end{pmatrix}\begin{pmatrix} C_1' \\ C_2' \end{pmatrix} = \begin{pmatrix} 0 \\ \frac{2K}{(2+K)}u_1' \end{pmatrix} \Longrightarrow \begin{pmatrix} C_1' \\ C_2' \end{pmatrix} = \begin{pmatrix} N_1 & N_2 \\ N_1' & N_2' \end{pmatrix}^{-1}\begin{pmatrix} 0 \\ \frac{2K}{(2+K)}u_1' \end{pmatrix} \tag{4.58}$$

$$\Longrightarrow \begin{pmatrix} N_1 & N_2 \\ N_1' & N_2' \end{pmatrix}^{-1} = \frac{1}{\det}\left[\mathrm{adj}\begin{pmatrix} N_1 & N_2 \\ N_1' & N_2' \end{pmatrix}\right]^t = \frac{1}{\sqrt{D}}\begin{pmatrix} N_1' & -N_1 \\ -N_2' & N_2 \end{pmatrix} = \frac{1}{\sqrt{D}}\begin{pmatrix} \sqrt{D}\mathrm{ch}(\sqrt{D}y) & \mathrm{sh}(\sqrt{D}y) \\ -\sqrt{D}\mathrm{sh}(\sqrt{D}y) & \mathrm{ch}(\sqrt{D}y) \end{pmatrix}$$

From equation (4.58) we obtained:

$$\begin{cases} C_1' = -\frac{2K}{(2+K)\sqrt{D}}\mathrm{sh}\left(\sqrt{D}y\right).u_1' \\ C_2' = \frac{2K}{(2+K)\sqrt{D}}\mathrm{ch}\left(\sqrt{D}y\right).u_1' \end{cases} \Longrightarrow \begin{cases} \int C_1' = -\frac{2K}{(2+K)\sqrt{D}}\int \mathrm{sh}\left(\sqrt{D}y\right).u_1' \\ \int C_2' = \frac{2K}{(2+K)\sqrt{D}}\int \mathrm{ch}\left(\sqrt{D}y\right).u_1' \end{cases}$$

$$\Longrightarrow \begin{cases} C_1 = -\frac{2K}{(2+K)\sqrt{D}}\int \mathrm{sh}\left(\sqrt{D}y\right).u_1' \\ C_2 = \frac{2K}{(2+K)\sqrt{D}}\int \mathrm{ch}\left(\sqrt{D}y\right).u_1' \end{cases} \Longrightarrow \begin{matrix} C_1 = -\frac{2K}{(2+K)\sqrt{D}}\left(\mathrm{sh}\left(\sqrt{D}y\right)u_1 - \sqrt{D}\mathrm{ch}(\sqrt{D}y)\right) \\ C_2 = \frac{2K}{(2+K)\sqrt{D}}\left(\mathrm{ch}\left(\sqrt{D}y\right)u_1 - \sqrt{D}\mathrm{sh}(\sqrt{D}y)\right) \end{matrix}$$

The relations of C_1 et C_2 obtained above, thus this equality: $\frac{2K}{(2+K)\sqrt{D}} = \frac{\sqrt{D}}{2}$, are replaced in (4.56), the equation (4.55) becomes:

$$N = c_7\,\mathrm{ch}\left(\sqrt{D}.y\right) + c_8\,\mathrm{sh}\left(\sqrt{D}.y\right) + \frac{GR}{2(2+K)}\left[c_1y^2 + 2c_2y + \frac{2c_1}{D}\right] \tag{4.59}$$

$$N' = \sqrt{D}c_7\,\mathrm{sh}\left(\sqrt{D}.y\right) + \sqrt{D}c_8\,\mathrm{ch}\left(\sqrt{D}.y\right) + \frac{GR}{(2+K)}[c_1y + c_2] \tag{4.60}$$

With: ch & sh, present the hyperbolic cosine & sine.

From the equations (4.46) & (4.47) we obtained:

$$u_1' = -\frac{K}{(1+K)}\left[c_7 ch\left(\sqrt{D}y\right) + c_8 sh(\sqrt{D}y)\right] - \frac{2GR}{(2+K)}\left(\frac{c_1}{2}y^2 + c_2 y\right) - c_7 \quad (4.61)$$

$$u_1 = -\frac{K}{\sqrt{D}(1+K)}\left[c_5 sh\left(\sqrt{D}y\right) + c_6 ch(\sqrt{D}y)\right] - \frac{2GR}{(2+K)}\left(\frac{c_1}{6}y^3 + \frac{c_2}{2}y^2\right) - c_7 y - c_8 \quad (4.62)$$

4.4.2. Calculation of Constants

A. Particular case, Newtonian-viscous fluid (K=0)

The equations that govern the fluids motions in both regions become:

$$\theta_1 = c_1 y + c_2 \quad (4.63)$$

$$\theta_2 = c_3 y + c_4 \quad (4.64)$$

$$u_1 = -GR\frac{c_1}{6}y^3 - GR\frac{c_2}{2}y^2 + e_1 y + e_2 \quad (4.65)$$

$$u_2 = -h^{*2}.\rho^*.\mu^*.\beta^*.GR\frac{c_3}{6}y^3 - h^{*2}.\rho^*.\mu^*.\beta^*.GR\frac{c_4}{2}y^2 + e_3 y + e_4 \quad (4.66)$$

$$u_1' = \frac{h^*}{\mu^*}u_2' \text{ ; à } y = 0 \quad (4.67)$$

The interface and boundary conditions become:

$$\text{When, } y = -1 \Rightarrow \begin{cases} u_1 = 0 \\ \theta_1 = 1 \end{cases} \Leftrightarrow \begin{cases} \frac{GR}{6}c_1 - \frac{GR}{2}c_2 - e_1 + e_2 = 0 & (4.68) \\ c_2 - c_1 = 1 & (4.69) \end{cases}$$

$$\text{When, } y = 1 \Rightarrow \begin{cases} u_2 = 0 \\ \theta_2 = 0 \end{cases} \Leftrightarrow \begin{cases} -\frac{h^{*2}\rho^*.\mu^*.\beta^*GR}{6}c_3 - \frac{h^{*2}\rho.\mu^*.\beta^*GR}{2}c_4 + e_3 + e_4 = 0 & (4.70) \\ c_3 + c_4 = 0 & (4.71) \end{cases}$$

$$\text{When, } y = 0 \Rightarrow \begin{cases} u_1 = u_2 \\ u_1' = \frac{1}{\mu^*.h^*}u_2' \\ \theta_1 = \theta_2 \\ \theta_1' = \frac{1}{h^*k^*}\theta_2' \end{cases} \Leftrightarrow \begin{cases} e_2 = e_4 & (4.72) \\ e_1 = \frac{1}{\mu^*.h^*}e_3 & (4.73) \\ c_2 = c_4 & (4.74) \\ c_1 = \frac{1}{h^*k^*}c_3 & (4.75) \end{cases}$$

By using equations (4.43) - (4.50), we obtained the following results:

$$c_1 = -\frac{1}{1+h^*k^*};\ c_2 = c_4 = -h^*k^*c_1;\ c_3 = h^*k^*c_1;\ e_1 = -\frac{GR(1+3h^*k^*+2h^{*3}\rho^*.\mu^*.\beta^*k^*)}{6(1+\mu^*h^*)(1+h^*k^*)};$$

$$e_2 = e_4 = \frac{\mu^* h^* . GR(1 + 3h^* k^* - 2h^{*2}\rho^* . \beta^* k^*)}{6(1 + \mu^* h^*)(1 + h^* k^*)};\ e_3 = \mu^* h^* . e_1$$

B. Micropolar fluid case (K ≠ 0)

Calculation of constants: $C_1, C_2, C_3, C_4, C_5, C_6, C_7, C_8, C_9$, by using the interface and boundary conditions we obtained.

At:

$y = -1 \Rightarrow$

$$\begin{cases} u_1 = 0 \\ N = 0 \\ \theta_1 = 1 \end{cases} \Leftrightarrow \begin{cases} \frac{GR}{3(2+K)} c_1 - \frac{GR}{(2+K)} c_2 + \frac{K\sinh(-\sqrt{D})}{\sqrt{D}(1+K)} c_7 + \frac{K\cosh(-\sqrt{D})}{\sqrt{D}(1+K)} c_8 - c_9 + c_{10} = 0 & (4.76) \\ \frac{GR(D+2)}{2D(2+K)} c_1 - \frac{GR}{(2+k)} c_2 + \cosh(-\sqrt{D}) c_7 + \sinh(-\sqrt{D}) c_8 = 0 & (4.77) \\ c_2 - c_1 = 1 & (4.78) \end{cases}$$

At :

$y = 0 \Rightarrow$

$$\begin{cases} u_1' + \frac{K}{(1+K)} N = \frac{1}{\mu^* h^* (1+K)} u_2' \\ N' = 0 \\ \theta_1 = \theta_2 \\ \theta_1' = \frac{1}{h^* k^*} \theta_2' \\ u_1 = u_2 \end{cases} \Leftrightarrow \begin{cases} \frac{GR.K}{D(2+K)} c_1 - \frac{1}{\mu^* h} c_5 + 2K c_7 = 0 & (4.79) \\ \frac{GR}{(2+K)} c_2 + \sqrt{D} c_8 = 0 & (4.80) \\ c_2 = c_4 & (4.81) \\ c_1 = \frac{1}{h^* k^*} c_3 & (4.82) \\ c_6 - \frac{K}{\sqrt{D}(1+K)} c_8 - c_{10} = 0 & (4.83) \end{cases}$$

À :

$y = 1 \Rightarrow$

$$\begin{cases} u_2 = 0 \\ \theta_2 = 0 \end{cases} \Leftrightarrow \begin{cases} -\frac{\rho^* . \mu^* . \beta^* h^{*2} . GR}{6} c_3 - \frac{\rho^* . \mu^* . \beta^* h^{*2} . GR}{2} c_4 + c_5 + c_6 = 0 & (4.84) \\ c_3 + c_4 = 0 & (4.85) \end{cases}$$

By the sum of equations (4.53) (4.54) et (4.58) we obtained:

$$c_2 - \frac{1}{h^* k^*} c_3 = 1 \ \& \ c_2 = c_4 \Rightarrow\ c_4 - \frac{1}{h^*} c_3 = 1 \qquad (4.86)$$

and : $c_3 = h^* k^* . c_1$, $c_4 = c_2 = -h^* k^* . c_1$ & $c_1 = -\frac{1}{(1+h^* k^*)}$

From the equations (4.48), (4.51), (4.52) , (4.55), (4.56) we obtained:

$$c_8 = a_2 + c_7;\ c_7 = \frac{a_3 + a_5 - a_2 - a_4}{(1 + \mu^* h^* (1 + k^*))}$$

Where: tanh(....): present the hyperbolic tangent.

$$c_5 = \frac{a_1 + c_6 \sinh(\sqrt{D})}{\cosh(\sqrt{D})}$$

$$c_6 = -\frac{c_2 GR}{((2+K)\sqrt{D})}$$

$$c_{10} = c_6 - \frac{K}{\sqrt{D}(1+K)} c_8$$

$$c_9 = a_3 - c_{10}$$

Accordingly to the results obtained later, the constants a_1, a_2, a_3, a_4 & a_5, are us follows:

$$\begin{cases} a_1 = \frac{GR(c_1 - 2c_2 + \frac{2c_1}{D})}{2(2+K)} - \frac{2A}{D(2+K)} \\ a_2 = -h^*k^*.c_1 \\ a_2 = \frac{K(c_5 \sinh(\sqrt{D}) - c_6 \cosh(\sqrt{D}))}{(1+K)} + \frac{2GR}{(2+K)}(\frac{c_1}{6} - \frac{c_2}{2}) \\ a_3 = -\rho^*.\mu^*.\beta^*.h^{*2}.GR(\frac{c_3}{6} + \frac{c_4}{6}) \\ a_4 = \frac{c_6 K}{(1+K)\sqrt{D}} \\ a_5 = \mu^*.h^*.K.(c_1 R + 2E) \\ E = \frac{GR.L_1}{L_2} \\ L_1 = 2(1+K)(2+K)D\sqrt{D}[3\mu^* h^*.c_1 K - \mu^*.\beta^* h^{*2} c_1] - c_1 + 3c_2 - \rho^*.\mu^*.\beta^*.h^{*2}(2+K) \\ +2K\sqrt{D}(2Dc_2 + c_1(2+D)\tanh(\sqrt{D})) + 2Kc_2\sqrt{D}(1+\cosh(\sqrt{D})) - c_1 D\sqrt{D}(1+K) \\ L_2 = 2D\sqrt{D}(1+K)(3+K-4\mu^* h^* K) - 4K\tanh(\sqrt{D}) \end{cases}$$

The functions defined the dimensionless linear and microrotation velocities are determined and provided by Annex A:

$u_1(y, GR), u_2(y, GR)$ et $N(y, GR), u_1(y, \mu^*), u_2(y, \mu^*)$ et $N(y, \mu^*), u_1(y, h^*), u_2(y, h^*)$ et $N(y, h^*)$

$u_1(y, k^*), u_2(y, k^*)$ et $N(y, k^*), u_1(y, K), u_2(y, K), N(y, K), u_1(y, \beta^*), u_2(y, \beta^*)$ et $N(y, \beta^*)$,

$u_1(y, \rho^*), u_2(y, \rho^*), N(y, \rho^*)$.

$y \in [-1,1]; GR = \{5,10,15\}; \mu^* = \{1,2,3\}; h^* \in \{0.1,1,2,3\}; k^* \in \{0.1,1,2,3\}; K = \{1,2,3\};$

$\beta^* = \{0.2,0.5,0.7\}; \rho^* = \{0.2,0.5,0.7\}$

4.5. Physical model in presence of a magnetic field

4.5.1. Mathematical Formulation

In using the same hypothesis indicated in paragraph (4.3.2) we obtained.

$$V_1 = V_2 = 0 \tag{4.87}$$

$$\frac{dU_1}{dX} = \frac{dU_2}{dX} = 0 \tag{4.88}$$

The motion equations of region1.

$$\frac{dU_1}{dX} = 0 \tag{4.89}$$

$$(\mu_1 + \sigma)\frac{d^2U_1}{dY^2} + \rho_1 g\beta_1(T_1 - T_1^*) - \sigma^* B_0^2 U_1 + \sigma\frac{dn}{dY} = 0 \tag{4.90}$$

$$\gamma\frac{d^2n}{dY^2} - \sigma(2n + \frac{dU_1}{dY}) = 0 \tag{4.91}$$

$$\frac{\sigma^* B_0^2}{\rho_1 C_{p1}} U_1^2 + \alpha_1 \frac{d^2T_1}{dY^2} = 0 \tag{4.92}$$

The motion equations of region 2 :

$$\frac{dU_2}{dX} = 0 \tag{4.93}$$

$$\mu_2 \frac{d^2U_2}{dY^2} + \rho_2 g\beta_2(T_2 - T_2^*) - \sigma^* B_0^2 U_2 = 0 \tag{4.94}$$

$$\frac{\sigma^* B_0^2}{\rho_2 C_{p2}} U_2^2 + \alpha_2 \frac{d^2T_2}{dY^2} = 0 \tag{4.95}$$

4.5.2. Numerical results of the model

The differential equations system from (4.90)-(4.95) doesn't admit analytical solutions, in this case, we will use of variable change techniques to arrive at a dimensionless mathematical model, this step of work is similar to that in section (4.4.1,B), so the procedure is as follows:

$$y = \frac{Y}{h_{i=1,2}} \implies Y = y.h_{i=1,2} \; ; \; u_{i=1,2} = \frac{U_{i=1,2}}{U_0} \implies U_{i=1,2} = U_0.u_{i=1,2} \; \& \; N = \frac{h_1}{U_0} n$$

- Non-Newtonian micropolar/Newtonian-viscous fluids system.

- Region1.

- step1.

$$\frac{\mu_1 U_0}{h_1^2}(1+K)\frac{d^2u_1}{dy^2}+\rho_1 g\beta_1(T_1-T_1^*)+\sigma\frac{U_0}{{h_1}^2}\frac{dN}{dy}-\sigma^* B_0^2 U_0 u_1=0$$

$$\frac{\mu_1 U_0}{h_1}\left(\frac{2+K}{2}\right)\frac{h_1^2}{h_1^2}\frac{d^2N}{dy^2}-\frac{\sigma U_0}{h_1}(2N+\frac{du_1}{dy})=0$$

$$\frac{\sigma^* B_0^2 U_0^2}{\rho_1 C_{p1}}u_1^2+\frac{k_1}{\rho_1 C_{P1} h_1^2}\frac{d^2T_1}{dy^2}=0$$

- step2.

$$(1+K)\frac{d^2u_1}{dy^2}+\frac{\rho_1 g\beta_1 h_1^2}{\mu_1 U_0}(T_1-T_1^*)+K\frac{dN}{dy}-\frac{\sigma^* B_0^2 h_1^2}{\mu_1}u_1=0$$

$$\left(\frac{2+K}{2}\right)\frac{d^2N}{dy^2}-K(2N+\frac{du_1}{dy})=0$$

$$\frac{\sigma^* B_0^2 h_1^2}{\mu_1}u_1^2+\frac{k_1}{U_0^2\mu_1}\frac{d^2T_1}{dy^2}=0$$

According to the following data:

$T_1-T_1^*=(T_1^*-T_2^*)\theta_1;\ (T_1^*-T_2^*)=\Delta T\Longrightarrow T_1=\Delta T\theta_1+T_1^*\ \&\ T_2-T_2^*=(T_1^*-T_2^*)\theta_1$, we derive these equation, we obtain: $\frac{d^2T_1}{dy^2}=\Delta T\frac{d^2\theta_1}{dy^2}\ \&\ \frac{d^2T_2}{dy^2}=\Delta T\frac{d^2\theta_2}{dy^2}$.

- Step 3.

$$(1+K)\frac{d^2u_1}{dy^2}+\frac{\rho_1 g\beta_1 h_1^2}{\mu_1 U_0}(T_1-T_1^*)+K\frac{dN}{dy}-\frac{\sigma^* B_0^2 h_1^2}{\mu_1}u_1=0$$

$$\left(\frac{2+K}{2}\right)\frac{d^2N}{dy^2}-K(2N+\frac{du_1}{dy})=0$$

$$\frac{\sigma^* B_0^2 h_1^2}{\mu_1}u_1^2+\frac{k_1\Delta T}{U_0^2\mu_1}\frac{d^2\theta_1}{dy^2}=0$$

- Step 4.

$$\frac{d^2u_1}{dy^2}+\frac{1}{(1+K)}\frac{\mu_1}{\rho_1 h_1 U_0}\left(\frac{h_1^3\rho_1^2 g\beta_1\Delta T}{\mu_1^2}\right)\theta_1+\frac{K}{(1+K)}\frac{dN}{dy}-\frac{1}{(1+K)}\left(\frac{h_1^2\sigma^* B_0^2}{\mu_1}\right)u_1=0$$

$$\frac{d^2N}{dy^2} - \frac{4K}{(2+K)}N - \frac{2K}{(2+K)}\frac{du_1}{dy} = 0$$

$$\left(\frac{h_1^2\sigma^* B_0^2}{\mu_1}\right)u_1^2 + \frac{k_1\Delta T}{U_0^2\mu_1}\frac{d^2\theta_1}{dy^2} = 0$$

- Step 5.

$$\frac{d^2u_1}{dy^2} + \frac{1}{(1+K)}\frac{Gr}{Re}\theta_1 + \frac{K}{(1+K)}\frac{dN}{dy} - \frac{Ha}{(1+K)}u_1 = 0$$

$$\frac{d^2N}{dy^2} - \frac{4K}{(2+K)}N - \frac{2K}{(2+K)}\frac{du_1}{dy} = 0$$

$$Ha.u_1^2 + \frac{k_1\Delta T}{U_0^2\mu_1}\frac{d^2\theta_1}{dy^2} = 0$$

- Step 6.

$$\frac{d^2u_1}{dy^2} + \frac{GR}{(1+K)}\theta_1 + \frac{K}{(1+K)}\frac{dN}{dy} - \frac{Ha}{(1+K)}u_1 = 0$$

$$\frac{d^2N}{dy^2} - \frac{4K}{(2+K)}N - \frac{2K}{(2+K)}\frac{du_1}{dy} = 0$$

$$Ha.u_1^2 + \frac{k_1\Delta T}{U_0^2\mu_1}\frac{d^2\theta_1}{dy^2} = 0$$

- Step 7.

$$u_1'' + \frac{GR}{(1+K)}\theta_1 + \frac{K}{(1+K)}N' - \frac{Ha}{(1+K)}u_1 = 0$$

$$N'' - \frac{4K}{(2+K)}N - \frac{2K}{(2+K)}u_1' = 0$$

$$Ha.u_1^2 + \frac{k_1}{C_{P1}\mu_1}\frac{C_{P1}\Delta T}{U_0^2}\theta_1'' = 0$$

- Step 8.

$$u_1'' + \frac{GR}{(1+K)}\theta_1 + \frac{K}{(1+K)}N' - \frac{Ha}{(1+K)}u_1 = 0$$

$$N'' - \frac{4K}{(2+K)}N - \frac{2K}{(2+K)}u_1' = 0$$

$$Ha.u_1^2 + \left(\frac{k_1}{C_{P1}\rho_1\nu_1}\right)\frac{1}{\left(\frac{U_0^2}{C_{P1}\Delta T}\right)}\theta_1'' = 0$$

- Step 9.

$$u_1'' + \frac{GR}{(1+K)}\theta_1 + \frac{K}{(1+K)}N' - \frac{Ha}{(1+K)}u_1 = 0$$

$$N'' - \frac{4K}{(2+K)}N - \frac{2K}{(2+K)}u_1' = 0$$

$$Ha.u_1^2 + \left(\frac{\alpha_1}{\nu_1}\right)\frac{1}{E_C}\theta_1'' = 0$$

In using the following data: $u_1 = f(y), u_2 = g(y)$ et $Y = \frac{y}{h_2}$, we obtain:

- step10.

$$f'' - \frac{Ha}{(1+K)}f + \frac{K}{(1+K)}N' + \frac{GR}{(1+K)}\theta_1 = 0$$

$$N'' - \frac{4K}{(2+K)}N - \frac{2K}{(2+K)}f' = 0$$

$$\theta_1'' + Ha.P_r.E_C.f^2 = 0$$

- step11.

$$f'' + K_1.GR.\theta_1 + K_2.N' - K_1.Ha.f = 0 \quad (4.96)$$

$$N'' - 2K_3N - K_3f' = 0 \quad (4.97)$$

$$\theta_1'' + Br.Ha.f^2 = 0 \quad (4.98)$$

- Region 2

$$\mu_2\frac{d^2U_2}{dY^2} + \rho_2 g\beta_2(T_2 - T_2^*) - \sigma^*B_0^2U_2 = 0$$

$$\frac{\sigma^* B_0^2}{\rho_2 C_{p2}} U_2^2 + \alpha_2 \frac{d^2 T_2}{dY^2} = 0$$

- Step 1.

$$\frac{d^2 U_2}{dY^2} + \frac{\rho_2 g \beta_2 \Delta T}{\mu_2} \theta_2 - \frac{\sigma^* B_0^2}{\mu_2} U_2 = 0$$

$$\frac{\sigma^* B_0^2}{\rho_2 C_{p2}} U_2^2 + \frac{k_2}{\rho_2 C_{P2}} \frac{d^2 T_2}{dY^2} = 0$$

- Step 2.

$$\frac{U_0}{h_2^2} \frac{d^2 u_2}{dy^2} + \frac{\rho_2 g \beta_2 \Delta T}{\mu_2} \theta_2 - \frac{\sigma^* B_0^2 U_0}{\mu_2} u_2 = 0$$

$$\frac{\sigma^* B_0^2 U_0^2}{\rho_2 C_{p2}} u_2^2 + \frac{k_2 \Delta T}{\rho_2 C_{P2} h_2^2} \frac{d^2 \theta_2}{dy^2} = 0$$

- Step 3.

$$\frac{d^2 u_2}{dy^2} + \frac{\rho_2 \mu_1 h_2^2 \beta_2}{\rho_1 \mu_2 h_1^2 \beta_1} \frac{1}{\left(\frac{\rho_1 U_0 h_1}{\mu_1}\right)} \left(\frac{\rho_1^2 g h_1^3 \beta_1 \Delta T}{\mu_1^2}\right) \theta_2 - \frac{\mu_1 h_2^2}{\mu_2 h_1^2} \left(\frac{\sigma^* B_0^2 h_1^2}{\mu_1}\right) u_2 = 0$$

$$\frac{h_2^2}{h_1^2} \left(\frac{\sigma^* B_0^2 h_1^2}{\mu_1}\right) u_2^2 + \frac{k_2}{k_1} \left(\frac{k_1 \Delta T}{\mu_1 U_0^2}\right) \frac{d^2 \theta_2}{dy^2} = 0$$

- Step 4.

$$\frac{d^2 u_2}{dy^2} + \rho^* \mu^* H^2 \beta^* \frac{Gr}{Re} \theta_2 - \mu^* H^2 Ha. u_2 = 0$$

$$H^2 Ha. u_2^2 + \frac{1}{k^* P_r E_C} \frac{d^2 \theta_2}{dy^2} = 0$$

- Step 5.

$$u_2'' + \rho^* \mu^* H^2 \beta^* \frac{Gr}{Re} \theta_2 - \mu^* H^2 Ha. u_2 = 0$$

$$H^2. Ha. u_2^2 + \frac{1}{k^*. P_r. E_C} \theta_2'' = 0$$

- Step 6.

$$g'' - \frac{\mu^*. Ha}{H^2} g + . \frac{GR. \mu^*}{\rho^*. H^2. \beta^*} \theta_2 = 0 \qquad (4.99)$$

$$\theta_2'' + \frac{Ha. k^*. Br}{H^2} . g^2 = 0 \qquad (4.100)$$

With: $GR = \frac{Gr}{Re}$; $Gr = \frac{h_1^3 \rho_1^2 \beta_1 g \Delta T}{\mu_1^2}$; $Re = \frac{\rho_1 h_1 U_0}{\mu_1}$; $\mu^* = \frac{\mu_1}{\mu_2}$; $h^* = \frac{h_1}{h_2}$; $k^* = \frac{k_1}{k_2}$; $\beta^* = \frac{\beta_1}{\beta_2}$; $\rho^* = \frac{\rho_1}{\rho_2}$

$$\mathrm{Ha} = \frac{\sigma^* B_0^2 h_1^2}{\mu_1}\ ;\ \mathrm{E_C} = \frac{U_0^2}{C_{P1}\Delta T};\ \mathrm{P_r} = \frac{\nu_1}{\alpha_1}\ ; \mathrm{Br} = \mathrm{Pr.Ec};\ \mathrm{K_1} = \frac{1}{1+\mathrm{K}}\ ;\ \mathrm{K_2} = \frac{\mathrm{K}}{1+\mathrm{K}}\ ; \mathrm{K_3} = \frac{2\mathrm{K}}{2+\mathrm{K}}\ ;$$

Particulate case: $\mathrm{K} \to 0$ (viscous/viscous fluids system):

$$f'' - \mathrm{Ha}.f + \mathrm{GR}.\theta_1 = 0 \tag{4.101}$$

$$\theta_1'' + \mathrm{Br}.\mathrm{Ha}.f^2 = 0 \tag{4.102}$$

$$g'' - \frac{\mu^*.\mathrm{Ha}}{H^2} g + . \frac{\mathrm{GR}.\mu^*}{\rho^*.H^2.\beta^*}\theta_2 = 0 \tag{4.103}$$

$$\theta_2'' + \frac{Ha.k^*.Br}{H^2}.g^2 = 0 \tag{4.104}$$

4.5.3. Calculation of local friction coefficients, C_{f1} et C_{f2}

In our study, the main interest physical quantities are the local friction coefficients close to the channel walls, the shear rate and the Nusselt number which represents the heat transfer rate, except that the calculation of the friction coefficients and the shear rate is done in function of a variable y, while the calculation of the Nusselt number is given as a function of a variable x, which requires the writing of balance equations in two dimensions in boundary layer.

The general formula of local friction coefficient and the shear rate are given by.

A wall in contact with a non-Newtonian Micropolar fluid**.**

$$C_{f1} = {\tau_{1Y}}\Big/{\left(\frac{1}{2}\rho_1.U_0^2\right)} \tag{4.105}$$

$$\tau_{1Y} = -(\mu_1 + \sigma)\left(\frac{dU_1}{dY}\right)_{(Y=-h_1)} + \sigma(n)_{Y=-h_1} \tag{4.106}$$

A wall in contact with a Newtonian-viscous fluid.

$$C_{f2} = {\tau_{2Y}}\Big/{\left(\frac{1}{2}\rho_2.U_0^2\right)} \tag{4.107}$$

$$\tau_{2Y} = -\mu_2\left(\frac{dU_2}{dY}\right)_{(Y=h_2)} \tag{4.108}$$

To calculate the local friction coefficient values in relations (4.105) and (4.107), we should write them in dimensionless form. In considering that: $n = 0, \sigma(n)_{Y=-h_1}$

- Region1.

$$C_{f1} = -\frac{(\mu_1 + \sigma)}{\left(\frac{1}{2}\rho_1 . U_0^2\right)}\left(\frac{dU_1}{dY}\right)_{(Y=-h_1)} \Rightarrow C_{f1} = -\frac{\mu_1\left(1+\frac{\sigma}{\mu_1}\right)}{\left(\frac{1}{2}\rho_1 . U_0^2\right)}\left(\frac{d(u_1 U_0)}{d(-h_1 y)}\right)_{(y=-1)}$$

$$\Longrightarrow C_{f1} = \frac{2U_0(1+K)}{\left(\frac{\rho_1 . h_1 . U_0^2}{\mu_1}\right)}\left(\frac{du_1}{dy}\right)_{(y=-1)} \Longrightarrow C_{f1} == \frac{2(1+K)}{\left(\frac{\rho_1 . h_1 U_0}{\mu_1}\right)}\left(\frac{du_1}{dy}\right)_{(y=-1)}$$

$$\Longrightarrow C_{f1} = \frac{2(1+K)}{Re_1}\left(\frac{du_1}{dy}\right)_{(y=-1)}$$

$$C_{f1} = \frac{2(1+K)}{Re_1} f'(-1) \qquad (4.109)$$

- Region2.

$$C_{f2} = -\frac{\mu_2}{\left(\frac{1}{2}\rho_2 . U_0^2\right)}\left(\frac{d(u_2 U_0)}{d(h_2 y)}\right)_{(y=1)} \Rightarrow C_{f2} = -\frac{U_0 . \mu_2}{\left(\frac{1}{2}\rho_2 . h_2 . U_0^2\right)}\left(\frac{du_2}{dy}\right)_{(y=1)}$$

$$\Rightarrow C_{f2} = -\frac{\rho_1 . h_1 . \mu_2}{\rho_2 . h_2 . \mu_1} . \frac{2}{\left(\frac{\rho_1 . h_1 . U_0}{\mu_1}\right)}\left(\frac{du_2}{dy}\right)_{(y=1)} \Rightarrow -\frac{\frac{\rho_1}{\rho_2}.\frac{h_1}{h_2}}{\frac{\mu_1}{\mu_2}} . \frac{2}{\left(\frac{\rho_1 . h_1 . U_0}{\mu_1}\right)}\left(\frac{du_2}{dy}\right)_{(y=1)} \Rightarrow$$

$$C_{f2} = -\frac{2.\rho^* . H}{\mu^* R_e} g'(1) \qquad (4.110)$$

4.6. Conclusion

The development of the differential equations system, either in the absence or in the presence of the magnetic field, went through a mathematical technique to change the variables in aim to make it in dimensionless form, keeping a same hypothesis and a same boundary conditions, in first hand, with Successful, we have two different final system of differential equations of both studied cases, in the other hand, we found that the presence of the magnetic diffusivity term allows the appearance of three dimensionless numbers and ratio, Prandtl, Eckert, Hartmann and thermal conductivities ratio, alongside, five other dimensionless ratios are found in the case a channel without magnetic field effect case: Grashoff and Reynolds ratio, widths ratio, dynamic viscosity ratio, thermal dilation coefficients ratio and densities ratio.

Chapter 5

Results and discussions

5.1. Introduction

In this last chapter, it finds two means of figures, curves obtained from analytical solution using Microsoft Excel for the model without magnetic field effect. Thus a numerical solution is done for the model with a magnetic field effect by computing "Matlab". The obtained figures show us dimensionless linear velocities and dimensionless microrotation velocity into both regions of a channel. So the structure of the flow is represented by dimensionless velocities u_1, u_2 *et* N.

First part (**5.2**) present the validation part study. In this point, we should improve that our analytic solutions are the same of those obtained by **J. P. Kumar** [9].

Second part of the solution (**5.3**) presents our proper work of the physic model under a magnetic field effect.

5.2. The effect of the parameters on linear and microrotation velocities without magnetic field

5.2.1. The mixed convection parameter

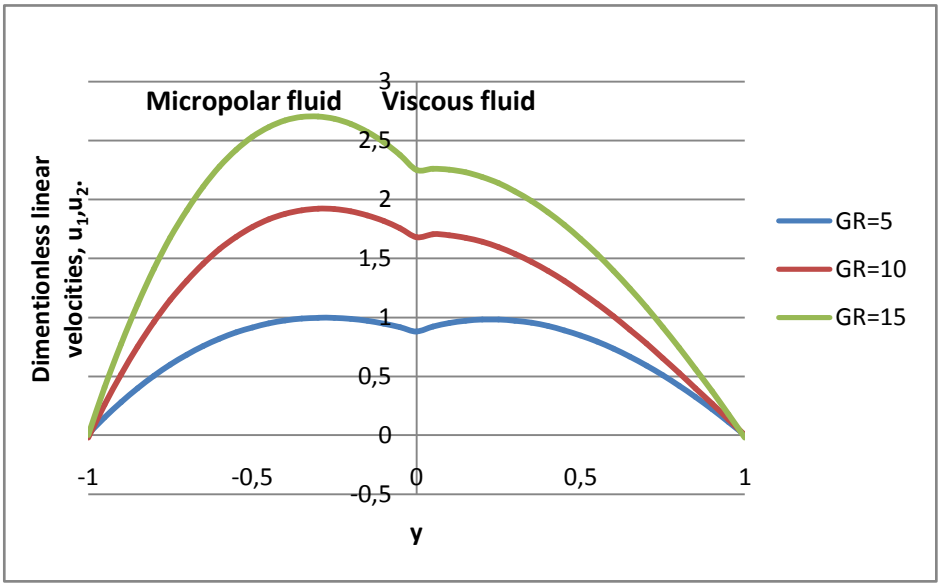

Figure 5.1: Dimensionless linear velocities profiles for different values of the mixed convection parameter with «K=0, **h***=1, k*=1, μ*=1, β*=1, ρ*=1».

Looking at Figure 5.1, 5.2 and 5.3, we have observed that the parameter of the mixed convection, also called, ratio of Grashoff to the Reynolds numbers (GR=Gr/Re) have a similar

effect on the dimensionless linear and microrotation velocities profile (u_1, u_2 et N). About the micropolar fluid, we have noticed that the increase of the mixed convection parameter causes an increase of the buoyancy force which support the motion, therefore in the case when the micropolar fluid is replaced by a Newtonian viscous fluid($K \to 0$), the effect of the variation of mixed convection parameter causes the increase of the buoyancy forces. However the attractive is that the increase in velocity profiles is significant in case of viscous-viscous fluids system.

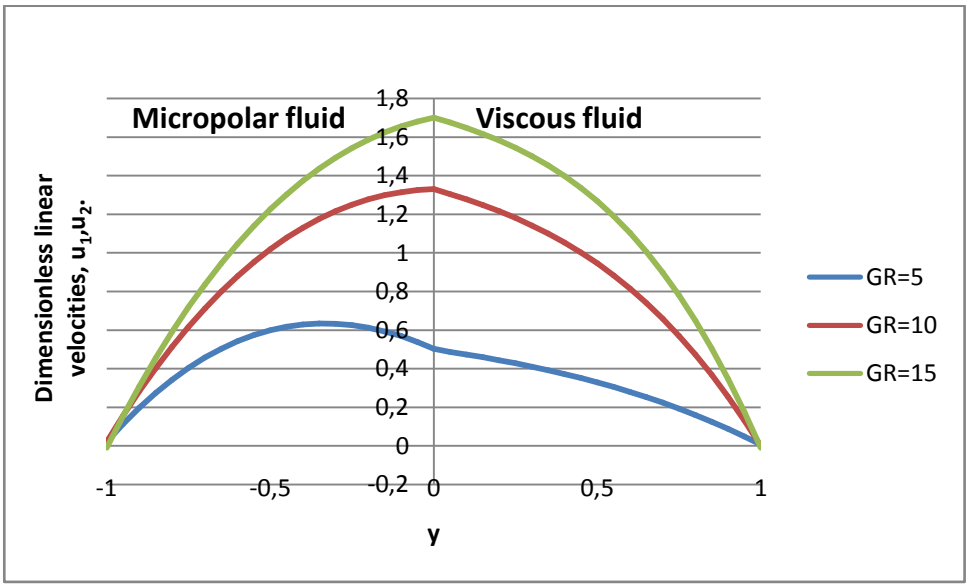

Figure 5.2: Dimensionless linear velocities profiles for different values of the mixed convection parameter with «K=1, h*=1, k*=1, μ*=1, β*=1, ρ*=1».

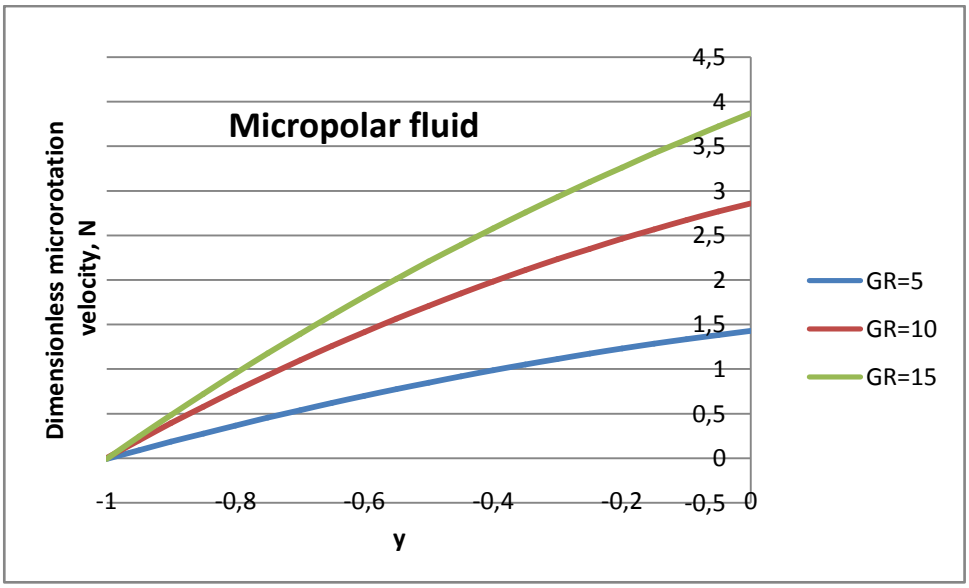

Figure 5.3: Dimensionless microrotation velocity profile for different values of the mixed convection parameter with **«** K=1, h*=1, k*=1, μ*=1, β*=1, ρ*=1**».**

5.2.2. The viscosity coefficients ratio

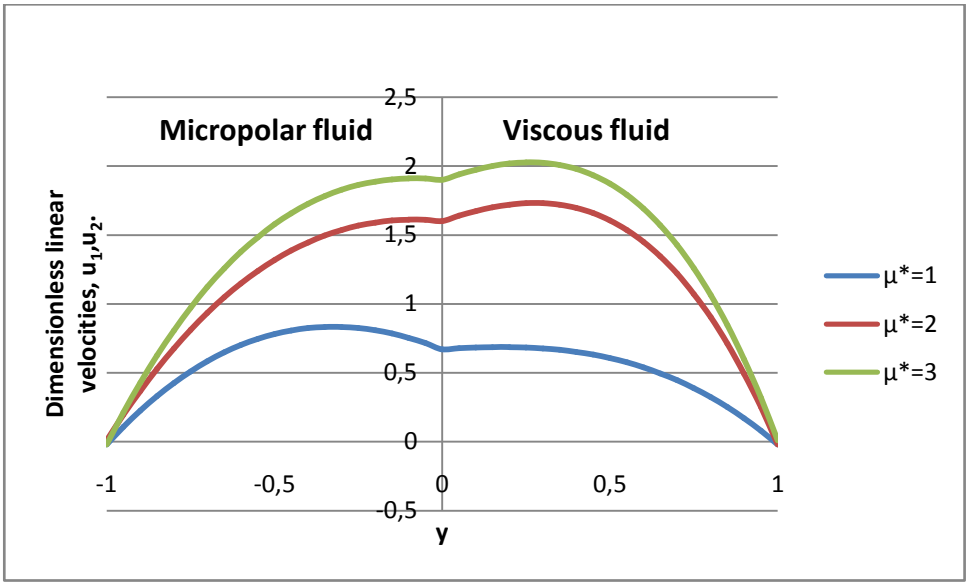

Figure 5.4: Dimensionless linear velocities profile for different values of viscosities ratio with « K=0, h^*=1, k*=1, GR=5, β*=1, ρ*=1».

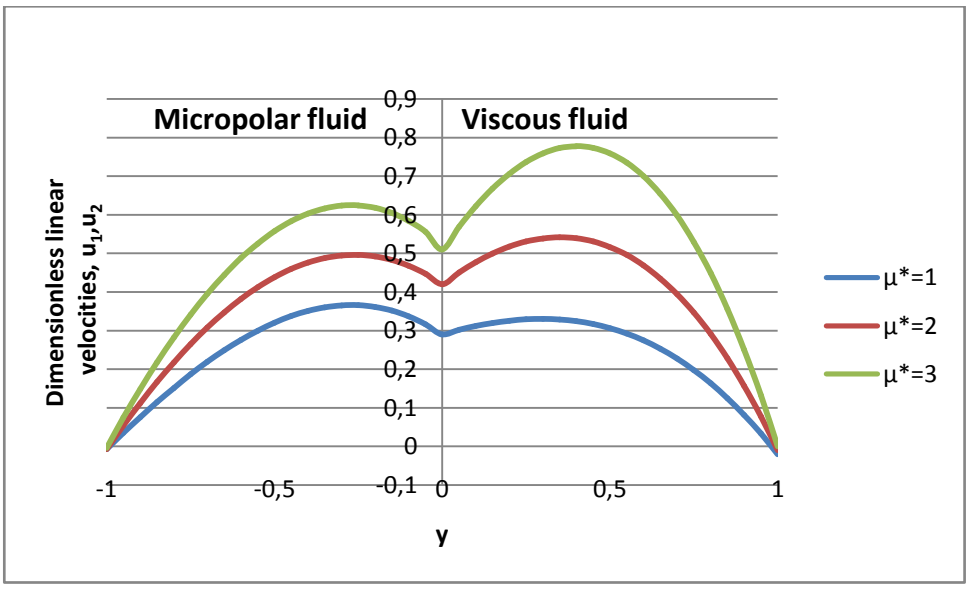

Figure 5.5: Dimensionless linear velocities profile for different values of viscosities ratio with « K=1, h^*=1, k*=1, GR=5, β*=1, ρ*=1».

From figures 5.4, 5.5 & 5.6, we note that the variation of viscosity coefficients ratio of the micropolar-non-Newtonian and Newtonian viscous fluid has an apparent effect on the linear and micro-rotation velocities field, it is clear that the increase in the viscosities ratio, causes an increase in the linear velocities of both fluid regions, we also say that the

increase is significant in the case of a viscous-viscous fluid system (K→0). When the viscosity ratio increases causes a decrease in the microrotation velocity profile.

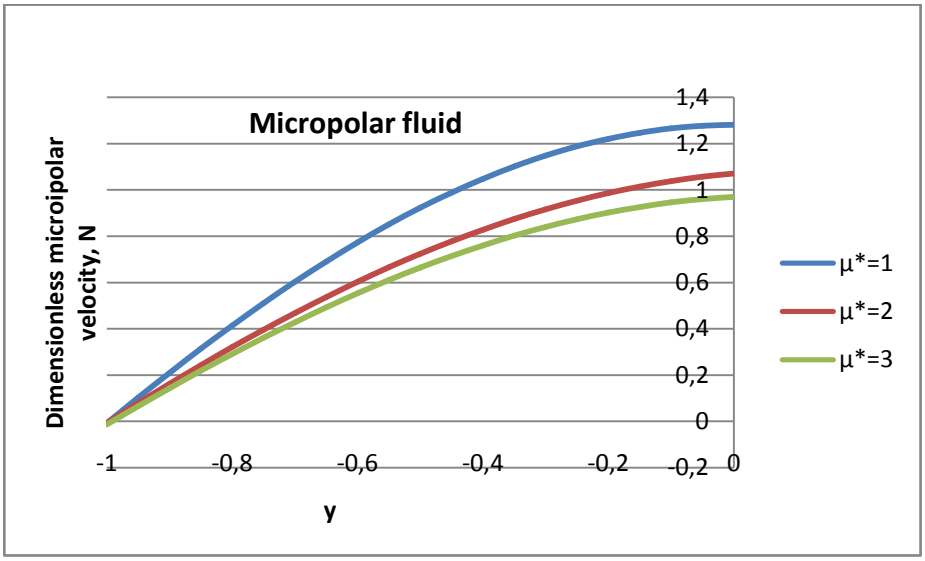

Figure 5.6: The dimensionless microrotation velocity profile for different values of the viscosities ratio with «K=1, h^*=1, k*=1, GR=5, β*=1, ρ*=1».

5.2.3. The widths ratio of fluids

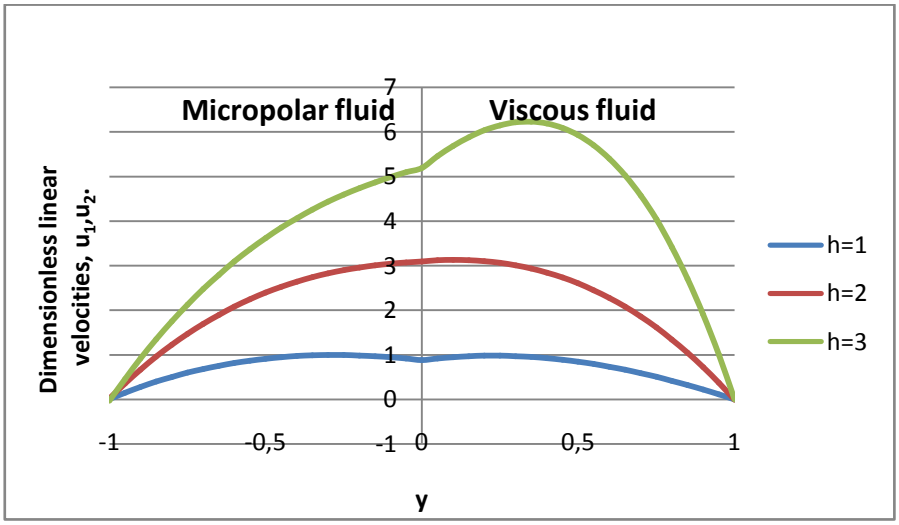

Figure 5.7: Dimensionless linear velocities profile for different values of channel widths ratio with « K=0, μ^*=1, k*=1, GR=5, β*=1, ρ*=1».

By observing the curves in Figure 5.7, 5.8 & 5.9, we observe that the widths ratio of both regions has an apparent effect on the linear and microrotation velocities, when the ratio of the widths increases the dimensionless linear and microrotation velocities increase, furthermore in the case which the viscous-micropolar fluid system is replaced

by viscous-viscous fluids system (K→0), the increase in the profile of linear and microrotation velocities according to the widths ratio h is greater.

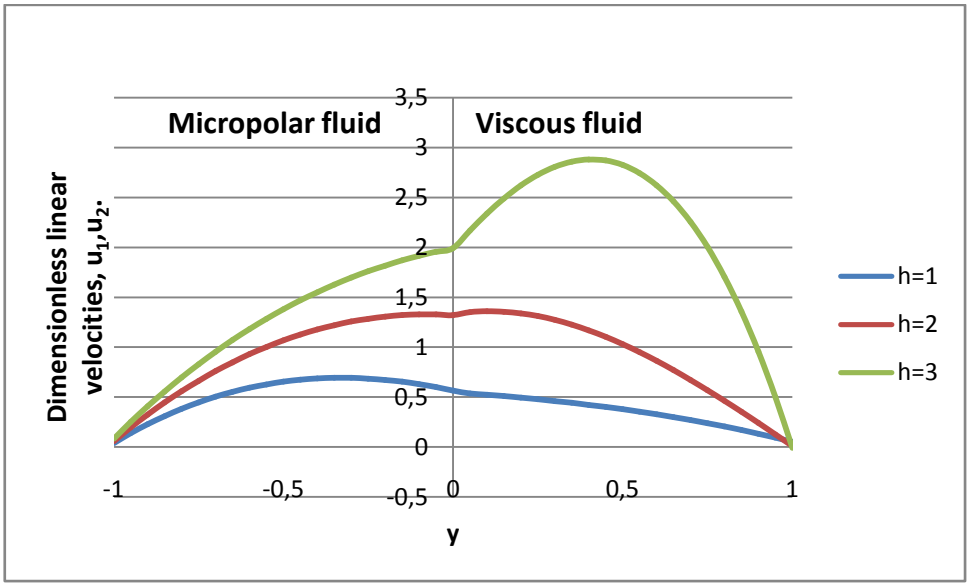

Figure 5.8: Dimensionless linear velocities profile for different values of channel widths ratio with **«**K=1, μ^*=1, k*=1, GR=5, β*=1, ρ*=1**».**

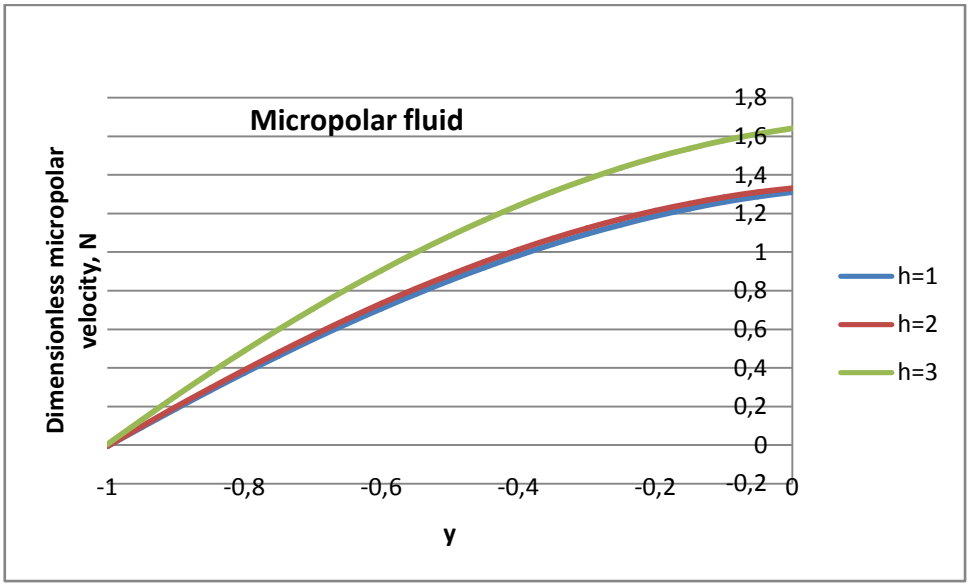

Figure 5.9: variation of dimensionless microrotation velocity for different values of widths ratio h of the channel, with «K=1, μ^*=1, k*=1, GR=5, β*=1, ρ*=1».

In other way, in observing the curves in figs. 5.4 – 5.6, facing the others in fig. 5.7 – 5.9, we can say that the width ratio of both regions support the microrotion velocity more than dynamics viscosities ratio. A fig. 5.6 shows that the spin velocity takes values from 0.9 to 1.3, but in fig. 5.9, the velocity of spin start over than the value 1.3 and takes more this value. We can also observe the same for the linear velocity variations. Values of

the linear velocities curves do not exceed more than 0.8 in fig. 5.5 but in fig. 5.8 the velocities exceed than a value 2.5.

5.2.4. The thermal conductivities ratio

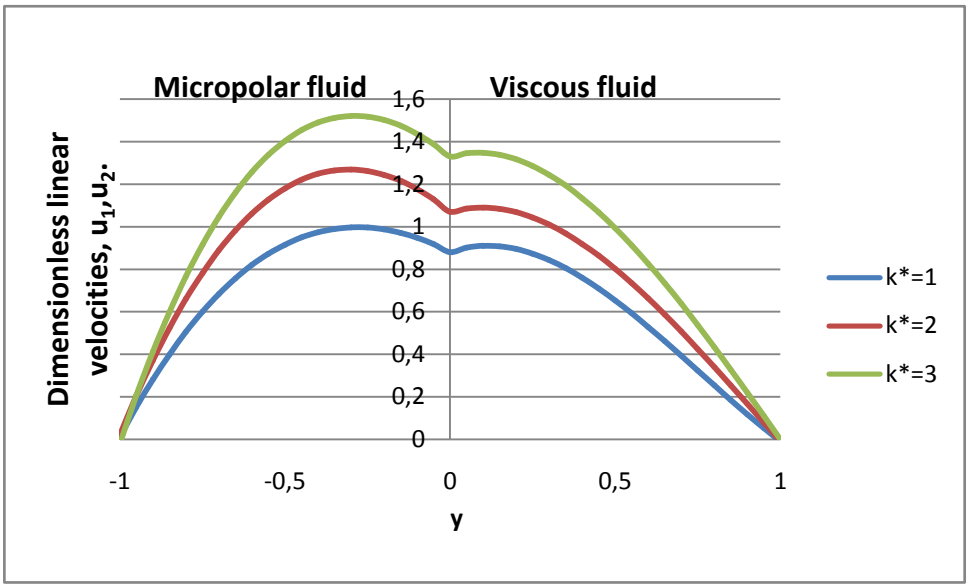

Figure 5.10: Dimensionless linear velocities profile for different values of thermal conductivities ratio with «K=0, μ^*=1, h^*=1, GR=5, β*=1, ρ*=1».

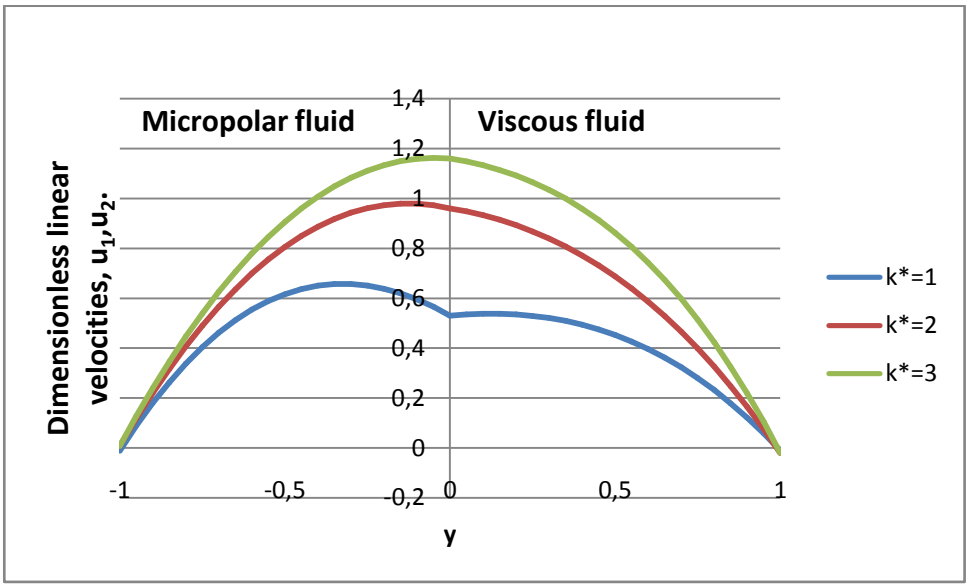

Figure 5.11: Dimensionless linear velocities profile for different values of thermal conductivities ratio with «K=1, μ^*=1, h^*=1, GR=5, β*=1, ρ*=1».

In analyzing the curves in figure 5.10, 5.11 & 5.12, the linear velocities profile in both regions increase when the thermal conductivities ratio increase for the both cases when K=0 and K=1, but the microrotation velocity decrease in the first region when the thermal conductivities ratio increase.

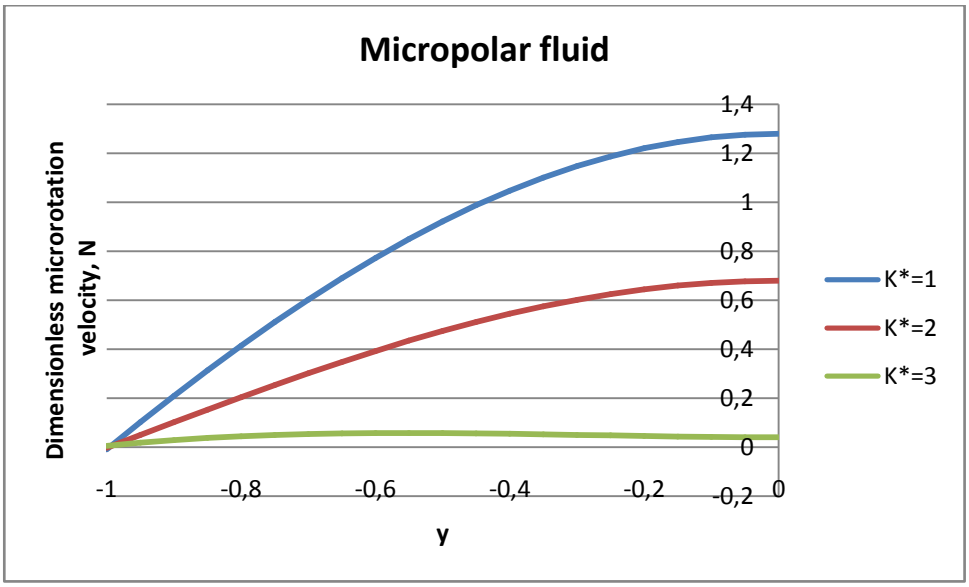

Figure 5.12: variation of dimensionless microrotation velocity for different values of widths ratio h of the channel, with with «K=1, μ^*=1, h^*=1, GR=5, β*=1, ρ*=1».

5.2.5. The material parameter and thermal dilation coefficients

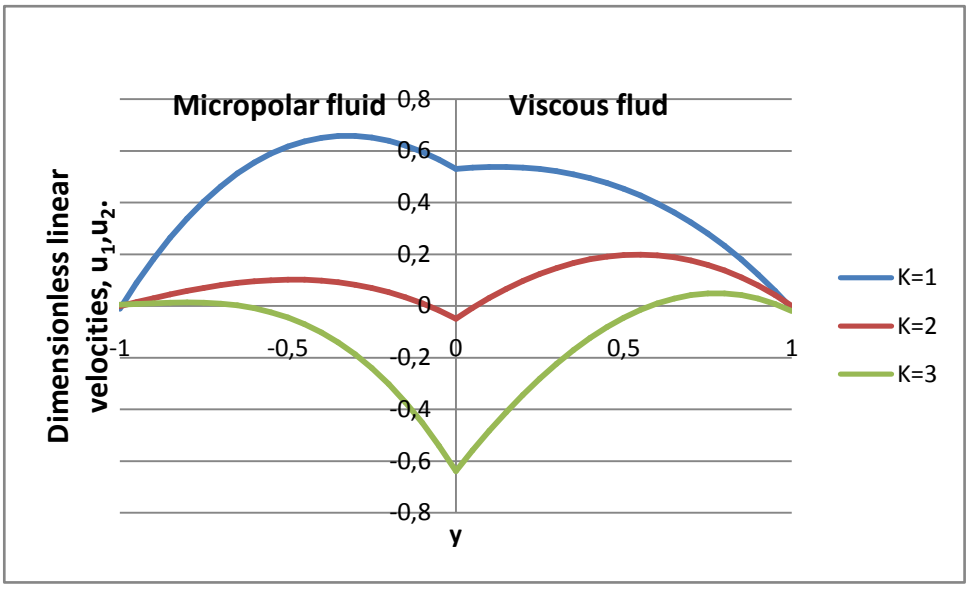

Figure 5.13: variation of dimensionless linear velocities profile for different values of material parameter, with «k^*=1, μ^*=1, h^*=1, GR=5, β*=1, ρ*=1».

Furthermore, the curves in fig. 5.10 & 5.11 facing the others in fig. 5.15 & 5.16, and curves in fig. 5.12 facing the others in fig. 5.17, we can say that the thermal conductivities ratio of both regions support, respectively, the linear and microrotion velocities more than thermal dilations ratio. A fig. 5.10 and fig. 5.11 show that the linear velocity takes values from 0.9 to 1.5, but in fig. 5.15 and fig. 5.16, the linear velocity starts over than the

value 0.15 to 0.45. We can also observe the same for the spin velocities, values of the linear velocities curves don't exceed more than 1.4 in fig. 5.12, but in fig. 5.17, the microrotation values exceed than a value 1.4 to 1.6.

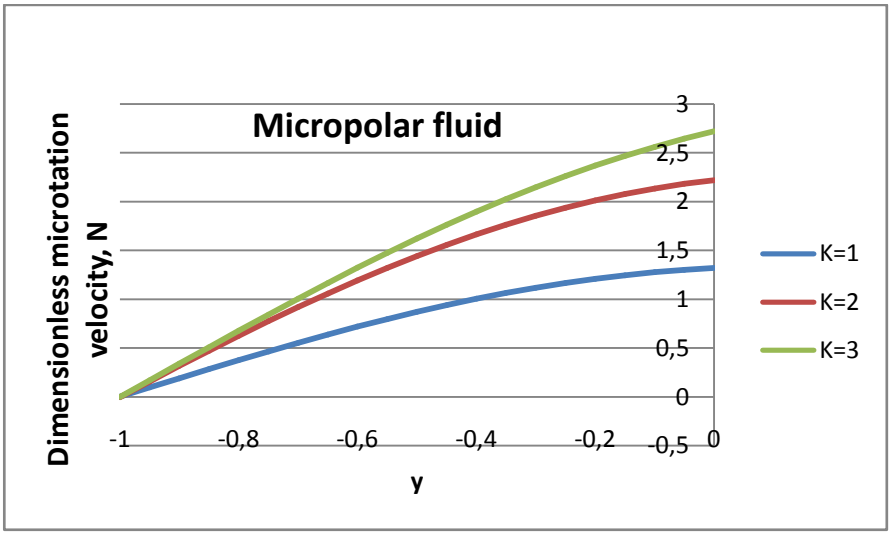

Figure 5.14: variation of dimensionless microrotation velocities profile for different values of material parameter with «k^*=1, μ^*=1, h^*=1, GR=5, β*=1, ρ*=1».

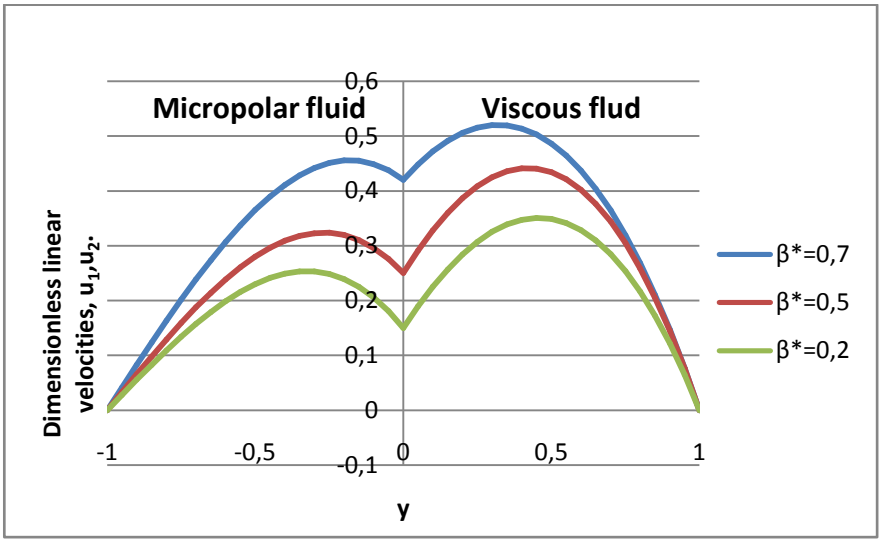

Figure 5.15: variation of dimensionless linear velocities profile for different values of thermal dilation coefficients ratio, with «K=0, k^*=1, μ^*=1, h^*=1, GR=5, ρ*=1».

We observed in figures 5.13-5.16, that when the material parameter - which characterize the variation of the form and the structure of the suspended fine particles within a non-Newtonian-micropolar-fluid - and the dilation thermal coefficients ratio (in cases K=0 & K=1) increase, the linear velocities increase, but in figures 5.14 & 5.17, the

microrotation velocity decrease according to the increase of the material parameter and dilation thermal coefficients ratio.

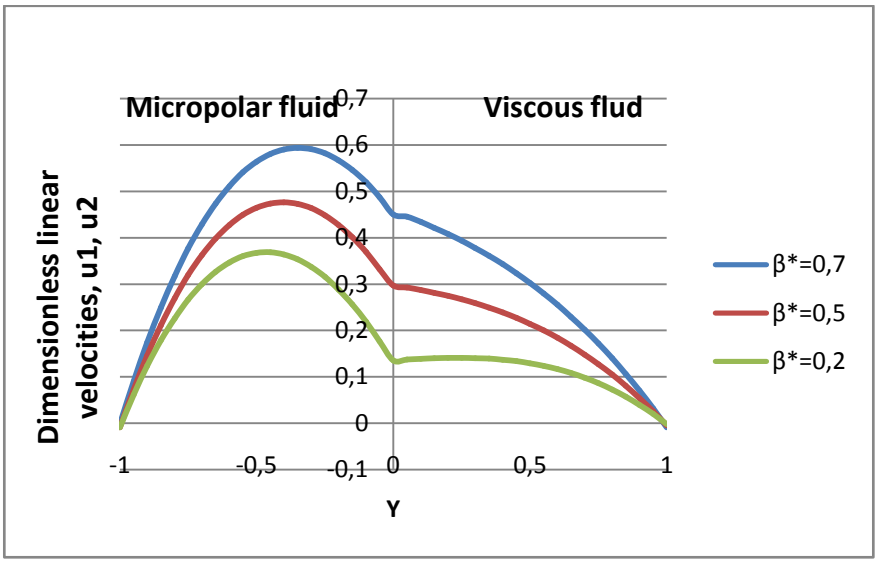

Figure 5.16: variation of dimensionless linear velocities profile for different values of thermal dilation coefficients ratio, with «K=1, k^*=1, μ^*=1, h^*=1, GR=5, ρ^*=1».

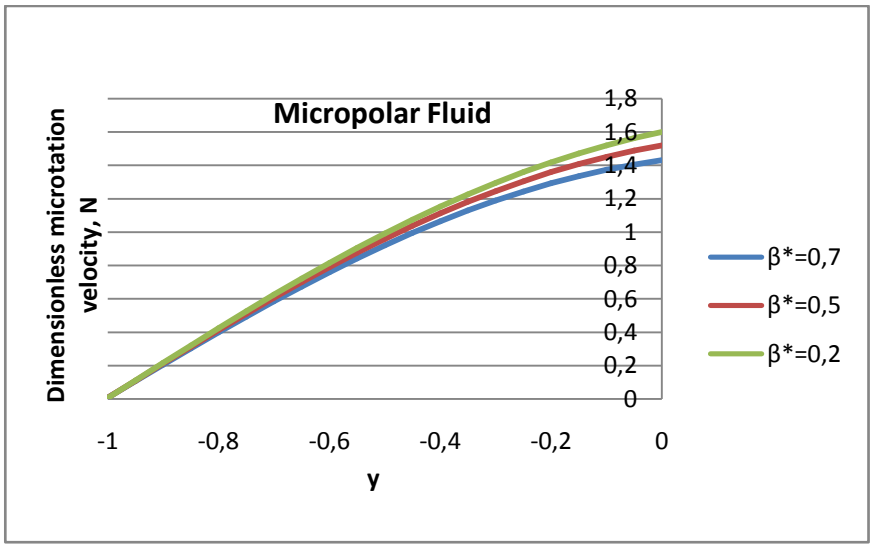

Figure 5.17: variation of dimensionless microrotation velocities profile for different values of thermal dilation coefficients ratio, with «K=1, k^*=1, μ^*=1, **h***=1, GR=5, ρ^*=1».

5.2.6. The densities ratio

by analyzing the curves obtained in Figures 5.18-5.20, it is clear that the variation of densities ratio have an effect on the linear and the microrotation velocities profile in both regions of a channel, we note that the increase in densities ratio causes a decrease in a linear and microrotation velocity profiles of case $K \to 0$ and $K = 1$.

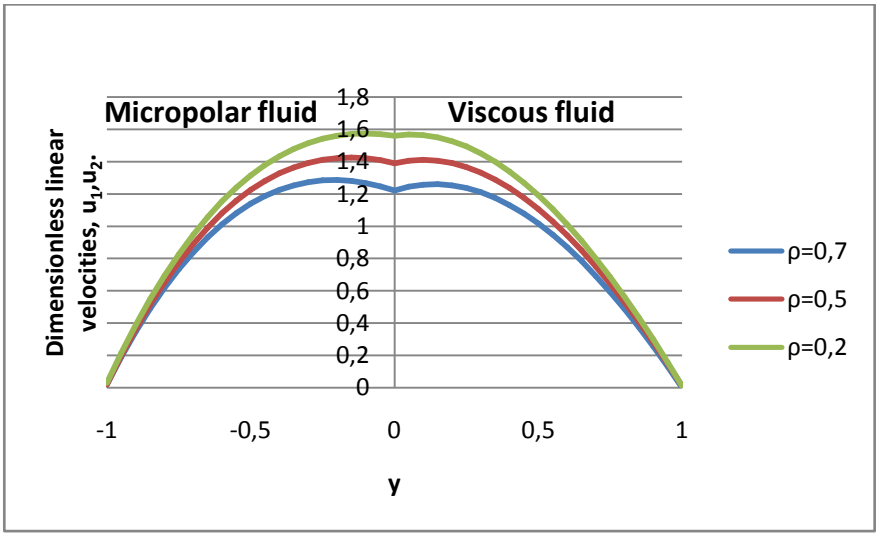

Figure 5.18: variation of dimensionless linear velocities profile for different values of densities ratio, with «K=0, k^*=1, μ^*=1, h^*=1, GR=5, β*=1».

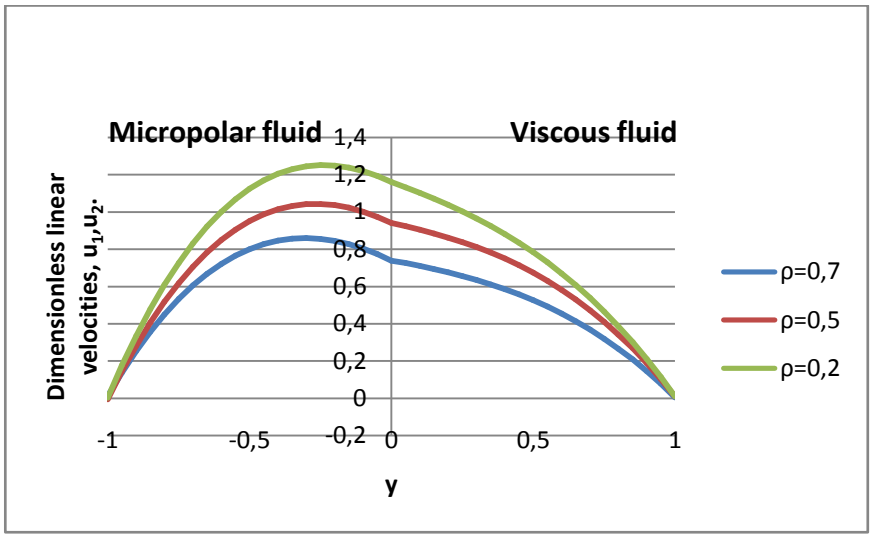

Figure 5.19: variation of dimensionless linear velocities profile for different values of densities ratio, with «K=1, k^*=1, μ^*=1, h^*=1, GR=5, β*=1».

In addition, the curves in fig. 5.10 & 5.11, facing the others in fig. 5.18 & 5.19, and curves in fig. 5.12 facing the others in fig. 5.20, we can say that the thermal conductivities ratio of both regions and the densities ratio might be have a same effect, so, they support the micropolar fluid flow. We also, observe that the curves in fig. 5.12, 5.17 and fig. 5.20 show that the densities ratio has more effect on the spine velocity than the thermal dilation and conductivities ratio within micropolar fluid flow.

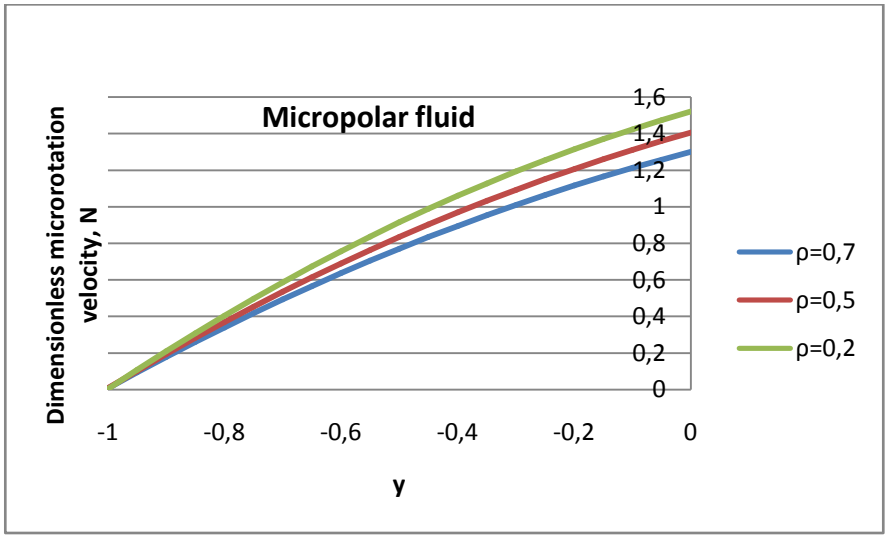

Figure 5.20: variation of dimensionless microrotation velocities profile for different values of densities ratio, with «K=1, k^*=1, μ^*=1, h^*=1, GR=5, β*=1».

5.3. The effect of dimensionless parameters in presence of magnetic field

The dimensionless differential equations obtained are programmed under MATLAB, as a result, curves obtained in this investigate; represent the flow structure (velocity profile). The structure of a flow is represented by dimensionless linear or axial velocity curves (u_1, u_2) and dimensionless microrotation velocity curves (N).

5.3.1. The material parameter effect in varying the magnetic parameter for $Pr \leq 1$

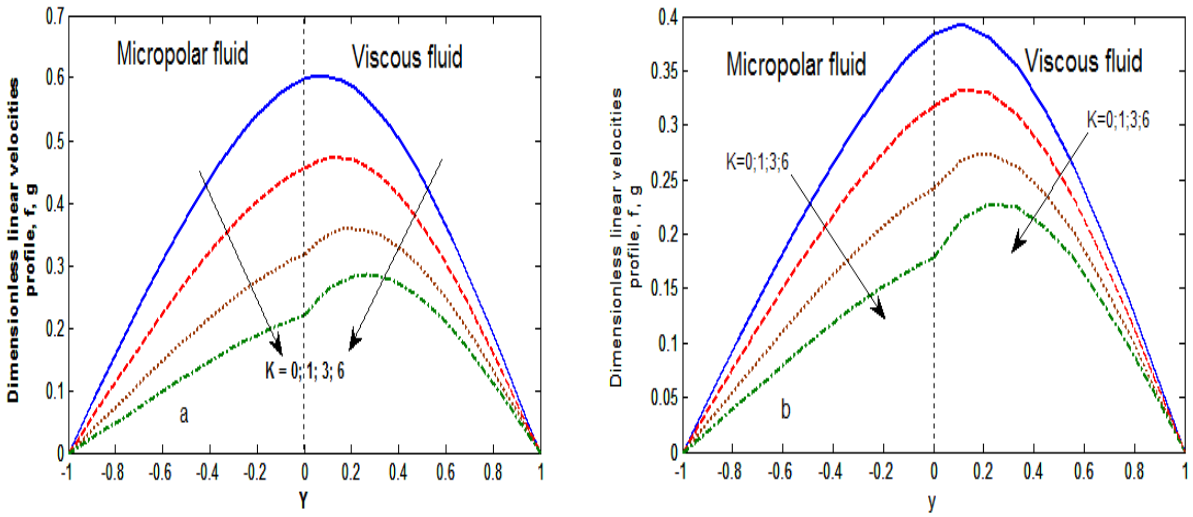

Figure 5.21: variation of dimensionless linear velocities profile for different values of material parameter with « **(a) Ha=1, (b) Ha=3, Pr=0.7**, Ec=1, GR=5, h^*=1, k*=1, μ*=1, β*=1, ρ*=1».

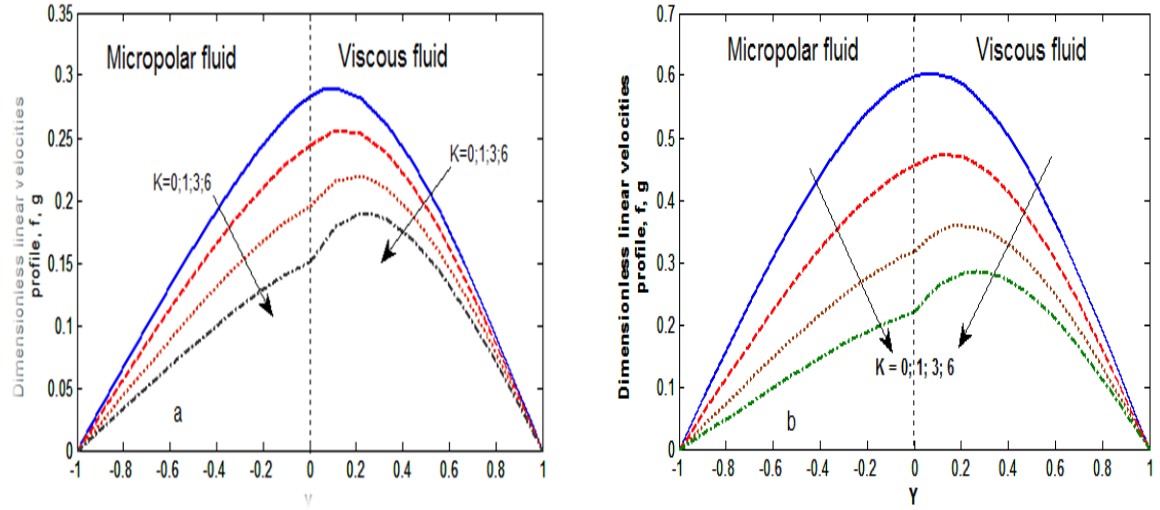

Figure 5.22: variation of dimensionless linear velocities profile for different values of material parameter with **« (a) Pr=0.7, Ha=5**, **(b) Pr=0.1, Ha=1** & Ec=1GR=5, **h***=1, k*=1, μ*=1, β*=1, ρ*=1».

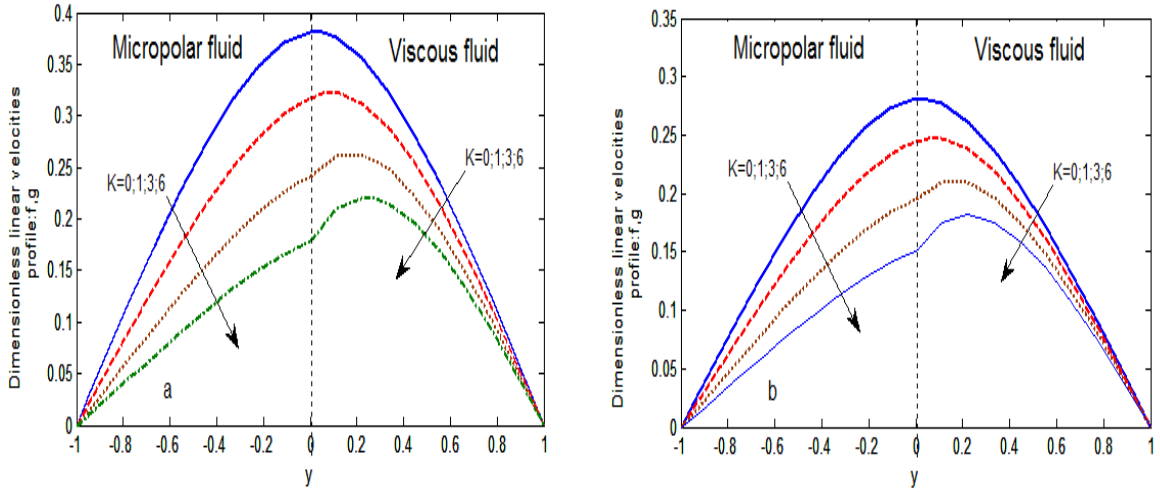

Figure 5.23: : variation of dimensionless linear velocities profile for different values of material parameter with « **(a) Pr=0.1, Ha=3**, **(b) Pr=0.1, Ha=5,** Ec=1, GR=5, **h***=1, k*=1, μ*=1, β*=1, ρ*=1»

First, by observing the curves obtained in figures 5.21-5.31, we note that the material parameter variation has an apparent effect on the linear and microrotation velocities profile, it's clear that an increase in the material parameter, as Prandtl number of 0.1-3 and Hartmann number of 1-5 causes a decrease in the linear velocity profiles in both regions (i.e. a decrease in buoyancy forces) of non-Newtonian-micropolar and Newtonian-viscous fluids, except in figure 5.32-a, case Pr=3, Ha=5 & K=0-2, the linear velocities increase within a micropolar fluid region, but about Newtonian-viscous fluid region-

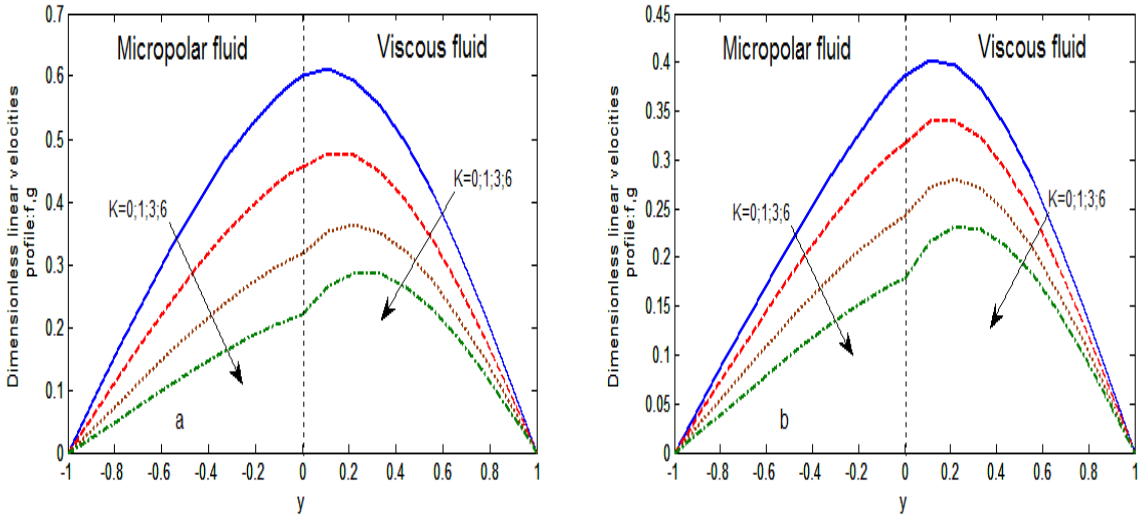

Figure 5.24: variation of dimensionless linear velocities profile for different values of material parameter with « **(a) Ha=1**, **(b) Ha=3** & **Pr=1,** Ec=1, GR=5, **h***=1, k*=1, μ*=1, β*=1, ρ*=1»

5.3.2. The material parameter effect in varying the magnetic parameter for $1 < Pr \leq 20$

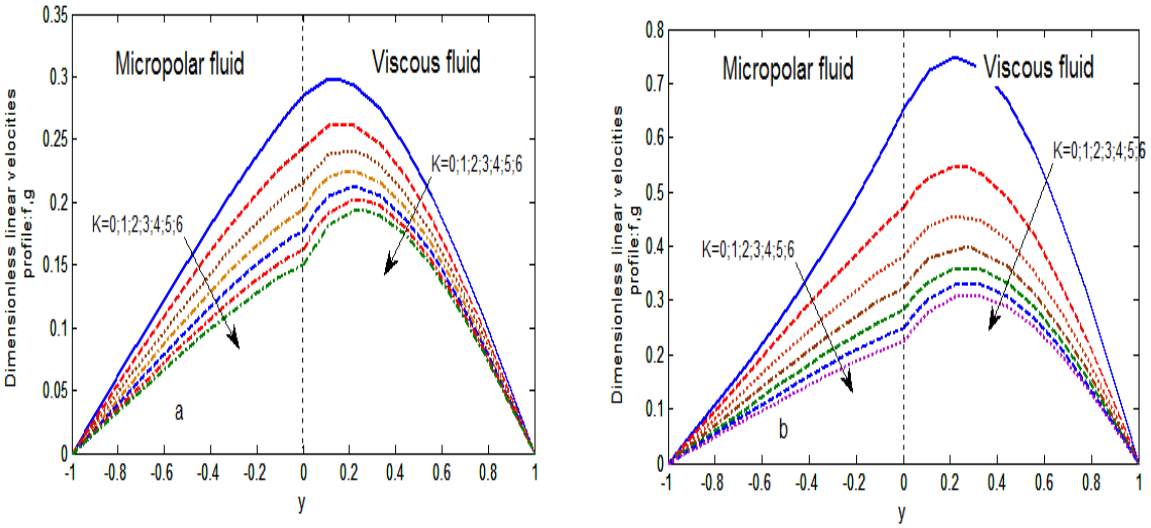

Figure 5.25: variation of dimensionless linear velocities profile for different values of material parameter with « **(a) Ha=5**, **Pr=1, (b) Ha=1, Pr=3** & Ec=1, GR=5, **h***=1, k*=1, μ*=1, β*=1, ρ*=1»

Moreover, the curves in fig. 5.21 – 5.25, facing the others in fig. 5.26 – 5.31, we can say that, in presence of magnetic effect, curves obtained in fig. 5.21 – 5.25, Prandtl number values from 0.1-1.0 had not a strong effect to raise velocities of both fluids. But curves obtained in fig. 5.26 – 5.31 show that while Pr takes values more than 1 the velocity curves in both regions will be more active for magnetic parameter values from 3 – 5.

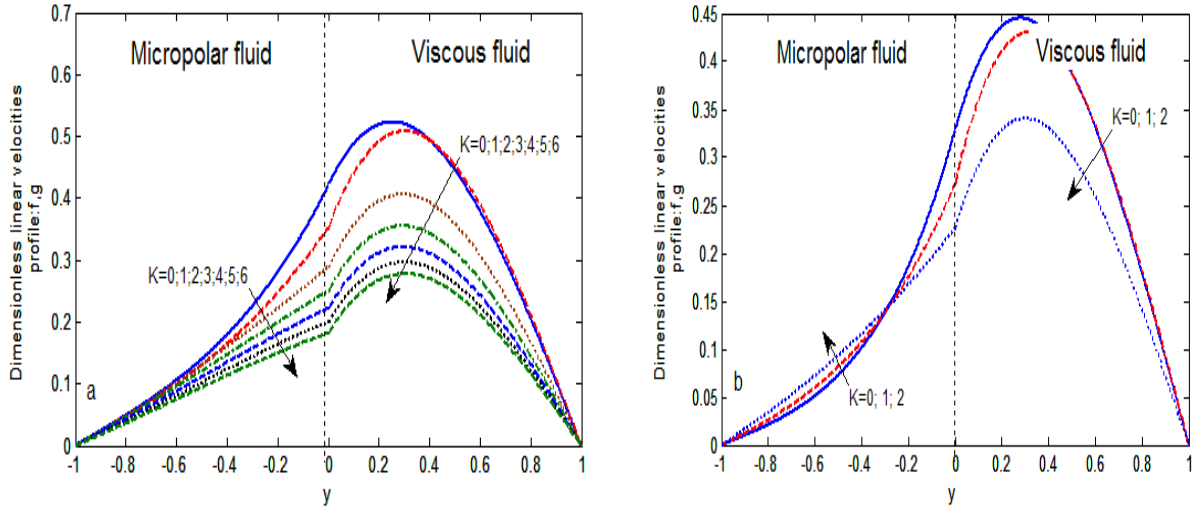

Figure 5.26: variation of dimensionless linear velocities profile for different values of material parameter with « **(a) Ha=3**, **Pr=3**, **(b) Ha=5**, **Pr=3, K=0-2** & Ec=1, GR=5, **h***=1, k*=1, μ*=1, β*=1, ρ*=1»

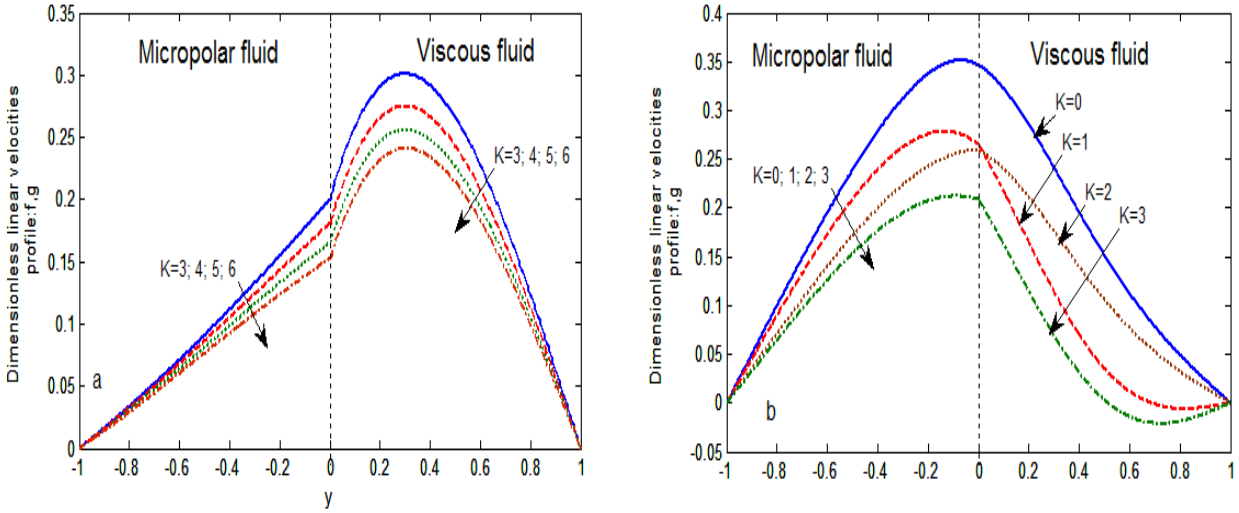

Figure 5.27 variation of dimensionless linear velocities profile for different values of material parameter with « **(a) Ha=5**, **Pr=3, K=3-6**, **(b) Ha=1**, **Pr=20, K=0-3**, Ec=1, GR=5, **h***=1, k*=1, μ*=1, β*=1, ρ*=1».

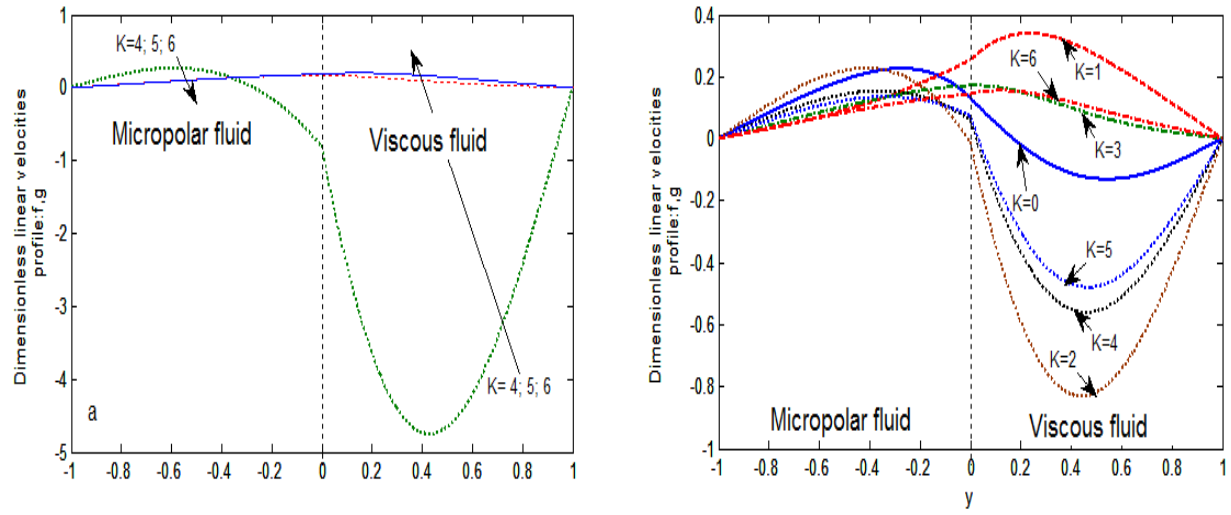

Figure 5.28 variation of dimensionless linear velocities profile for different values of material parameter with « **(a) Ha=1**, **Pr=20, K=4-6, (b) Ha=3**, **Pr=20, K=0-6** & Ec=1, GR=5, h*=1, k*=1, μ*=1, β*=1, ρ*=1»

In figures 5.28-5.30, we observed an increase in the linear velocities profile for K<3, 10 <Pr <50, Ha=1-5, we can also noticed a perturbation in velocities profile for K>3 in both regions, up and equal value 3 of Hartmann number including figure 5.31.

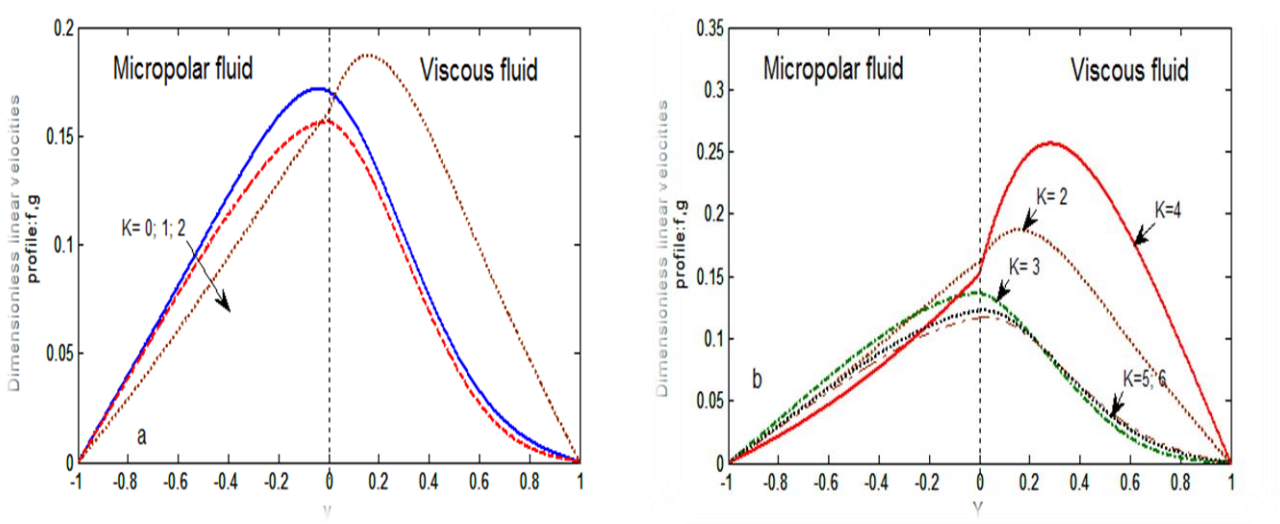

Figure 5.29 : variation of dimensionless linear velocities profile for different values of material parameter with « **Ha=5**, **Pr=20, (a) K=0-2, (b), K=2-6** & Ec=1, GR=5, **h***=1, k*=1, μ*=1, β*=1, ρ*=1»

5.3.3. The material parameter effect with varying the magnetic parameter for $20 < Pr < 100$

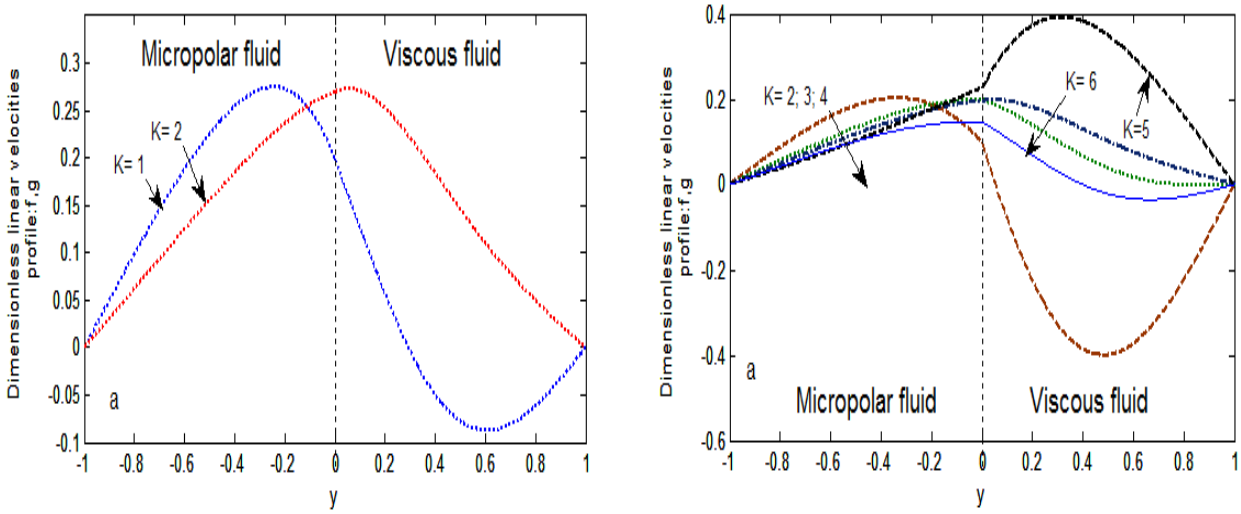

Figure 5.30 : variation of dimensionless linear velocities profile for different values of material parameter with « **Ha=1**, **Pr=40, (a) K=1-2, (b) K=2-6** & Ec=1, GR=5, **h***=1, k*=1, μ*=1, β*=1, ρ*=1»

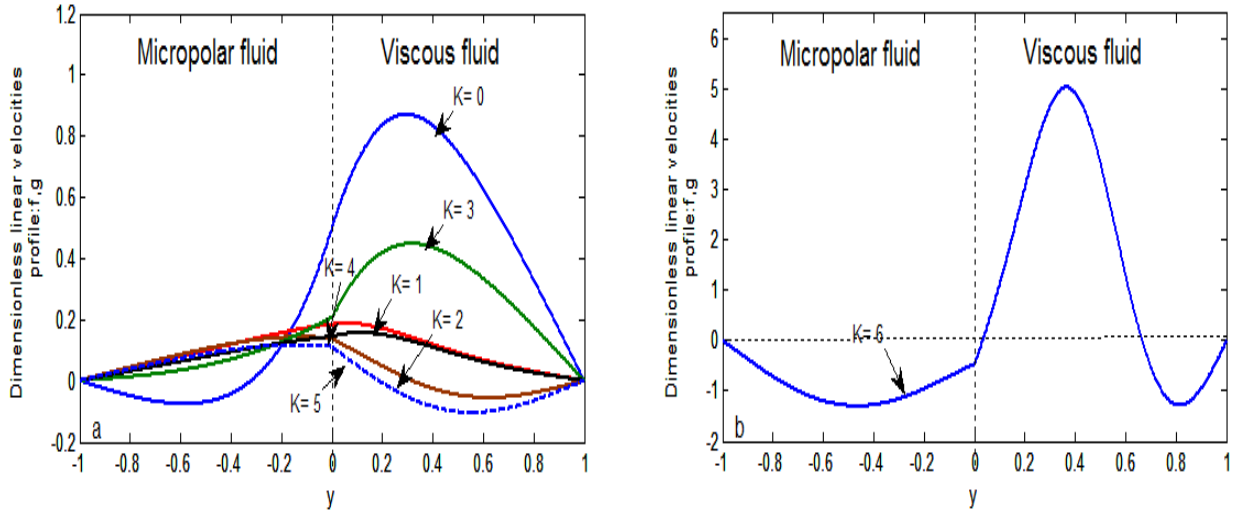

Figure 5.31: variation of dimensionless linear velocities profile for different values of material parameter with « **Ha=3**, **Pr=40, (a) K=1-5, (b) K=6** & Ec=1, GR=5, h*=1, k*=1, μ*=1, β*=1, ρ*=1»

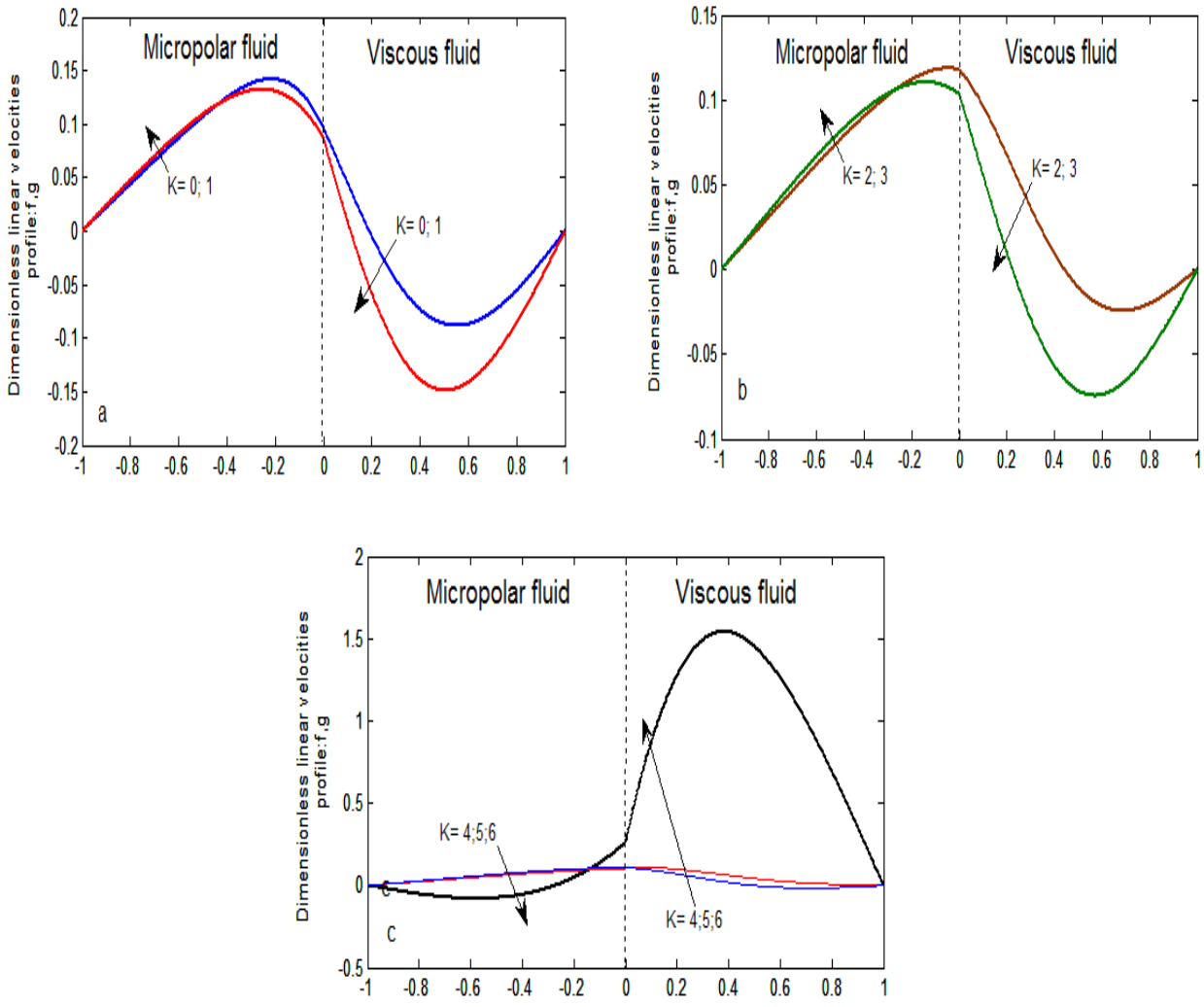

Figure 5.32 : variation of dimensionless linear velocities profile for different values of material parameter with « **Ha=5**, **Pr=40, (a) K=0-1, (b) K=2-3, (c)K=4-6** & Ec=1, GR=5, h*=1, k*=1, μ*=1, β*=1, ρ*=1»

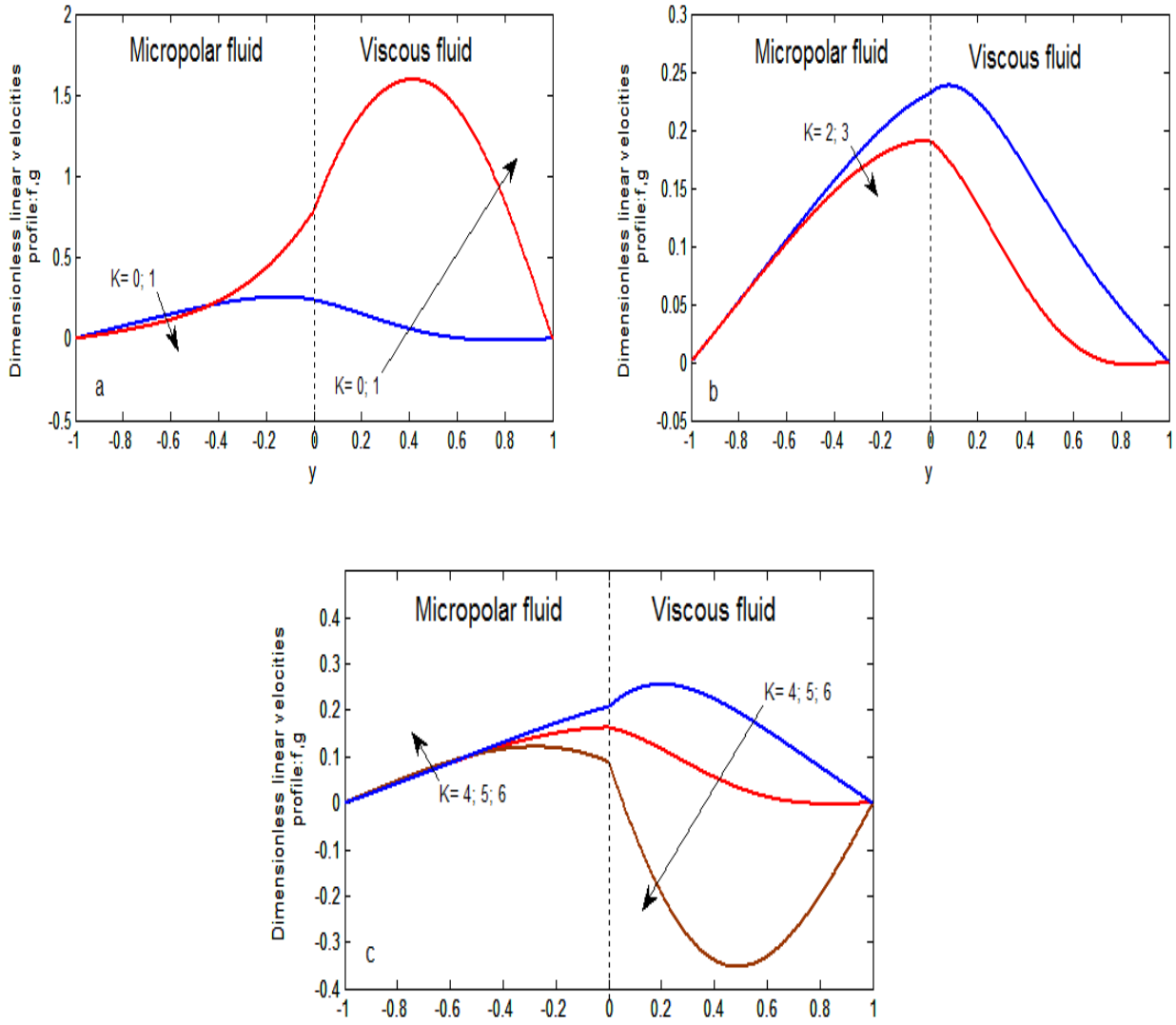

Figure 5.33: variation of dimensionless linear velocities profile for different values of material parameter with « **Ha=1**, **Pr=50, (a) K=0-1, (b) K=2-3, (c) K=4-6** & Ec=1, GR=5, h^*=1, k*=1, μ*=1, β*=1, ρ*=1»

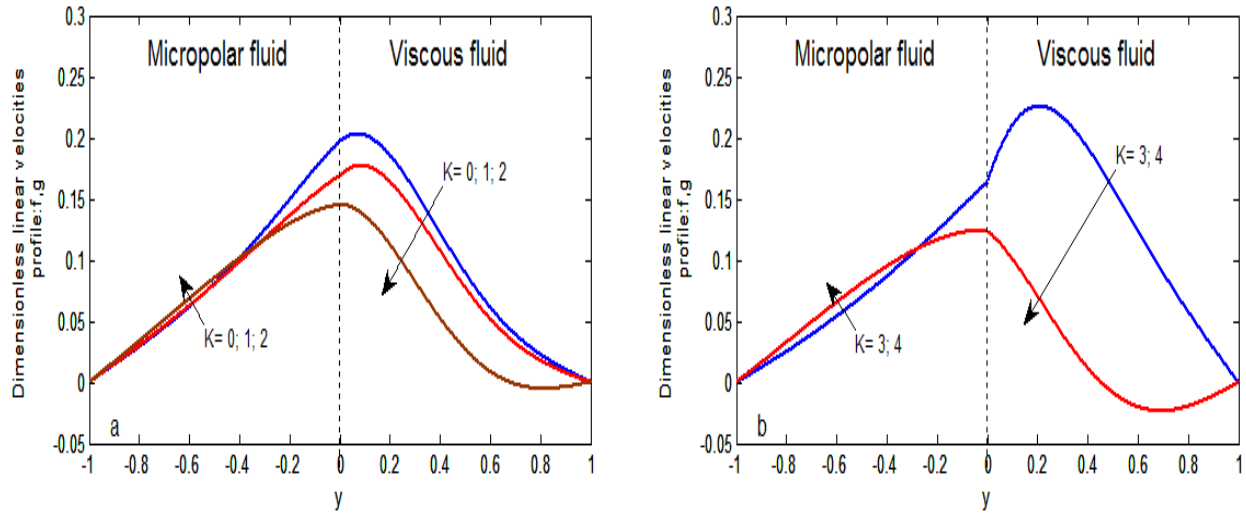

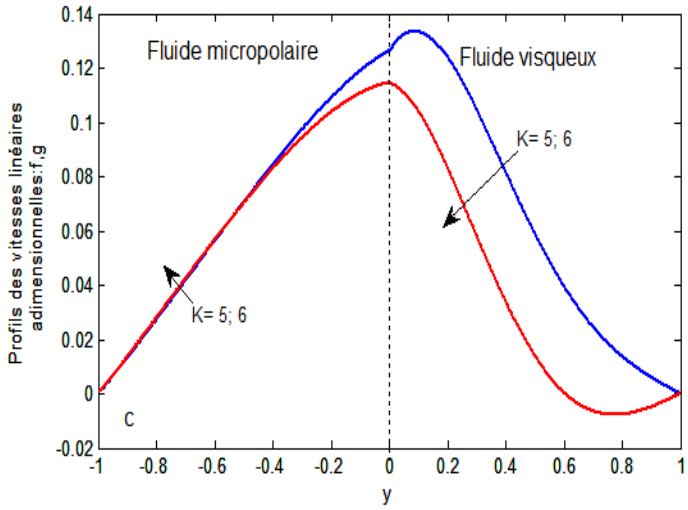

Figure 5.34 : variation of dimensionless linear velocities profile for different values of material parameter with « Ha=3, Pr=50, (a) K=0-2, (b) K=3-34, (c) K=5-6 & Ec=1, GR=5, h*=1, k*=1, μ*=1, β*=1, ρ*=1»

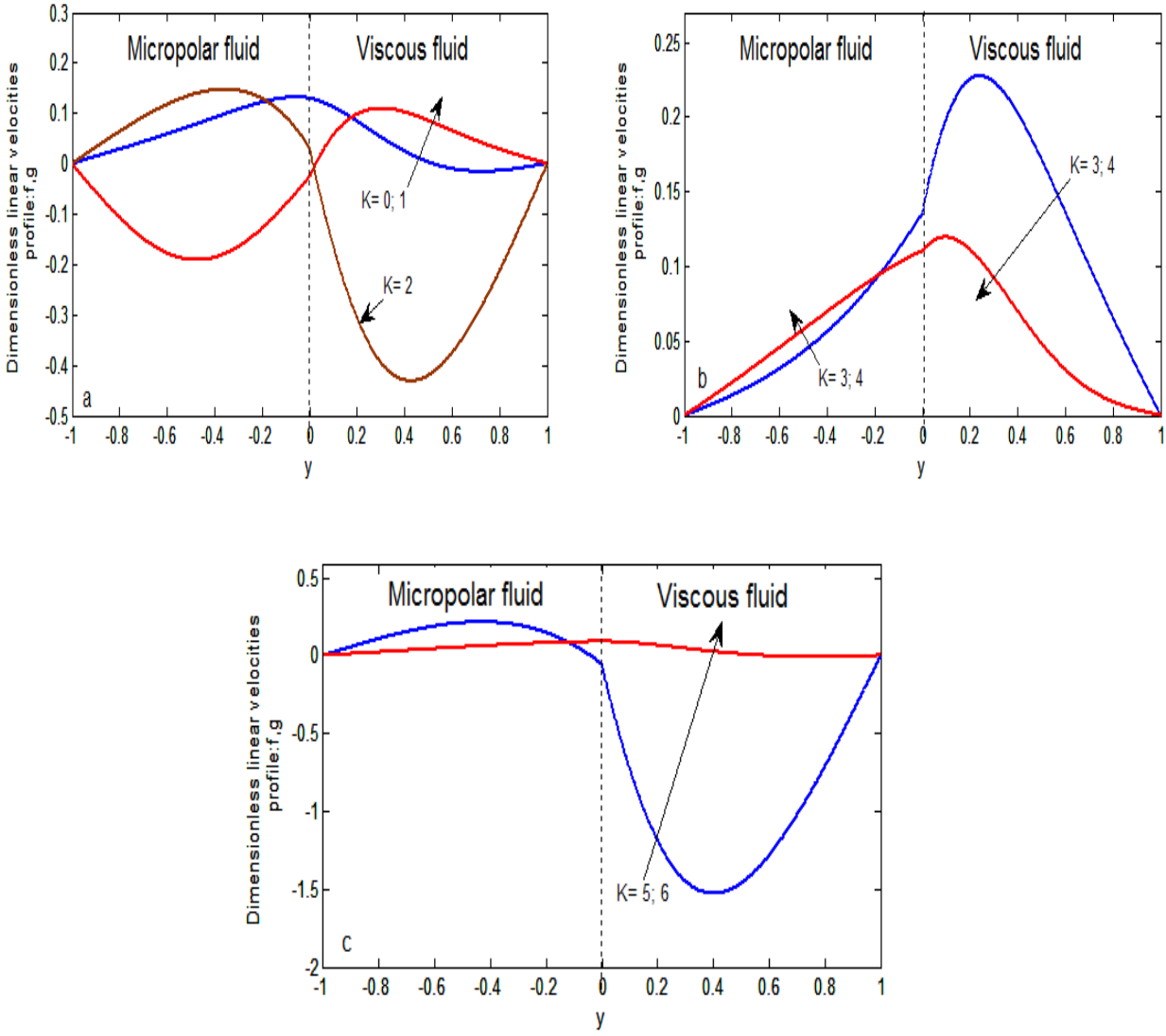

Figure 5.35 : variation of dimensionless linear velocities profile for different values of material parameter with « **Ha=5**, **Pr=50, (a) K=0-2, (b) K=3-4, (c) K=5-6** & Ec=1, GR=5, h*=1, k*=1, μ*=1, β*=1, ρ*=1»

In analyzing the effect of material parameter variation by varying Prandtl number and magnetic field (figures 5.32-5.38), we note that a high values of material parameter, Prandtl and Hartmann numbers have a significant effect on the linear and microrotation velocities profile, so the increase of the three dimensionless parameters provoke a perturbation in the linear velocity profiles in both regions. In other way we can note that, in same time, the linear velocities profile increase within non-Newtonian micropolar fluid, and decrease within Newtonian-viscous fluid, when the material parameter increase.

5.3.4. The material parameter effect with varying the magnetic parameter for $Pr = 100$

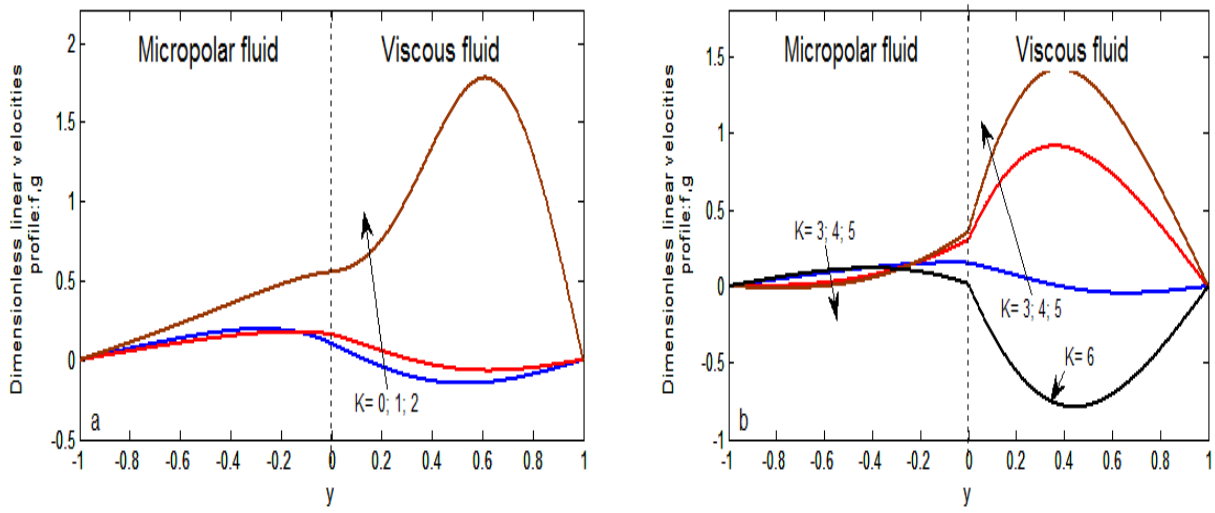

Figure 5.36: : variation of dimensionless linear velocity profiles for different values of material parameter with « **Ha=1**, **Pr=100, (a) K=0-2, (b) K=3-6** & Ec=1, GR=5, h*=1, k*=1, μ*=1, β*=1, ρ*=1».

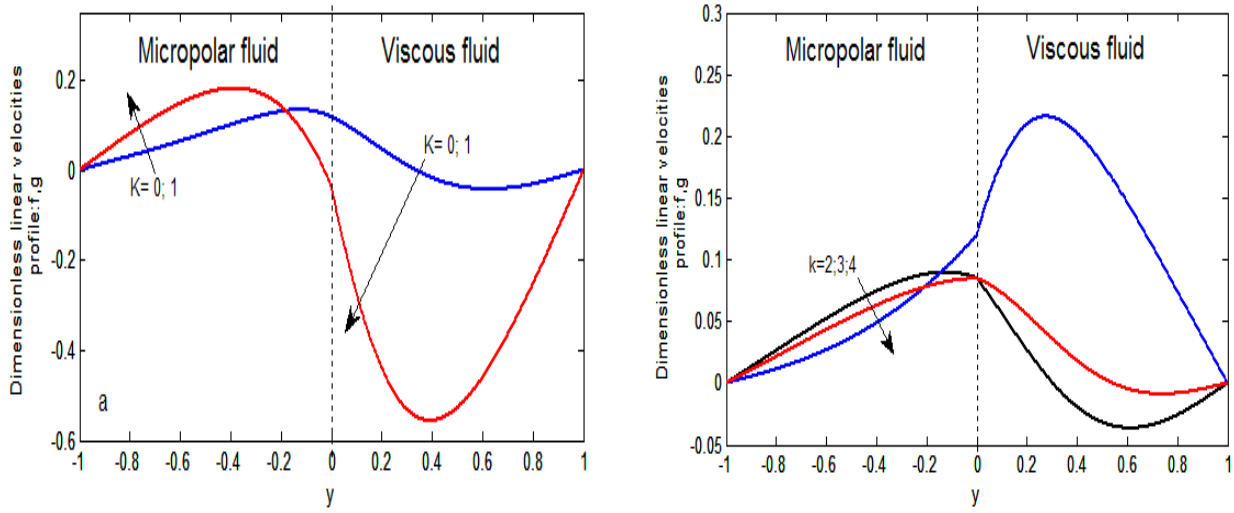

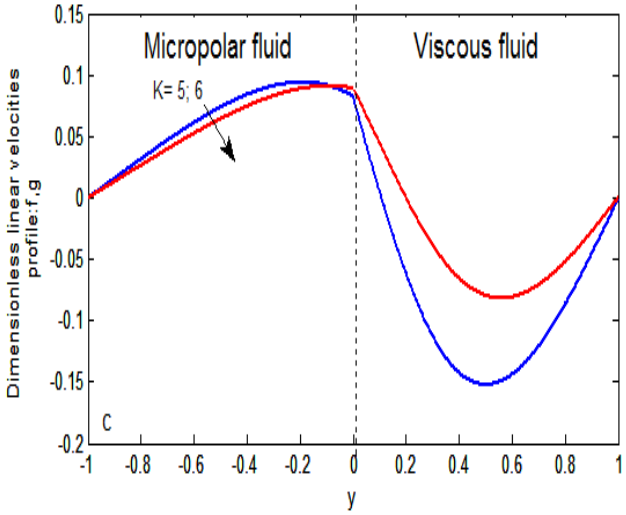

Figure 5.37: variation of dimensionless linear velocities profile for different values of material parameter with « **Ha=3**, **Pr=100, (a) K=0-2, (b) K=2-4, (c) K=5-6** & Ec=1, GR=5, h^*=1, k*=1, μ*=1, β*=1, ρ*=1».

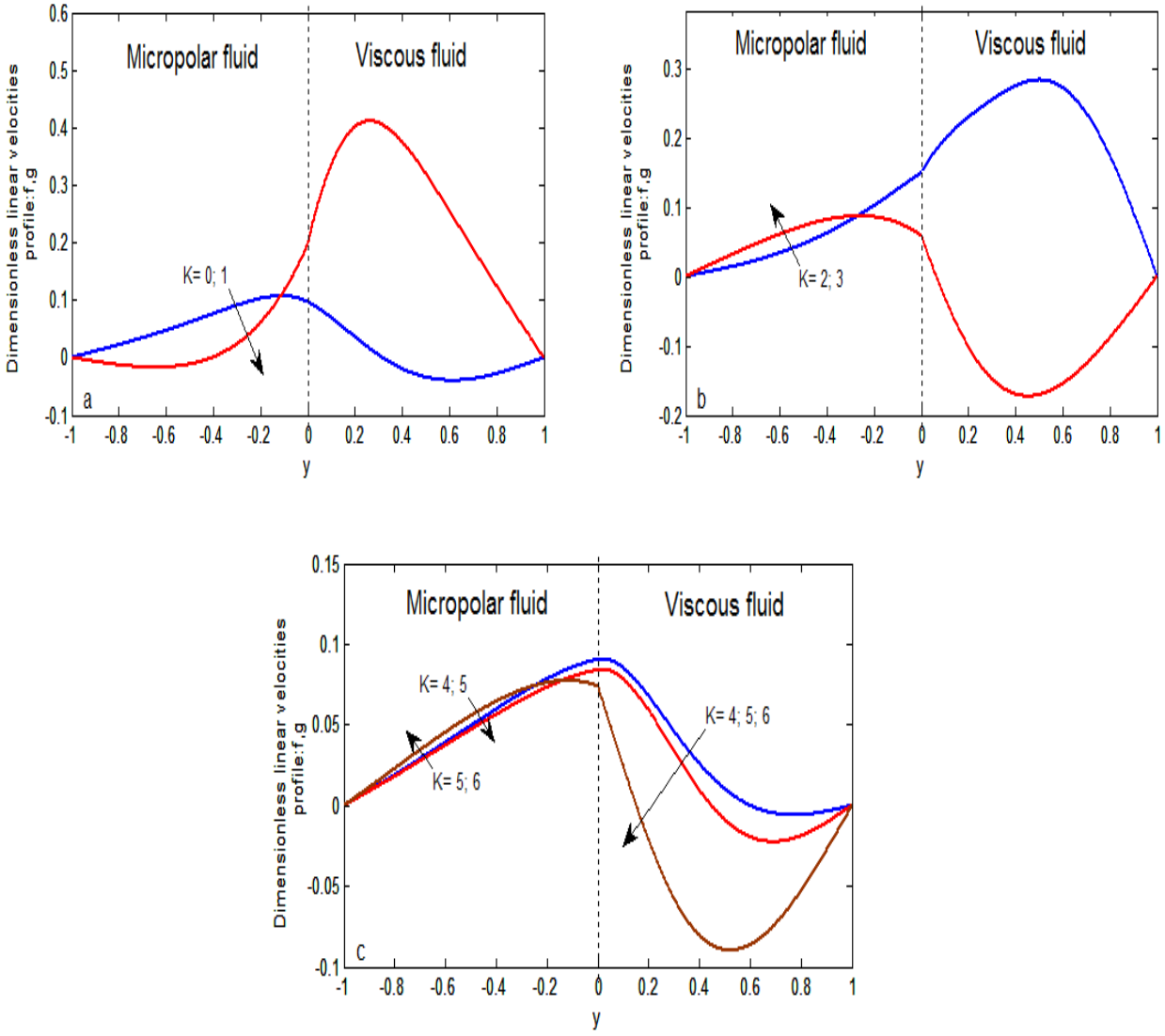

Figure 5.38: variation of dimensionless linear velocities profile for different values of material parameter with « **Ha=5**, **Pr=100, (a) K=0-1, (b) K=2-3, (c) K=4-6** & Ec=1, GR=5, h^*=1, k*=1, μ*=1, β*=1, ρ*=1».

5.4. The effect of parameter variations on microrotation velocity in presence of magnetic field

5.4.1. The material parameter effect in varying the magnetic parameter for $0.1 \leq Pr \leq 3$

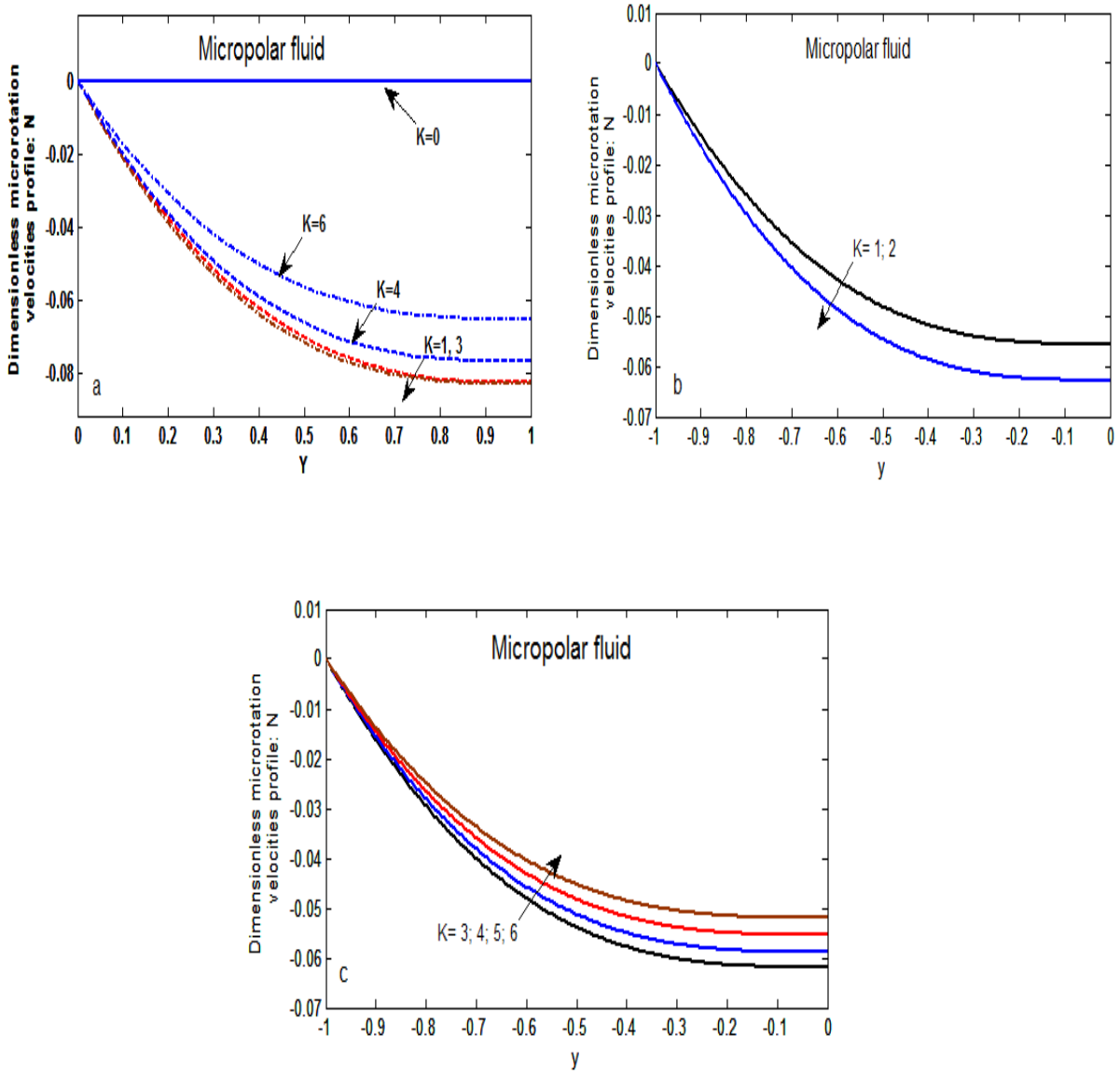

Figure 5.39: variation of dimensionless microrotation velocity profile for different values of material parameter with « **Pr=0.1, (a) Ha=1**, **K=0-6, , (b) Ha=3, K=1-2, (c) K=3-6** & Ec=1, GR=5, h^*=1, k*=1, μ*=1, β*=1, ρ*=1».

In figures 5.39-a,b,c, above we observed that the increase in the material parameter causes a decrease in microrotation velocity profiles for K = 0.0-3.0, but the microrotation velocities increase when the material parameter takes values 3-6.

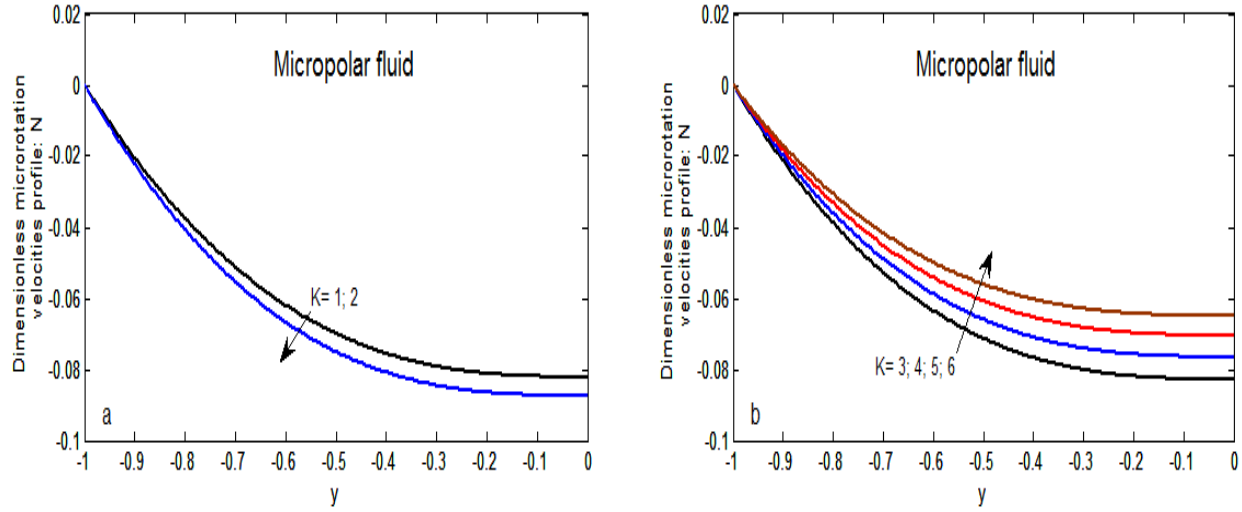

Figure 5.**40** : variation of dimensionless microrotation velocity profile for different values of material parameter with « **Pr=0.7, Ha=1, (a)**, **K=1-2, , (b) K=3-6** & Ec=1, GR=5, h^*=1, k*=1, μ*=1, β*=1, ρ*=1».

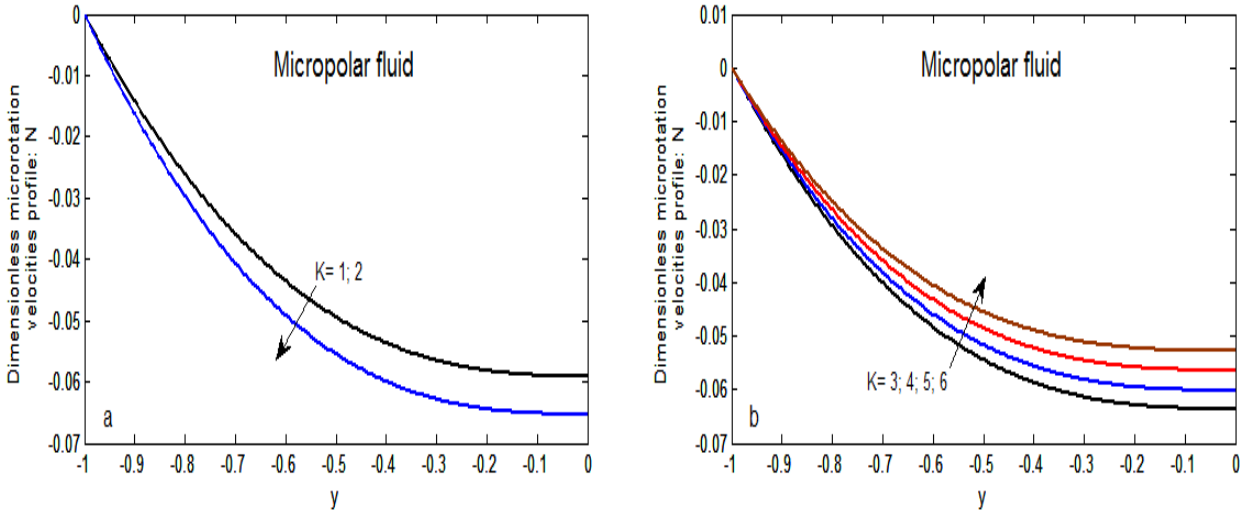

Figure 5.41: variation of dimensionless microrotation velocity profile for different values of material parameter with « **Pr=0.7, Ha=3, (a)**, **K=1-2, , (b) K=3-6** & Ec=1, GR=5, h^*=1, k*=1, μ*=1, β*=1, ρ*=1».

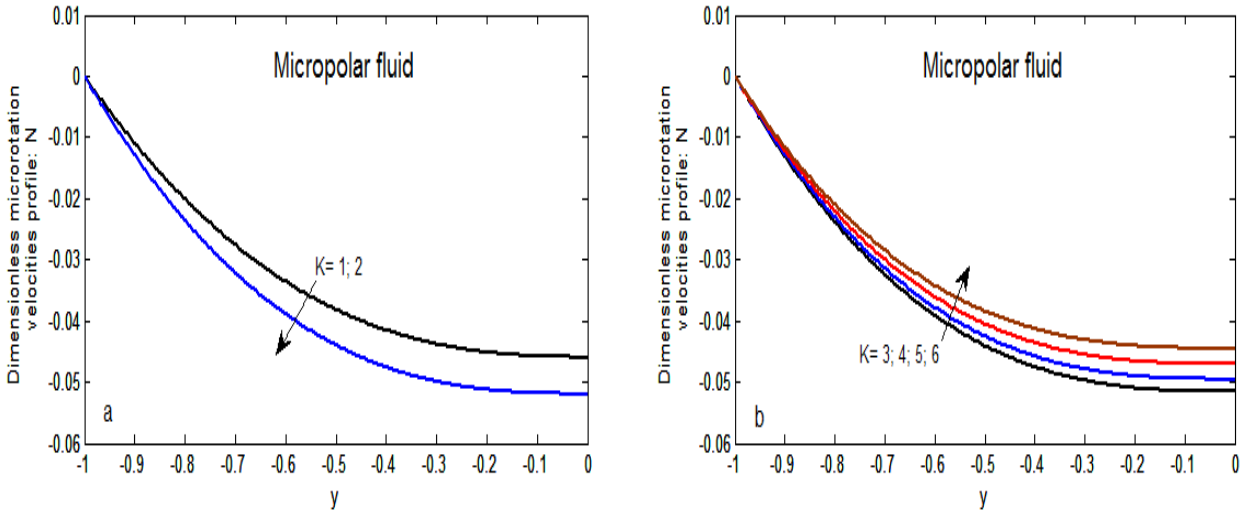

Figure 5.42: variation of dimensionless microrotation velocity profile for different values of material parameter with « **Pr=0.7, Ha=5, (a)**, **K=1-2, , (b) K=3-6** & Ec=1, GR=5, h^*=1, k*=1, μ*=1, β*=1, ρ*=1».

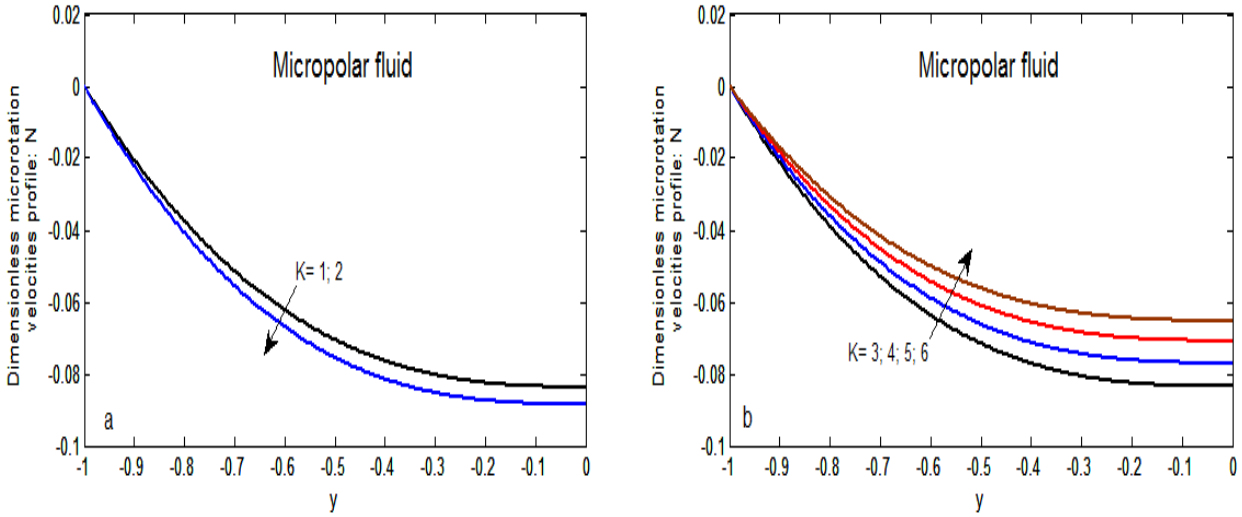

Figure 5.43: variation of dimensionless microrotation velocity profile for different values of material parameter with « **Pr=1, Ha=1, (a)**, **K=1-2, , (b) K=3-6** & Ec=1, GR=5, h^*=1, k*=1, μ*=1, β*=1, ρ*=1».

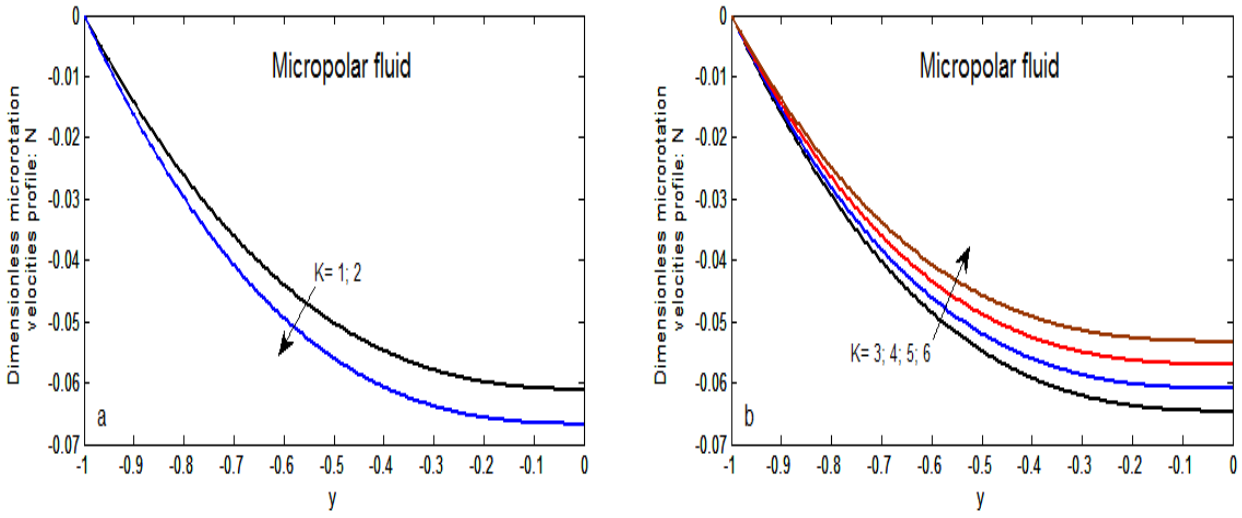

Figure 5.44: variation of dimensionless microrotation velocity profile for different values of material parameter with « **Pr=1, Ha=3, (a)**, **K=1-2, , (b) K=3-6** & Ec=1, GR=5, h^*=1, k*=1, μ*=1, β*=1, ρ*=1».

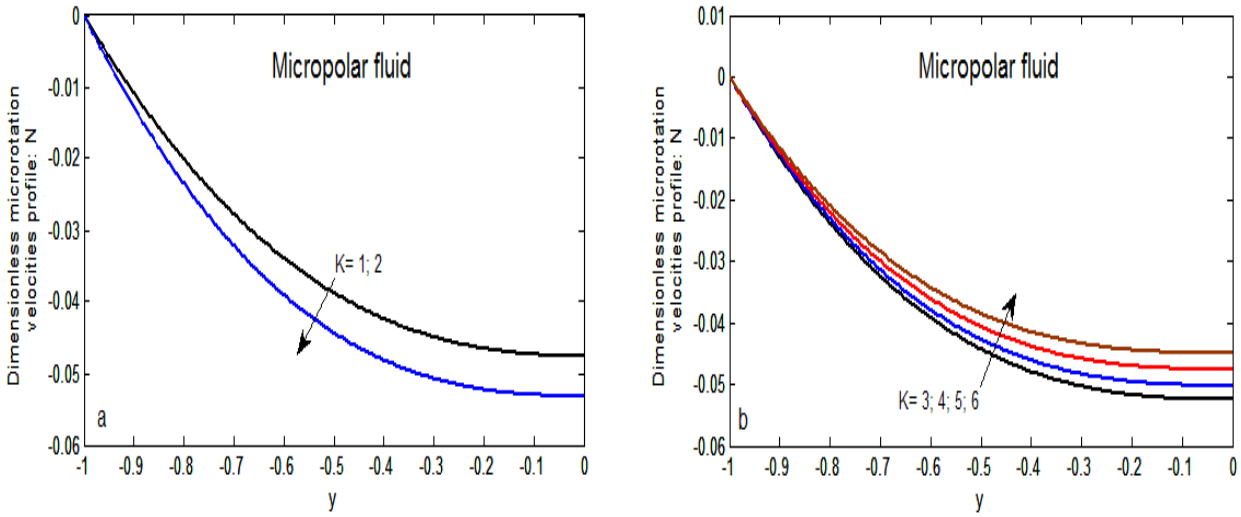

Figure 5.45: variation of dimensionless microrotation velocity profile for different values of material parameter with « **Pr=1, Ha=5, (a)**, **K=1-2, (b) K=3-6** & Ec=1, GR=5, h^*=1, k*=1, μ*=1, β*=1, ρ*=1».

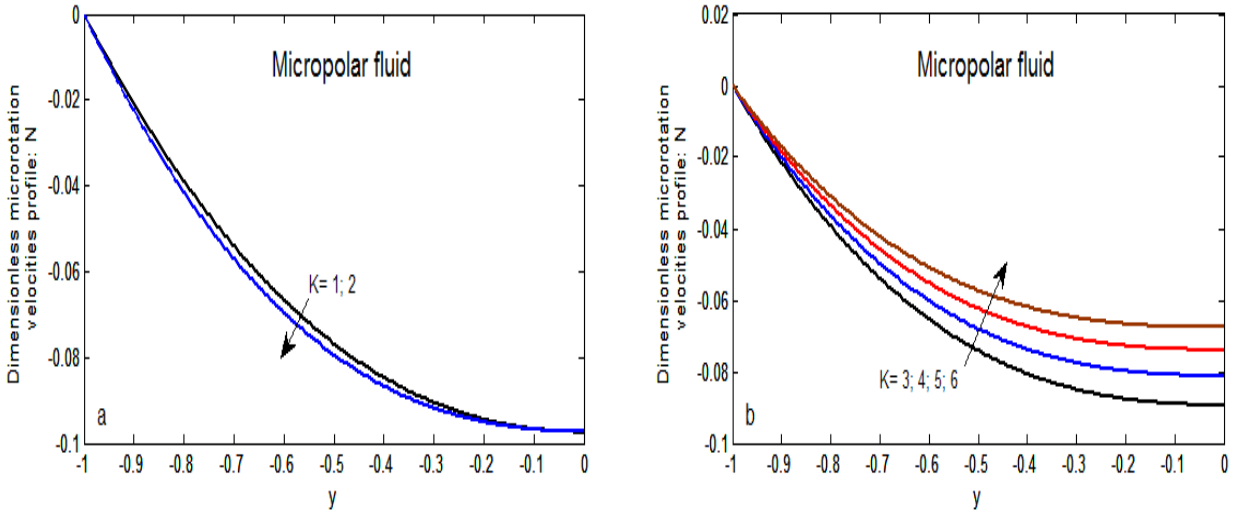

Figure 5.46: variation of dimensionless microrotation velocity profile for different values of material parameter with « **Pr=3, Ha=1, (a)**, **K=1-2, (b) K=3-6** & Ec=1, GR=5, h^*=1, k*=1, μ*=1, β*=1, ρ*=1».

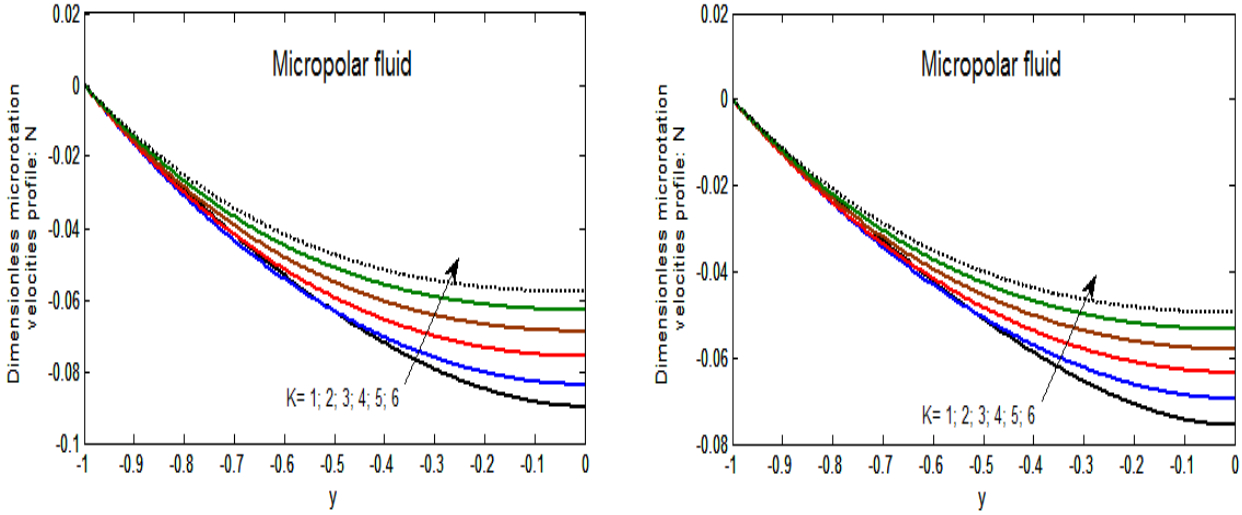

Figure 5.47: variation of dimensionless microrotation velocity profile for different values of material parameter with « **Pr=3, K=1-6, (a) Ha=3, (b) Ha=5** & Ec=1, GR=5, h^*=1, k*=1, μ*=1, β*=1, ρ*=1».

5.4.2. The material parameter effect in varying the magnetic parameter for $3 < Pr \leq 50$

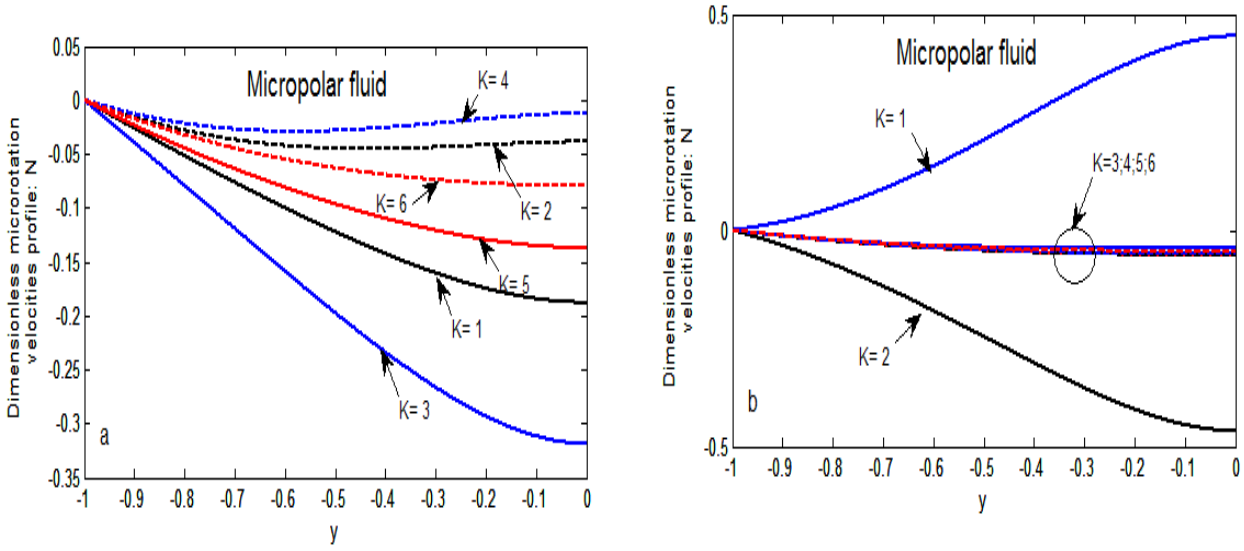

Figure 5.48: variation of dimensionless microrotation velocity profile for different values of material parameter with « Pr=10, K=1-6, (a) Ha=1, (b) Ha=3 & Ec=1, GR=5, h^*=1, k*=1, μ*=1, β*=1, ρ*=1».

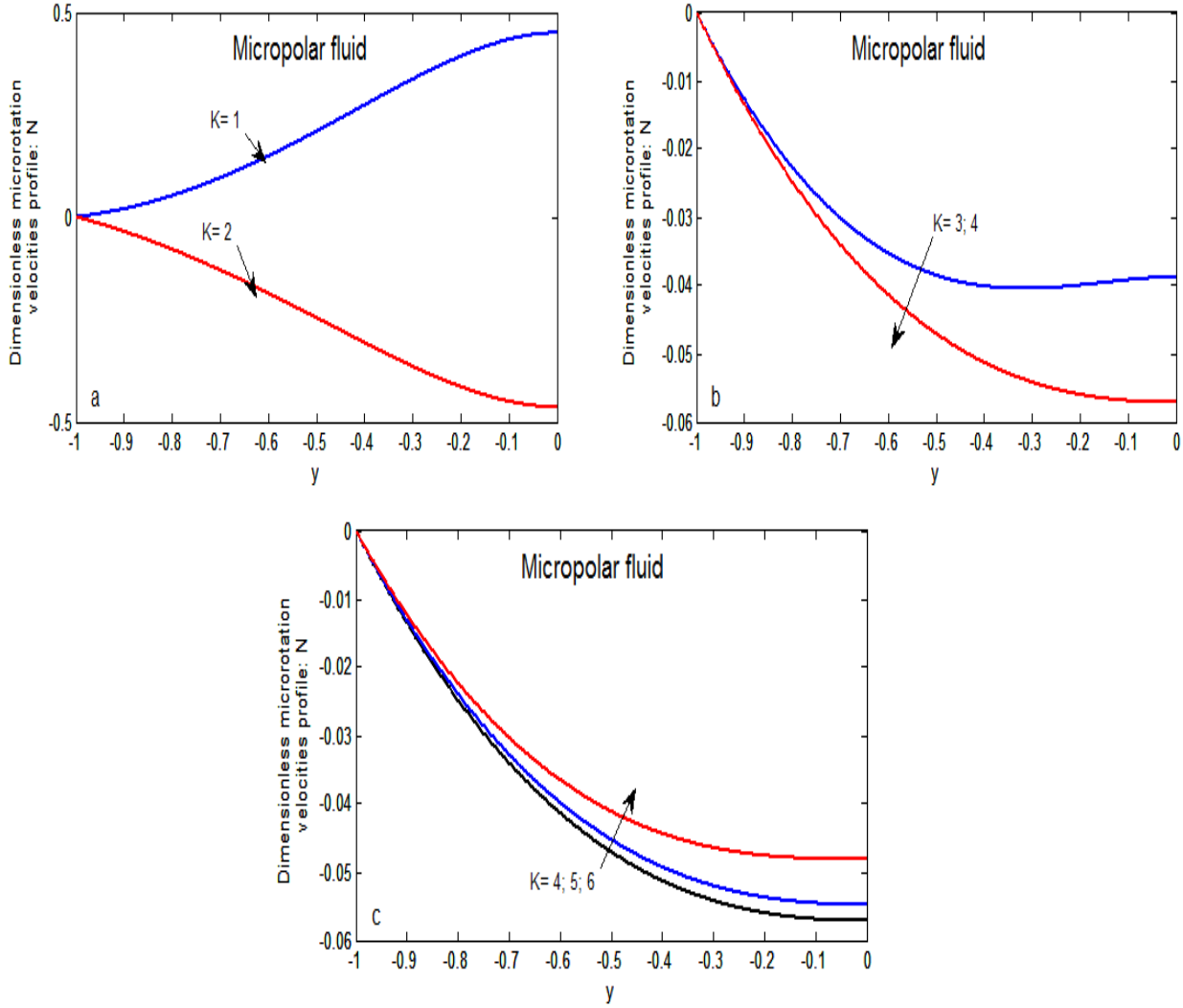

Figure 5.49: variation of dimensionless microrotation velocity profile for different values of material parameter with « **Pr=10, Ha=3, (a) K=1-2, (b) K=3-4, (c) K=4-6** & Ec=1, GR=5, h^*=1, k*=1, μ*=1, β*=1, ρ*=1».

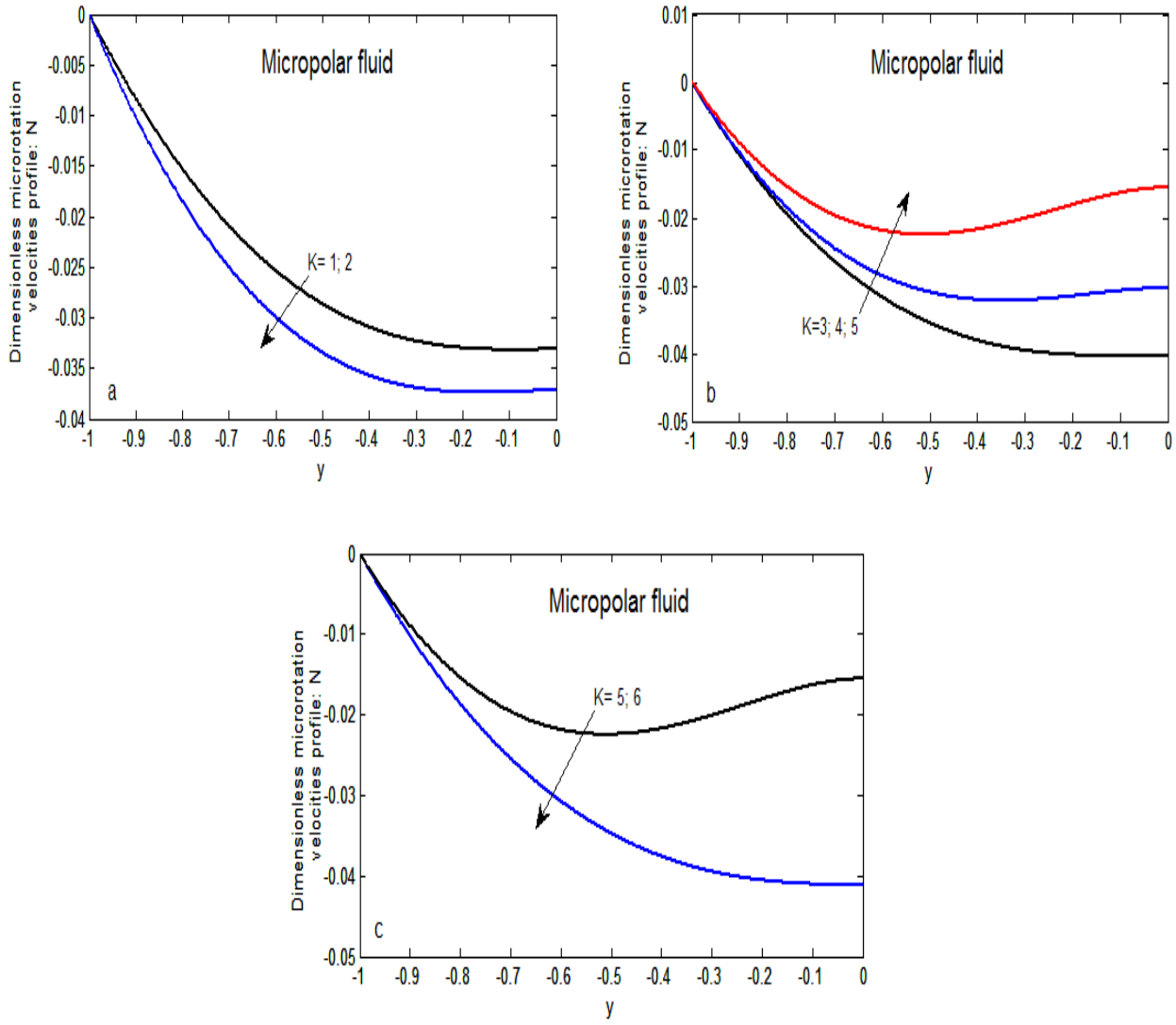

Figure 5.50: variation of dimensionless microrotation velocity profile for different values of material parameter with « **Pr=10, Ha=5, (a) K=1-2, (b) K=3-5, (c) K=5-6** & Ec=1, GR=5, h^*=1, k*=1, μ*=1, β*=1, ρ*=1».

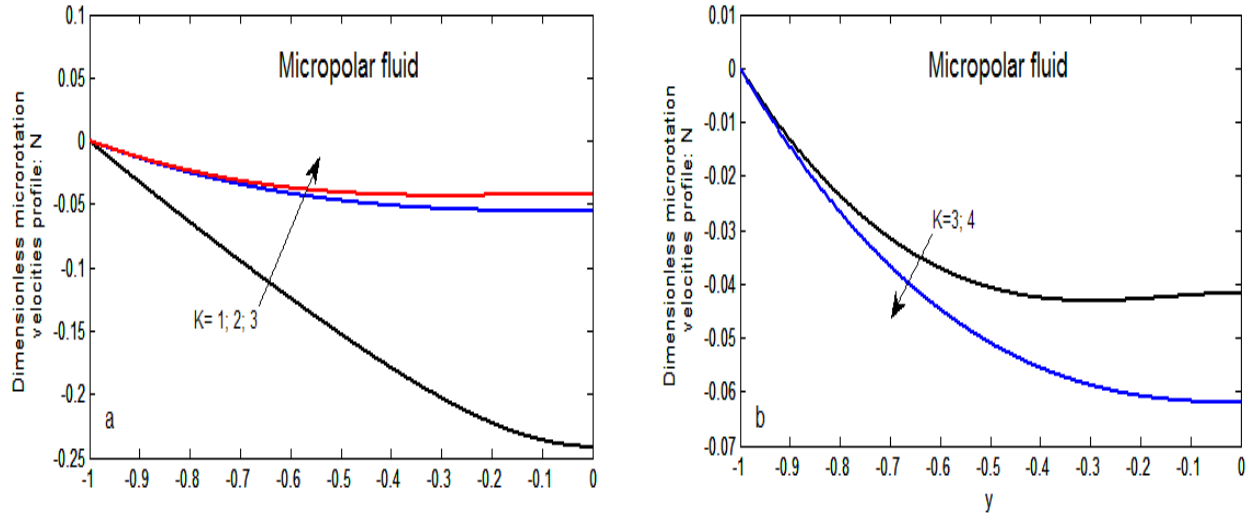

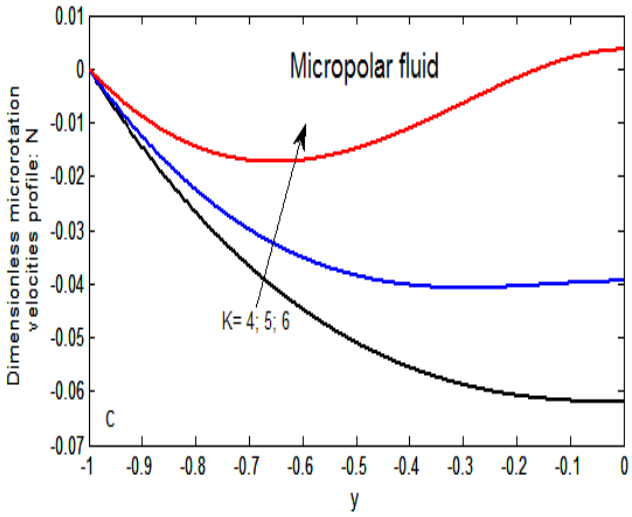

Figure 5.51: variation of dimensionless microrotation velocity profile for different values of material parameter with « **Pr=50, Ha=1, (a) K=1-3, (b) K=3-4, (c) K=4-6** & Ec=1, GR=5, h^*=1, k*=1, μ*=1, β*=1, ρ*=1».

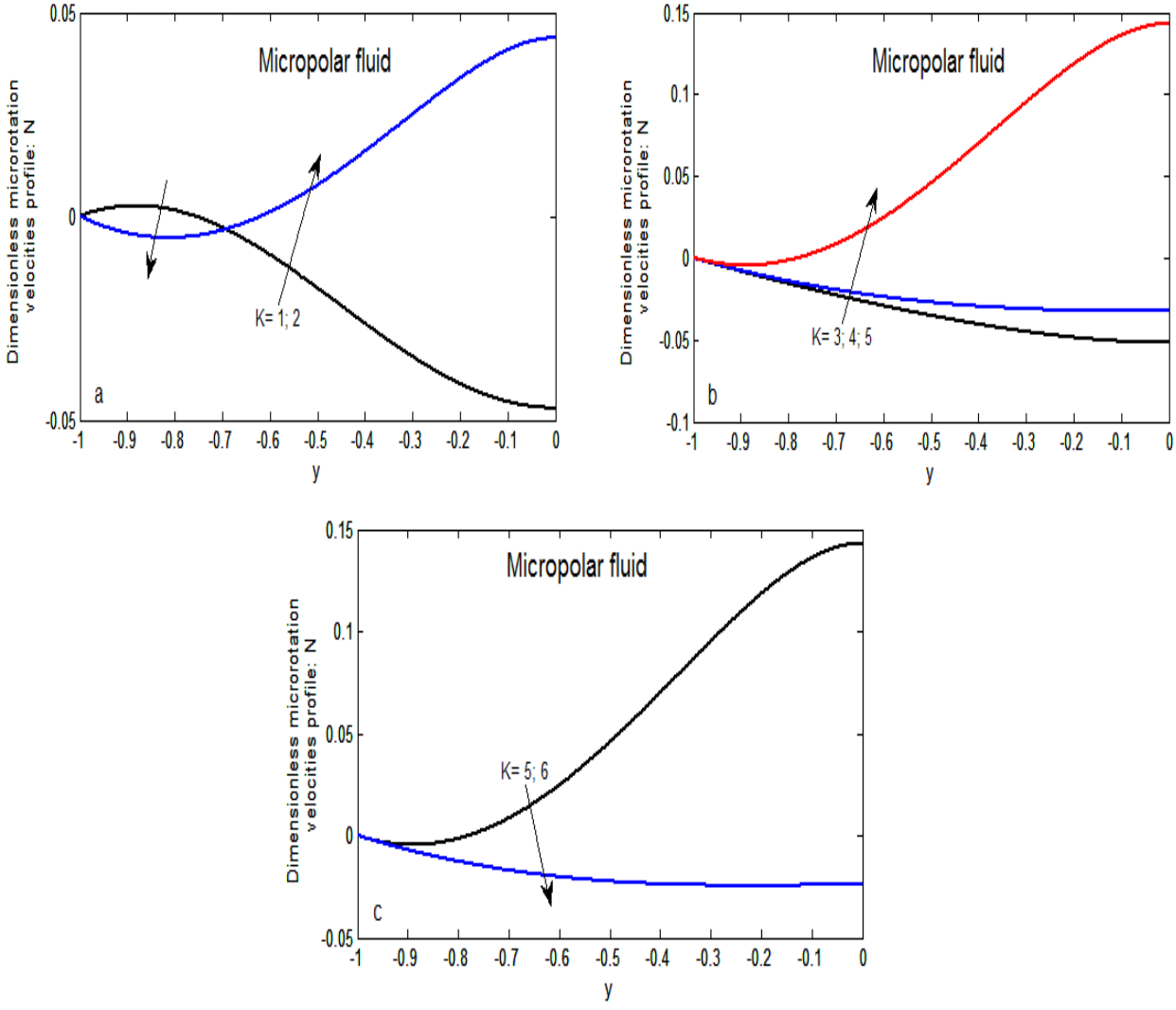

Figure 5.52: variation of dimensionless microrotation velocity profile for different values of material parameter with « **Pr=50, Ha=5, (a) K=1-2, (b) K=3-5, (c) K=5-6** & Ec=1, GR=5, h^*=1, k*=1, μ*=1, β*=1, ρ*=1».

5.4.3. The material parameter effect in varying the magnetic parameter for $Pr = 100$

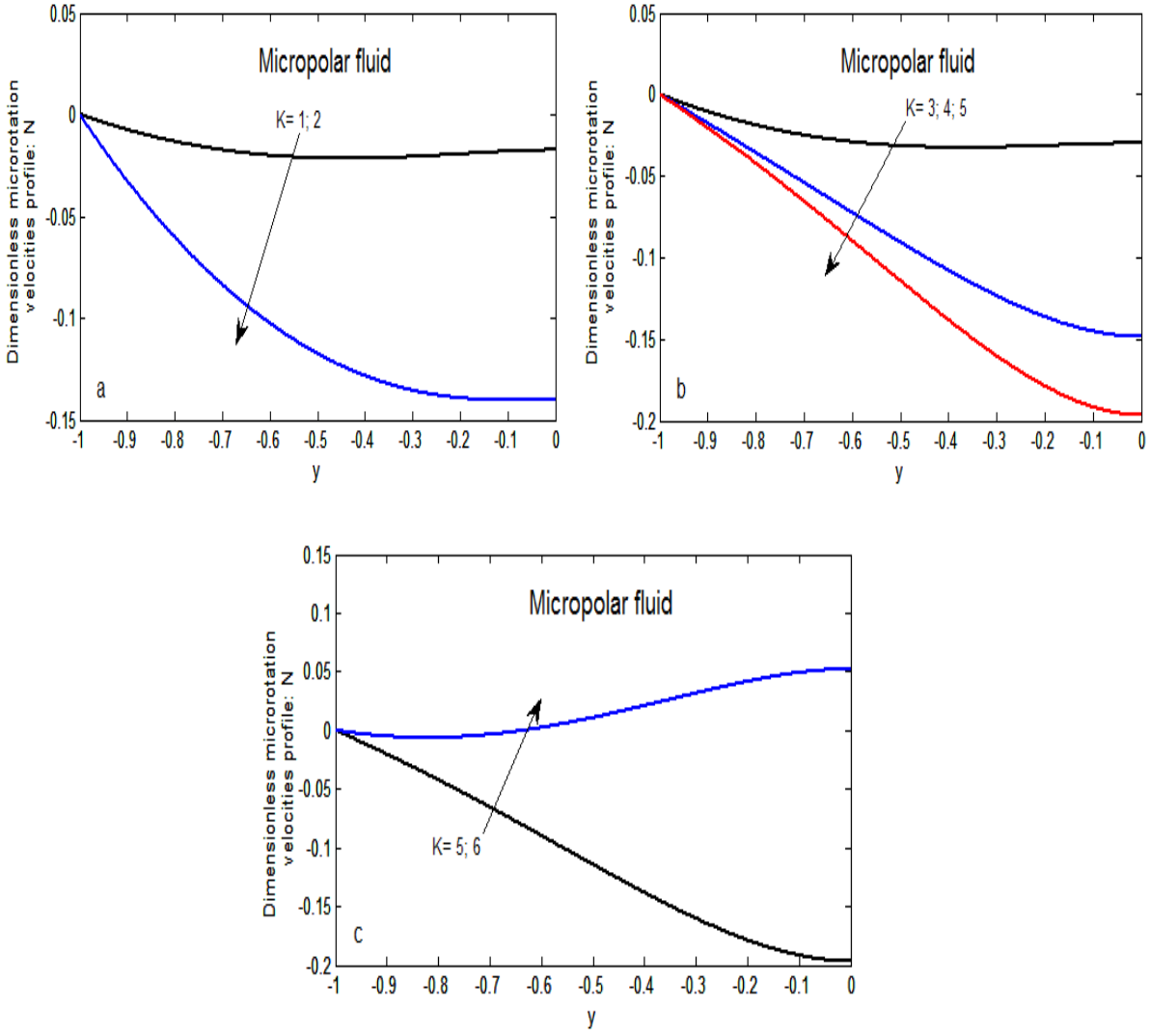

Figure 5.53: variation of dimensionless microrotation velocity profile for different values of material parameter with « **Pr=100, Ha=1, (a) K=1-2, (b) K=3-5, (c) K=5-6** & Ec=1, GR=5, h^*=1, k^*=1, μ^*=1, β^*=1, ρ^*=1».

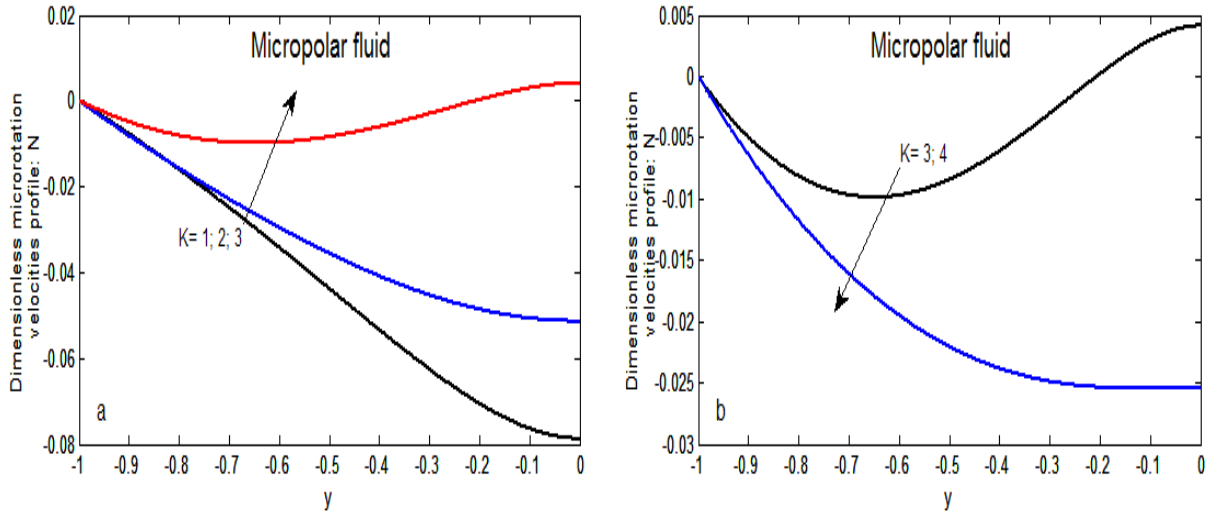

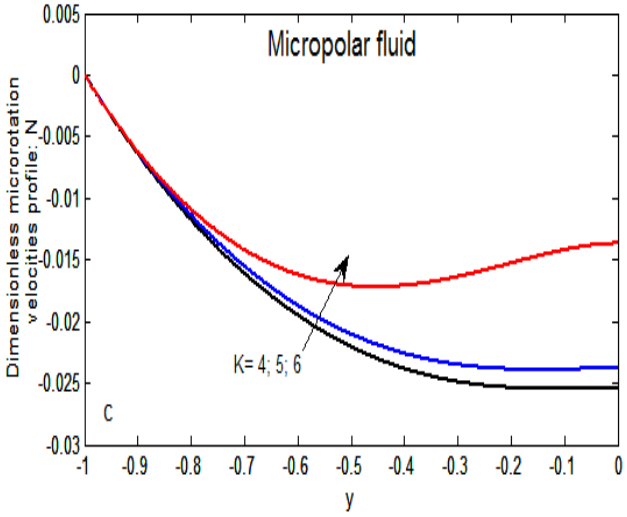

Figure 5.54: variation of dimensionless microrotation velocity profile for different values of material parameter with « **Pr=100, Ha=5, (a) K=1-3, (b) K=3-5, (c) K=5-6** & Ec=1, GR=5, h^*=1, k*=1, μ*=1, β*=1, ρ*=1».

5.4.4. The thermal conductivities ratio, magnetic parameter effect for $10 \leq Pr \leq 100$

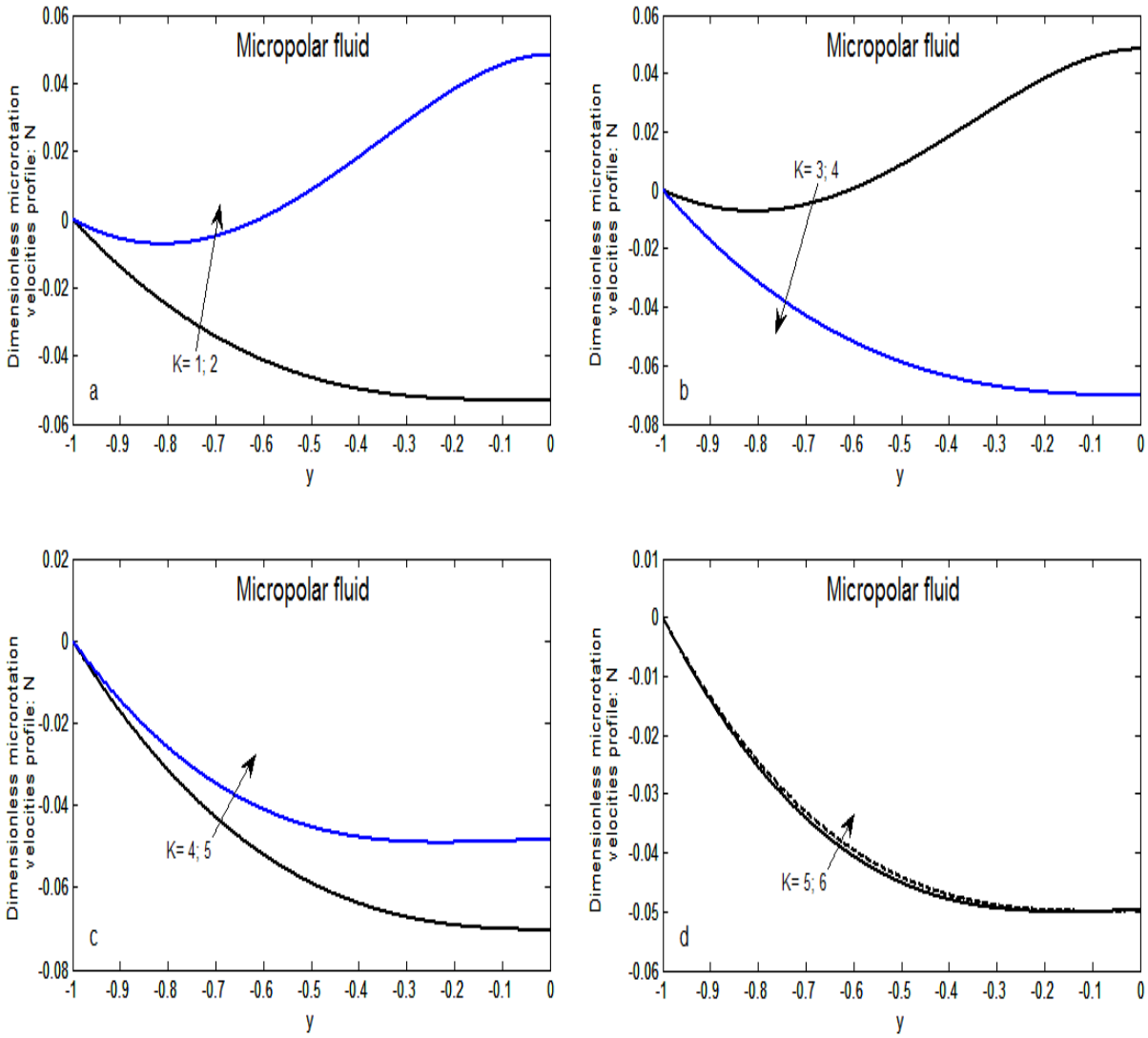

Figure 5.55: variation of dimensionless microrotation velocity profile for different values of material parameter with « **Ha=1, Pr=10, k*=2,, (a) K=1-2, (b) K=3-4, (c) K=4-5, (d) K=5-6** & Ec=1, GR=5, h^*=1, μ*=1, β*=1, ρ*=1».

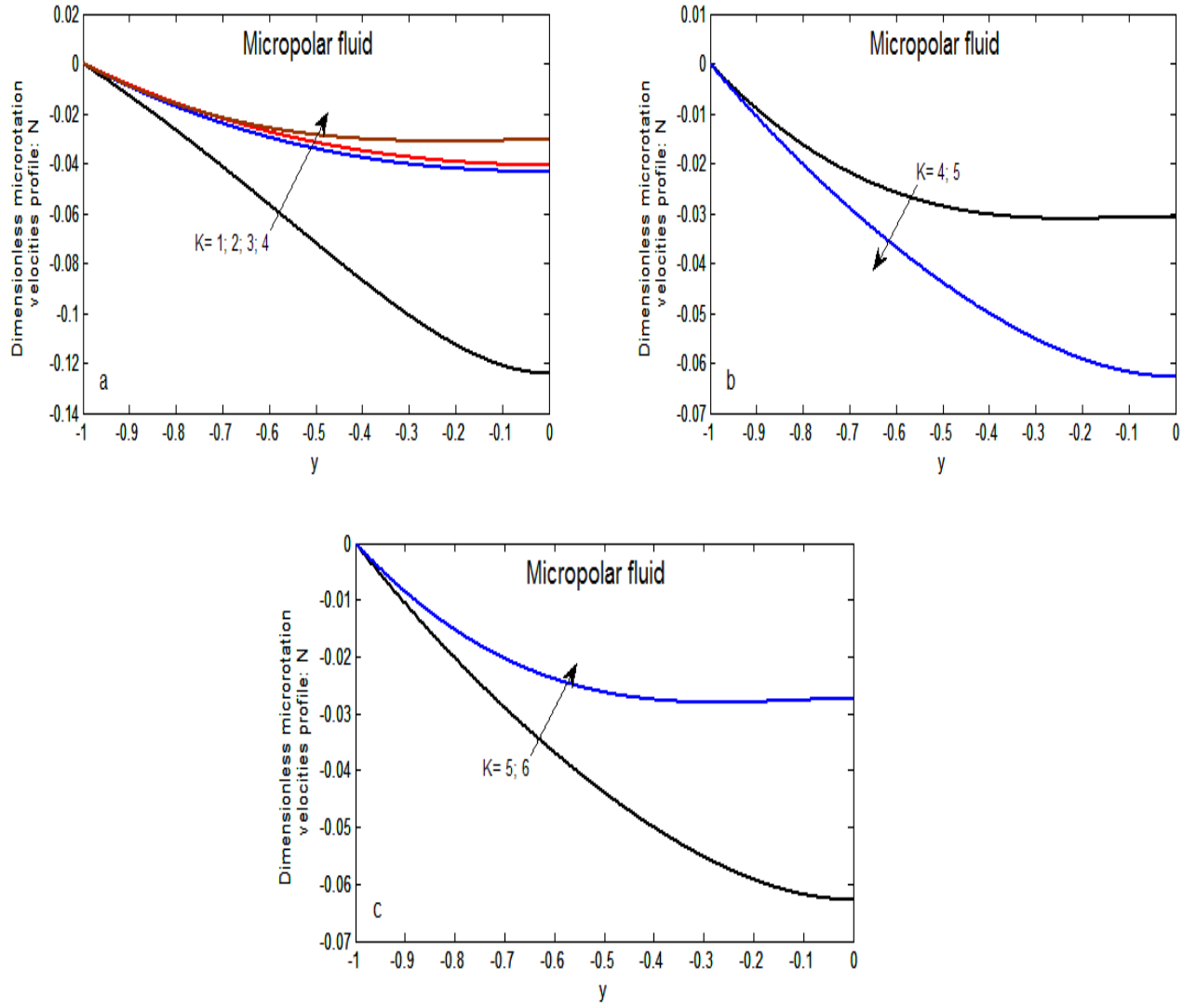

Figure 5.56: variation of dimensionless microrotation velocity profile for different values of material parameter with « **Pr=10, Ha=5, k*=2,, (a) K=1-4, (b) K=4-5, (c) K=5-6** & Ec=1, GR=5, h^*=1, μ*=1, β*=1, ρ*=1».

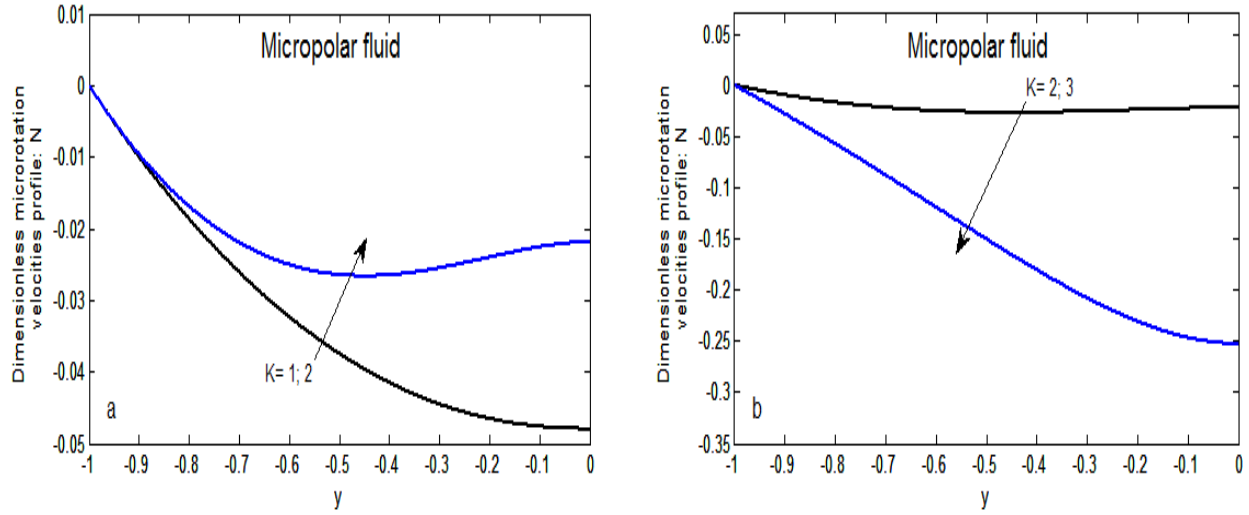

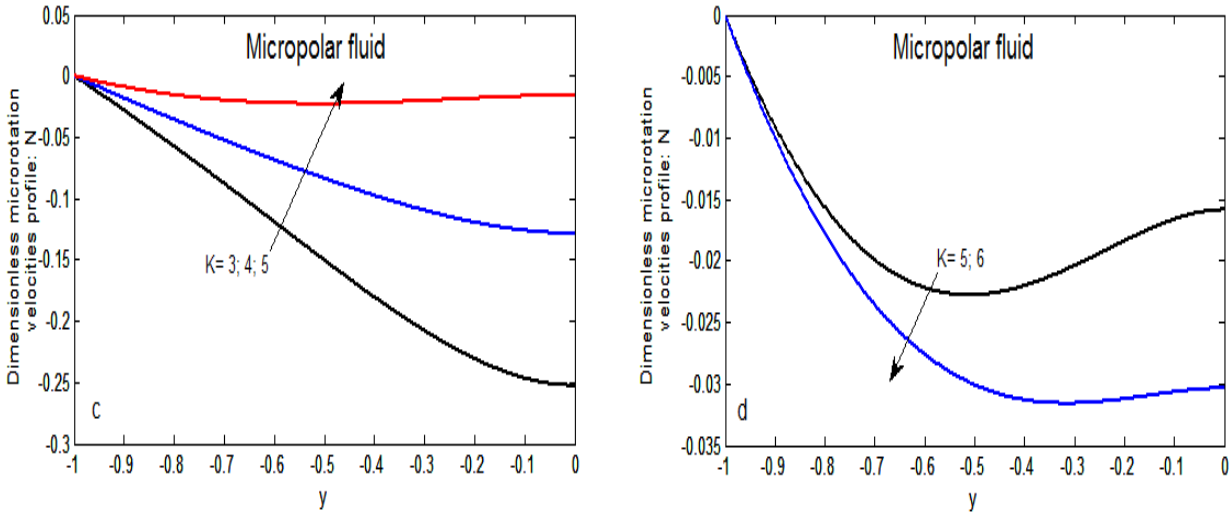

Figure 5.57: variation of dimensionless microrotation velocity profile for different values of material parameter with « **Ha=1, Pr=50, k*=2**, **(a) K=1-2, (b) K=2-3, (c) K=3-5, (d) K=5-6** & Ec=1, GR=5, h^*=1, μ*=1, β*=1, ρ*=1».

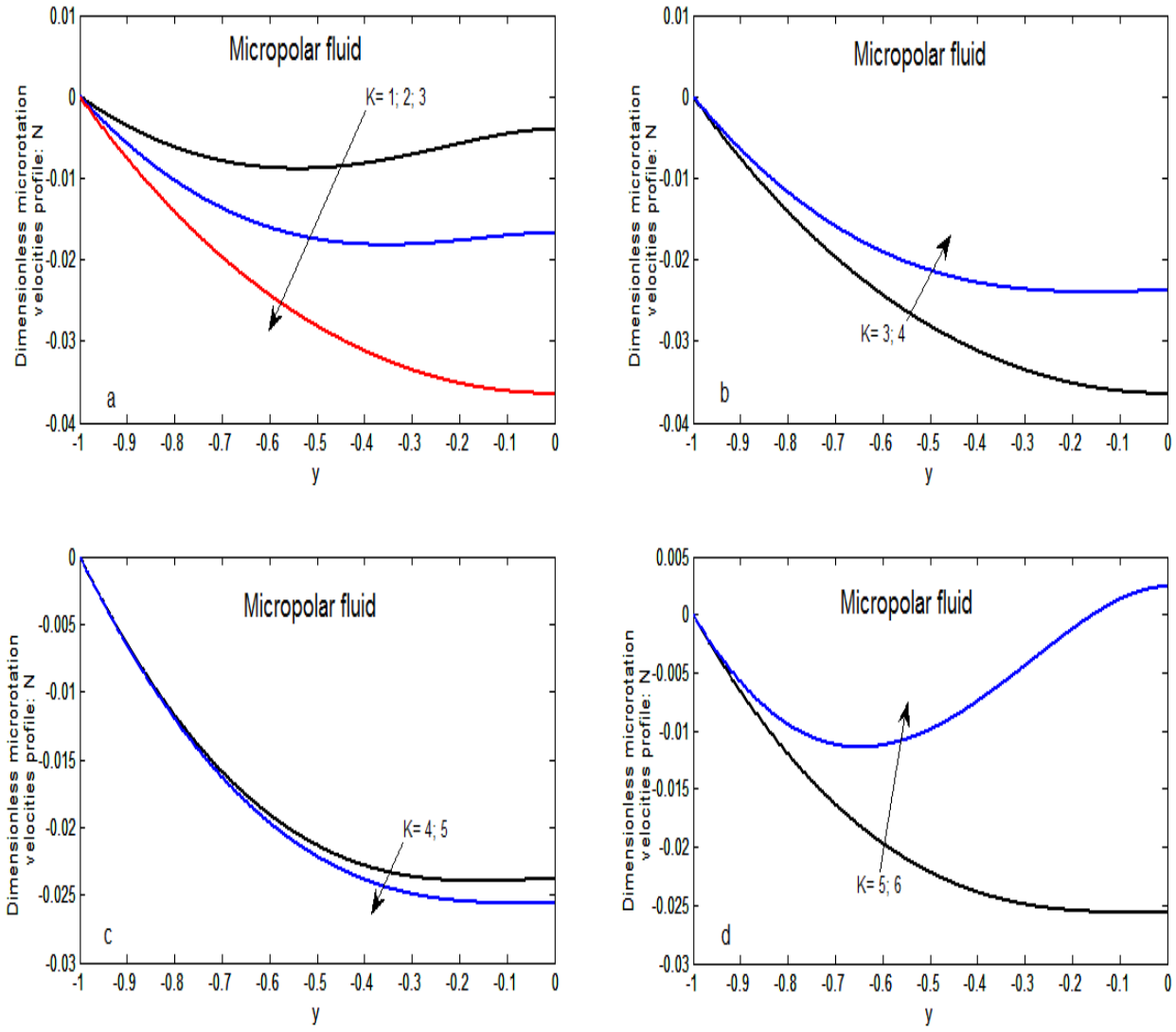

Figure 5.58: variation of dimensionless microrotation velocity profile for different values of material parameter with « **Ha=5, Pr=50, k*=2,, (a) K=1-3, (b) K=3-4, (c) K=4-5, (d) K=5-6** & Ec=1, GR=5, h^*=1, μ*=1, β*=1, ρ*=1».

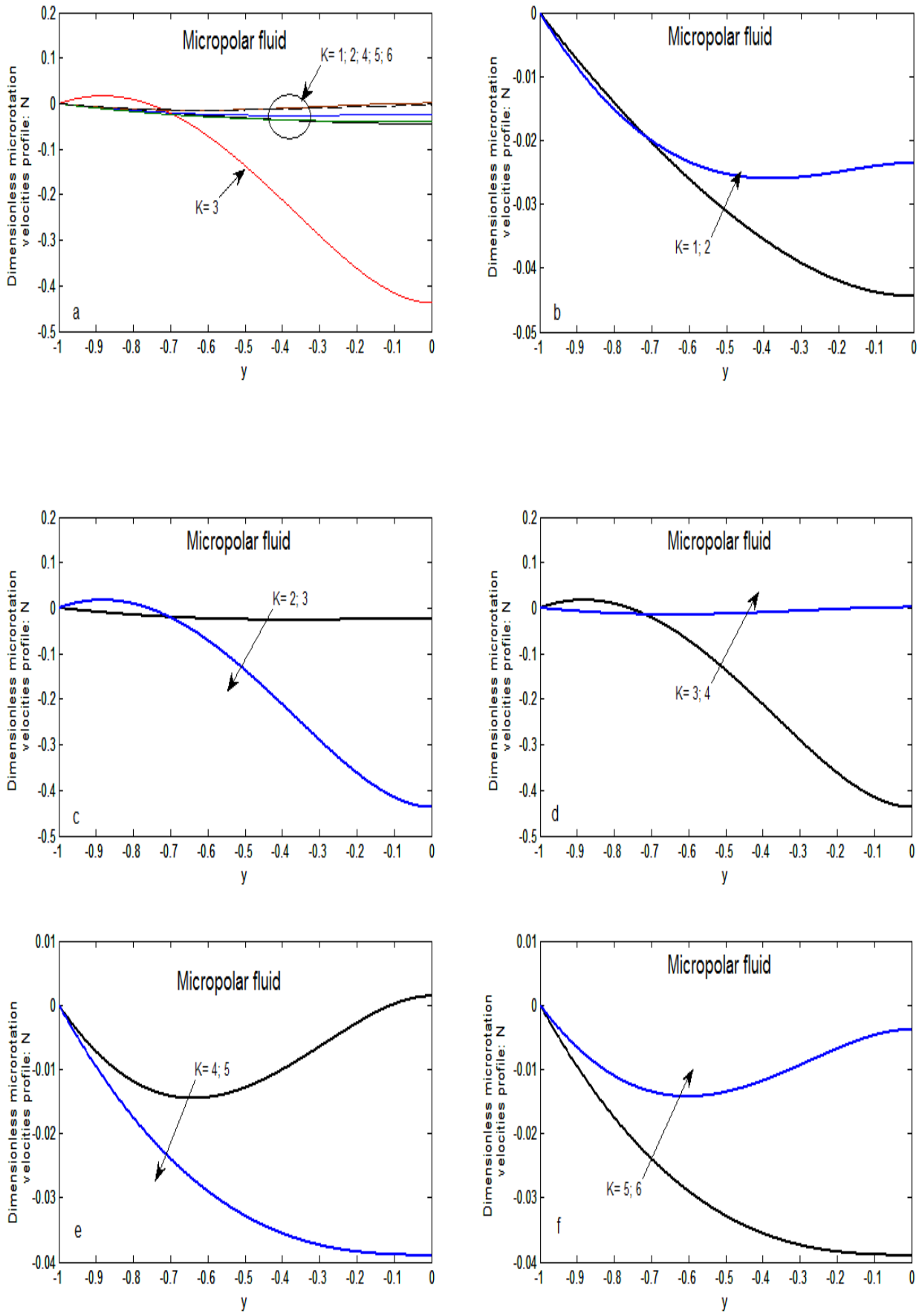

Figure 5.59: variation of dimensionless microrotation velocity profile for different values of material parameter with « **Ha=1, Pr=100, k*=2,, (a) K=1-6, (b) K=1-2, (c) K=2-3, (d) K=3-4, (e) K=4-5, (f) K=5-6** & Ec=1, GR=5, h*=1, μ*=1, β*=1, ρ*=1».

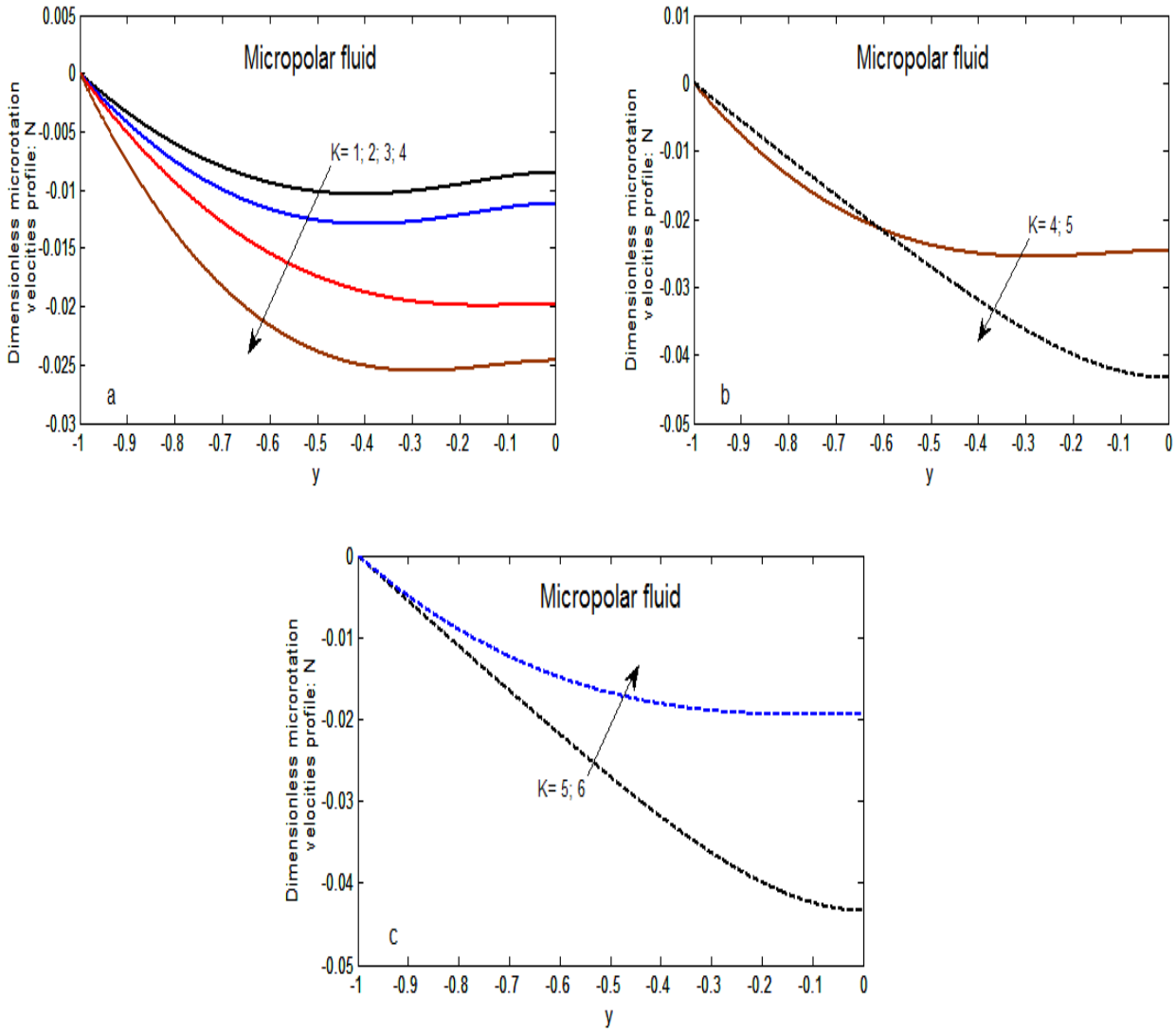

Figure 5.60: variation of dimensionless microrotation velocity profile for different values of material parameter with « **Ha=5, Pr=100, k*=2**, **(a) K=1-4, (b) K=4-5, (c) K=5-6 &** Ec=1, GR=5, h^*=1, μ*=1, β*=1, ρ*=1».

5.4.5. The Eckert number and width ratio effects for $Pr = 50$

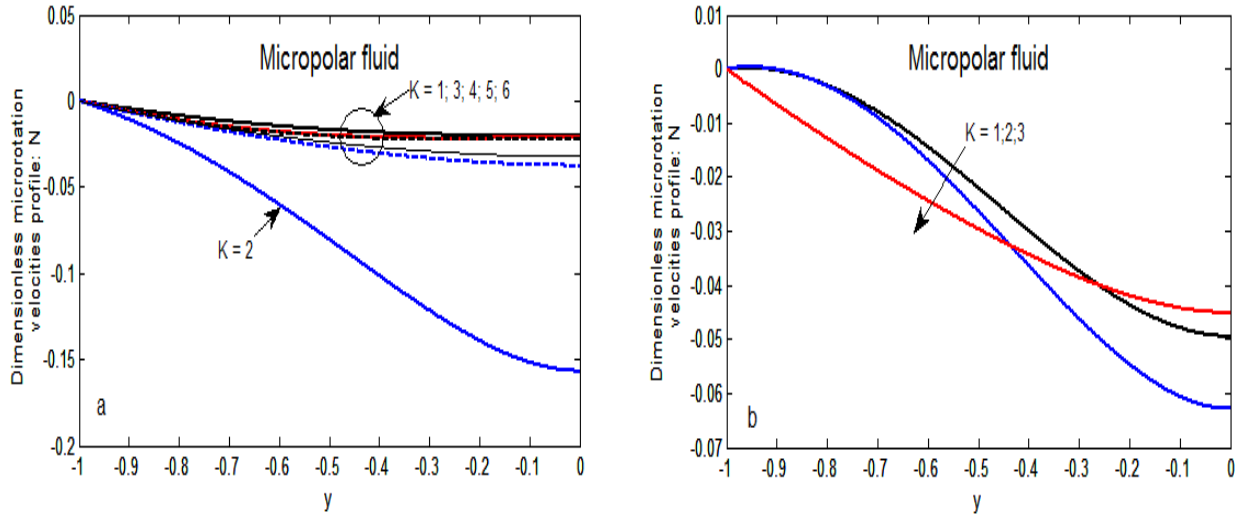

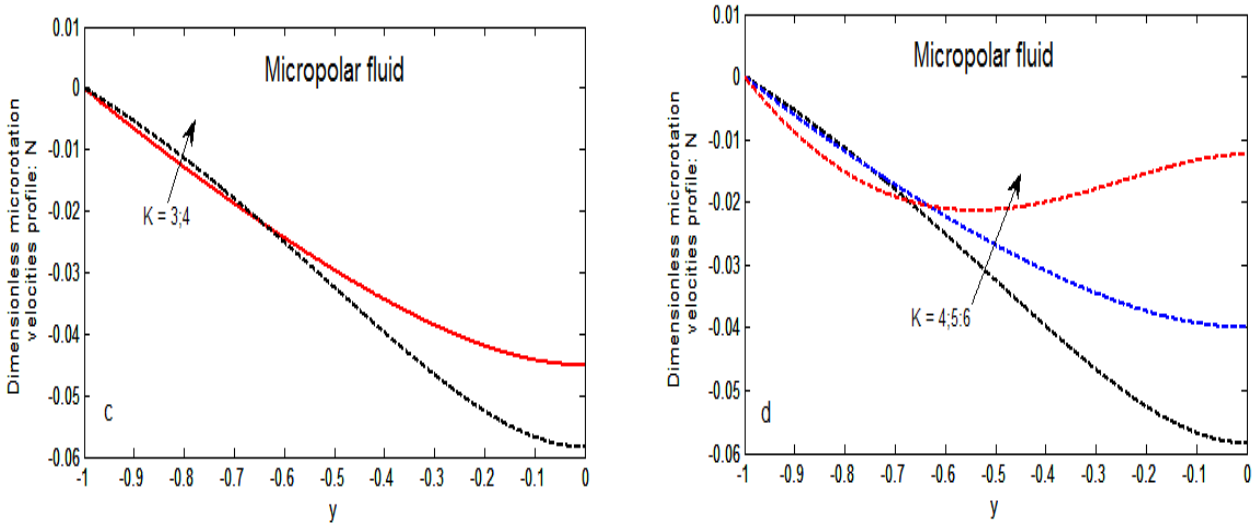

Figure 5.61: variation of dimensionless microrotation velocity profile for different values of material parameter with « **Ha= 3, Pr=50, k*=2, Ec=2, h*=2, (a) K=1-6, (b) K=1-3, (c) K=3-4, (d) K=4-6 &** GR=5, μ*=1, β*=1, ρ*=1».

5.4.6. The dynamical viscosities ratio effect for $Pr = 50$

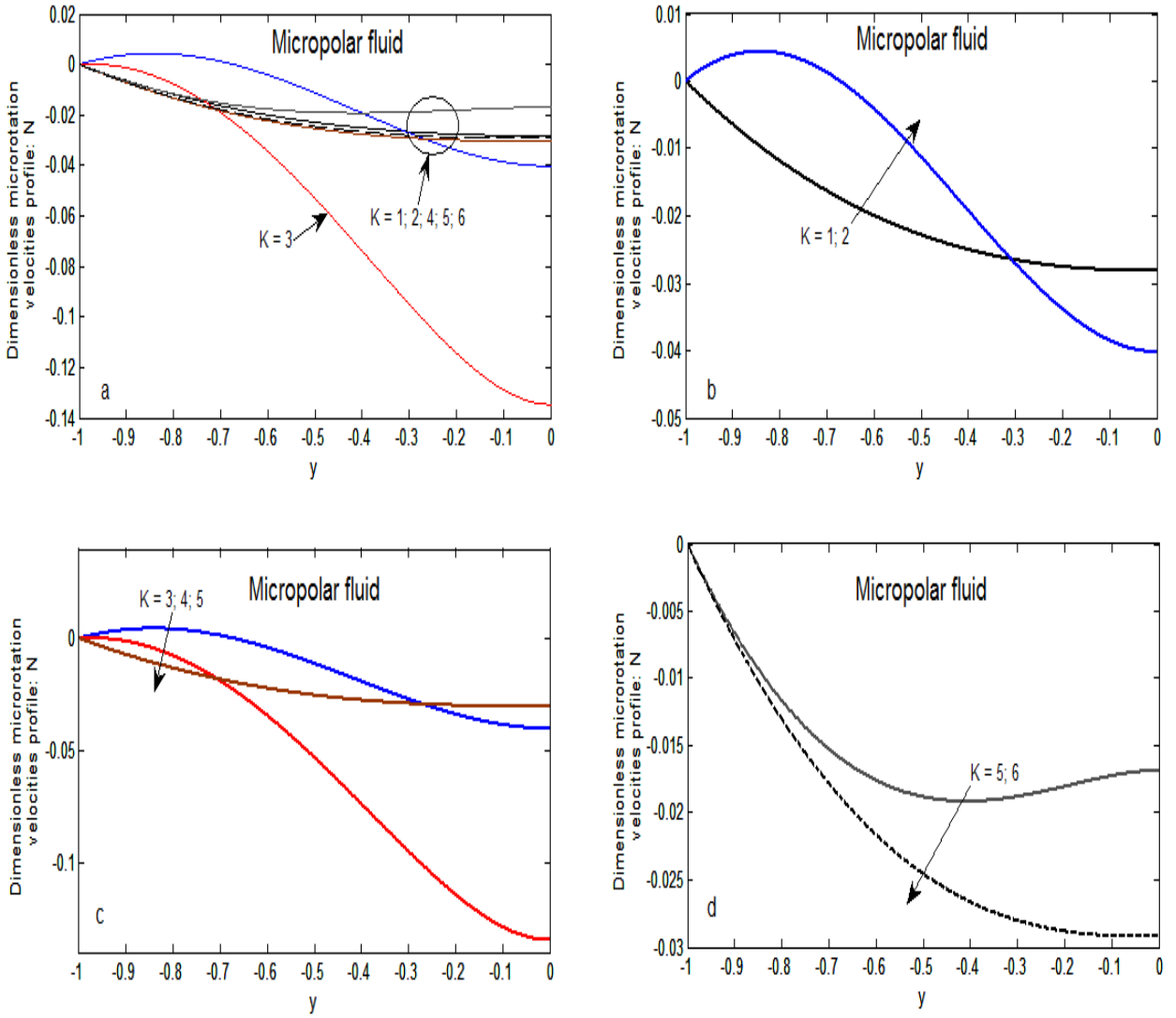

Figure 5.62: variation of dimensionless microrotation velocity profile for different values of material parameter with « **Ha= 3, Pr=50, k*=2, Ec=2, h*=3, μ*=2, (a) K=1-6, (b) K=1-2, (c) K=3-5, (d) K=5-6 &** GR=5, , β*=1, ρ*=1».

Indeed J.**P Kumar & al.** [9], **N. Kumar et al.** [21], and **B. Suresh Babu et al.** [59], have concluded a same results about the microrotation velocity (K=1, 2, 3) and the linear velocity profile of a Newtonian-viscous and non-Newtonian micropolar fluids when Prandtl number is low of 1 and Hartmann number doesn't exceed 1, thus which for the linear velocities profile of Newtonian viscous fluid in absence of a magnetic field. But the results obtained by **A. Ishak et al.** [7] in studying the forced flow in the presence of a magnetic field are different, for the microrotation velocity they have proved that the increase in the material parameter causes a decrease in the microrotation velocity of the suspended fine particles.

5.4.7. The mixed convection parameter effect for $Pr = 50$

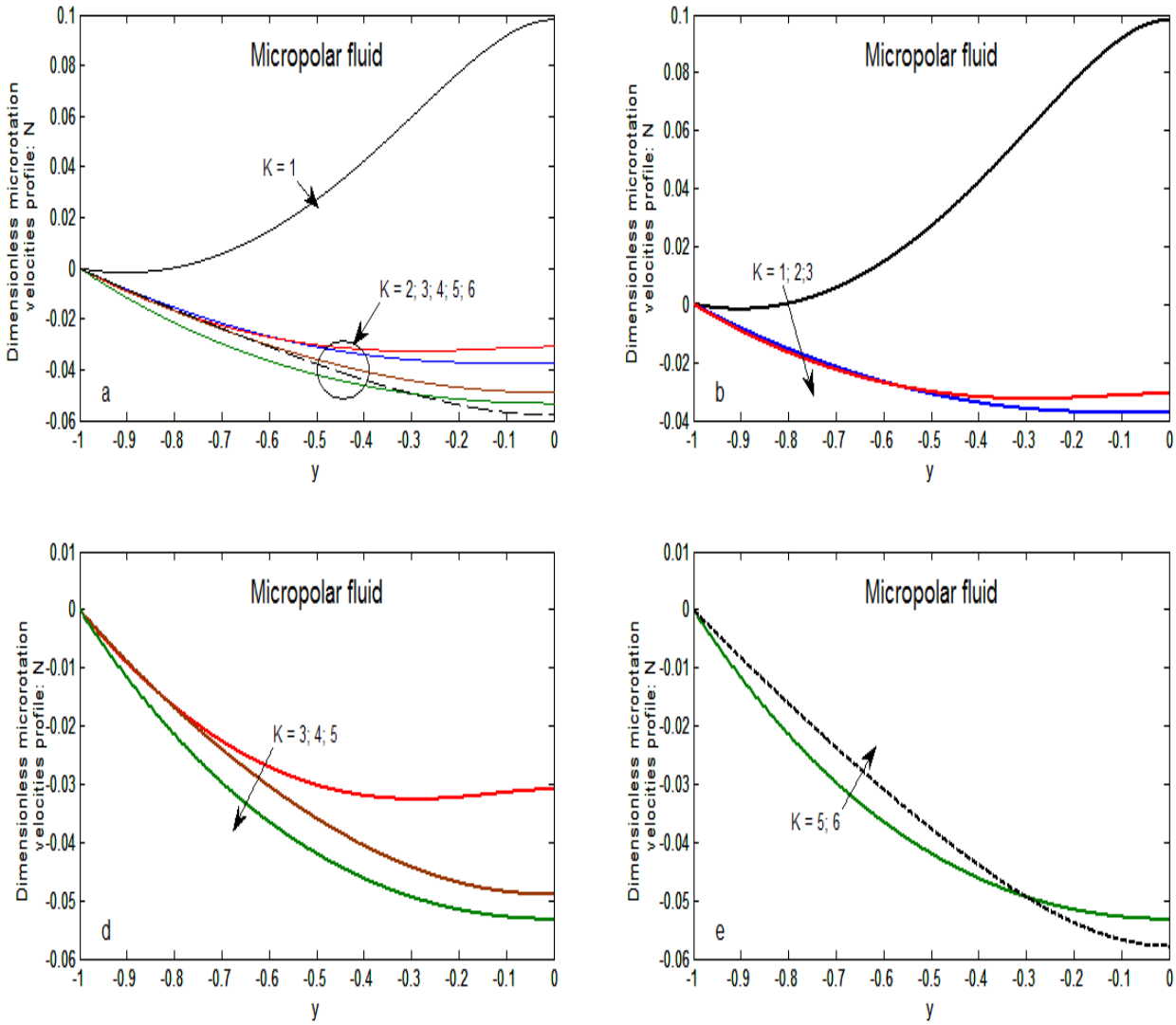

Figure 5.63: variation of dimensionless microrotation velocity profile for different values of material parameter with « **Ha= 3, Pr=50, k*=2, Ec=2, h*=2, μ*=2, GR=10, (a) K=1-6, (b) K=1-2, (c) K=3-5, (d) K=5-6 &** β*=1, ρ*=1».

5.4.8. The densities ratio effect for $Pr = 50$

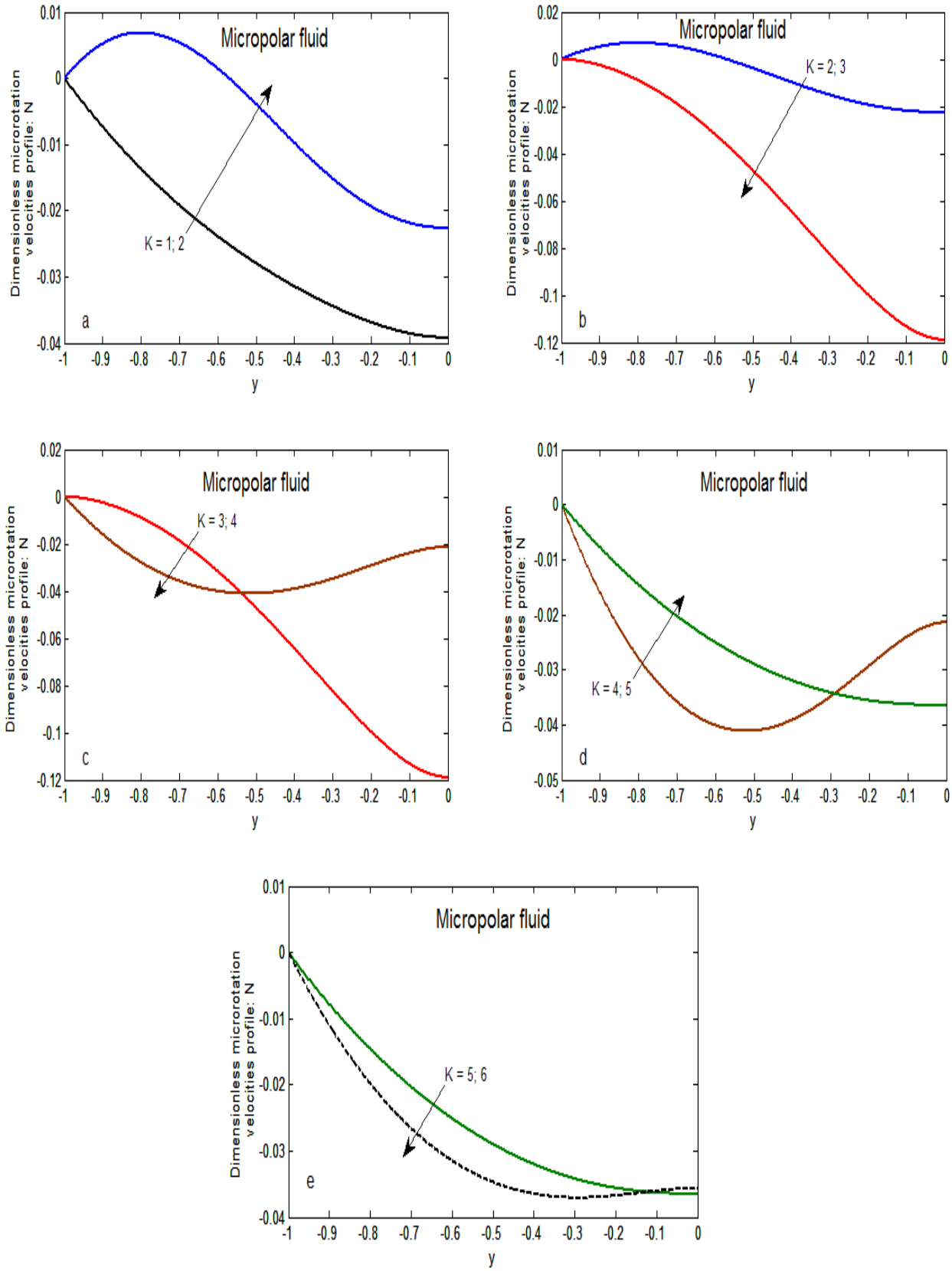

Figure 5.64: variation of dimensionless microrotation velocity profile for different values of material parameter with « **Ha= 3, Pr=50, k*=2, Ec=2, h*=2, μ*=2, GR=10, ρ*=2 (a) K=1-2, (b) K=2-3, (c) K=3-4, (d) K=4-5, (e) K=5-6 &** β*=1».

5.4.9. The thermal dilation parameter effect for $Pr = 50$

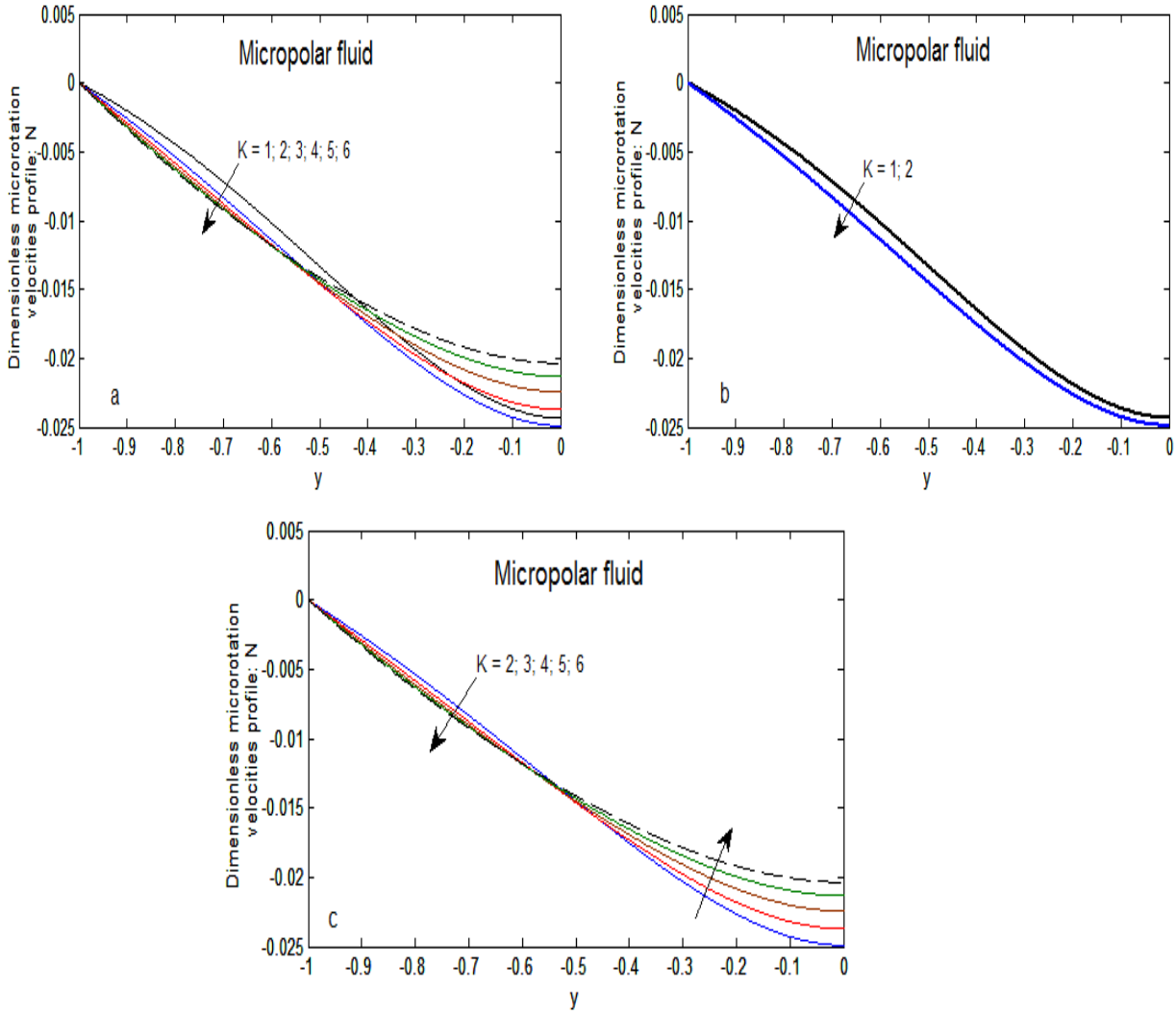

Figure 5.65: variation of dimensionless microrotation velocity profile for different values of material parameter with « **Ha= 3, Pr=50, k*=2, Ec=2, h*=2, μ*=2, GR=10, β*=2, ρ*=2, (a) K=1-2, (b) K=2-3, (c) K=3-4, (d) K=4-5, (e) K=5-6** ».

5.5. The effect of parameter variations on the linear velocity profiles for $K = 0$ & 1, $Ha = 1$ & $5, Pr \leq 1$

5.5.1. The thermal conductivity ratio effect in varying Ha and Pr

Also, by examining the curves obtained in figure 5.65-5.75, we can observe a minor variation in velocity profiles in both regions of fluids, first from fig. 5.65-5.70, the variation of Prandtl number – which means that the rate of a viscous diffusivity is low compared to the rate of thermal diffusivity – of 0.1-1.0 (figure 5.65.-a,b,c,d) causes a slight decrease in the linear velocity profiles within a non-Newtonian micropolar fluid for cases K=1 & K → 0 with Ha=1, which means that, a low viscous diffusivity rate relative to a thermal diffusion rate causes a slight increase in the linear velocity profiles.

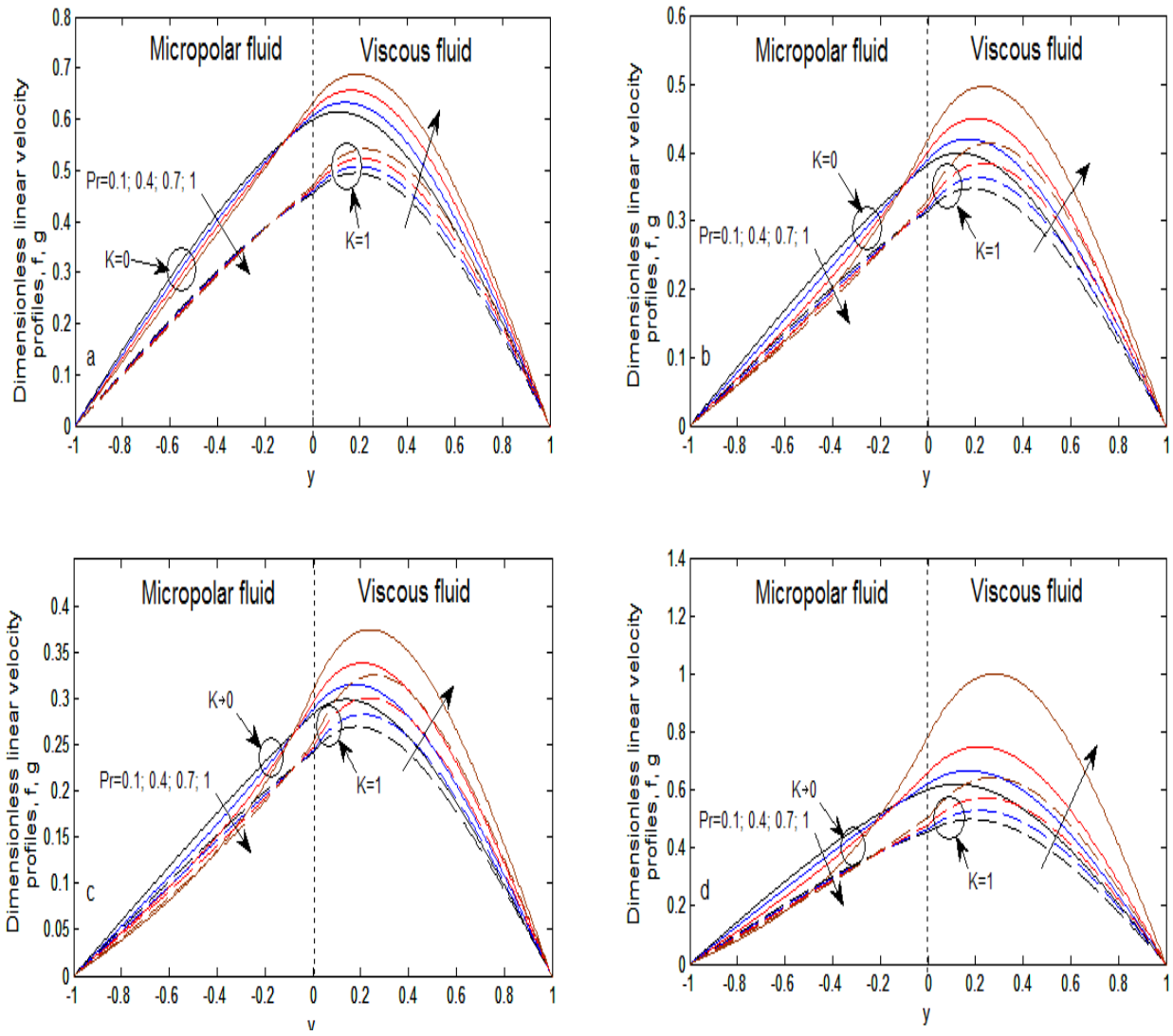

Figure 5.66: Dimensionless linear velocities profile according to Prandtl number variation, « **K=1, K→0, k*=2, Ec=1, h*=1, μ*=1, GR=5, β*=1, ρ*=1, (a) Ha= 1, (b) Ha=3, (c) Ha=5, (d) Ha=1, Pr=0.1, Ec=2** ».

5.5.2. The Eckert number effect in varying Pr

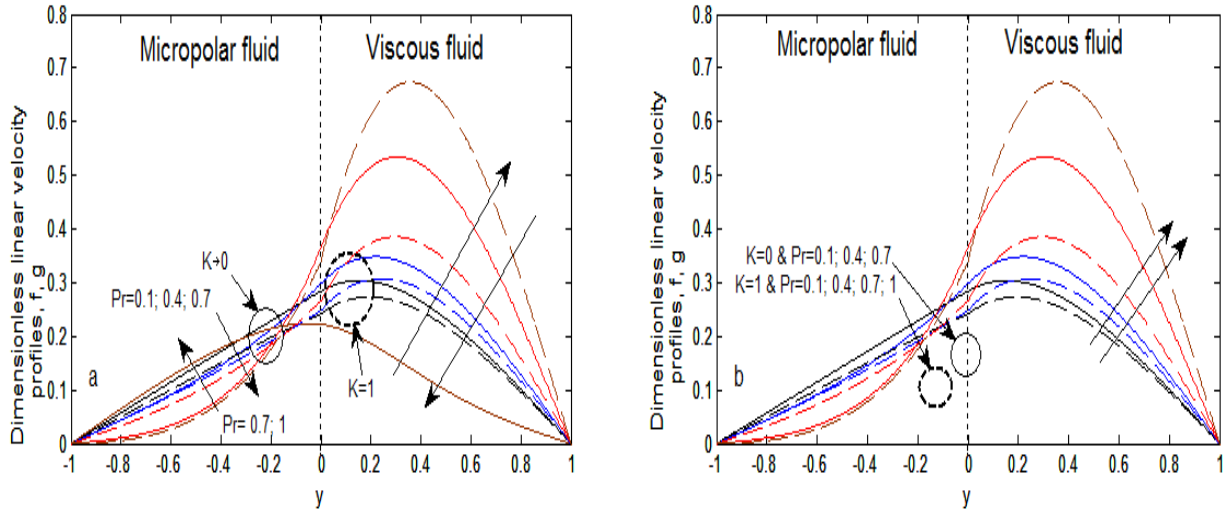

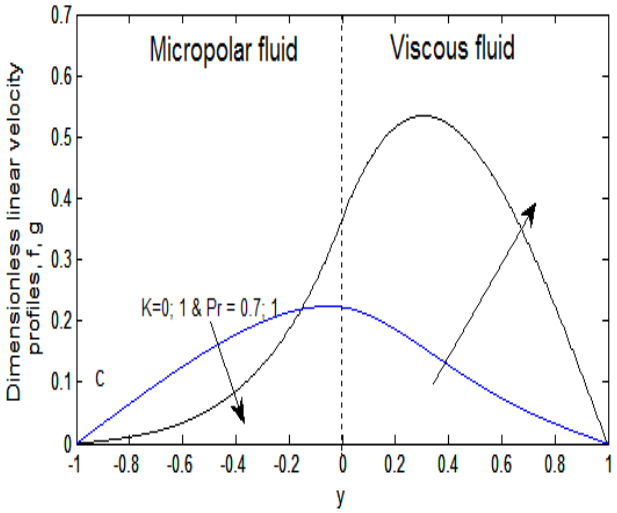

Figure 5.67: variation of dimensionless linear velocities profile for different values of Prandtl number with « **k*=2, Ec=2,** h^***=5, μ*=1, GR=5, β*=1, ρ*=1, (a) K=1, K→0, Pr=0.1-0.7, (b) K→0, Pr=0.7-1 & K=1; Pr=0.1-1, (c) K→0; K=1, Pr=0.7-1 Ha=5** ».

But in the second region, the increase in dimensionless linear velocities profile is important compared to the first region. We think that, the variation of linear velocity profiles hasn't a significant effect when the values of Prandtl number vary of 0.1-1.0 & Ha<=1.

5.5.3. The mixed convection parameter effect in varying Ha and Pr

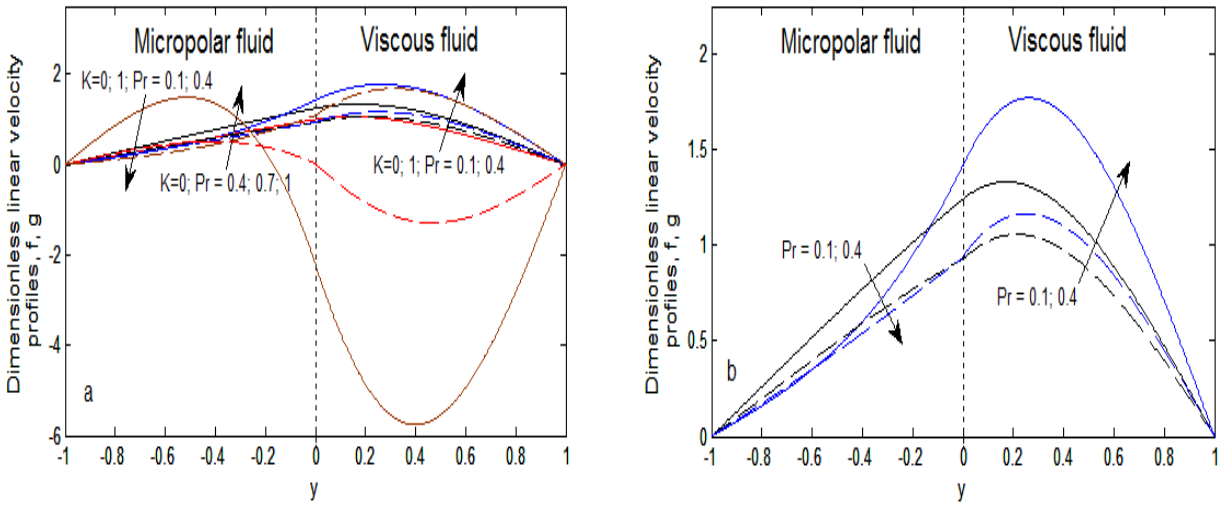

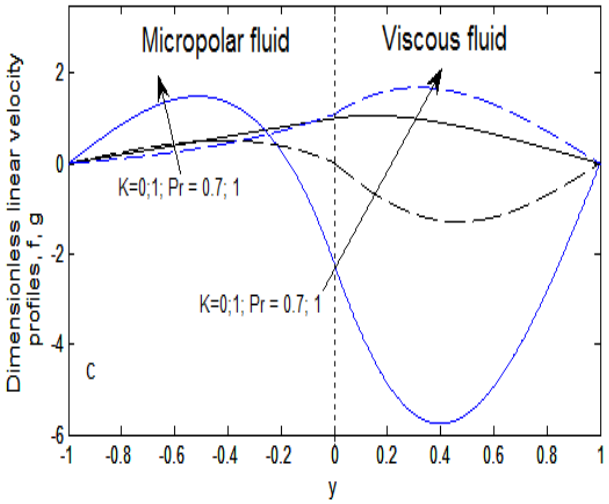

Figure 5.68: variation of dimensionless linear velocities profile for different values of Prandtl number with « **Ha=1, k*=2, Ec=2, GR=10, (a) Pr= 0.1 – 0.4, K→0; K=1; K→0, 0.4-1, (b) K→0; K=1 Pr=0.1 – 0.4; (c) K→0; K=1, Pr=0.7 – 1** & $h^*=1$, $\mu^*=1$, $\beta^*=1$, $\rho^*=1$»».

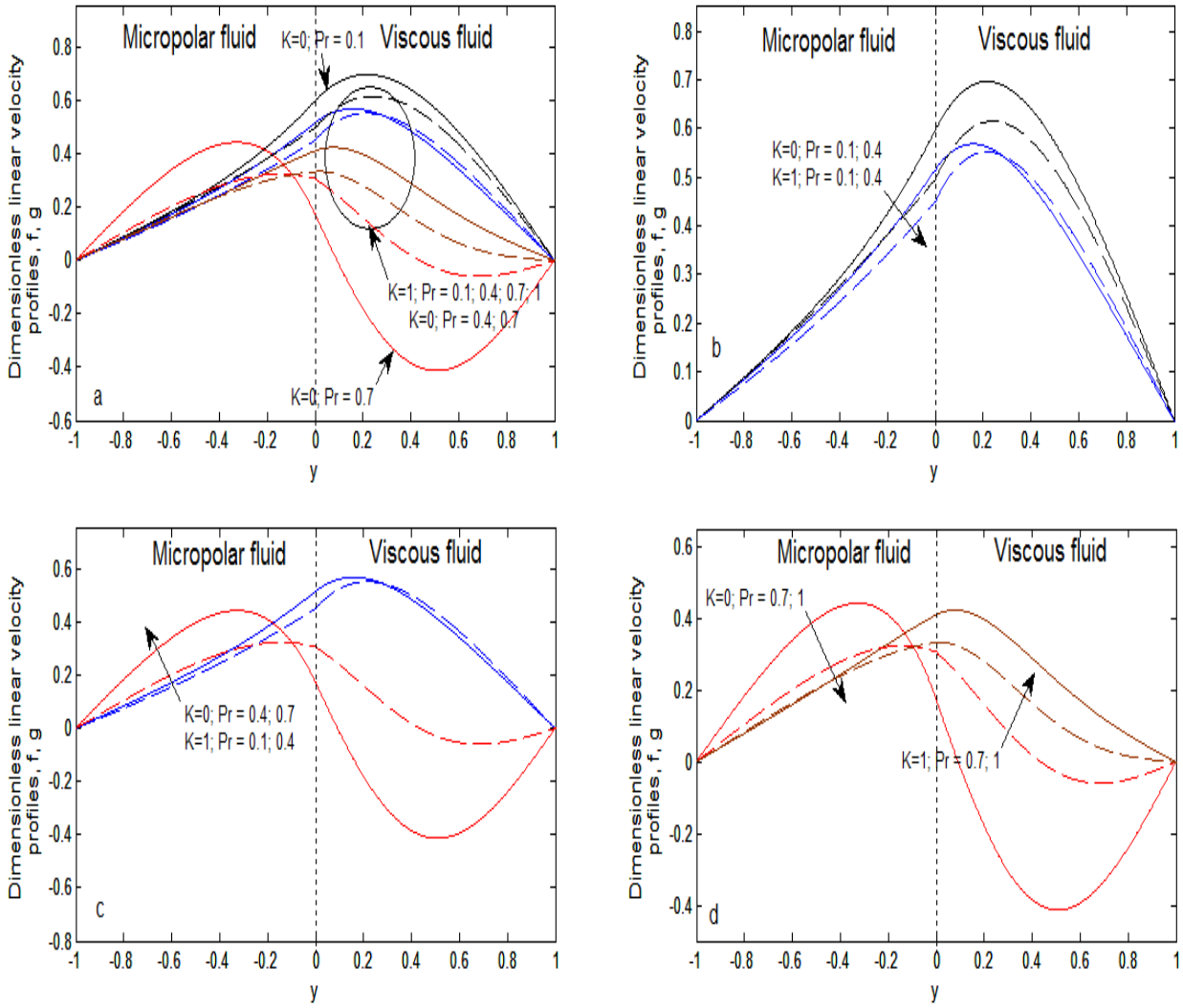

Figure 5.69: variation of dimensionless linear velocities profile for different values of Prandtl number with « **Ha=5, k*=2, Ec=2, GR=10, (a) K→0, Pr= 0.4– 0.7 ; K=1; Pr=0.1-1, (b) K→0; K=1 Pr=0.1 – 0.4; (c) K→0; Pr=0.4 – 0,7, K=1, Pr=0.1 – 0.4, (d) K→0, K=1; Pr=0.7 – 1** & $h^*=1$, $\mu^*=1$, $\beta^*=1$, $\rho^*=1$».

Therefore, in the region filled of Newtonian-viscous fluid, we can note down an increase in the linear velocity profiles (figures 5.67 & 5.68) for Prandlt number values varying from low than 1, but for Hartmann number values vary more than 3, we observe a perturbation in the field of linear velocities in both regions of fluids.

5.5.4. The widths ratio and dynamical viscosities ratio effects in varying Ha and Pr

We have also in figure 5.69, a visible effect of the magnetic field, we can note that for Prandtl number varies of low than 1 (fig. 5.69-a,b,c,d), Hartmann equal 1-5 and the ratio of widths varies of 1-2, ratio of dynamical viscosities varies of 1-2 the linear velocities field decrease in the micropolar fluid region, but in viscous fluid region we observe an increase in the linear velocities field.

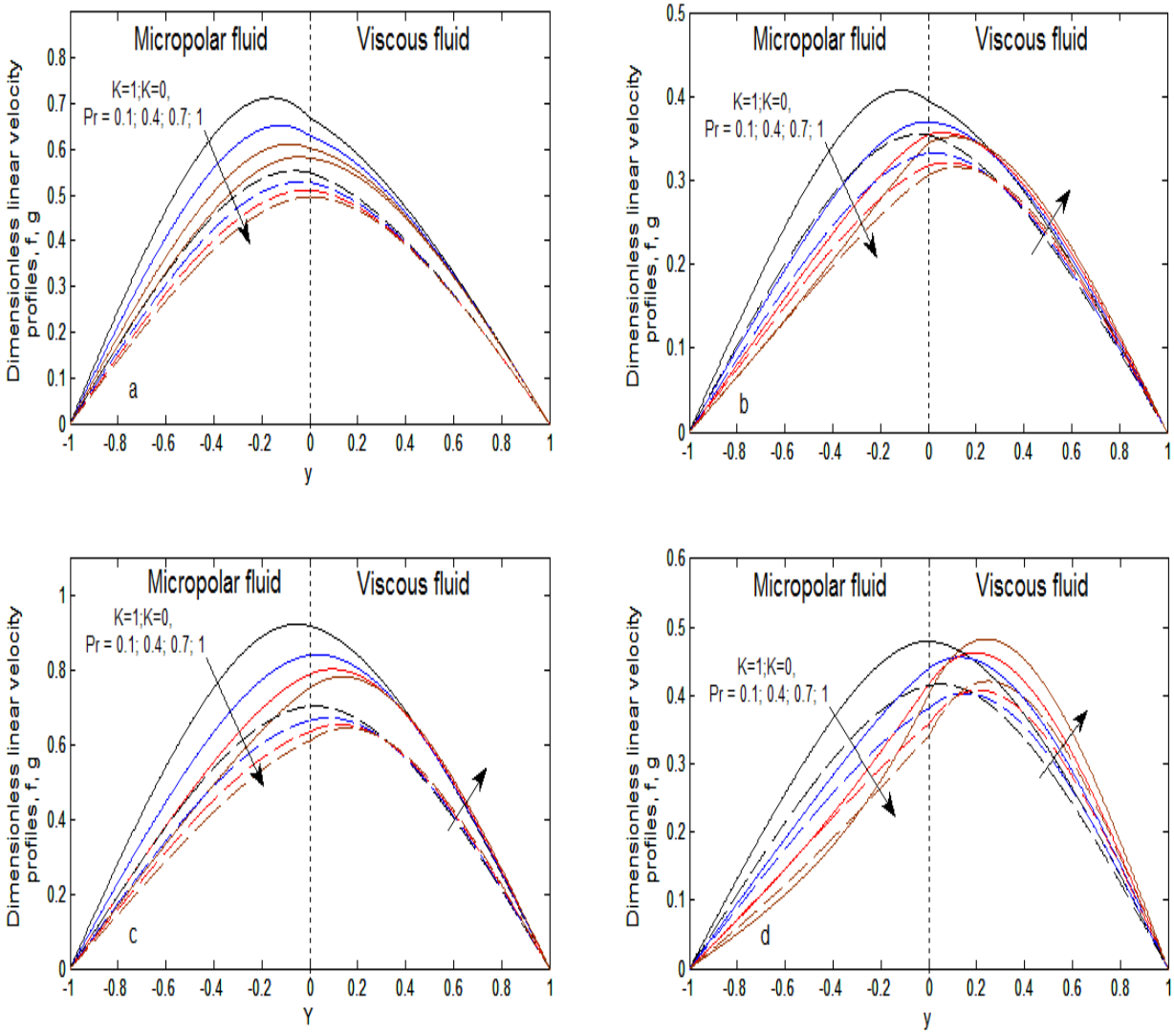

Figure 5.70: variation of dimensionless linear velocities profile for different values of Prandtl number with « **(a) Ha=1,** h^***=1, μ*=1; (b) Ha=5,** h^***=1, μ*=1, (c) Ha=1,** h^***=2, μ*=2 (d) Ha=5,** h^***=2, μ*=2** &, K→0; K=1, k*=2, Ec=2, GR=10, Pr= 0.1– 1, β*=1, ρ*=1».

5.5.5. The Thermal dilations ratio effect in varying Ha and Pr

We can also note that, an increase in the rate of viscous diffusivity compared to the rate of thermal diffusivity (fig. 5.70 -5.75) causes an apparent decrease in the linear velocity profiles within micropolar and viscous fluids for Prandlt values vary low than 1, in cases K=1, K→0, Hartmann number of 1-5, Eckert number equal 2, Mix parameter up then 5, ratio of widths equal 2, ratio of thermal conductivities equal 2 and thermal dilation equal 2, but when Praudtl number takes value more than 10, we observe a perturbation in velocities field distribution in both regions of the channal.

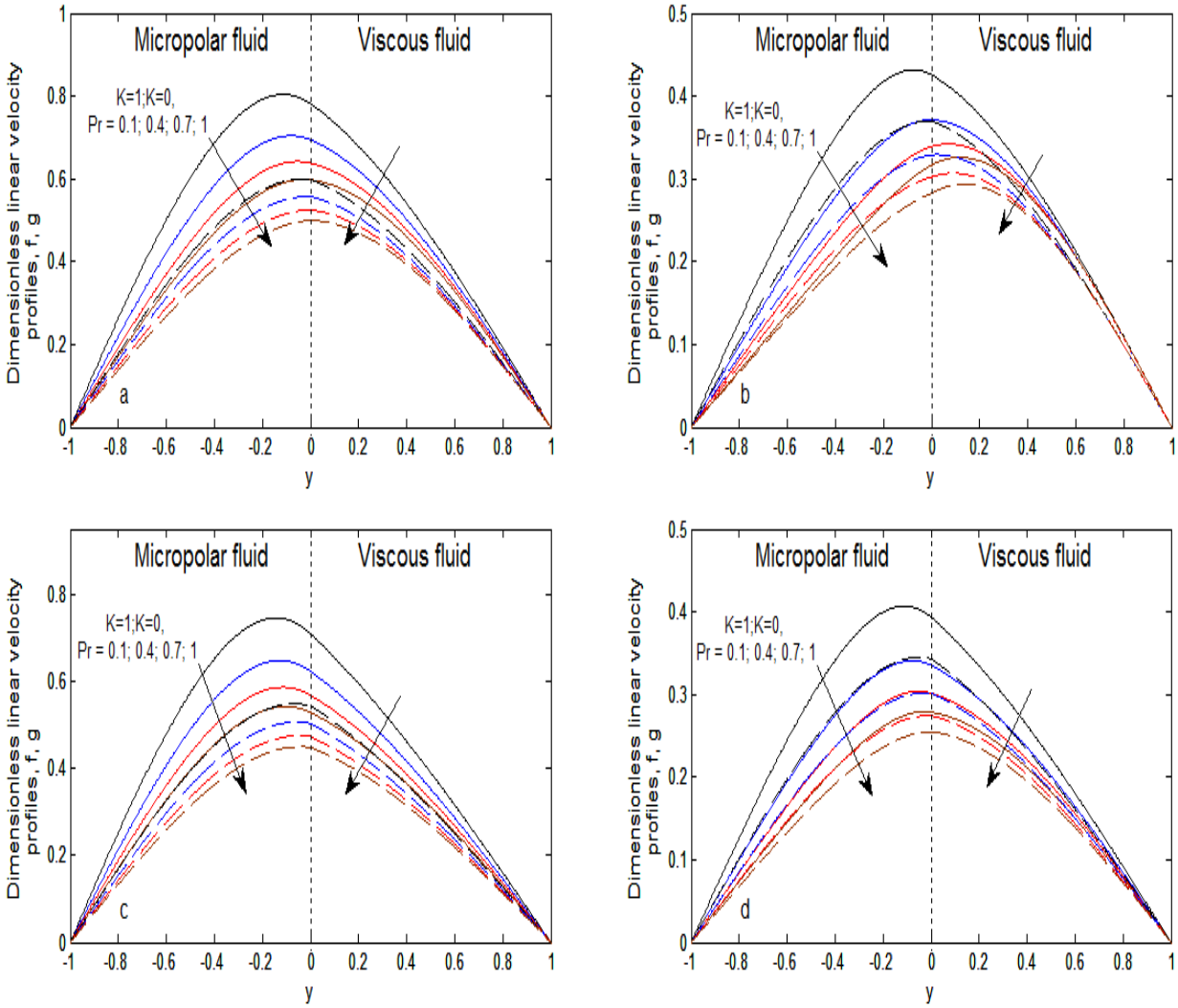

Figure 5.71: variation of dimensionless linear velocities profile for different values of Prandtl number with « **K→0; K=1, k*=2, Ec=2, GR=10, Pr= 0.1– 1, μ*=1 (a) h*=2, Ha=1, β*=2; (b) h*=2, Ha=5, β*=2, (c) Ha=1, h*=2, μ*=2, ρ*=2 (d) h*=2, Ha=5, μ*=2, ρ*=1**».

5.6. The dimensionless parameter and number effects on linear velocities for $1 < Pr \leq 90$

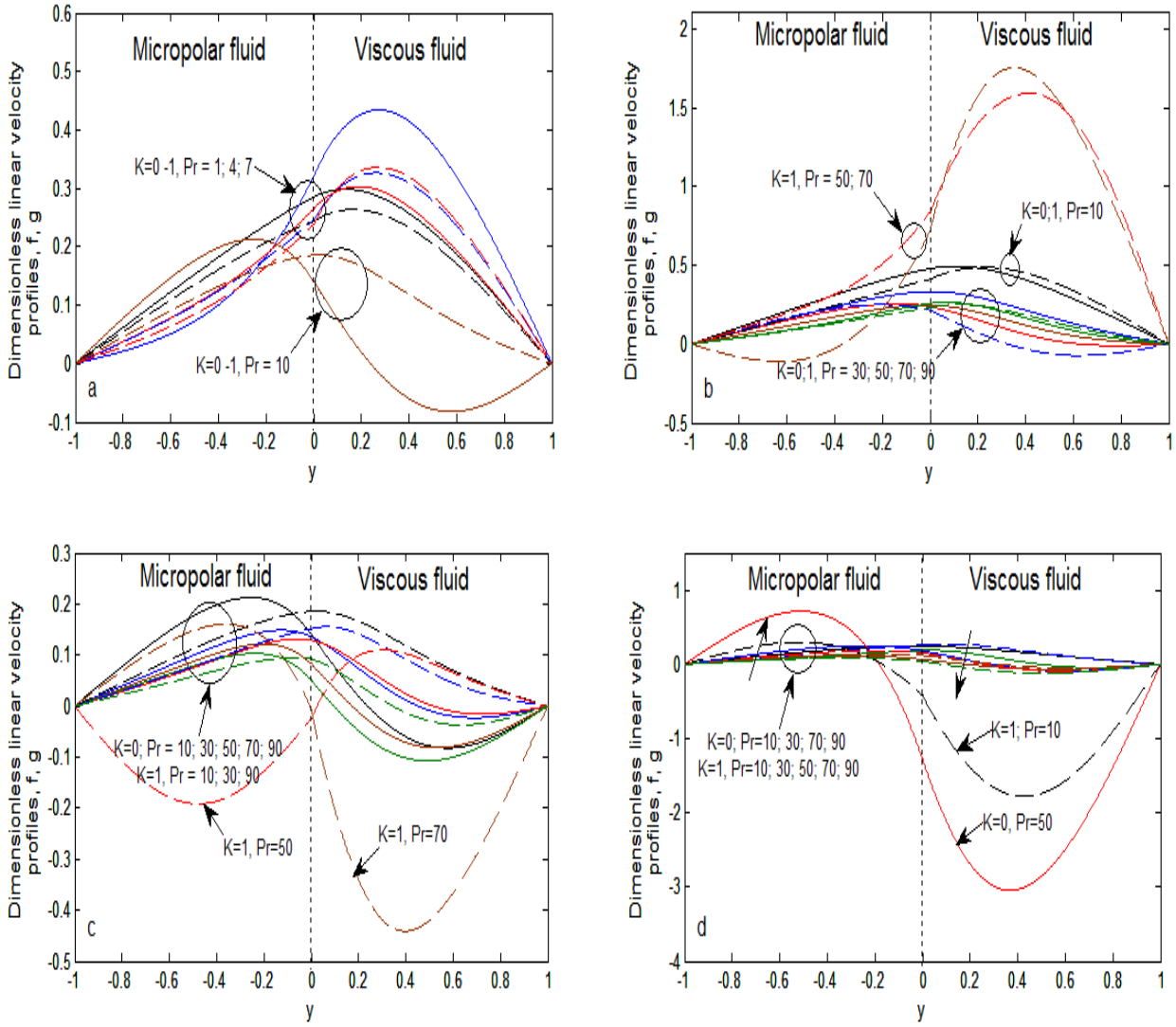

Figure 5.72: variation of dimensionless linear velocities profile for different values of Prandtl number with « K→0; K=1, **(a) Ha=5, Pr= 1– 10, (b) Ha=1, Pr= 10– 90, (c) Ha=5, Pr= 10-90, (d) Ha=1, k*=2, Pr= 10-90** & GR=5 **,** Ec=1, k*=1, **h***=1, μ*=1, β*=1, ρ*=1».

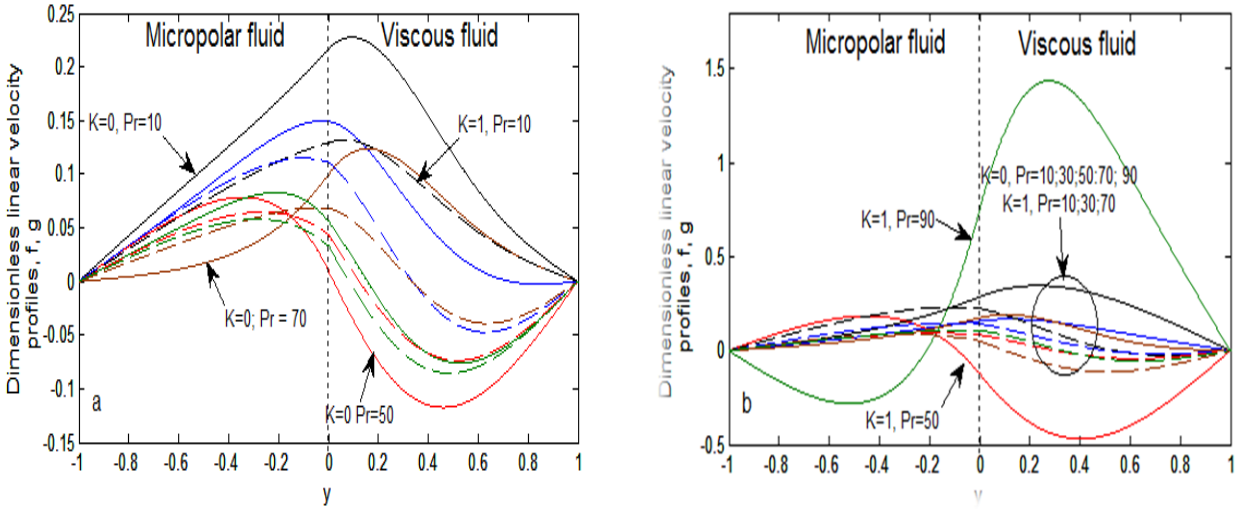

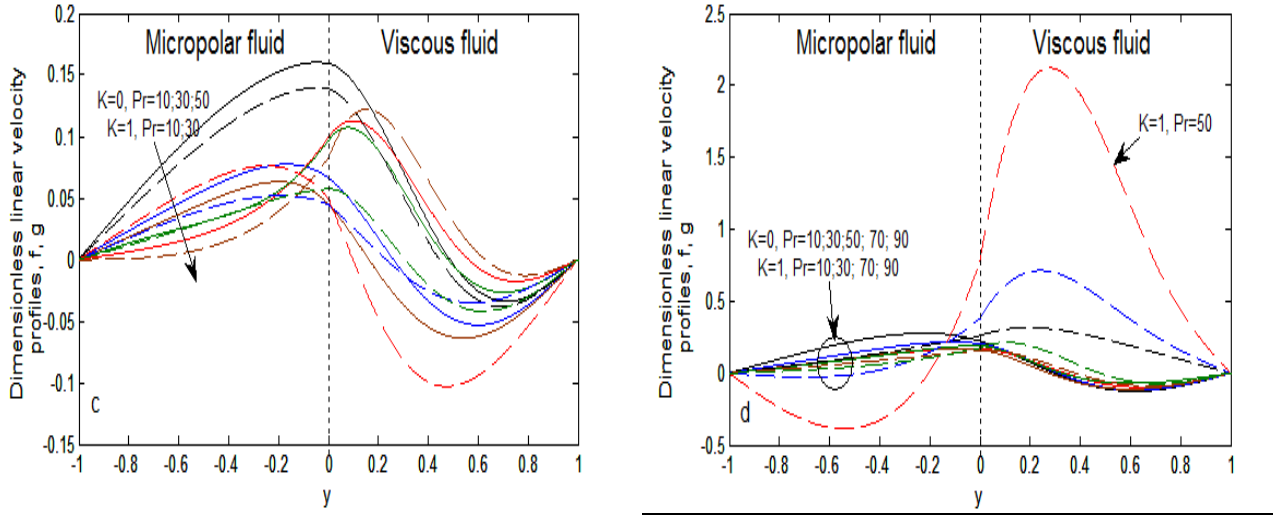

Figure 5.73: variation of dimensionless linear velocities profile for different values of Prandtl number with « GR=5 **, h***=1, μ*=1, β*=1, ρ*=1, K→0; K=1, Pr= 10– 90;**(a) k*=2, Ha=1, (b) Ha=1, k*=2, Ec=2, (c) k*=2, Ec=2, Ha=5, (d) Ha=1, k*=2, Ec=2, GR=10** ».

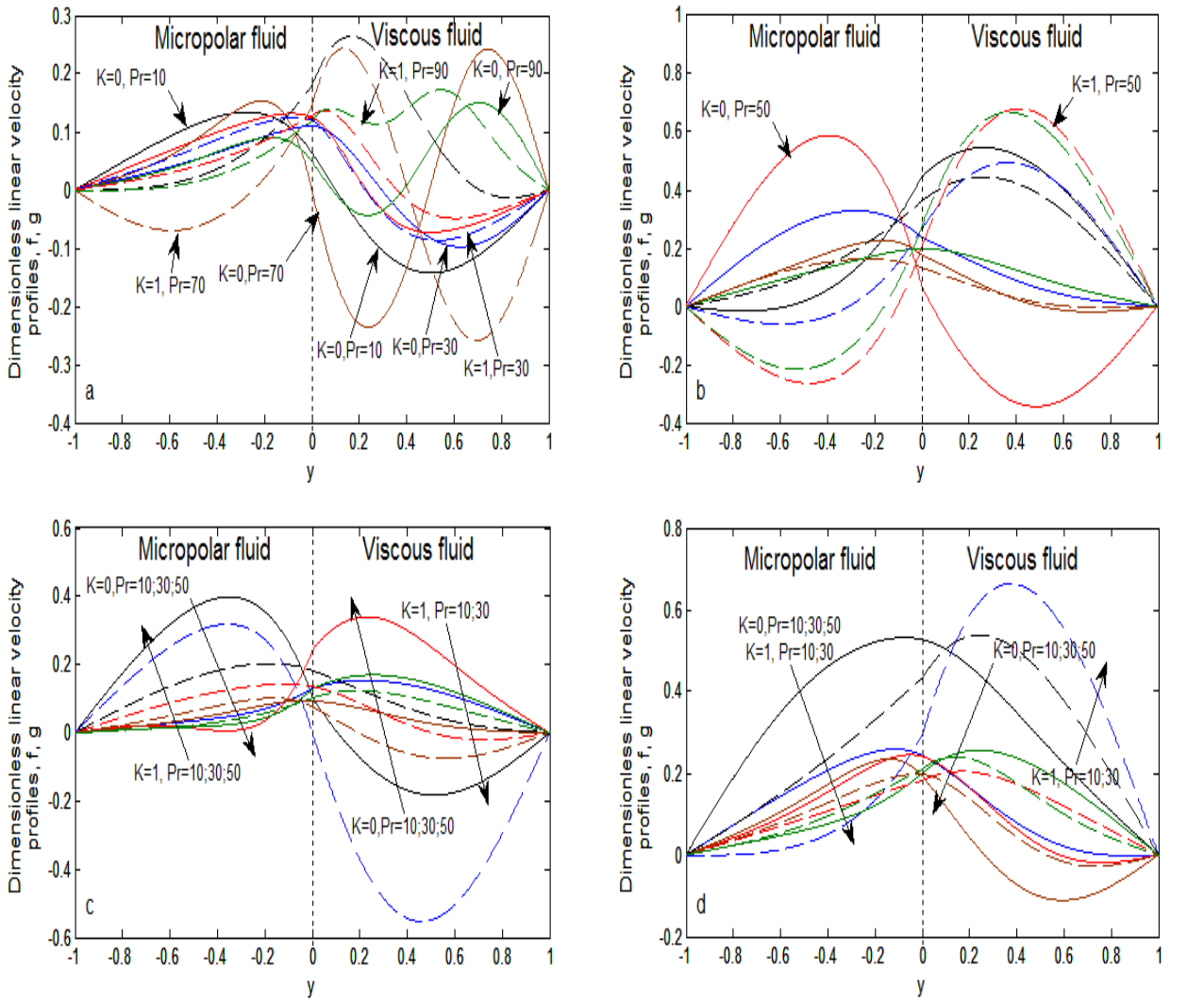

Figure 5.74: variation of dimensionless linear velocities profile for different values of Prandtl number with « **h***=1, μ*=1, β*=1, ρ*=1, K→0; K=1, Pr= 10– 90;**(a) Ha=5, k*=2, Ec=2, GR=10, (b) Ha=1, k*=2, Ec=2, GR=10, h*=2, (c) Ha=1, k*=2, Ec=2, GR=10, h*=2, (d) Ha=5, k*=2, Ec=2, GR=10, h*=2, μ*=2** ».

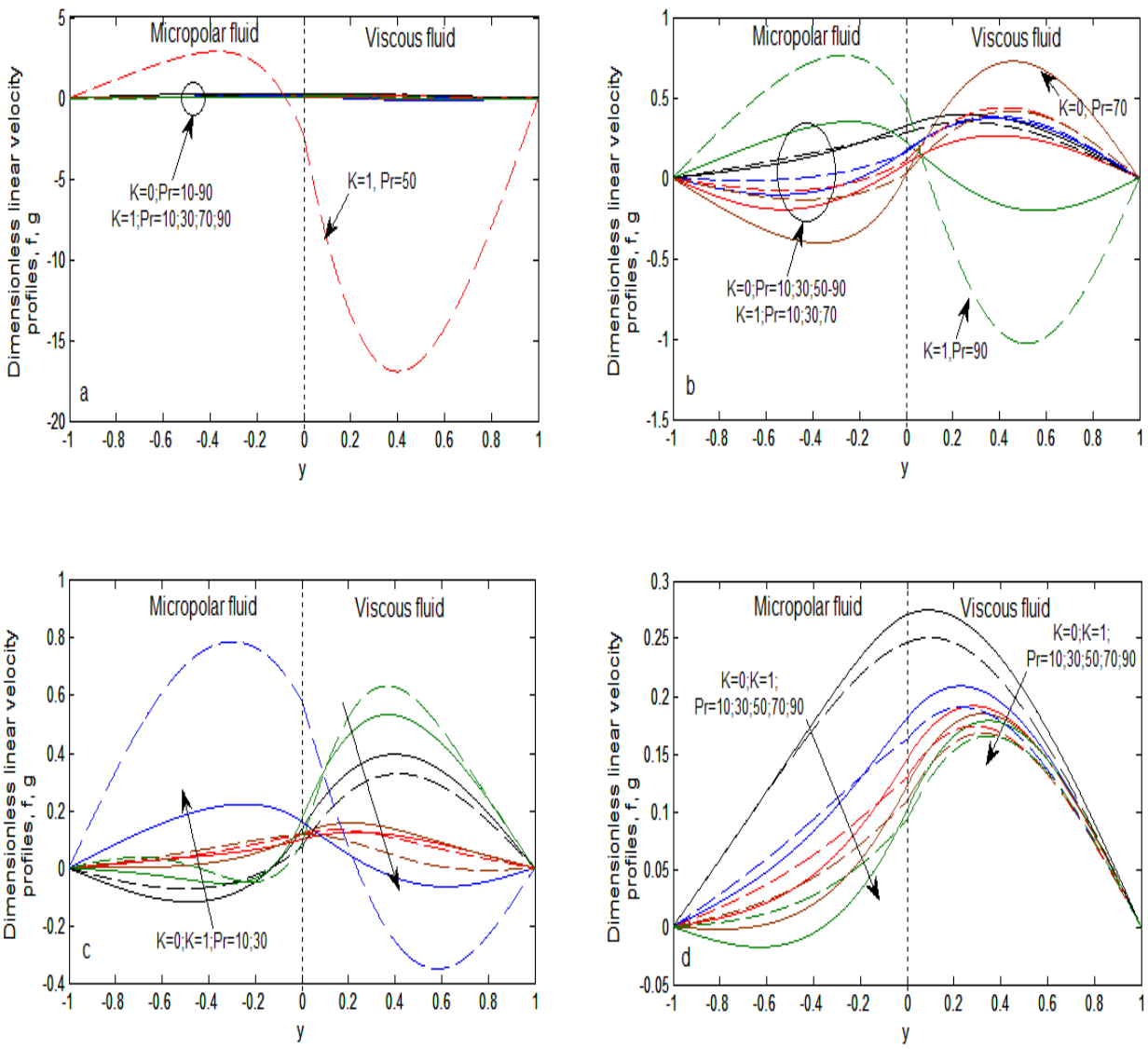

Figure 5.75: variation of dimensionless linear velocities profile for different values of Prandtl number with « **(a) Ha=5, k*=2, Ec=2, GR=10, h*=2, μ*=2, (b) Ha=1, k*=2, Ec=2, GR=10, h*=2, μ*=2, , β*=2, (c) Ha=5, k*=2, Ec=2, GR=10, h*=2, μ*=2, , β*=2, (d) Ha=1, k*=2, Ec=2, GR=10, h*=2, μ*=2, β*=2, ρ*=2**».

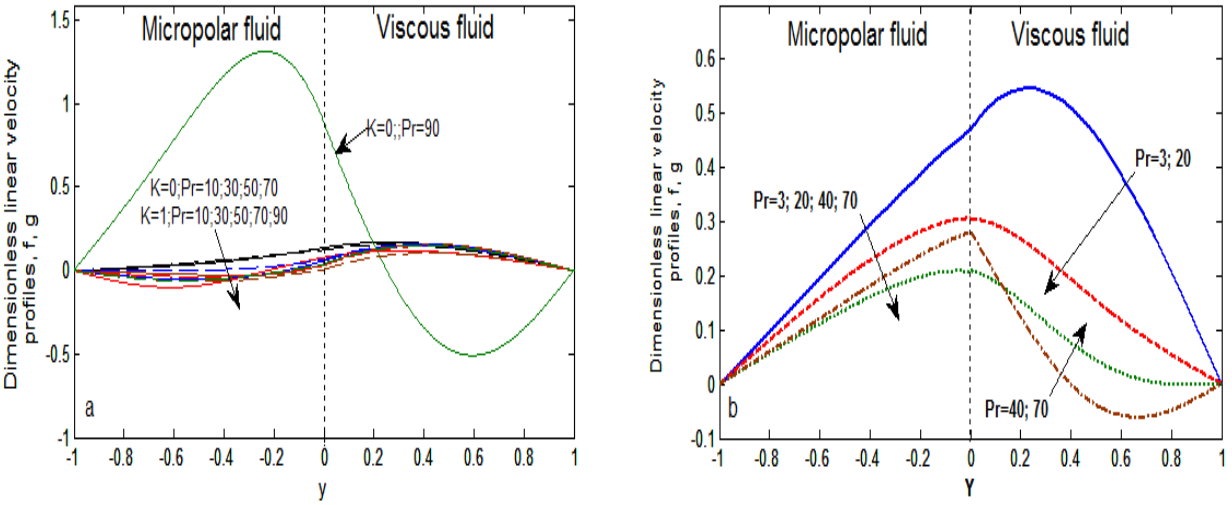

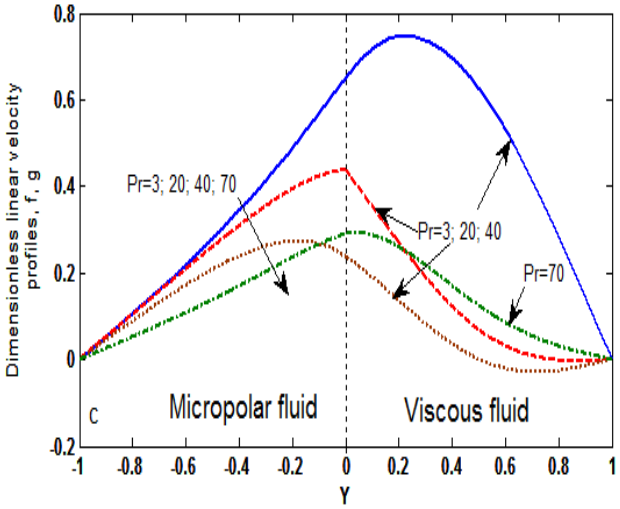

Figure 5.76: variation of dimensionless linear velocities profile for different values of Prandtl number with « **(a) Pr= 10– 90, Ha=5, k*=2, Ec=2, GR=10, μ*=2, β*=2, ρ*=2, (b) Pr= 3-70, K=1, Ha=1, (c)K=0** & k*=1, Ec=1, GR=5, **h***=1, μ*=1 , β*=1».

5.7. The dimensionless parameter and number effects on microrotaion velocity for $1 < Pr \leq 50$

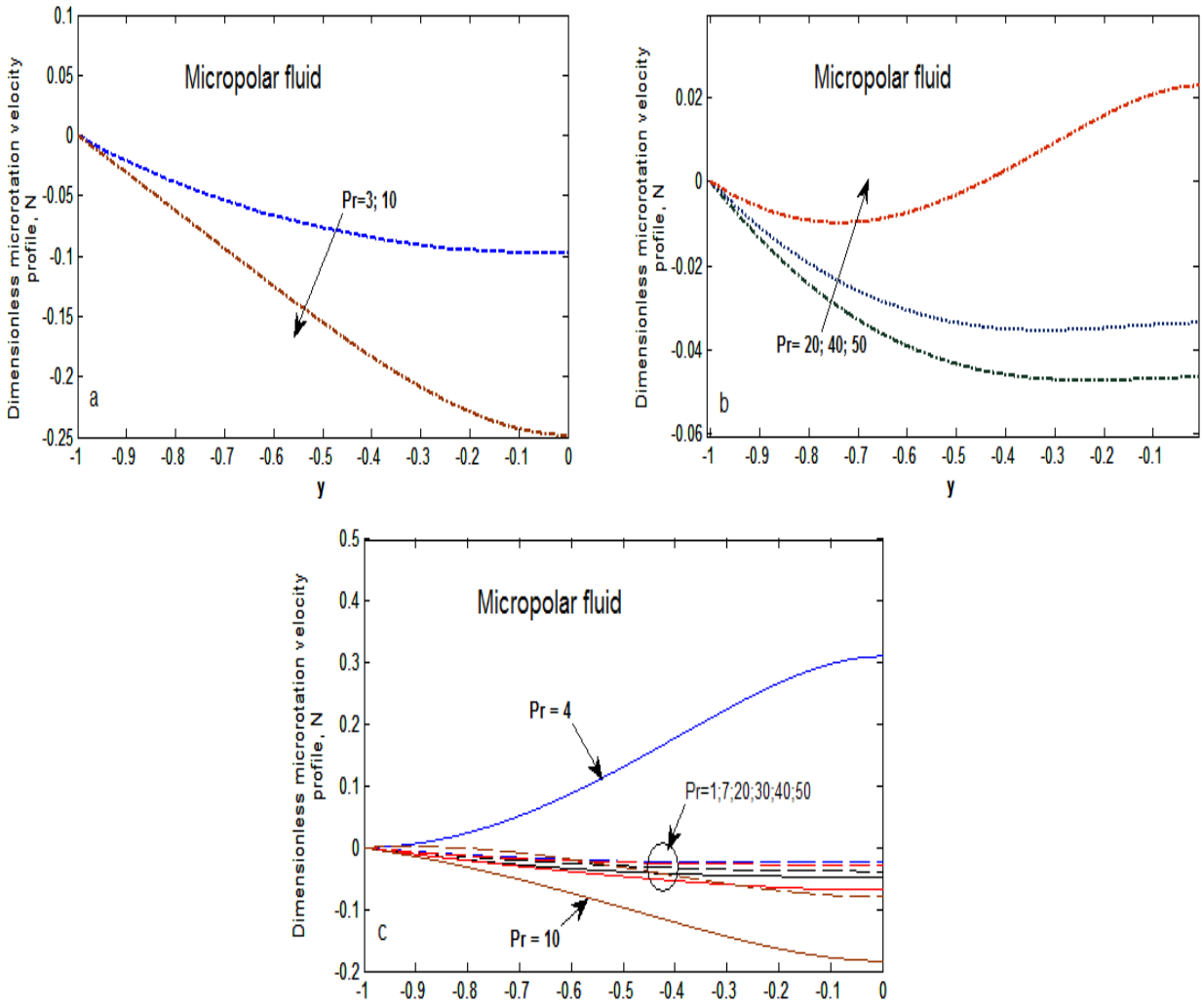

Figure 5.77: variation of dimensionless microrotation velocity profile for different values of Prandtl number with « **(a) & (b) K=1**, **Ha=1, (c) K=1, Ha=5 &** h*, Ec=1, GR=5, μ*=1, β*=1, ρ*=1, k*=1».

5.8. The effects of mixed convection parameter, Eckert and Hartmann numbers on velocities profiles

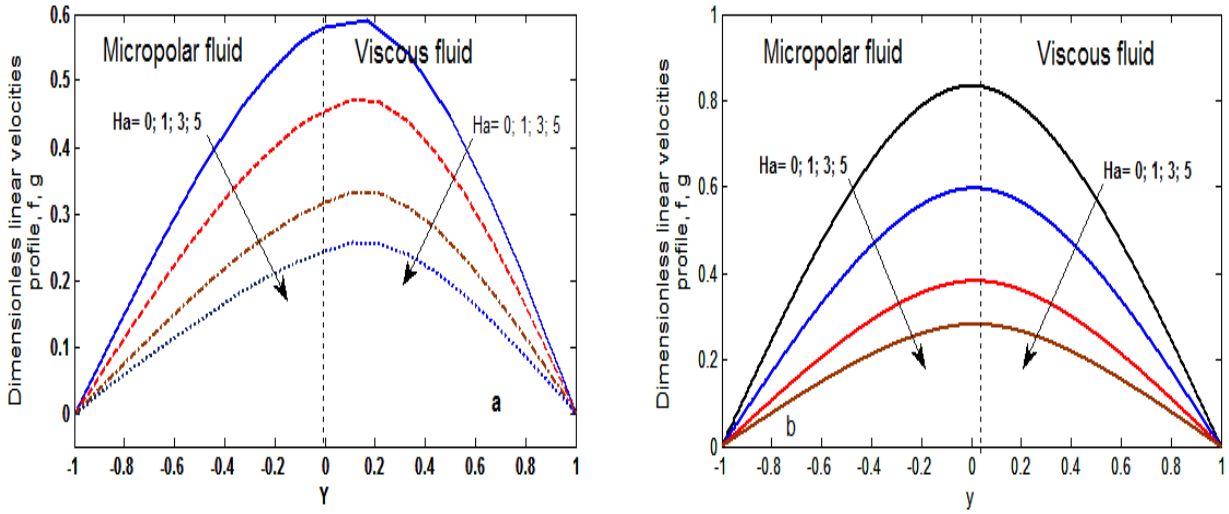

Figure 5.78: variation of dimens ionless linear velocities profile for different values of Hartmann number with « **(a) K=1, (b) K=0, Ha=1,** & **Pr= 0.1, k*=2, Ec=1, GR=5, h*=1, μ*=1, β*=1, ρ*=1**».

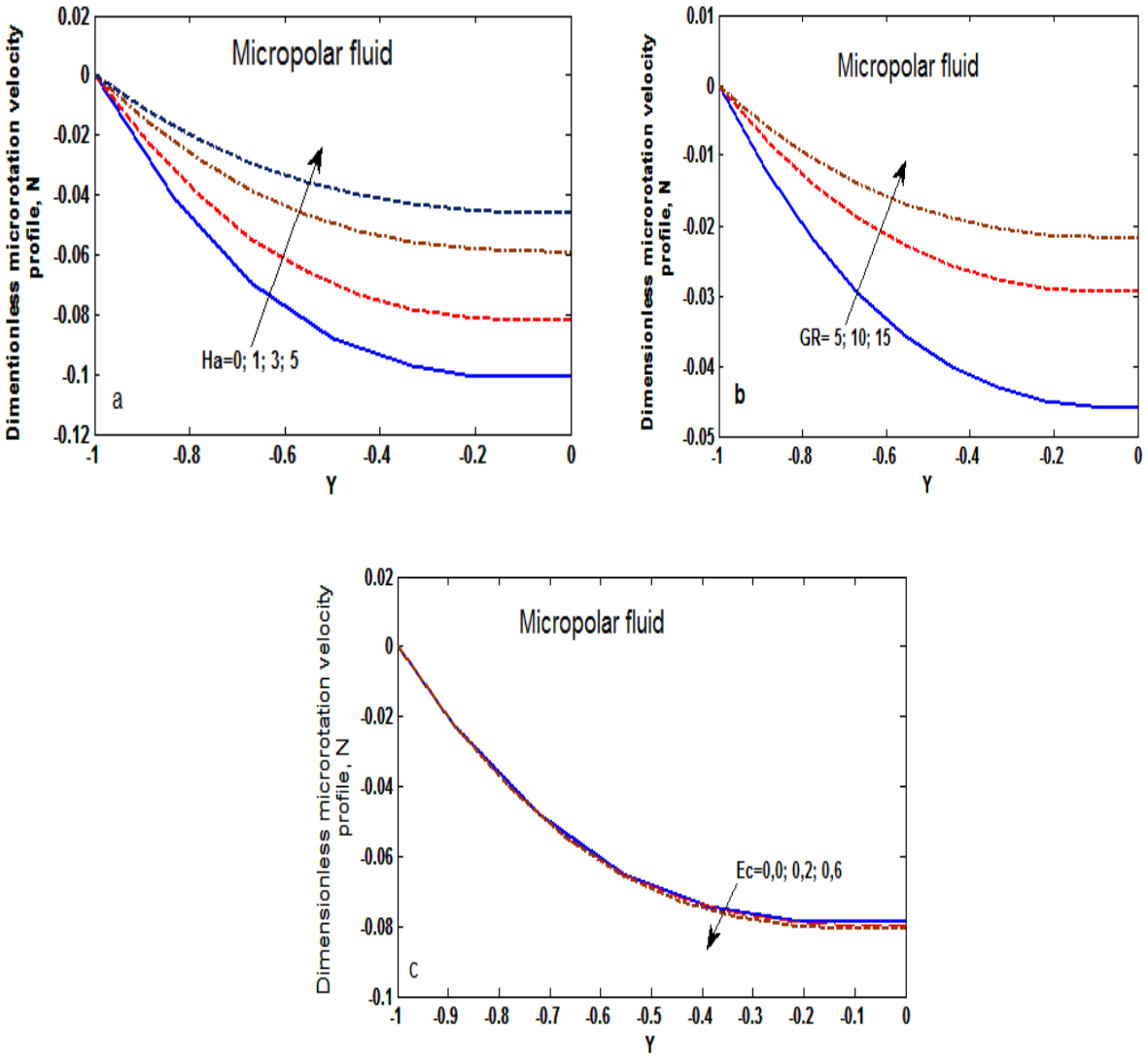

Figure 5.79: variation of dimensionless microrotation velocity, with « **(a) Ha=0-5, (b) GR=5-15, (c) Ec=0-0.6 &** K=1, Pr=0.1, Ec=1, GR=5, h*=1, k*=1, μ*=1, β*=1, ρ*=1».

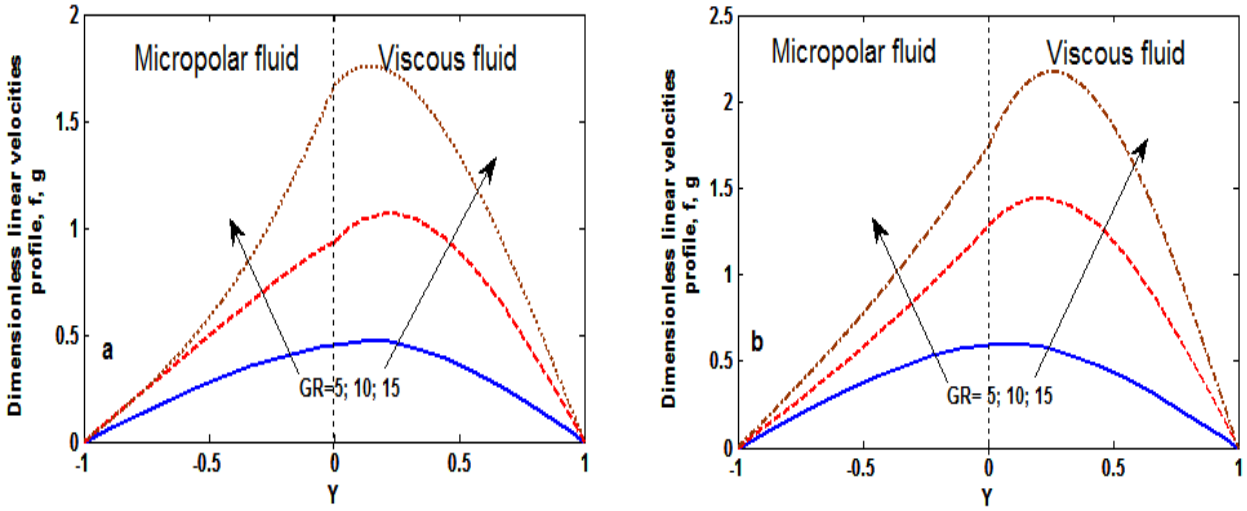

Figure. 5.80: variation of dimensionless linear velocities profile for different values of mix convection parameter with « **(**a). K=1, (b) K→0 Pr=0.7, Ha=1, Ec=1, h*=1, k*=1, μ*=1, β*=1, ρ*=1».

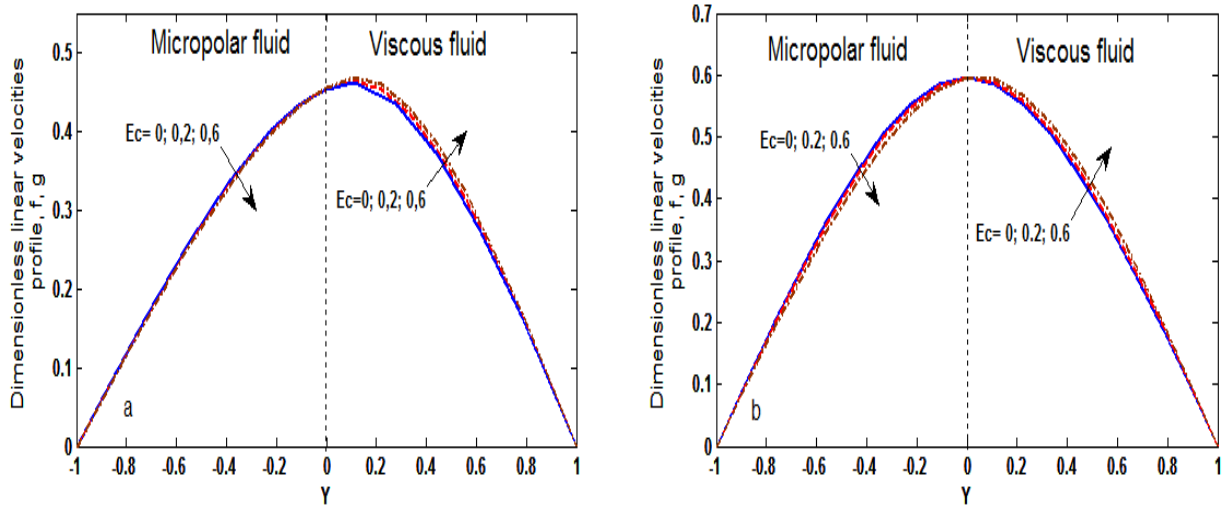

Figure 5.81: variation of dimensionless linear velocities profile for different values of Eckert number with « **(**a) K=1, (b) K→0, Pr=0.7, Ha=1, GR=5, h*=1, k*=1, μ*=1, β*=1, ρ*=1».

5.9. The calculation of Local skin friction Coefficients

One is calculated in using the both formulations of the local skin friction coefficient, one obtained results which are filled in tables, 5.1 and 5.2.

Table 5.1: Local skin-friction Coefficient results for different values of Ha, K and Re ≤ 2000, with $\rho^* = 1$, $\beta^* = 1$, $\mu^* = 1$, $h^* = 1$, Pr = 0.7, Ec=1. $C_{f1} = \frac{2}{\mathrm{Re}}(1+K).f'(-1)$, $C_{f2} = -\frac{2}{\mathrm{Re}}g'(1)$.

Ha	K	Non-Newtonian micropolar fluid, Gr =2×10^3, Re =10^3		Newtonian viscous fluid, Gr = 4×10^3, Re = 2×10^3	
		f'(-1)	C_{f1}	g'(1)	C_{f2}
1	1	0,2329	0,0009316	-0,3068	0,0003068
	2	0,1770	0,0001062	-0,2782	0,0002782
	5	0.1051	0,0012612	-0,2336	0,0002336
2	1	0.1902	0,0007608	-0,2476	0,0002476
	2	0,1497	0,0008982	-0,2298	0,0002298
	5	0,0936	0,0011232	-0,1998	0,0001998
3	1	0.1608	0,0006432	-0.2065	0.0002065
	2	0.1299	0,0007794	-0.1948	0.0001948
	5	0.0845	0,0010140	-0.1738	0.0001738

Table 5.2: Local skin-friction Coefficient results for different values of Ha, K and Re ≤ 1000, with $\rho^* = 1$, $\beta^* = 1$, $\mu^* = 1$, $h^* = 1$, Pr = 0.7, Ec =1. $C_{f1} = \frac{2}{\mathrm{Re}}(1+K).f'(-1)$, $C_{f2} = -\frac{2}{\mathrm{Re}}g'(1)$

Ha	K	Non-Newtonian micropolar fluid, Gr =103, Re =0.5×103		Newtonian viscous fluid, Gr = 2×103, Re = 103	
		f'(-1)	C_{f1}	*g'(1)*	C_{f2}
1	1	0,2329	0,0018632	-0,3068	0,0006136
	2	0,1770	0,0002124	-0,2782	0,0005564
	5	0.1051	0,0025224	-0,2336	0,0004672
2	1	0.1902	0,0015216	-0,2476	0,0004952
	2	0,1497	0,0017964	-0,2298	0,0004596
	5	0,0936	0,0022464	-0,1998	0,0003996
3	1	0.1608	0,0012864	-0.2065	0,0004130
	2	0.1299	0,0015588	-0.1948	0,0003896
	5	0.0845	0,0020280	-0.1738	0,0003476

5.10. Conclusion

In this chapter we presented a graphic result of two cases of the proposed model. First case present (validation part) a system of fluid without magnetic field effect, indeed this mathematical model was studied by **J. P. Kumar et al**. [9], we have obtained the same

results, so, for the second case, a model was under a magnetic field effect as we have focus our studied on is different and the results obtained, present a comparative study with **N. Kumar**'s results[63], therefore, we can conclude that:

In general, high values of magnetic fields (i.e. Hartmann number more than 1), Prandtl number value more than 1, the parameter value of the mixed convection more than 5 and ratio values of; widths, dynamic viscosities, thermal expansion coefficients, thermal conductivities coefficients and fluid densities, more than 1, cause a decrease and disturbance in field of dimensionless linear velocities in both regions of the channel.

In details, the effects of; the mixed convection parameter, the ratio of a dynamical viscosities, the widths ratio (h^*) and a thermal dilation coefficients ratio maintained the dimensionless linear velocities which involve that -an increase of buoyancy forces, favor the lubrication systems, but the increase in viscous effect provoke a decrease in the linear velocities (which means a reduction in the buoyancy forces),

Overall conclusion and prospects

Overall conclusion and prospects

This work consists in studying the flow of two immiscible fluids in a vertical channel in mixed convection. Complexities not considered in the literature have emerged: One of both fluids is of non-Newtonian micropolar type; the channel is subjected to a magnetic field with dissipation of thermal and magnetic energy not ignored; the convection is mixed.

After a mathematical formulation characterized by strong couplings between movement equations and taking into account these complexities. Dimensionless equations were obtained by the application of the similarity method while using an efficient procedure for the boundary conditions, has led to following results:

1. The variation of the material parameter (K: means the shape and the structure) from 3 to 6, the low magnetic parameter of Prandtl <1 (α> ν: significant energy transfer by conduction), or moderately low (Pr<20, α<ν: energy transfer by viscous dissipation is important), increases the profile of the microrotation;
2. Also, the variation of “K” provokes an increase in the viscosity of the micro-inertia. Whereas, for values of Pr> 20, the microrotation velocity decreases, this causes a decrease in the micro-inertia.

It can also be concluded that:

3. First, the increase of Prandtl number (Pr: means a high viscous diffusivity rate relative to a thermal diffusivity rate) with a large magnetic flux, "Ha", does not favour the field of linear velocities. Energetically, the decrease in the velocity means that the buoyancy forces decrease within the FM, which represents a disadvantage for systems using lubricant fluids;
4. However, in the case of Newtonian viscous fluid, an increase of “Pr” and a strong magnetic field "Ha" favour the field of linear velocities, which means that the buoyancy forces increase; this is an advantage for systems using lubricant fluids. So, the presence of both types of fluids will lead to an optimization of “Ha” give meaning to studied objectives.
5. Then, the increase in mixed parameter (GR: means an increase in buoyancy forces relative to inertia forces) favours linear velocities within the Newtonian viscous fluid. Also, an increase of “GR” favours the micro-rotation velocity within micropolar fluid, which this increases the viscosity of micro-inertia ;

6. Also, the increase in Eckert number (Ec: means the kinetic energy rate is higher than the enthalpy energy rate) does not favour linear and microrotation velocities within the micropolar fluid. On the other hand, an increase of "Ec" favours the linear velocity within the Newtonian viscous fluid, which represents in presence of magnetic field:
   a) First, a disadvantage for lubrication systems using a type of micropolar fluids with high polarity;
   b) Second, the micropolar fluid with low polarity ($K \rightarrow 0$) can be used as a method of accumulation heat, which represents an advantage. For example, controlling certain joint diseases (rheumatism) in human joints.

Finally, as prospects as resulting from this work, we can predict that:

It is possible to study more complex configuration with more than two regions of different types of fluids. For example, fluid models of CARREAU and modified CARREAU, Cristo-liquids, plastic fluids, ANDRADE fluid, and ARHENIUS fluid, as well that of horizontal, vertical or inclined channels.

References

[1] A. Cemal Eringen, "Nonlocal Continuum Field Theories", Sheridan Books Springer-Verlag NewYork, USA, 2001.

[2] A. C. Eringen, "Simple Microfluids," International Journal of Engineering Science, Vol. 2, No. 2, 1964, pp. 205-217. doi:10.1016/0020-7225(64)90005-9.

[3] A. C. Eringen, "Theory of Micropolar Fluids," International Journal of Mathematics and Mechanics, Vol. 16, 1966, pp. 1-18.

[4] A. C. Eringen, "Theory of Micropolar Fluids," Journal of Mathematical Analysis and Applications, Vol. 38, No. 2, 1972, pp. 480-496. doi:10.1016/0022-247X(72)90106-0.

[5] A.C. Eringen, "Microcontinuum Field Theories". II: Flu-ent Media," Springer, New York, 2001.

[6] A. C. Eringen, "Continuum Physics", Academic Press Inc., New York USA, (1976), page 2–29.

[7] Anuar Ishak, Roslinda Nazar, Ioan Pop, Magnetohydrodynamic (MHD) flow of a micropolar fluid towards a stagnation point on a vertical surface (Elsevier, Computer and Mathematics with Applications 56, 2008), page 3188 – 3194.

[8] Z. Chaohui & all. In: Exploring micropolare effects in thin film lubrication (Science in China Ser. G. Physics, Mechanics & Astronomy, Vol. 47 supp, 2004), page 65 – 71.

[9] J. Prathap Kumar, J. C. Umavathi, Ali J. Chamkha, and Ioan Pop, Fully-developed free-convective flow of micropolar and viscous fluids in a vertical channel, Applied Mathematical Modeling, (2009), page 1 – 12.

[10] Youn J. Kim, Unsteady MHD convection flow of polar fluids past a vertical moving porous plate in a porous medium, International journal of heat and mass transfer, 44, (2001), page 2791 – 2799.

[11] K. L. Hsiao, Heat and mass mixed convection for MHD visco-elastic fluid past a stretching sheet with ohmic dissipation, Commun. Nonlinear Sci. Numer. Simul, 15 (2010) 1803–1812.

[12] K. L. Hsiao, Corrigendum to "Heat and mass mixed convection for MHD viscoelastic fluid past a stretching sheet with ohmic dissipation, Commun Nonlinear Sci Numer Simulat 15, (2010) 1803–1812.

[13] K. L. Hsiao, Corrigendum to "Heat and mass mixed convection for MHD viscoelastic fluid past a stretching sheet with ohmic dissipation" [Commun Nonlinear Sci Numer Simulat 15 (2010) 1803–1812], Commun. Nonlinear Sci. Numerical Simulation, 28, (2015) 232.

[14] K.L. Hsiao, MHD mixed convection for viscoelastic fluid past a porous wedge, Int. J. Non Linear Mech. 46 (2011) 1–8.

[15] K. L. Hsiao, Nanofluid flow with multimedia physical features for conjugate mixed convection and radiation, Comput. Fluids 104 (2014) 1–8.

[16] A. Kucaba-Piętal, Microchannels flow modelling with the micropolar fluid theory, Bulletin of the Polish Academy of Sciences, Technical Sciences, vol. 52, No. 3, 2004, pp. 35-59.

[17] Md. Ziaul Haque, Md. Mahmud Alam, M. Ferdows, A. Postelnicu, Micropolar fluid behaviors on steady MHD free convection and mass transfer flow with constant heat and mass fluxes, joule heating and viscous dissipation, Journal of King Saud University–Engineering Sciences (2011) xxx, xxx–xxx.

[18] J. Zueco, P. Eguía, L.M. López-Ochoa, J. Collazo, D. Patiño, Unsteady MHD free convection of a micropolar fluid between two parallel porous vertical walls with convection from the ambient, Int. Commun. Heat Mass Transfer, 36, (2009) page 203–209.

[19] M. A. El-Hakiem, J. P. Hartnett, W. J. Minkowycz, Viscous dissipation effects on MHD free convection flow over a non-isothermal surface in a micropolar fluid, Int. Comm. Heat Mass Transfer, 27, 4, (2000), page 581–590.

[20] Afzal A. Siddiqui, A. Lakhtakia, Debye-Hûckel solution for steady electro-osmotic flow of micropolar fluid in cylindrical microcapillary, Applied Mathatematics and Mechanics, English Edition, vol. 34, N°. 11 (2013) page 1305 –1326.

[21] Navin Kumar and Sandeep Gupta, MHD free-convective flow of micropolar and Newtonian fluids through porous medium in a vertical channel, Meccanica, 47, (2012), page 277–291.

[22] Matej Zadravec, Matjazˇ Hribersˇek, Leopold Sˇkerget, Natural convection of micropolar fluid in an enclosure with boundary element method, Engineering Analysis with Boundary Elements, vol. 33 (2009) page 485–492.

[23] Diksha Gupta, Non-linear problems in micropolar fluid flows, doctorate thesis, Department of Mathematics, JAYPEE Institute of Information Technology (JIIT), A-10, SECTOR-62, NOIDA, INDIA (September 2014).

[24] Xinhui Si, Mingyang Pan, Liancun Zheng, Jianhui Zhou2 and Lin Li, The solutions for the flow of micropolar fluid through an expanding or contracting channel with porous walls, Boundary Value Problems, Springer Open journals,176 (2016).

[25] P. Muthu, B. V. Rathish Kumar and Peeyush Chandra, A study of micropolar fluid in an annular tube with application to blood flow, Journal of Mechanics in Medicine and Biology, Vol. 8, No. 4 (2008) page 561‑576.

[26] Gamal M. Abdel-Rahman, Effect of Magnetohydrodynamic on Thin Films of Unsteady Micropolar Fluid through a Porous Medium, Journal of Modern Physics, vol. 2 (2011) page 1290-1304.

[27] M. M. Rahman, Convective flows of micropolar fluids from radiate isothermal porous surfaces with viscous dissipation and Joule heating, Communication Nonlinear Sci. Numerical Simulation, 14 (2009), page 3018–3030.

[28] Yuri A. Buyevichn, Advances in the flow and Rheology of non-Newtonian fluids Elsevier, Science B. V. (1999), page 1237 – 1240.

[29] Theodore L. Bergman, Adrienne S. Lavine, Fundamentals of heat and mass transfer, JOHN WILEY & SONS, 7th edition, (2011), pages 627 – 628.

[30] W. M. Kays, M. E. Crawford, Convective Heat and Mass Transfer, McGraw-Hill Series in Mechanical Engineering, Third edition (1993), pages 413 – 414.

[31] D. R. Pitts, Theory and problems of heat transfer, Mc-Grow-Will Companies, Inc. USA, 3rd Edition, (1998), page 221-232.

[32] C. I. Chen, Non-linear stability characterization of the thin micropolar liquid film flowing down the inner surface of a rotating vertical cylinder (ELSEVIER, Science Direct, Nonlinear Science and Numerical simulation 12, 2007), page 760 – 775.

[33] M. A. Hossain and M. K. Chowdhury, Mixed convection flow of micropolar fluid over an isothermal plate with variable spin gradient viscosity, Acta Mechanica 131, (1998), page 139 – 151.

[34] S. P. Singh, G. C. Chadda and A. K. Sinha, Model for Micropolar fluid film mechanism with reference to human joints (Indian Journal of pure applied Mathematics, vol.19, No.4, (1988), page 385 – 386.

[35] Y. Y. Lok and all, Unsteady mixed convection flow of a micropolar fluid near a stagnation point on a vertical surface (ELSEVIER, Science Direct, International of Thermal Science 45, 2006), page 1149 – 1157.

[36] Ching-Yang Cheng, Natural convection of a micropolar fluid from a vertical truncated cone with power-low variation in surface temperature (ELSEVIER, International Communications in Heat and Mass Transfer 35, 2008), page 39 – 46.

[37] Jawad Raza, Azizah Mohd Rohni and Zurni Omar, Rheology of Micropolar Fluid in a Channel with Changing Walls: Investigation of Multiple Solutions, Journal of Molecular Liquids, accepted paper, PII: S0167-7322(16)30928-X, (2016).

[38] Md. A. Ikbal, S. Chakravarty, Kelvin K.L. Wong, J. Mazumdar, P.K. Mandal, Unsteady response of non-Newtonian blood flow Throw a stenosed artery in magnetic field, Journal of Computational and Applied Mathematics, 230 (2009), page 243 – 259.

[39] V. P. Srivastava and Rashmi Srivastava, Particulate suspension blood flow through a narrow catheterized artery, Computers and Mathematics with Applications, 58, (2009), page 227 – 238.

[40] F. Shahzad, M. Sajid, T. Hayat, M. Ayub, Analytic solution for flow of a micropolar fluid, Acta Mechanica, 188, (2007), page 93–102.

[41] Rajesh Sharma, R. Bhargava, I. V. Singh, Combined effect of magnetic field and heat absorption on unsteady free convection and heat transfer flow in a micropolar fluid past a semi-infinite moving plate with viscous dissipation using element free Galerkin method, Applied Mathematics and Computation, 217, (2010), page 308–321.

[42] Fadzilah Md Ali, Roslinda Nazar, Norihan Md Arifin and Ioan Pop, Dual solutions in MHD flow on a nonlinear porous shrinking sheet in a viscous fluid, Ali et al. Boundary Value Problems, Springer Open Journal, (2013) page 01 – 07.

[43] Z. Abbas , and B. Ahmad, and S. Ali, Chemically reactive hydromagnetic flow of a second-grade fluid in a semi-porous channel, Journal of Applied Mechanics and Technical Physics, No. 5, Vol. 56, , (2015), page 878–888.

[44] S. M. M. EL-Kabeir, M. A. EL-Hakiem, and A. M. Rashad, Lie group analysis of unsteady MHD three dimensional by natural convection from an inclined stretching surface saturated porous medium, Journal of Computational and Applied Mathematics, 213, (2008), page 582 – 603.

[45] Nabil T. M. Eldabe, Sallam N. Sallam, Mohamed Y. Abou-zeid, Numerical study of viscous dissipation effect on free convection heat and mass transfer of MHD non-Newtonian fluid flow through a porous medium, Journal of the Egyptian Mathematical Society , 20, (2012), page 139–151.

[46] O. A. Bég, J. Zueco, H.S. Takhar, Unsteady magnetohydrodynamic Hartmann–Couette flow and heat transfer in Darcian channel with hall current ion-slip viscous and Joule heating effects Network Numerical solutions, Commun. Nonlinear Sci. Numer. Simul. 14 (2009) 1082–1097.

[47] Madhusudhana Rao, G. Viswanatha Reddy, M. C. Raju, S. V. K. Varma, Unsteady MHD free convective heat and mass transfer flow past a semi-infinite vertical permeable moving plate with heat absorption, radiation, chemical reaction and soret effects, International Journal of Engineering Sciences & Emerging Technologies, V. 6, I. 2 (2013) page 241-257.

[48] M. Ashraf and A. R. Wehgal, MHD flow and heat transfer of micropolar fluid between two porous disks, Applied Mathatematics and Mechanics, vol. 33, N°. 1, (2012) page 51–64.

[49] Yapeng Liu, Yongjun Jian , Quansheng Liu and Fengqin Li, Electro-osmotic Magnetohydrodynamic flow of Maxwell fluids between two micro-parallel plates Alternating current, Journal of Molecular Liquids, 211, (2015), page 784–791.

[50] Chonghua Gao and Yongjun Jian, Analytical solution of magnetohydrodynamic flow of Jeffrey fluid through a circular micro-channel, Journal of Molecular Liquids, 211, (2015), page 803–811.

[51] A. A. Mohammadein, R. S. R. Gorla, and Cleveland Ohio, Effects of transverse magnetic field on mixed convection in a micropolar fluid on a horizontal plate with vectored mass transfer, Acta Mechanica, 118, (1996), page 1 – 12.

[52] Z. Y. Huang, Y. J. Liu, Characteristics of laminar MHD fluid hammer in pipe, Journal of Magnetism and Magnetic Materials, 397, (2016), page 213–224.

[53] Ruchika Dhanai, Puneet Rana, Lokendra Kumar, Critical values in slip flow and heat transfer analysis of non-Newtonian nanofluid utilizing heat source/sink and variable magnetic field: Multiple solutions, Journal of the Taiwan Institute of Chemical Engineers, 58, (2016), page 155–164.

[54] M. Turkyilmazoglu, Dual and triple solutions for MHD slip flow of non-Newtonian fluid over a shrinking surface, Computers & Fluids, 70, (2012), page 53–58.

[55] Hari R. Kataria , Harshad R. Patel , Rajiv Singh, Effect of magnetic field on unsteady natural convective flow of a micropolar fluid between two vertical walls, Ain Shams Engineering Journal, (2015), in press.
[56] M. M. Rashidi, S. Bagheri, E. Momoniat, N. Freidoonimehr, Entropy analysis of convective MHD flow of third grade non-Newtonian fluid over a stretching sheet, Ain Shams Engineering journal, (2015), in press.

[57] Neela Rani , S.K. Tomar, EHD convection in dielectric micropolar fluid layer, Journal of Electrostatics, 78, (2015) page 60 – 67.

[58] M. Madhu and N. Kishan, MHD BOUNDARY-LAYER FLOW OF A NON-NEWTONIAN NANOFLUID PAST A STRETCHING SHEET WITH A HEAT SOURCE/SINK, Journal of Applied Mechanics and Technical Physics, Vol. 57, No. 5 (2016) page 908–915.

[59] B. Suresh Babu, G. Srinivas and B. R. K. Reddy, Finite element analysis of free convection flow with MHD micropolar and viscous fluids in a vertical channel with dissipative effects, Journal of Naval Architecture and Marine Engineering, (2011), DOI: 10.3329.

[60] Cha'o-Kuang Chen, Bo-Shiuan Chen, Chin-Chia Liu, Entropy generation in mixed convection magnetohydrodynamic nanofluid flow in vertical channel, International Journal of Heat and Mass Transfer, 91, (2015), page 1026 – 1033.

[61] M. Ashraf and M. M. Ashraf, MHD stagnation point flow of a micropolar fluid towards a heated surface, Applied Mathematics and Mechanics - English Edition – Vol. 32, N°. 1 (2011) page 45–54.

[62] M. Ashraf, N. JAMEEL, K. ALI, MHD non-Newtonian micropolar fluid flow and heat transfer in channel with stretching walls, Applied Mathematics and Mechanics. -Engl. Edition – Vol.34, N°.10 (2013) page 1263–1276.

[63] M. Kumari, I. Pop, and G. Nath, Transient MHD stagnation flow of a non-Newtonian fluid due to impulsive motion from rest, International Journal of Non-Linear Mechanics, 45, (2010), page 463–473.

[64] R. Ellahi, The effects of MHD and temperature dependent viscosity on the flow of non-Newtonian nanofluid in a pipe: Analytical solutions, Applied Mathematical Modelling, 37, (2013), page 1451–1467.

[65] K. Tzirakis, L. Botti , V. Vavourakis , Y. Papaharilaou, Numerical modeling of non-Newtonian biomagnetic fluid flow, Computers and Fluids, 126, (2016), page 170–180.

[66] B. Suresh Babu, G. Srinivas, B. R. K. Reddy, Finite element analysis of free convection flow MHD micropolar and viscous fluids in a vertical channel with dissipative effect, Journal of Naval Architecture and Marine Engineering (2011).

[67] N. Midoux, Mécanique et Rhéologie des fluides en génie chimique TEC & DOC-LAVOISIER, (1993), page 71 – 120.

[68] D. Quemada, Modélisation Rhéologique Structurelle TEC & DOC-LAVOISIER, (2006), page 115 – 142.

[69] R. P. Chhabra and all, Non-Newtonian Flow and Applied Rheology, Engineering Applications, Elsevier Science, PLANTA TREE, 1st Edition, (1999), page 316 – 372.

[70] D. P. Kessler and all. In: Momentum, Heat and Mass Transfer Library of Congress Cataloging-in-Publication Data, Marcel Dekker, Inc. Basel, New-York USA, (1999), page 73–822.

[71] J. L. Battaglia and all, Introduction aux Transferts Thermiques DUNOD, Paris, (2010), page 91–135.

[72] J. F. Sacadura, Initiation aux Transferts Thermiques TEC & DOC. 4ième tirage, (1993), page 253–266.

[73] A. Bejan, Convection Heat Transfer 2nd editions, Wiley inter-science, (1995), page 156 –202.

[74] H. A. Barnes, A Hand Book of Elementary Rheology, Institute of Non-Newtonian Fluid Mechanics, University of Wales, Penglais Aberystwyth, (2000), page 55 –185.

[75] D. A. Siginer, D. De Kee and R. P. Chhabra. In: Advances in the flow and Rheology of non-Newtonian fluids (Elsevier, Science B. V. 1999), page 1237 – 1240.

[76] J. P. Holman, Heat Transfer, McGraw-Hill in Mechanical Engineering, Tenth edition, (2002), 358 – 362.

[77] Michel Favre-Marinet, Sedat Tardu, Convective Heat Transfer Solved Problems, ISTE Ltd and John Wiley & Sons, Inc (2009), pages 189 – 210.

[78] W. M. Rohsenow and all, Hand Book of Heat Transfer, Mc-Grow-Will Companies, Inc. USA, 3rd Edition, (1998), page 202 – 288.

[79] O. G. Martynenko Pavel P. Khramtsov, Free-Convective Heat Transfer with Many Photographs of Flows and Heat Exchange, Springer-Verlag Berlin Heidelberg, (2005), page 245 – 263.

[80] J. A. Schetz, A. E. Fuhs, Handbook of Fluid Dynamics and Fluid Machinery, John Wiley & Sons, Inc., (1996), page 733–871.

[81] C. P. Kothandaraman, Fundamental of Heat and Mass Transfer, New Age International (P) Ltd., Revised Third Edition, Publishers, (2006), page 434–479.

[82] John H. Lienhard IV and John H. Lienhard V, A Heat Transfer Textbook, Phlogiston Press, Cambridge, Massachusetts, U.S.A., Third Edition, (2005), page 397 – 428.

[83] F. Durst, Fluid mechanics, An Introduction to the Theory of Fluid Flows, Library of Congress, Springer-Verlag Berlin Heidelberg, (2008), page 633–634.

[84] E. Krause. In: Fluid mechanics 2 (Springer, Verlag Berlin Heidelberg Germany, 2005), page 31 – 66.

[85] Vector A. Eremeyev, Leonid P. Lebedev and Holm Altenbach, Fundations of Micropolar Mechanics, Applied Sciences and Technology, SpringerBriefs (2013), pages 01 – 66.

[86] H. K. Moffat, Magnetic field generation in electrically conducting fluids, Cambridge monographs on mechanics and applied mathematics Bibliography, (1978), page 01 – 60.

[87] R. Bronson. In: Differential Equations, SCHAUM'S EASY OUTLINES, Mc-Grow-Hill, 2nd edition (2003), page 39 – 46.

Equations in following form: $u_1(y, GR), u_2(y, GR), N(y, GR)$**, (figures 5.1, 5.2, 5,3)**

K = 0 **:**

$$m = 1, \rho = 1, k = 1, b = 1 \ et \ h^* = 1$$

GR=5 :

$$u_1 = 0.42y^3 - 1.25y^2 - 0.80y + 0.88$$

$$u_2 = 0.35y^3 - 2.15y^2 + 0.92y + 0.88$$

GR=10 :

$$u_1 = 0.83y^3 - 2.5y^2 - 1.63y + 1.68$$

$$u_2 = 0.97y^3 - 2.92y^2 + 0.25y + 1.7$$

GR=15 :

$$u_1 = 1.25y^3 - 3.75y^2 - 2.75y + 2.25$$

$$u_2 = 0.9y^3 - 3.55y^2 + 0.38y + 2.25$$

K = 1 **;**

GR = 5 :

$$u_1 = -0.528sinh(y) - 0.417cosh(y) + 0.278y^3 - 0.833y^2 - 0.234y + 0.92 \ ;$$

$$-1 \le y \le 0$$

$$u_2 = -0.117y^3 - 0.125y^2 - 0.25y + 0.5; \ 0 \le y \le 1$$

$$N = 1.22cosh(y) + 0.57sinh(y) - 1.10y^2 + 0.33y + 0.21$$

GR=10 :

$$u_1 = -0.45 * sinh(y) - 0.42 * cosh(y) + 0.28 * y^3 - 0.83 * y^2 + 0.50 * y + 1.75$$

$$u2 = -0.58 * y^3 - 0.25 * y^2 - 0.5 * y + 1.33$$

$$N = 1.37 * cosh(y) + 1.14 * sinh(y) - 1.6 * y^2 + 0.66 * y + 1.49$$

GR=15 :

$$u_1 = -0.15 * sinh(y) - 0.42 * cosh(y) + 0.312 * y^3 - 0.85 * y^2 + 0.496 * y + 2.12$$

$$u2 = -0.96 * y^3 - 0.25 * y^2 - 0.5 * y + 1.7$$

$$N = 1.99cosh(y) + 1.75sinh(y) - 1.78y^2 + 1.12y + 1.88$$

Equations in following form: $\boldsymbol{u_1(y,\mu^*), u_2(y,\mu^*), N(y,\mu^*)}$**, (figures 5.4, 5.5, 5.6)**

K = 0 :

GR = 5, μ^* = 1 :

$$u_1 = 0.33 * y^3 - 1.33 * y^2 - 0.97 * y + 0.67$$

$$u_2 = -0.53 * y^3 - 0.33 * y^2 + 0.17 * y + 0.67$$

GR = 5, μ^* = 2 :

$$u_1 = 0.42 * y^3 - 1.42 * y^2 - 0.25 * y + 1.6$$

$$u_2 = -1.62 * y^3 - 0.83 * y^2 + 0.83 * y + 1.6$$

GR = 5, μ^* = 3 :

$$u1 = 0.75 * y^3 - 1.42 * y^2 - 0.25 * y + 1.9$$

$$u2 = -1.89 * y^3 - 0.83 * y^2 + 0.83 * y + 1.9$$

K = 1 :

GR = 5, μ^* = 1

$$u_1 = -0.42 * sinh(y) - 0.83 * cosh(y) - 0.32 * y^3 - 0.83 * y^2 - 0.17 * y + 1.12$$

$$u_2 = -0.25 * y^3 - 0.31 * y^2 + 0.25 * y + 0.29$$

$$N = 2.11 * cosh(y) - 0.83 * sinh(y) - 2.58 * y^2 + 0.83 * y - 0.83$$

GR = 5, μ^* = 2 :

$$u_1 = -0.42 * sinh(y) - 0.83 * cosh(y) - 0.18 * y^3 - 0.83 * y^2 - 0.18 * y + 1.25$$

$$u_2 = -0.33 * y^3 - 0.75 * y^2 + 0.65 * y + 0.42$$

$$N = 1.19 * cosh(y) - 0.491 * sinh(y) - 1.58 * y^2 + 0.72 * y - 0.12$$

GR = 5, μ^* = 3 :

$$u_1 = -0.61 * sinh(y) - 0.83 * cosh(y) - 0.18 * y^3 - 1.15 * y^2 - 0.18 * y + 1.35$$

$$u_2 = -0.51 * y^3 - 1.25 * y^2 + 1.25 * y + 0.51$$

$$N = 1.19 * cosh(y) - 0.57 * sinh(y) - 1.58 * y^2 + 0.72 * y - 0.22$$

Equations in following form: $\boldsymbol{u_1(y,h^*), u_2(y,h^*), N(y,h^*)}$**, (figures 5.7, 5.8, 5.9)**

$\boldsymbol{K=0}$**:**

$\boldsymbol{GR=5, h^*=1}$ **:**

$$u_1 = 0.42 * y^3 - 1.25 * y^2 - 0.80 * y + 0.88$$

$$u_2 = 0.35 * y^3 - 2.150 * y^2 + 0.92 * y + 0.88$$

$\boldsymbol{GR=5, h^*=2}$ **:**

$$u_1 = 1.12 * y^3 - 1.67 * y^2 + 0.28 * y + 3.0922$$

$$u_2 = -1.12 * y^3 - 2.55 * y^2 + 0.56 * y + 3.10$$

$\boldsymbol{GR=5, h^*=3}$ **:**

$$u_1 = 1.52 * y^3 - 1.88 * y^2 + 1.82 * y + 5.19$$

$$u_2 = -5.19 * y^3 - 5.54 * y^2 + 5.54 * y + 5.19$$

$\boldsymbol{K=1}$**:**

$\boldsymbol{GR=5, h^*=1}$ **:**

$$u_1 = -0.528 * sinh(y) - 0.417 * cosh(y) + 0.32 * y^3 - 0.833 * y^2 - 0.234 * y + 0.98$$

$$u_2 = -0.12 * y^3 - 0.13 * y^2 - 0.25 * y + 0.55$$

$$N = 0.65 * cosh(y) - 0.92 * sinh(y) - 1.42 * y^2 + 1.33 * y + 0.66$$

$\boldsymbol{GR=5, h^*=2}$ **:**

$$u_1 = -1.33 * sinh(y) - 0.56 * cosh(y) + 0.29 * y^3 - 1.11 * y^2 + 1.12 * y + 1.88;$$

$$-1 \le y \le 0$$

$$u_2 = 0.88 * y^3 - 2.76 * y^2 + 0.56 * y + 1.33; 0 \le y \le 1$$

$$N = 0.65 * cosh(y) - 0.98 * sinh(y) - 1.51 * y^2 + 1.33 * y + 0.68; \ -1 \le y \le 0$$

$\boldsymbol{GR=5, h^*=3}$ **:**

$$u_1 = -0.56 * sinh(y) - 0.56 * cosh(y) + 0.29 * y^3 - 0.76 * y^2 + 1.21 * y + 2.55;$$

$$-1 \le y \le 0$$

$$u_2 = -2.91 * y^3 - 2.99 * y^2 + 3.91 * y + 1.98;\ 0 \le y \le 1$$

$$N = 0.42 * cosh(y) - 0.83 * sinh(y) - 1.51 * y^2 + 1.33 * y + 1.22;\ -1 \le y \le 0$$

Equations in following form: $u_1(y, k^*), u_2(y, k^*), N(y, k^*)$, (figures 5.10, 5.11, 5.12)

$K = 0$:

$GR = 5, k^* = 1$:

$$u_1 = 0.42 * y^3 - 1.25 * y^2 - 0.80 * y + 0.88;\ -1 \le y \le 0$$

$$u_2 = 1.12 * y^3 - 2.55 * y^2 + 0.54 * y + 0.88;\ 0 \le y \le 1$$

$GR = 5, k^* = 2$:

$$u_1 = 0.48 * y^3 - 1.82 * y^2 - 1.25 * y + 1.07;\ -1 \le y \le 0$$

$$u_2 = 0.83 * y^3 - 2.33 * y^2 + 0.42 * y + 1.07; 0 \le y \le 1$$

$GR = 5, k^* = 3$:

$$u_1 = 0.78 * y^3 - 1.82 * y^2 - 1.25 * y + 1.33;\ -1 \le y \le 0$$

$$u_2 = 0.88 * y^3 - 2.63 * y^2 + 0.42 * y + 1.33; 0 \le y \le 1$$

$K = 1$:

$GR = 5, k^* = 1$:

$u_1 = -0.53 * sinh(y) - 0.45 * cosh(y) + 0.32 * y\text{^}3 - 0.83 * y\text{^}2 - 0.23 * y + 0.98;\ -1 \le y \le 0$

$$u_2 = -0.22 * y\text{^}3 - 0.44 * y\text{^}2 + 0.12 * y + 0.53;\ 0 \le y \le 1$$

$$N = 2.11 * cosh(y) - 0.83 * sinh(y) - 2.58 * y\text{^}2 + 0.83 * y - 0.83;\ -1 \le y \le 0$$

$GR = 5, k^* = 2$:

$$u_1 = -0.98 * sinh(y) - 0.56 * cosh(y) + 0.19 * y^3 - 0.94 * y^2 + 0.67 * y + 1.52;$$

$$-1 \le y \le 0$$

$$u_2 = -0.22 * y\text{^}3 - 0.54 * y\text{^}2 - 0.22 * y + 0.96;\ 0 \le y \le 1$$

$$N = 1.24 * cosh(y) - 1.11 * sinh(y) - 1.55 * y\text{^}2 + 1.11 * y - 0.56;\ -1 \le y \le 0$$

$GR = 5, k^* = 3$:

$$u_1 = -0.98 * sinh(y) - 0.56 * cosh(y) + 0.19 * y^3 - 0.94 * y^2 + 0.87 * y + 1.72;$$

$$-1 \le y \le 0$$

$$u_2 = -0.42 * y\text{^}3 - 0.54 * y\text{^}2 - 0.22 * y + 1.16;\ 0 \le y \le 1$$

$$N = 0.79 * cosh(y) + 1.45 * sinh(y) - 0.21 * y\text{^}2 - 1.45 * y - 0.75;\ -1 \le y \le 0$$

Equations in following form: $u_1(y, K), u_2(y, K), N(y, K)$, (figures 5.13, 5.14)

$GR = 5, K = 1$:

$$u_1 = -0.53 * sinh(y) - 0.45 * cosh(y) + 0.32 * y\text{^}3 - 0.83 * y\text{^}2 - 0.23 * y + 0.98;$$

$$-1 \le y \le 0$$

$$u_2 = -0.22 * y\text{^}3 - 0.44 * y\text{^}2 + 0.12 * y + 0.53;\ 0 \le y \le 1$$

$$N = 1.95 * cosh(1.15 * y) - 0.46 * sinh(1.15 * y) - 2.58 * y\text{^}2 + 0.83 * y - 0.63;$$

$$-1 \le y \le 0$$

$GR = 5, K = 2$:

$u_1 = -1.77 * sinh(1.15 * y) - 0.47 * cosh(1.15 * y) + 0.21 * y\text{^}3 - 0.55 * y\text{^}2 + 1.36 * y + 0.42;\ -1 \le y \le 0.$

$u_2 = -0.11 * y\text{^}3 - 0.72 * y\text{^}2 + 0.88 * y - 0.05;\ 0 \le y \le 1$

$N = 2.55 * cosh(1.15 * y) - 0.44 * sinh(1.15 * y) - 3.55 * y\text{^}2 + 1.18 * y - 0.33;$

$$-1 \le y \le 0$$

$GR = 5, K = 3$:

$$u_1 = -2.82 * sinh(1.22 * y) - 0.47 * cosh(1.22 * y) + 0.21 * y\text{^}3 - 1.75 * y\text{^}2 + 1.36 * y - 0.17;\ -1 \le y \le 0$$

$$u_2 = -0.21 * y\text{^}3 - 0.82 * y\text{^}2 + 1.65 * y - 0.64;\ 0 \le y \le 1$$

$$N = 3.24 * cosh(1.15 * y) - 0.43 * sinh(1.15 * y) - 3.80 * y\text{^}2 + 1.92 * x - 0.52;$$

$$-1 \le y \le 0$$

Equations in following form: $u_1(y,\beta^*), u_2(y,\beta^*), N(y,\beta^*)$, (figures 5.15, 5.16, 5.17)

$\mu^* = 1, \rho = 1, k^* = 1, GR = 5 \ \ et \ h^* = 1.$

$K = 0, \beta^* = 0.7$:

$$u_1 = -0.42 * y\text{^}3 - 1.25 * y\text{^}2 - 0.41 * y + 0.42$$

$$u_2 = -0.15 * y\text{^}3 - 0.88 * y\text{^}2 + 0.61 * y + 0.42$$

$K = 0, \beta^* = 0.5$:

$$u_1 = -0.42 * y\text{^}3 - 1.25 * y\text{^}2 - 0.58 * y + 0.25$$

$$u_2 = -0.23 * y\text{^}3 - 0.89 * y\text{^}2 + 0.87 * y + 0.25$$

$K = 0, \beta^* = 0.2$:

$$u_1 = -0.42 * y\text{^}3 - 1.25 * y\text{^}2 - 0.68 * y + 0.15$$

$$u_2 = -0.23 * y\text{^}3 - 0.75 * y\text{^}2 + 0.83 * y + 0.15$$

$K = 1, \beta^* = 0.7$:

$$u_1 = -0.51 * sinh(y) - 0.42 * cosh(y) + 0.28 * y\text{^}3 - 0.833 * y\text{^}2 - 0.29 * y + 0.87$$

$$u_2 = -0.115 * y\text{^}3 - 0.142 * y\text{^}2 - 0.208 * y + 0.446$$

$$N = 2.06 * cosh(1.15 * y) - 0.33 * sinh(1.15 * y) - 2.58 * y\text{^}2 + 0.83 * y - 0.63$$

$K = 1, \beta^* = 0.5$:

$$u_1 = -0.51 * sinh(y) - 0.42 * cosh(y) + 0.28 * y\text{^}3 - 0.77 * y\text{^}2 - 0.38 * y + 0.71$$

$$u_2 = -0.12 * y\text{^}3 - 0.092 * y\text{^}2 - 0.09 * y + 0.297$$

$$N = 2.15 * cosh(1.15 * y) - 0.22 * sinh(1.15 * y) - 2.58 * y\text{^}2 + 0.83 * y - 0.63$$

$K = 1, \beta^* = 0.2$:

$$u_1 = -0.51 * sinh(y) - 0.42 * cosh(y) + 0.28 * y\text{^}3 - 0.7 * y\text{^}2 - 0.47 * y + 0.55$$

$$u_2 = -0.147 * y\text{^}3 - 0.03 * y\text{^}2 + 0.04 * y + 0.135$$

$$N = 2.23 * cosh(1.15 * y) - 0.12 * sinh(1.15 * y) - 2.58 * y\text{^}2 + 0.83 * y - 0.63$$

Equations in following form: $u_1(y,\rho), u_2(y,\rho), N(y,\rho)$, (figures 5.18, 5.19, 5.20)

$$\mu^* = 1, \beta^* = 1, k = 1, GR = 5 \ \ et \ h^* = 1.$$

$\boldsymbol{K = 0, \rho = 0.7}$:

$$u_1 = 0.55 * y\text{^}3 - 1.25 * y\text{^}2 - 0.60 * y + 1.22$$

$$u_2 = 0.35 * y\text{^}3 - 2.150 * y\text{^}2 + 0.58 * y + 1.22$$

$\boldsymbol{K = 0, \rho = 0.5}$:

$$u_1 = 0.55 * y\text{^}3 - 1.25 * y\text{^}2 - 0.43 * y + 1.39$$

$$u_2 = 0.35 * y\text{^}3 - 2.150 * y\text{^}2 + 0.42 * y + 1.39$$

$\boldsymbol{K = 0, \rho = 0.2}$:

$$u_1 = 0.55 * y\text{^}3 - 1.25 * y\text{^}2 - 0.27 * y + 1.56$$

$$u_2 = 0.35 * y\text{^}3 - 2.150 * y\text{^}2 + 0.25 * y + 1.56$$

$\boldsymbol{K = 1, \rho = 0.7}$:

$$u_1 = -0.528 * sinh(y) - 0.462 * cosh(y) + 0.498 * y\text{^}3 - 0.833 * y\text{^}2 - 0.234 * y + 1.2$$

$$u_2 = -0.33 * y\text{^}3 - 0.12 * y\text{^}2 - 0.285 * y + 0.74$$

$$N = 1.21 * cosh(y) + 0.54 * sinh(y) - 1.02 * y\text{^}2 + 0.295 * y + 0.09$$

$\boldsymbol{K = 1, \rho = 0.5}$:

$$u_1 = -0.52 * sinh(y) - 0.49 * cosh(y) + 0.56 * y\text{^}3 - 0.95 * y\text{^}2 - 0.22 * y + 1.43$$

$$u_2 = -0.39 * y\text{^}3 - 0.21 * y\text{^}2 - 0.33 * y + 0.94$$

$$N = 1.21 * cosh(y) + 0.59 * sinh(y) - 1.05 * y\text{^}2 + 0.31 * y + 0.195$$

$\boldsymbol{K = 1, \rho = 0.2}$:

$$u_1 = -0.52 * sinh(y) - 0.55 * cosh(y) + 0.63 * y\text{^}3 - 1.05 * y\text{^}2 - 0.21 * y + 1.71$$

$$u_2 = -0.39 * y\text{^}3 - 0.21 * y\text{^}2 - 0.55 * y + 1.16$$

$$N = 1.21 * cosh(y) + 0.59 * sinh(y) - 1.15 * y\text{^}2 + 0.33 * y + 0.31$$